Investigation into the Application of Turbo-compounding for Downsized Gasoline engines

Lu, Pengfei

Award date:
2017

Awarding institution:
University of Bath

Investigation into the Application of Turbo-compounding for Downsized Gasoline engines

Pengfei Lu

A thesis submitted for the degree of Doctor of Philosophy

University of Bath

Department of Mechanical Engineering

June 2017

Abstract

This thesis sets out to evaluate six novel arrangements of internal combustion engine air path designed to improve the degree of exhaust energy recovery from a practical passenger car engine system. The study was conducted using 1D engine simulation based on two experimentally validated models of modern turbocharged spark ignition engines. Improvements of up to 5% in fuel efficiency are presented, along with reductions of up to 30% in the torque rise time are presented.

For at least 7 decades, efforts have been made to recover waste energy from the internal combustion engine. Heat engines, governed by the second law of thermodynamics, inevitably reject a significant proportion of the fuel energy as heat to the environment. Technologies, such as turbo-compounding, (organic) Rankine cycle and thermoelectric generators have been proven effective for waste energy recovery in high load applications. Inverted Brayton cycle is also under investigation currently due to the high exergy availability in exhaust stream and the potential to enhance the overall performance of vehicle engines.

However, none of these technologies has been given extensive application in the field of automobiles, especially passenger cars, despite their effectiveness in reducing fuel consumption and CO_2 emission. This thesis reviews current and previous studies to summarise the advantages and disadvantages of these technologies as well as the factors that constrain them from wide application. Transient performance, which is rarely considered in the literature, is considered here to allow a more realistic assessment of the technologies merits.

Among these approaches, turbo-compounding has the advantage of compact volume, lower complexity and application cost, and is now employed to recover waste heat in heavy duty vehicles, such as mining equipment and road haulage. This thesis reviews the most recent research on turbo-compounding to identify the variables that make the greatest difference to the engine performance.

The potential for the augmentation of the fuel economy and power output by a novel implementation of turbo-compounding in light duty vehicles has been demonstrated. The concept of a variable ratio supercharger drive has been studied as part of a novel boosting system to improve the low-speed torque output by up to 55% and overall fuel economy by 3%. After a careful optimisation of the specifications of the variable ratio unit, it is combined with a turbo-compounding system to fully overcome the inherent drawbacks of turbo-

compounding, namely the tendency to reduce the power output and engine efficiency at low speed. Finally, the concept of divided exhaust period has been introduced in a novel turbo-compounded arrangement to regulate the exhaust flow for a better gas exchange process and improve fuel consumption by up to 5% while improving transient response times by 30%.

Acknowledgements

First of all, I would like to express my great appreciation and gratitude to Professor Chris Brace for his consistent supervision, support and guidance. It was his patience, specialised knowledge and vision that helped me to keep direction and proceed effectively towards my goals. And also, I would like to thank Dr Sam Akehurst for the countless helps he provided in technical aspects.

Besides, the discussions with Ford, Torotrak and Honeywell have also been greatly appreciated, most notably: Arnd Sommerhoff and Harald Stoffels from Ford; Andrew De Freitas, Dave Burtt and James Shawe from Torotrak and Ludek Pohorelsky from Honeywell.

And also, I cannot forget the assistance I received from Calogero Avola and Dr. Andy Lewis in helping me to understand the operation of the test cell. I also must thank my colleagues Dr Bo Hu, Dr. Huayin Tang, Dr. Nic Zhang and Dr. Dai Liu for their considerable assistance in helping me to understand the engine modelling and validation theory. I cannot imagine how tough my works will become without your supports.

I also would like to express my sincere thanks to all the colleagues at PVRC for their emotional and technical support throughout my research, Dr. Pin Lu, Dr Dian Liu, Dr Colin Copeland, Dr. Chris Bannister, Dr. Richard Burke, Dr. Pavlos Dimitriou, Dr. Simon Pickering, Dr Ramkumar Vijayakumar, Bingxing Luo, Qiyou Deng, Yuxiang Feng, Zhihang Chen, …Thank you so much for making my experience in these three and half years such an enjoyable one.

Finally, I would like to thank my family for their unconditional support and encouragement. I can never finish this study without your love!

Further Publications

The work has led to the publication or peer review of a number of journal and conference articles. A list of these publications is given below and references to these will be provided as necessary within the chapters of this thesis.

Refereed journal articles:

1. Analysis and comparison of the performance of an inverted Brayton cycle and turbo-compounding with decoupled turbine and CVT driven compressor for small automotive engines

P. Lu et al, *Journal of Engineering for Gas Turbines and Power: Transactions of the ASME*, 139 (7), 072801.

Peer reviewed journal articles:

2. System Validation of the V-charge Variable Drive Supercharger System on a 1.0 L GTDI Engine

P. Lu et al Journal: Energy Conversion and Management

Refereed conference articles

3. Explore and Extend the Effectiveness of Turbo-Compounding in a 2.0 Litre Gasoline Engine

P. Lu, et al, SAE Technical Paper 2015-01-1279, 2015, doi:10.4271/2015-01-1279.

4. **Explore and Extend the Effectiveness of Turbo-Compounding in a 2.0 Litre Gasoline Engine (Second report: fuel economy under part load condition, transient performance and effect of pressure ratio)**

P. Lu, et al, SAE Technical Paper, 2016-01-0564, 2016, doi:10.4271/2016-01-0564.

Peer reviewed conference articles:

5. Implementing full electric turbocharging systems on highly boosted gasoline engines

P. Lu et al Proceedings of ASME Turbo Expo 2017: Turbomachinery Technical Conference and Exposition.

Contents

List of Figures

List of Tables

Abbreviations

1-D	1-Dimensional	LIVC	Late Intake Valve Closing (deg)
AFR	Air fuel ratio	LP	Low Pressure
BDC	Bottom Dead Centre (deg)	MOP	Mean Opening Position
BMEP	Brake Mean Effective Pressure (bar)	NA	Naturally Aspirated
BSFC	Brake Specific Fuel Consumption (g/Kw-H)	NA	Naturally aspirated
CCP	CAD Calibration Protocol	NEDC	New European Drive Cycle
CFD	Computational Fluid Dynamics	NVH	Noise Vibration Harshness
CPU	Central Processing Unit	OEM	Original Equipment Manufacturer
CVT	Continuously Variable Transmission	PI	Proportional Integration
DEP	Divided Exhaust Period	PID	Proportional Integration Differentiation
DoE	Design of Experiment	PMEP	Pumping Mean Effective Pressure (bar)
DOHC	Double OverHead Camshaft	PR	Pressure Ratio
ECU	Electronic Control Unit	R2S	Regulated 2-Stage
EEVO	Early Exhaust Valve Opening (deg)	RGF	Residual Gas Fraction
EGR	Exhaust Gas Recirculation	RPM	Revolutions Per Minute
EIVC	Early Intake Valve Closing (deg)	SC	Supercharger
EIVO	Early Intake Valve Opening (deg)	SI	Spark Ignition
FEAD	Front End Accessory Drive	TDC	Top Dead Centre (deg)
FGT	Fixed Geometry Turbine	TGDI	Turbocharged gasoline direct injection engine
FMEP	Friction Mean Effective Pressure (bar)	TSI	Twincharger Fuel Stratified Injection
GDI	Gasoline Direct Injection	VCR	Variable Compression Ratio

GTDI	Gasoline Turbocharged Direct Injection	VGT	Variable Geometry Turbine
HCCI	Homogeneous Charge Compression Ignition	VVT	Variable Valve Timing
HP	High Pressure	WEDACS	Waste Energy Driven Air Conditioning System
IMEP	Indicate Mean Effective Pressure (bar)	WLTP	Worldwide Harmonized Light Vehicle Test Procedures
ISG	Integrated starter generator	WOT	Wide Open Throttle
KLSA	Knock Limited Spark Advance	DCE	Differential Compound Engine
LEVC	Late Exhaust Valve Closing (deg)		

Chapter 1 - Introduction

Turbo-compounding has been proven effective for waste energy recovery in heavy duty engines. However, this technology has not been given extensive application in the field of automobile, especially the passenger car, so far, because of the drawback of imposing high back pressure which obstructs gas exchange of premier cycle. Weakened power output at low engine speed is also one of the major issues preventing it from wide application.

Accordingly, the concept of variable speed supercharger and divided exhaust period will be combined with turbo-compounding engine trying to solve the aforementioned problem. DEP, which is of the capability of allocating brake load between internal combustion engine and waste energy recovery devices, could enhance the competitive advantages that are already achieved by turbo-compounding while mitigating the inherent deficiencies in engine breathing simultaneously. At the same time, a variable-drive supercharging concept has the potential to enable a higher power output and better fuel efficiency at low engine speed and rapid transient response in transient.

This chapter will firstly lay out the background for this project, and will then present the aims and principle objectives. A description of each chapter in this thesis will follow.

1.1. Background

Over the years, in order to meet the customer expectation in gasoline engine performance while limit the CO_2 emission fuel consumption, a long term (year 2050) roadmap showing the transition from current gasoline & diesel fuels to a majority renewable energy portfolio has been made, as shown in figure 1.1. It suggests a drop in conventional fuel engines and an increasing use of electricity in battery electric and plug-in vehicles. However, since the hybrid and electric vehicles have not move into the mainstream until now, efforts are still being invested on improving the efficiency of conventional internal combustion engines [1]. In spite of a number of issues such as the rising of knock and backpressure, boosting systems are now the most dominant technology applied in modern cars to achieve a better power-to-weight

ratio and fuel efficiency.

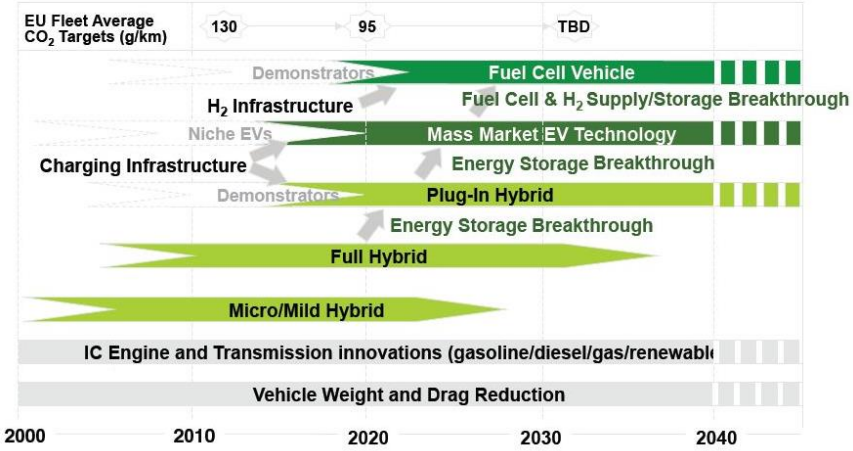

Figure 1.1. Passenger car low carbon technology road map [220].

Another most concerning issue is waste heat management. As shown in figure 1.2, more than a half of the fuel energy is lost through irreversibility (in the form of chemical combustion, heat transfer and cooling circulation) and exhaust gas for a typical medium sized car under the combined FTP75 City and Highway cycle [17] [202]. Therefore, in order to enhance the utilization of combustion energy and eventually improve the overall efficiency of the engine system, it is worth investigating exhaust energy recovery technologies.

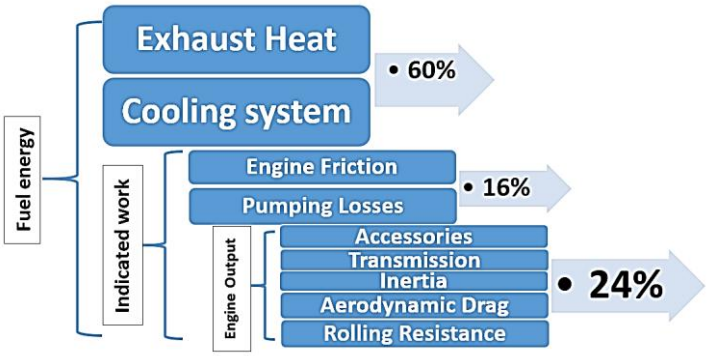

Figure 1.2. The schematic diagram of fuel energy distribution in a medium-sized passenger car.

An extensive sensitivity analysis was carried out in a high energy engine technologies program conducted in 2010 using engine simulation tools to determine the approaches to achieve 10% improvement in internal combustion engine thermal efficiency [203]. Considering the balance between the risks of exceeding the strength limits of the components and maximising the

opportunity of fulfilling the target performance, six technical factors was chosen as the objects for the further development, as shown in Figure 1.3. The percentage numbers in figure 1.3 represent the contributions from each factor that was expected to the thermal efficiency improvement. 10% improvement can be achieved when they work together.

From figure 1.3, it is also indicated that the thermal energy recovery from the engine exhaust stack made the biggest contribution (40%) to the total engine thermal efficiency improvement followed by the improvement in turbine and compressor performance that were expected to enhance the thermal efficiency of the engine by 3% and 0.7% in respectively [204]. Even though it was an ambitious goal for the study in this chapter, especially when the engine operation deviated from the high load region, it gives the general impression of the high potential of exhaust energy recovery technologies in upgrading the overall engine efficiency.

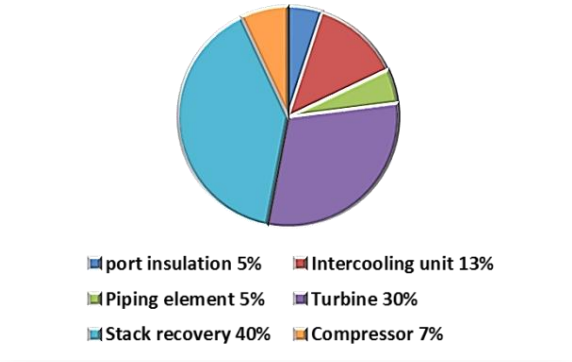

Figure 1.3. **Technical objects for strategy optimization to achieve 10% improvement in fuel economy.**

In addition to the substantial energy that can be recovered from and the fuel efficiency that can be improved by, exhaust heat utilization in internal combustion engines can also lower the carbon emissions.

In 2002, Volvo became the first one to design a prototype engine which recovers exhaust gas energy through compound turbines mechanical transmission. That is to say, the remaining pressure energy was converted into engine shaft power by turbine [12]. In this way, exhaust gas energy was recycled by 20% and fuel was saved by 5% at most. However, pumping loss increased with exhaust gas back pressure going up, and engine even did negative work under low-load operating conditions. Therefore, only when the engine was under high-load

conditions and the turbocharger was of high efficiency, did it save fuel. In addition, American Environmental Protection Agency (EPA) and the FEV did some research on engine exhaust gas dual-expander. The study results indicated that the dual-expander work of exhaust gas is not enough to overcome the additional friction loss under low speed and low load conditions. Only when the engine operated under high speed and high load conditions would the exhaust gas dual-expander work be surplus. B. The indirect method of exhaust gas energy recovery Doyle and Patel, both are engineers of American Mack Trucks, designed an equipment to recover exhaust heat energy by using Rankine cycle based on a truck engine with 288 horsepower. After commissioning for 450km, it saved fuel by 12.5% [13]. With the exhaust gas energy recovered, Cummins Corporation improved thermal efficiency by 5.4% through using Rankine cycle on a truck engine [14]. By selecting the best working medium of thermal cycle and optimizing the thermal cycle parameters as well as compound energy system, Italian Pamar University improved the engine thermal efficiency by 12% compared to the engine without bottom cycle [15]. In 1971, American scholar Pefley [16] put forward a new method to recover exhaust gas heat energy on dual-fuel engine (methanol and gasoline). By using exhaust heat energy, the methanol was dissociated into H2 and CO; then, the two kinds of gases were mixed with gasoline and sent into cylinder. German BMW started to study exhaust gas energy recovery on passenger cars. They put forward Rankine two cycle system and applied it to 1.8 L, 4 cylinder engines used in 3 series cars of BMW. The test results showed that engine fuel efficiency, output power and torque increased by 15%, 10kW and 20N·m [3]. In one word, exhaust gas energy recovery on engine is being developed and has made some preliminary achievements. The earlier study suggests that recovering exhaust gas energy through heat transmission has more advantages. With the energy and environmental problems becoming serious day by day, the research on this aspect will be more systematic, comprehensive and thorough. The energy recovery efficiency will be improved and the cost of equipment will be reduced. The waste energy recovery technology is a great revolutionary on engine.

In general, there are four dominating technologies for waste energy recovery [9]:

- Adding a power turbine in series after the main turbine of the turbocharger to

generate mechanical power form the enthalpy change of the exhaust gas and feed it back to the output crankshaft via gear train (Mechanical Turbo-compounding) [4-6]. Specifically, a series of nozzles increases the velocity of the fluid stream in the stator stage. This creates a pressure drop and an increase in velocity. Then the fluid stream is directed to the rotor blades, which are also acting as nozzles. This further reduces the pressure, but the velocity also drops as a result of transfer of kinetic energy to rotor blades. Therefore, in the power turbine, not only the kinetic energy of the fluid, but also the energy in the fluid in the form of pressure is converted into mechanical energy of the rotor shaft.

- Coupling of an electrical generator to the power turbine to directly convert the excess energy extracted from the exhaust into electricity (Electrical Turbo-compounding) [7].
- Implementation of a Rankine Cycle [8] system utilizing steam or organic fluid as working media where additional power is produced through an expander (Either a piston expander or a turbine expander)
- Direct conversion of exhaust gas heat to electric power through thermoelectric phenomenon (Thermoelectric Generators) [9]

As described above, the popular layout of the turbo-compounding engine at present can be roughly divided into two categories, namely mechanical turbo-compounding and electrical turbo-compounding. The difference between which lies in whether the power turbine output shaft is connected to the engine crank shaft mechanically (via gear sets, like that in a differential compound engine firstly proposed by F J Wallace [10]) or connected to a generator and then an energy storage device like a battery. While the mechanical turbo-compounding engine is considered as the standard technology that deserves further investigation to examine the potential for application and improvement, the electrical turbo-compounding has not been widely investigated to the same extent despite of its superiority in flexibility of layout according to some vehicle manufacturers.

The main disadvantage of turbo-compounding technology lies in the fact that it increases the backpressure and thus the pumping losses of the engine, which results in reduction of brake engine power. Especially when considering light duty transport or when the engines running

under part load condition or at low engine speed, the mechanical power produced by the power turbine is even not enough to offset the increased pumping losses [11]. For this reason, it is now widely accepted that the turbo-compounding engine is only suitable for heavy-duty vehicles or the transports that are consistently operated under high-load condition.

The most frequently utilized technology in exhaust heat recovery is the turbocharger which extracts the kinetic energy from the exhaust flow to drive the compressor. However, the benefit for turbocharged engine always comes along with the drawbacks in delayed transient response and over-boost risk at high engine speed. Specifically, a large turbocharger can provide high boosting at high engine speed, but suffers from poor efficiency and delayed transient response at lower engine speed due to the lack of exhaust gas flow to overcome the inertia of the system. On the contrary, a small turbocharger is more effective in air boosting and transient response at low engine speed due to the reduced inertia. However, as the engine speed rises, it would be necessary to bypass the turbine, typically through a waste gate, to prevent excessive turbocharger from over speed which may otherwise leads to over boost and thus sacrificed efficiency.

Besides, the produced power from the main turbine of a turbocharger unit has to be totally consumed by the compressor, which means the capability as well as the efficiency of the turbine is limited by the power demand of the compressor and substantially the air demand of the engine. When the extracted energy from the exhaust is excess, a waste gate is needed to bypass the redundant exhaust energy, otherwise the inlet air to the engine will suffer from over boost which may cause damage to the combustion stability and also exceeding the limit of in-cylinder pressure. When equipped with the turbo compound arrangement, however, the power produced by the power turbine is feed back to the engine crank shaft mechanically or converted into electricity. In this way, the waste energy recovery is only limited by the inherent specification of the power turbine such as inertial and mechanical strength.

The turbo-compounding engine is not a new idea at all. The original application of this concept can be traced back to the late 1940s and 50s on two notable aircraft engines, namely the Wright Cyclone and the Napier Nomad [12], however, its advantage in low fuel consumption for transport aircraft was soon overtaken by the rapid development of the gas turbine and the

turboprop engines. In 1970's, a new concept of the differential compound engine (DCE) as an integrated engine transmission system was developed at Bath University by Frank. J. Wallace [10]. The tested experimental prototype achieved a significant advance in both torque and efficiency characteristics over the turbocharged engine of the same class. Nevertheless, DCE was built based on heavy duty diesel engine, and it benefited greatly from the application of an epicyclical gear train to reclaim power from the power turbine over a significant part of the load and speed range.

In a gasoline engine, on the other hand, the inlet air flow is provided with a relatively fixed ratio to the fuel injection and fundamentally determined by the power demand. Therefore, at lower engine speed the exhaust gas flow rate is not sufficient to drive the power turbine, which results in notable lag. Furthermore, the power turbine added in series to the main turbine will substantially increase the back pressure and then the pumping losses.

1.2. Aim and objectives

This project aims to develop a detailed system model to quantify the expected benefits by exploring method to relief the constraint on the application of this technology and to implement the optimised system onto an engine platform to evaluate its performance.

The primary objectives of this project were as following:

- Document the origin and historic development of turbo-compounding engine (see **chapter 2**).
- Analyse the thermodynamics behind the concept of turbo-compounding engine (see **chapter 2**).
- Study the state-of the-art in the field of turbo-compounding and engine simulation, and produce a literature review (see **chapter 2**).
- Carry out simulation exercises of conventional turbo-compounding engines, and explore improving method based on the basic model (see **chapter 6**).
- Analyse the simulating results to determine parameters, such as CVT ratio (see **chapter 7**, turbine size (see **chapter 8**) and valve timing (see **chapter 9**), in that those models are most sensitive to.

- Determine a solution to the inherent problems, such as high back pressure (see **chapter 9**), interfering with engine breathing (see **chapter 9**) and deteriorated low end output (see **chapter 7**), faced by turbo-compounding.
- Highlight aspects of the thermodynamic model which need particular attention trying to produce test procedure and instrumentation standard documents for future testing (see **chapter 5**).
- Produce technical papers on the key areas of this project.

1.3. Scope of thesis

Chapter 2 to Chapter 10 present the works according to each of the project objectives, respectively. The conclusions are summarised in **Chapter 11**. Here is an overview of the contents of these chapters:

Chapter 2 will review knowledge on the current state-of-the-art waste energy recovery technologies, and then a comparison will be given regarding the advantages and disadvantages of aforementioned approaches.

Chapter 3 will first review the history of the development of turbo-compounding technologies to trace back the early applications in automotive industry, followed by the introduction of the typical configurations of turbo-compounding. Finally, the sensitivity of turbo-compounding performance to a variety of parameters would be summarised based on previous studies.

Chapter 4 will describe a modelling and calibration theory foundation for the study that will take place over the following chapters. It mainly includes three sub-sections: engine model introduction and calibration for steady state and transient simulation and engine control theory and tuning.

Chapter 5 will investigate the CVT Supercharger concept in simulation by comparing with a conventional two-stage super-turbo system. The results will be utilised as the theoretical basis to determine the feasibility of adopting CVT Supercharger with turbo-compounding in one engine.

Chapter 6 will verify the performance of variable supercharged engine system in improving low end output and enhancing fuel economy and transient speed by real test in engine level. The test results in this chapter will also be used for calibrating the combustion model of the turbo-compounding engine.

Chapter 7 will optimise a de-coupled electric turbo-compounding system to achieve a better BSFC under full and partial load condition over a conventional turbocharged engine system as an extra knowledge. The results in this part is considered as evaluation of the baseline turbo-compounding system. The turbo-compounding model will be adopted as a basic part for the comprehensive engine system in the following chapters.

Chapter 8 will first present the simulation of combining CVT Supercharger and turbo-compounding concepts under full load condition load to examine the potential to improve power output and fuel economy by comparing with a conventional turbocharged engine. And then, further investigation into the performance of CVT Supercharged turbo-compounding engine for low load and transient operation will follow.

Chapter 9 will present a comparison between turbo-compounding (coupled with variable supercharger) and inverted Brayton cycle for the performance of improving fuel economy under and response speed.

Chapter 10 will model the concept of divided exhaust period and combine it with CVT Supercharged turbo-compounding engine. A sweep and a global optimization of a variety of parameters will be carried out successively to investigate the influence on engine performance before the novel model with the optimal setups is evaluated for steady state and transient simulation.

Chapter 2 –*Review of research on exhaust energy recovery technologies*

This chapter will first briefly review the current state of the art technologies for waste energy recovery, including Rankine cycle, Brayton cycle, thermoelectric and turbo-compounding. After the working principle of these technologies are introduced, a comparison will be demonstrated regarding the advantages and disadvantages of each. The factors that constrain these approaches from wide application will be analysed as well. Based on the review on previous research, it comes to the conclusion that turbo-compounding units have the advantage of compact volume, lower complexity and application cost when compare with other counterparts. They also show good efficiency in harvesting exhaust energy, despite of the drawbacks in highly interfering with the gas exchange in premier cycle.

This chapter will also review the most recent research on turbo-compounding to specify the variables that make the greatest difference to the engine performance. The transient performance that was rarely involved in the previous work will also be included in this part. A conclusion can been drawn from this review that optimization is necessary for the configuration of the turbo-compounding engine to minimize the negative impact of the raised back pressure to the exhaust. Finally, the potential for the augmentation of the fuel economy and power output of the novel implementation of turbo-compounding engine in both heavy and light duty vehicles will also been demonstrated.

2.1. Introduction

In recent years, great effort has been spent to meet the higher customer expectation in gasoline engine performance and limit the CO_2 emission and the fuel consumption [1]. The increasingly strict emission legislation also prompt the development of internal combustion engines (ICEs) towards the direction of better fuel economy and lower emission.

Despite a number of issues, such as the reduced knock resistance and higher backpressure, turbo and supercharger system are now the most dominant technology helping modern cars to achieve a more efficient pumping cycle and a better power-to-weight ratio [1]. After years

of study and improvement, turbochargers and superchargers in passenger cars now generally have very high efficiency of up to about 75% [46]. On one hand, this is beneficial for the miniaturization of the boost system and effectively increasing the intake air pressure, on the other hand, only a small proportion of the exhaust energy is able to be reused due to the relatively smaller power requirement from the compressor. Further recovery of waste heat is restricted by the constraints of mechanical strength and heat resistance of ICEs. From this point of view, waste energy recovery (WER) arrangement, such as turbo-compounding and Rankine cycle and so on, have significant advantage over air boosting units in the capability of reclaiming exhaust energy as they are immune to the upper power demand limit of the compressor. Therefore, the approaches of utilizing novel thermodynamic cycles and waste energy recovery devices to increase the overall efficiency of ICEs is recently of growing interests, especially when considering the fact that the heat expelled through the exhaust makes up about 22-46% of the fuel energy in an internal combustion engine which accounts for the largest part of waste energy in ICEs [2].

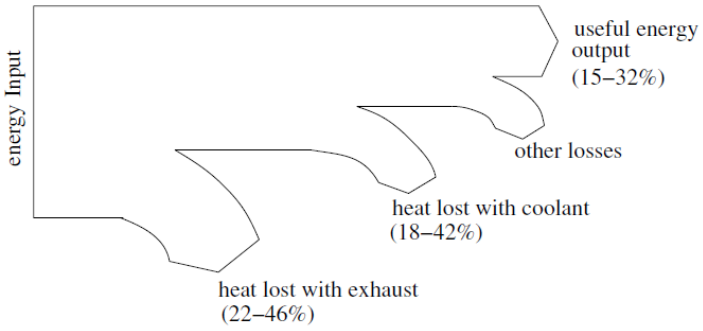

Figure 2.1. A Sankey diagram showing the fuel energy balance [5].

A recent study in [3] estimated that in a typical 2 litre gasoline engine which is commonly used on passenger cars, 21% of the produced energy is wasted through the exhaust at the commonest load and speed condition. Under full load condition, this loss increases to 44% [5]. Hendricks TJ and Lustbader JA estimated that [4] depending on engine size and torque-speed, the waste thermal energy from small passenger cars ranges from 20 Kw to 400 kW. According to statistics, the number of passenger cars hit 28.5 million in United Kingdom in 2011, which means about 5 billion gallons of gasoline fuel energy lost through the exhaust pipes annually. Figure 2.1. A Sankey diagram showing the energy balance of an internal combustion engine

[6]. According to the conclusion in [7], it is difficult for an ICE to achieve an efficiency higher than 42%, as large amount of fuel energy is lost through the heat transfer of the cylinder wall and the exhaust gas and coolant without being converted into useful work. According to figure 2.1, about 22-46% of the fuel energy in ICEs is expelled to the environment in the form of exhaust gas, which makes up the greatest part of the fuel energy. Therefore, it is worth investing efforts to harvest parts of this source of energy.

Generally, the temperature of the exhaust gas from light duty passenger cars ranges from 500 to 900 ◦C, and typically between 600 and 700 ◦C. In a high duty vehicle, it is slightly lower ranging from 500 to 650 ◦C [5]. This temperature can be further increased due to the ongoing development of the boost and after treat devices [7]. Those high exhaust temperatures provide significant opportunities for exhaust heat recovery system to produce useful work for various applications.

The benefit of converting exhaust heat into useful power lies in various aspects. First of all, it would bring measurable advantages for improving fuel economy. Secondly, it is capable of increase power output and the power density which are all beneficial for engine downsizing. Lastly, it may bring about further reducing in CO2 and other harmful exhaust emissions correspondingly. Vazaquez et al predicted in [8] that if only 6% of the heat contained in the exhaust gases were converted into to electric power, this would achieve a reduction of specific fuel consumption by 10% due to the additional power produced as well as the decrease in mechanical losses for overcoming the resistance of the alternator drive. Furthermore, in the experimental work conducted by Honda [9], the investigated thermal recovery system showed a maximum thermal cycle efficiency of 13%. At 100 km/h, this arrangement yields a cycle output of 2.5 kW (for the engine output of 19.2 kW), which increased the overall thermal efficiency of the engine from 28.9% to 32.7%.

At present, there are four dominating technologies for exhaust heat recovery [10]:

1. Adding a power turbine to the outlet port of the main turbo to extract kinetic energy from the exhaust gas and convert it into mechanical power and feed back to the output crankshaft via a gear train set (Mechanical Turbo-compounding) [11, 12, 13].
2. Coupling of an electrical generator to the power turbine to directly convert the excess

energy extracted from the exhaust into electricity (Electrical Turbo-compounding) [14].

3. Implementation of a Rankine Cycle [15] system that utilizes steam or organic fluid as working media to produce additional power through an expander (either a piston expander or a radial turbine).

4. Direct conversion from exhaust gas heat to electric power through thermoelectric phenomenon (Thermoelectric Generators) [16].

5. Standard Brayton cycle where compressed air is pushed through a heat exchanger to raise the temperature before it expands in the power turbine and output mechanical work [17].

2.2. Waste energy recovery technologies – a brief overview

2.2.1 Thermoelectric generation

As mentioned in the introduction, currently major technologies for exhaust heat recovery include turbo-compounding and thermal harvest arrangement based on Rankine cycle and thermoelectric regeneration. The thermoelectric regeneration is able to directly convert the exhaust heat into electric power based on the thermoelectric phenomenon. This technique provides some advantages including avoiding the use of mechanically rotating components, thus produce no noise or vibration in procession of work. It employs completely solid materials with no moving fluid involved, which ensures its stability and high reliability. Because of these advantages as well as, the revival of interests into clean energy production within the recent years has brought thermoelectric generation technology into the attention of many scientists and engineers.

Thermoelectric generation utilise the thermoelectric effects in the semiconductor material to convert thermal energy from different temperature gradients existing between hot and cold ends, as shown in figure 2.2. This phenomenon was firstly discovered by Thomas Johann Seebeck in 1821 and called the “Seebeck effect’’. One of the most commonly used thermoelectric material in waste energy recovery power generation is BiTe-based bulk. This is due to its availability in the market and high applicability in low and high exhaust gas

temperature range [20]. This material offers a simple and reliable way to convert thermal energy into electric current. The performance of a thermoelectric material can be expressed as $\mathrm{ZT} = S^2T/\rho\kappa$ where S is the thermos power; T is the absolute temperature; κ is the total thermal conductivity; and ρ is the electrical resistance [19].

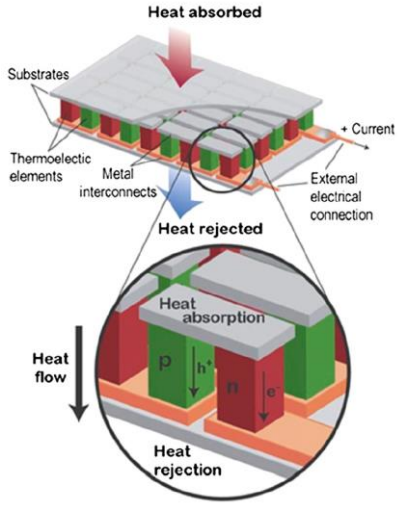

Figure 2.2. Schematic of a typical thermoelectric device [18].

Many researchers have studied the effects that thermoelectric waste energy recovery system have on modern vehicles. Mori et al [18] studied the potentials of thermoelectric technology in improving fuel economy of 2.0 litre gasoline engine powered vehicles. In the research conducted by Hussain et al [20] the effects of thermoelectric waste energy recovery for hybrid vehicles have been explored. From the results of Stobart and Milner's [21] studies on the possibility of utilising thermoelectric regeneration in passenger car, it was found out that 1.3 kW power could be produced by the thermoelectric generation device, which provides the potential to replace the alternator of a small passenger vehicle. Stobart et al [22] has also reviewed the potentials that the thermoelectric devices have in fuel saving for vehicles. It was concluded that up to 4.7% of improvement in fuel economy efficiency could be achieved. From these articles, the understanding of TEG technology has been comprehensively discussed. The employed materials are all available in the market. As the authors stated, the TEG technology is a promising new technology to recover waste heat from internal combustion engines. Studies on thermoelectric devices are still ongoing nowadays.

However, there are still some significant challenges preventing the development of the TE

technology. Basically, the hurdles come in two aspects Firstly, the conversion efficiency of the thermoelectric device is low with current technology. Secondly, the costs of the thermoelectric semiconductor materials which makes up the key component of the devices is relatively high [23-28, 194].

2.2.2 Rankine cycle

Basically, a Rankine cycle system consists of an evaporator, a pump, a condenser and a fluid expander. If heat is recovered to another working fluid for example, into water or into an organic fluid through the evaporator, the resulting vapour can then be expanded through the fluid expander and produce useful work, as shown in figure 2.4. The efficiency of the exhaust heat secondary fluid power cycle depends on the combined effectiveness of heat recovery (utilisation) method and the expansion cycle.

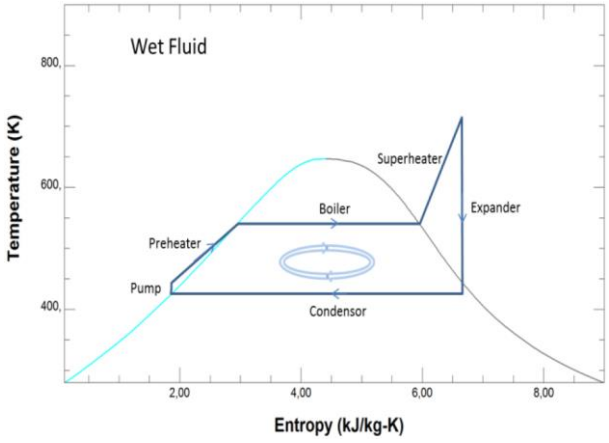

Figure 2.3. T-s diagram for heat recovery and utilisation options [6].

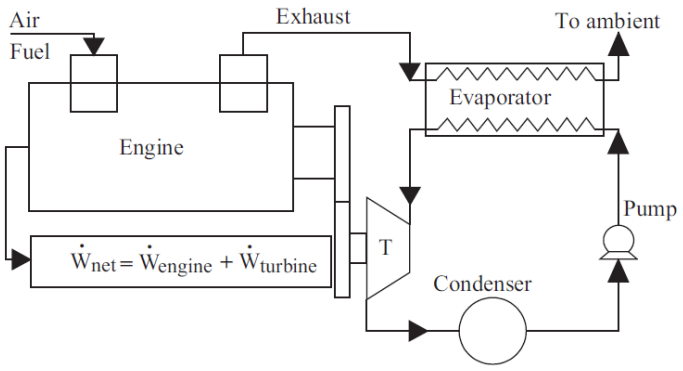

Figure 2.4. Schematic of setup used for RC HER [34].

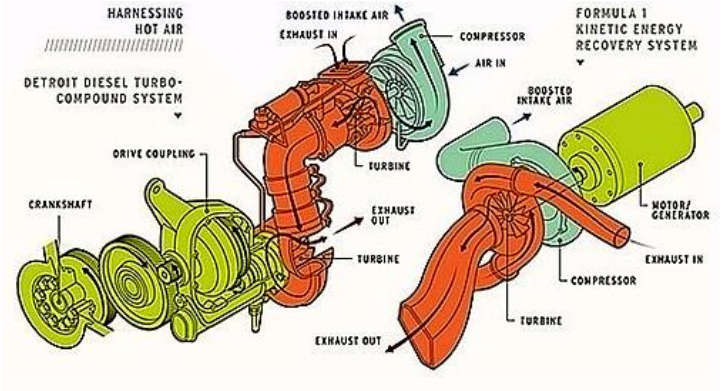

Figure 2.5. Schematic of Turbo-compounding [30].

According to figure 2.3, the working fluid is heated and vaporized by absorbing heat from the exhaust. The vaporized fluid is made to expand over an expander like turbine, piston expander and scroll expander to derive power. And then, the vapor condenses to liquid form in a condenser using air or an external fluid circuit as in power plants and then the process is repeated.

As for the working fluid in a Rankine cycle, water is one of the most popular choices in many applications due to its thermal stability. Usually, it is applied in the conditions where the temperature of the heat source is very high as there is no need to worry about the thermal decomposition of the steam. However, in the application where the heat need to be capture from a low-grade source, when the output is smaller than 1 MW for example, the organic working fluid becomes more favoured as it has higher efficiency than that of the steam turbines due to its higher molecular weight and thus lower saturated boiling temperature. Therefore, the application of the organic working fluid attracts much more attention in automotive industries. The organic Ranking cycle usually utilises the isentropic organic fluids due to their lower heat of vaporization and they do not need to be superheated to achieve a better efficiencies as the steam does [36]. But, it should be noted that the best working fluid with the highest efficiency in one operating condition may not be ideally suitable for another. Even though, researchers have provided some general roles for the working fluid selection. For example, after studied several working fluids Gu et al [34] found that the cycle efficiency is very sensitive to the evaporating pressure but insensitive to the expander inlet temperature. Hung [37] concluded that the system with lower irreversibility would more likely to produce

a better power output.

As above mentioned, the working fluid plays the most important role in determining the efficiency of the cycle. Therefore, the selection of working fluid should be given a careful consideration as it may affect various aspects of the entire system including the operating reliability, efficiency and the environmental impact. The type of the working fluid can be determined through a simplified Equation [38] as following:

$$\mathrm{E} = \frac{C_p}{T_H} - \frac{\left(\frac{nT_{rH}}{1} - T_{rH}\right) + 1}{T_H^2} \Delta H_H \qquad \textbf{2.1}$$

Where E (ds/dT) refers to the reverse of the slope of saturated vapour curve on T-s diagram, n is a constant which is suggested to be 0.375 or 0.38 in [39], $T_{rH} (= \frac{T_H}{T_C})$ refers to the reduced evaporation temperature and ΔH_H is the enthalpy of vaporization. When E<0, a wet fluid should be employed. When E=0, an isentropic fluid should be chosen. When E>0, a dry fluid should be chosen. More detailed criteria and properties of working fluids selection for Rankine cycle can be find in [40]

In recent years, Rankine cycle has increasingly attract interest of various automotive manufacturers. It is reported that Honda and BMW has respectively achieved an improvement in fuel economy up to 10% using this technology in their passenger cars [41-44]. Cummins, the commercial trucks company, stated that they decreased more than 10% of the fuel consumption with Rankine cycle [45]. Another one exciting research carried out by Miller et al [46] explored the potential of using the organic Rankine bottoming cycle integrated with thermoelectric generation. A comprehensive review of the research on thermal exhaust heat recovery with Rankine cycle can be found in [3]

2.2.3 Brayton cycle

In the standard Brayton cycle, as figure 2.6 shows, the air is compressed by a compressor driven by an expander before it enters the heat exchanger to absorb heat from the engine exhaust gas at a constant pressure.

The outlet air form the heat exchanger with higher temperature and increased volumetric flow rate is then flow into the expander. The thermal energy is converted into mechanical energy as the expander running. In this arrangement the energy conversion efficiency

increases with the air pressure. On the other hand, the temperature will increase as the working pressure rises. The temperature difference between the exhaust gas and the compressed air is then decreased which leads to a lower energy recovery efficiency. The arrangement in figure 2.6 (left) introducing a regeneration process that will improve the energy conversion efficiency comparing with the standard Brayton cycle. The compressed air is directed to a regenerator to draw heat from the after expansion air. In this way, the otherwise wasted thermal energy in the expelled air is recovered. It is beneficial for improving the energy conversion efficiency at lower working pressure. However, due to the aforementioned reason, the preheated air extracts less energy form the exhaust gas and the energy recovery efficiency is reduced accordingly. Consequently, the overall energy conversion efficiency is roughly the same [17] [50].

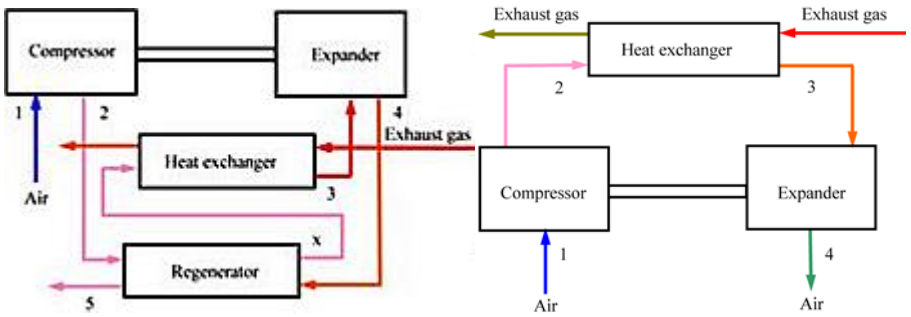

Figure 2.6. Schematic of Brayton cycle engine [17].

It leads to the compromise between the pressure and temperature of the compressed air and the energy extraction from the exhaust gas. Therefore, the compression ratio and regenerating process should be carefully adjusted to achieve the optimum overall efficiency.

A Brayton bottoming cycle is a real sense of heat recovery devices as it does not require for a high pressure exhaust gas from the primary cycle as the turbo-compounding does. Instead, it is the thermal energy remaining in the exhaust gas that is made use of.

Figure 2.7 demonstrates another way to make use of exhaust thermal energy. This approach is named as inverted Brayton cycle as it is opposite to the standard Brayton cycle in the layout. After expanded in the power turbine, the exhaust gas is directed into a heat exchanger to release heat. The cooled exhaust gas is then pressurised by a compressor to the atmospheric level and expelled to the ambient.

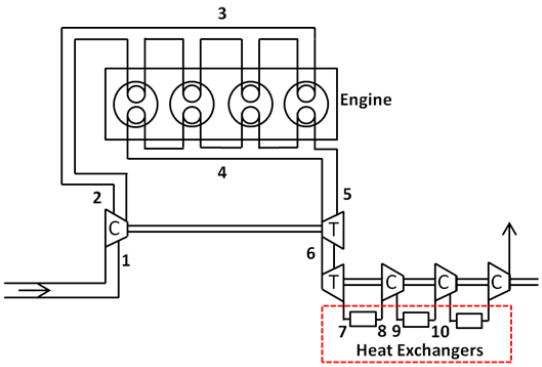

Figure 2.7. Schematic of inverted Brayton cycle engine [51].

This cycle allows the exhaust to be expanded under atmospheric pressure which increases the potential of removing from the exhaust gas. From this point of view, this arrangement can be considered as an extension to the turbo-compounding arrangement. Besides, the high temperature heat exchanger that is needed in the pressurized Brayton cycle and Rankine cycle is avoided, as the exhaust gas immediately goes into the power turbine, which is beneficial for further reducing the size and weight. The inverted Brayton cycle was studied in [51] as an alternative to turbo-compounding. Besides, a combination of the Brayton and inverted Brayton cycle, which was known as the mirror gas turbine, was studied in [52] based on the Brayton cycle that was firstly proposed by Frost at el [53]. The analysis in [54] also came to the conclusion that the inverted Brayton cycle is able to offer a more significant improvement in terms of the net engine power output.

2.2.4 Turbocharger

By now, the most frequently utilized technology in exhaust heat recovery is the turbocharger which extracts the kinetic energy from the exhaust flow to drive the compressor. The main turbine utilises the waste energy to drive the compressor providing boost pressure for the engine cylinder. The end objective of reduced fuel consumption is enabled through the reduced level of friction, reduced heat transfer across the cylinder walls and reduced pumping losses present in a downsized engine.

However, the benefit for a turbocharged engine always comes along with the drawbacks in transient response and over-boost with variable engine speed [54]. Specifically, a large

turbocharger can offer the power at high speed, but suffers from poor performance and transient response at lower engine speed due to the lack of exhaust gas flow to overcome the inertia of the system. On the contrary, a small turbocharger is able to improve the boost pressure and transient response due to the reduced inertia, however, as the engine speed rises, it would require turbine bypassing, typically a waste gate to prevent excessive turbocharger speed which may leads to over boost problem thus sacrificing efficiency.

Besides, as the produced power from the main turbine of a turbocharger unit has to be totally consumed by the compressor, which means the capability as well as the efficiency of the turbine is limited by the power demand of the compressor and substantially the air demand of the engine. When the extracted energy from the exhaust is excess, a waste gate is needed to bypass the redundant exhaust gas, otherwise the inlet air to the engine will be over boosted.

In spite of these challenges, the need to reduce carbon dioxide (CO2) emissions and fuel consumption is still the primary requirement for internal combustion (IC) engine development. Since the position of the IC engine as the engine type of choice for continued development seems to be unaffected by the advent of alternative propulsion systems (such as hybrids and fuel cells) and will probably remain so until at least well into the next decade [55], practically all new diesel engines feature boosting systems and 25% of all new gasoline engines in Europe also feature boosting systems today [56].

In general, the main needs of OEMs for both gasoline and diesel engines are the ability of the boosting system to provide high BMEP, EGR rates and efficiency throughout the whole operating range with reduced and/or variable back pressure. And also, rapid transient response, altitude performance, downsizing, down-speeding, hybrid powertrains and waste energy recovery are also desired [57]. In order to reach these targets, various technologies including the variable geometry turbine (VGT), twin-turbine, electric turbocharger and so on have been tried. The detailed introduction of these techniques can be found in [1].

With the turbo compound arrangement, however, the power produced by the power turbine is feed back to the engine crank shaft mechanically or converted into electricity, which is independent of the compressor working condition. Therefore, the waste energy recovery is

only limited to the inherent specification of the power turbine such as inertial and isentropic efficiency.

2.2.5 Turbo-compounding technology

By definition, the net power of an engine using a compound process is generated not only in the cylinder but also in a downstream expansion stage. In this sense, the exhaust gas turbine or another downstream turbine provides additional power to the crankshaft in a compound engine. The purpose of the process is to utilize the exhaust gas energy to a larger extent, resulting in better fuel economy. Calculations in [47] show that, at the design point of the engine, improvements in fuel economy exceeding 5% may be accomplished when the compressor and turbine efficiencies are excellent. Since this is true especially at high engine load, the most prominent examples of turbo-compounding engines are found in aircrafts and maritime ships which operate at constant high load for extended periods.

Turbo compound engine is not a new idea at all. The original application of this concept can be traced back to the late 1940s and ’50s on two notable aircraft engines, namely the Wright Cyclone and the Napier Nomad [58, 59], however, its advantage in low fuel consumption for transport aircraft was soon overtaken by the rapid development of the gas turbine and the turboprop engines. In 1970’s, a new concept of the differential compound engine (DCE) as an integrated engine transmission system was developed at Bath University by Frank. J. Wallace. [60, 61]. The tested experimental prototype achieved a significant advance in both the torque and efficiency characteristics over the turbocharged engine. Nevertheless, the DCE was built based on heavy duty diesel, and it benefited greatly from the application of epicyclical gear train to reclaim power from the power turbine over a significant part of the load and speed range. While in gasoline engine, the inlet air flow is fundamentally determined by the power demand. Therefore, at lower engine speed the exhaust gas flow rate is sufficient to drive the power turbine which results in notable lag. Furthermore, the power turbine added in series to the main turbine will substantially increase the back pressure and then the pumping losses. As above mentioned, the popular layout of the turbo compound engine at present can be Roughly divided into two categories, namely mechanical turbo-compounding and electrical turbo-compounding, The difference between which lies in whether the power turbine output

shaft is connected to the engine crank shaft mechanically (via gear sets, like that in a differential compound engine firstly proposed by F J Wallace [48]) or connected to a generator and then an energy storage device like battery. While the mechanical turbo-compounding engine is considered as the standard technology that deserves further investigation to examine the potential for application and improvement the electrical turbo-compounding has not been widely investigated to the same extent even though it is also a promising technique according to some vehicle manufacturers. The main disadvantage of turbo-compounding technology lies in the fact that it increases the backpressure of the engine and pumping losses that result to reduction of net engine power. Especially in a light load transport or under part load condition or during operating at low engine speed, the power produced by the power turbine is even not enough to offset the increased pumping losses [49]. For this reason, the original turbo-compounding engine is widely accepted only suitable for high-duty vehicles or the transport consistently operate at high load condition. All these issues in pumping work, turbo lag and exhaust energy distribution have forced an implementation of advanced boosting technologies such as variable speed supercharger and novel pipe routing for gas exchange of engine system such as divided exhaust period (DEP).

2.3. Comparison of the performance of waste energy recovery technologies

According to their working principle, the characteristics of all kinds of energy recovery technology are summarised as following.

2.3.1 Rankine cycle

The Ranking cycle is one of the most effective way to harvest waste heat in an internal combustion engine. For this approach, the feasible energy resources are not limited to exhaust gas, but also include cooling water and coolant for air boosting [42, 64].

The major working medium for Rankine cycles are usually water steam or organic fluid. The latter is more popular for the industrial application at present and gradually becoming the emphasis of research because of the relatively higher efficiency and less requirement in heat

exchange area despite of the risk in safety and toxicity of the working fluid. However, even with the more compact organic Rankine cycle, it takes up higher volume and weight than other waste energy recovery approaches do. For example, Weerasinghe et al made a comparison between Rankine cycle and turbo-compounding for the application in a diesel engine and concluded that the added weight of a Rankine cycle hybrid system is around 100 kg, which is about 15% heavier than that the turbo-compounding arrangement. According to the study in [65], the mass of the vehicles could undertake up to 74%, while other parameters, such as friction, heat loss and turbomachinery efficiency, undertake the rest, of the variation in the vehicle's fuel consumption. Therefore, the size and weight of Rankine cycles is regarded as the main issue hindering the application in passenger cars. It should be noted though, the gap in volume between Rankine cycle and turbo-compounding might be narrowed in gasoline engine implementation, since the turbomachinery in turbo-compounding could be significantly bigger for the need to reduce the back pressure imposed to the spark ignition engine.

2.3.2 Turbo-compounding

In an internal combustion engine, the remaining combustion pressure at the end of the power stroke will generate a pressure pulse when it is released from the exhaust valve. Turbo-compounding is able to make use of this energy directly by direct it through a power turbine to generate shaft work or electricity. As aforementioned, turbo-compounding is one of the most simple and compact technologies for waste energy recovery. With a properly arranged turbo-compounding system, the total brake power could be increased with a notable benefits in fuel efficiency. And also, the transient response of the whole system could be improved as well [66].

However, because of the simple working principle, turbo-compounding can only recover the remaining fuel energy from exhaust gas. Besides, as turbo-compounding relies on the pressure pulse from the primary cycle to play a role, its capability as a heat recovery devices is greatly depending on the expansion ratio and thermal efficiency of the power turbine. Furthermore, in contrast to Ranking cycles and thermoelectric generators, turbo-compounding highly interacts with the exhaust flow and causes back-pressure to the engine breathing, which leads to the main drawbacks of turbo-compounding. The high back-pressure causes resistance to

the exhaust flow and thus increases the parasitic pumping work. At the same time, higher exhaust back pressure on the engine results in increased residual gases, delayed combustion, increased heat transfer in the cylinder, and disruption to the global engine thermodynamic balance. Therefore, it is the most important topic to reduce the back pressure in order to fit a turbo-compounding system to the small gasoline engine. In a heavy duty diesel engines, however, rising BMEP levels and reducing EGR rates could improve the function of turbo-compounding [1].

Between the Rankine cycle system (figure 2.4) and turbo-compounding (figure 2.5), Weerasinghe et al [29] have made a numerical simulation to compare their effects in improving power output and fuel economy. The results showed that the Rankine cycle has relative advantages over turbo-compounding at various aspects: (1) at least 2% of more power can be developed; (2) 20% or more of fuel savings can be achieved by Rankine cycle compared to around 2.0% savings through turbo-compounding. However, there seems to be a question as to how a 2% difference in power generation can lead to an 18% increase in fuel economy. The author attributed this improvement to the heat storage ability of the secondary fluid employed in the exhaust heat harvest cycle. They stated that the "response" to temperature fluctuations in a turbo-compounding cycle is inferior to a heat recovery and expansion cycle. When the engine is heavily loaded, more energy will be found in the exhaust gas. The extra energy wasted is then recovered and stored in the secondary fluid reservoir. The secondary fluid (for example, steam in this case) reservoir does not only act as the working medium in the cycle but also act as an energy buffer. As a result, all the energy that is recovered is not consumed immediately, but is stored and expanded smoothly on demand. This feature enable the Rankine cycle to keep its overall efficiency at a maximum over a much wider operating range. On the other hand, in turbo-compounding cycle, the overall efficiency of the energy recovery process is limited by the top temperature and maximum flow rate through the power turbine. This is a significant difference that makes heat recovery and expansion cycles more favoured against turbo-compounding systems, and even against conventional electric hybrids. Except for the outstanding heat storage ability of the steam reservoir that is able to act as an energy buffer enhancing the overall efficiency of the system, another advantage provided by

Rankine cycle system was also highlighted to make Rankine cycle favoured against turbo-compounding systems. If a turbocharger is installed upstream of a Rankine cycle device the low-speed response of the turbocharger will be improved, while the turbo-compounding system cannot do it.

Generally, turbo-compounding is a heat recovery technique that has been successfully used in medium and large scale engines. Heat recovery to a secondary fluid and expansion is used in large scale engines, such as in power plants in the form of heat recovery steam generators (HRSG) [33]

However, the turbo-compounding engine does have advantages over Rankine cycle. Typically, the added weight of a turbo-compounding system of a Scania production engine that uses an electric turbo compound device is in the order of 75 kg (Scania press release) whereas a comparable Rankine cycle secondary fluid power system would weigh around 105 kg. The weight of a mechanical turbo compound drive of a Caterpillar engine would also be in the same order [35]. Besides, as a general rule, dry technologies are preferred opposed to fluid power systems, even though the air conditioning circuits have served extremely well over the past twenty to thirty years as an integral part of the engine. Some believe that a secondary fluid power system would probably have the same degree of complexity as an air conditioning system. However, it is no doubt that it will increase the complexity of the whole system. Another challenge is employing a relatively high pressure steam reservoir to build up the circuit. The technology is available but not mature, especially the expanders that are expected to be small scale steam expanders. This area is relatively underdeveloped by now.

The theoretical analysis of the effectiveness of these two waste energy recovery techniques can be found in [31, 32].

2.3.3 Thermoelectric

Nowadays, the research on thermoelectric devices are still ongoing. One of the biggest obstacles to the successful application of this technology is the low efficiency of the device. Besides, heat management could also be a problem regarding the thermal dissipation of the battery. In summary, the current level of materials science is not sufficiently developed to provide a thermoelectric device that is practical and cost effective [67, 68].

2.3.4 Heat insulation

Thermal insulation for an internal combustion engines is effective in increasing the exhaust gas energy availability for the secondary thermal cycle such as turbo-compounding [69-74]. Therefore, it is usually considered as an adjunct to the waste energy recovery techniques. Nevertheless, heat insulation may cause a significant drop in volumetric efficiency (because of the higher pre-ignition temperature) and an increase in nitrogen oxide emissions, which blocks it from extensive utilization. Besides, the work on insulated engines nowadays has been largely ceased due to the problems with the mechanical integrity of the ceramic materials used in the combustion chamber. Synthetically considering the aforementioned unfavourable characteristics gas exchange and NOx emission, heat insulation technics will not be included in the discussion in this report.

2.3.5 Brayton cycle

Theoretically, Brayton cycle has the advantages over Rankine cycle in thermodynamic and aerodynamic effectiveness since the thermodynamic irreversibility in the boiler of a combined gas and steam turbine system are completely eliminated.

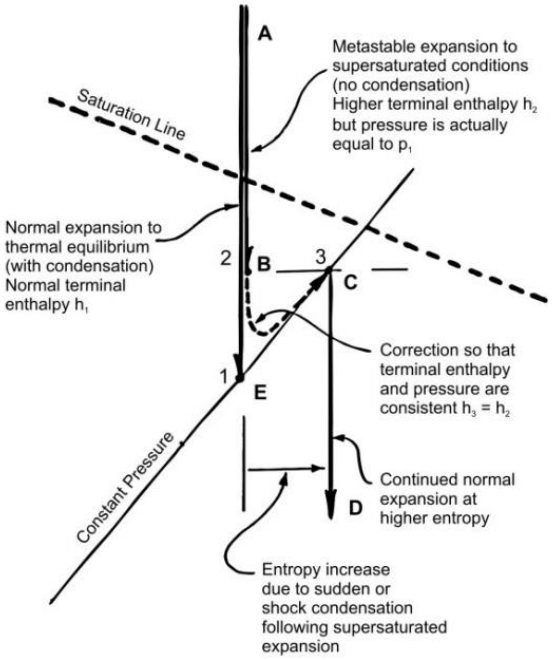

Figure 2.8. Expansion Supersaturated steam into wet region [86].

In addition, the efficiency penalty relating to the steam expansion in the wet region (During

the operation of a steam turbine, steam tends to condense during expansion when across the saturation line. This changes the status from metastable equilibrium into thermodynamic equilibrium irreversibly, and therefore a loss in availability takes place, as shown in (figure 2.8) is also avoided. Furthermore, it is reliable to reduce the plant complexity and develop a more environmental friendly system by applying Brayton cycle.

The comparison is summarised in table 2.1.

Table 2-1. Comparison between waste energy recovery technologies.

WER/WHR system	Advantages	Disadvantages
Rankine cycle (water)-WHR	• Good effectiveness in fuel saving • No interaction with engine breathing	• High complexity and cost • High volume and weight • Low expander efficiency for the steam turbine with common technology
Organic Rankine cycle-WHR	• Excellent BSFC reduction • Immune engine breathing • Lower heat exchange area	• High complexity and cost • High volume and weight • Working fluid toxicity risk
Turbo-compounding-WER	• Good BSFC reduction • Simple construction • Compact size and weight • Lower cost	• Highly affected engine breathing. • Limited fuel benefit at low load operation • Relatively low turbine efficiency
Thermo-electricity-WHR	• Compact in weight and size • No interaction with engine breathing	• Low efficiency • High heat dissipation • High cost • Large exhaust surface area needed
Heat insulation	• No extra attachment to the original system	• Limits in material technology • Degree the volumetric efficiency and combustion phase of original system
Brayton cycle (and Brayton cycle and mirror gas turbine)-WER	• Good BSFC reduction • Lower interaction with engine breathing when comparing with turbo-compounding	• Still interact with engine breathing • Very high complexity and cost • Sensitive to the effectiveness of compressor and cooler

For a Brayton cycle system, a low pressure turbine needs to be mounted to the outlet end of

the conventional gas turbine to expel the exhaust to higher vacuum. Besides, since the success or otherwise of the Brayton cycle critically depends on the heat transfer coefficients between the gas under compression and the stator rows, multistage intercooled compression is also needed to minimize the heat rejection. Therefore, a satisfactory level of intercooling and an effective method of producing hollow blades and heat pipes (low pressure power turbine) is required in real application to make the arrangement competitive in terms of specific power, initial cost and running cost [75]. As can be seen, a complete system of Brayton cycle is bulky in both size and complexity. Recent development in forced draught cooling towers operating with wet and dry cooling in parallel [76] brings about a significant reduction in size (but not in cost). Silverstein [77] has suggested a neat arrangement of achieving multistage intercooled compression for the research in this area by using an array of heat pipes located at the exit of each rotor and stator stage to reject heat inside the compressor casing to the forced draught medium surrounding the compressor housing. Besides, the mirror gas turbine which is a combination of the Brayton and inverted Brayton cycle was also proposed based on the principle of Brayton cycle and is in optimization now [78][79].

In practice, before these waste energy recovery technologies could be effectively utilised, a number of technique issues should be considered. Firstly, engine type is one of the most important factors. Wojciechowski et al conducted the comparison of two engine types (diesel and gasoline) for light-duty vehicles and came to the conclusion that waste energy recovery system is more suitable for spark ignition engines because of the higher exhaust gas temperatures and lower exhaust gas flow rates [80]. However, it was also indicated by other studies that the thermal energy availability which is a function of mass flow rate and temperature are highly dynamic in gasoline engine. This will greatly affect the heat transfer efficiency and degrade the functionality of the WER system to from its optimum [81]. Another example, as aforementioned, is that turbo-compounding is believed more suitable for the implementation in a diesel engine because of the higher tolerance to high back pressure. Besides, the added weight of the WER systems should also be taken into consideration as it will significantly deteriorate the net gain in fuel economy without proper handling. According to a sensitivity analysis about the effectiveness of different parameters on vehicle's fuel

consumption [65, 82], the mass of the vehicle overwhelms other parameters such as the aerodynamic drag and tyre rolling resistance. Therefore, turbo-compounding should be favoured because of the compactness in both size and weight when comparing with other WER technologies [83, 84]. Weerasinghe et al [85] compared a Rankine cycle system with turbo-compounding of a commercial Diesel engine of the similar size and weight and concluded that the added weight of a Rankine cycle hybrid system is around 100kg, which is 16 kg heavier than a mechanical turbo-compounding attachment and 21 kg than the electric version, as shown in table 2.2 [85]..

Table 2-2. Comparison in weight of typical turbo-compounding and Rankine cycle products

Scania-electric turbo-compounding		**Caterpillar turbo-compounding**		**Heat recovery fluid power cycle**	
Component	**Weight (kg)**	**Component**	**Weight (kg)**	**Component**	**Weight (kg)**
Turbine	20.0	**Turbine**	20.0	**Expander**	6.0
Compressor	20.0	**Compressor**	20.0	**Pump**	20.0
Electric motor	30.0	**Gear train**	30.0	**Working fluid**	25.0
Clutch	5.0	**Clutch**	10.0	**Condenser**	10.0
				Heat Exchanger	30.0
Auxiliaries	10.0	**Auxiliaries**	10.0	**Auxiliaries**	10.0
Total	85.0	**Total**	90.0	**Total**	106.0

2.4 History of the development of turbo-compounding

Before the gas turbine became the dominant technology in boosting aircraft piston engines, turbo-compounding was one of the most popular application to assist aeronautic propulsion which tended to operate constantly at high load. The working condition was especially favourable at high altitude where the ambient air pressure was very low. The power turbines were then able to achieve higher expansion ratio and then produce useful mechanical work.

As the field where turbo-compounding firstly found its application, a number of successful practices emerged during the early and middle 20th century. Two examples are briefly introduced as following.

2.4.1 Curtiss-Wright compound aircraft engine

One of the most powerful and fuel efficient gasoline piston engine for commercial aircraft was

the Curtiss-Wright compound aircraft engine (R-3350). Wright was also the first aircraft engine manufacturer to put a turbo-compounding engine into production. The first R-3350 was produced in the United States and started running in May of 1937. From then on, the later versions of this engine remained in production until the 1950s. During this period, thousands of Curtiss-Wright engines were built to provide power for both military and commercial aircrafts. The first major military application of it was found in the Boeing B-29 during World War II. Later on, subsequent versions became the power source of the C-119, C-121, A-1 Skyraider, and a number of Navy and commercial aircrafts. Curtiss-Wright compound engine was of double-row radial type with 18 cylinders (Figure 3.1).

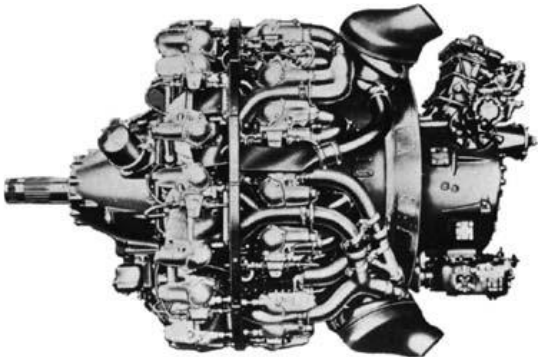

Figure 2.9. Curtiss-Wright compound aircraft engine with 18 cylinders in double-row radial configuration [46].

The rated take off power was 2,420 kW at 2,900 min−1. In this design, the charger was powered from the crankshaft at a fixed ratio, which possibly avoided the disadvantages coming with the propeller load characteristic. Three exhaust gas turbines, arranged in angular spacing of 120◦ were also connected to the crankshaft at a fixed ratio, supplying power to the crankshaft. The turbo-compounding assisted arrangement could produce up to 3,700 take-off horsepower when using the highest grade fuels available [58]. The specifications of the engine is shown in table 2.3.

Table 2-3. Details of the Curtiss-Wright compound aircraft engine (R-3350)

Engine Type	Twin-row 18-cylinder air-cooled radial
Power	3,700 hp (2760 kW) at 2,900 RPM, 59.5 in. MP
Weight	3,775 lb (1,712 kg)
Cylinders	bore 6.125 in (155 mm), stroke 6.312 in (160 mm)
Displacement	3,347 in3 (54.86 litre)

2.4.2 Napier Nomad

In addition to the application in gasoline engines, turbo-compounding was also used in aircraft diesel engines. A famous example was Nomad Napier which was a 12-cylinder two-stroke compound powertrain (figure 3.2).

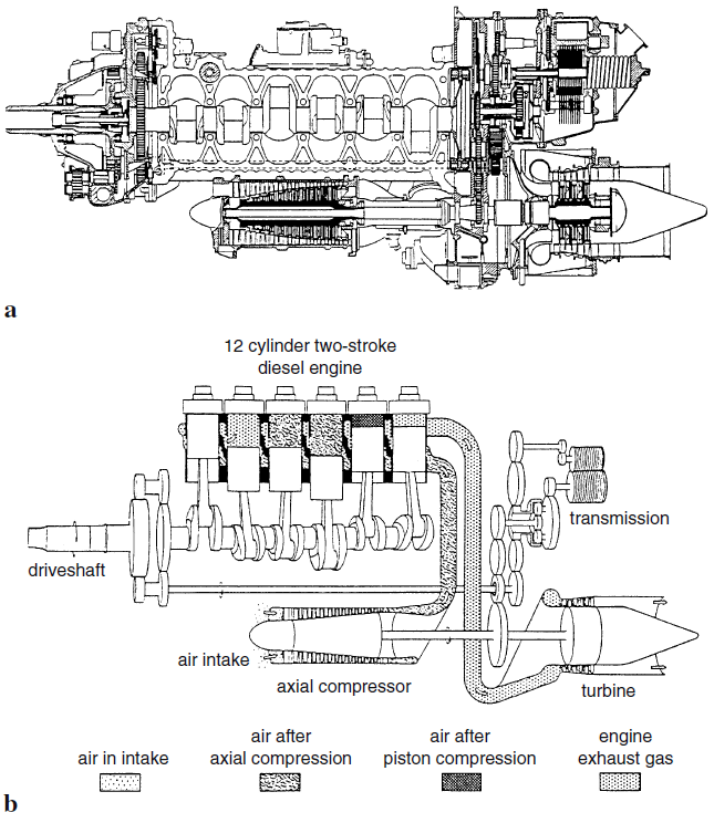

Figure 2.10. a, Napier diesel compound aircraft engine; b, diagram [46].

The Napier Nomad was a diesel aircraft engine designed and built in 1949 by a British company, D. Napier and Son, Ltd. The basic principle of this engine was to combine a piston engine with a power turbine recovering exhaust energy to produce mechanical work and improve the fuel economy. This engine was regarded as an exciting product which is likely to see a wide service in both military and civil applications as a result of its unique efficiency. In fact, its overall efficiency was higher than that of any other aero engine in its era. What was particularly remarkable was the fact that the engine was extremely competitive in parameters such as power/weight ratio, complexity, bulk, altitude performance, flexibility and control, and ease of installation in addition to the unrivalled economy. Furthermore, it could burn a

wide range of fuels (not only accepted aircraft fuels). It was the common opinion of its time that this engine brought the aero engine overall life and reliability to a new level. The Napier Nomad, from a technical standpoint, was one of the most interesting aero engines ever designed.

The layout shown in Figure 3.2 was an improved version which was known as Nomad Ⅱ (E.145). Actually, even before the initial design of Nomad Ⅰ (E.125) was brought into developing, the design work of Nomad Ⅱ was carried out synchronously. In this newer version, an engine driving supercharger was added to the axial compressor as an extra stage to ensure the boosting pressure. The downstream centrifugal compressor and the intercooler were deleted, so that the complexity of the overall system was reduced. The power turbine driven by the exhaust gas then only provided additional power to the compressor, and fed any excess power to the main shaft using a hydraulic clutch. The deputy propeller which was previously driven by the power turbine was deleted as well. Besides, the entire part of the "afterburner" system together with its valves were cancelled. Consequently, the system was greatly simplified and turned out to be a compact combination of a mechanical supercharger and a turbo-compounding without any need for bypass. The system turned out to be a much smaller and considerably lighter arrangement in which a single engine driving a single propeller. The overall weight of the engine was about 1,000 lb (450 kg).

In 1953, a further developed (and final) version known as the Nomad Nm.7 was launched. It was announced that it could produce 3,500 shp (2,600 kW). By 1954, the enthusiasm for the Nomad was waning, and the work on the engine was completely ended in April 1955, after an expenditure of £5.1 million.

2.4.3 Mitsubishi 10 ZF

During the late 1950s, turbo-compounding technology eventually became obsolete in aircraft applications. However, it shortly found applications in boat and high load vehicle engines in 1950s and 1960s [88]. One of the examples during that era was the Mitsubishi 10 ZF which was a diesel engine first developed in 1968 for a military tank.

Mitsubishi 10 ZF was a V-type 10-cylinder direct injection air-cooled two-cycle compression ignition engine equipped with a uniflow scavenging system. The cooling air system of this

engine was made up of two sets of cooling fans which were mounted horizontally in the upper space between the two cylinder banks. It was also equipped with four oil-coolers which was made of aluminium tubes. They were attached to both sides of the engine block with two sets on each side. One of them was also used for providing transmission oil for the vehicle. Two exhaust turbochargers were located in the front of the engine block. They were connected to the engine crankshaft through a gear set and a torque-limited clutch. This arrangement deleted the positive displacement blowers which were the common choice for boosting conventional high speed two-cycle engines at its time and led to a much more compact structure of the boosting system.

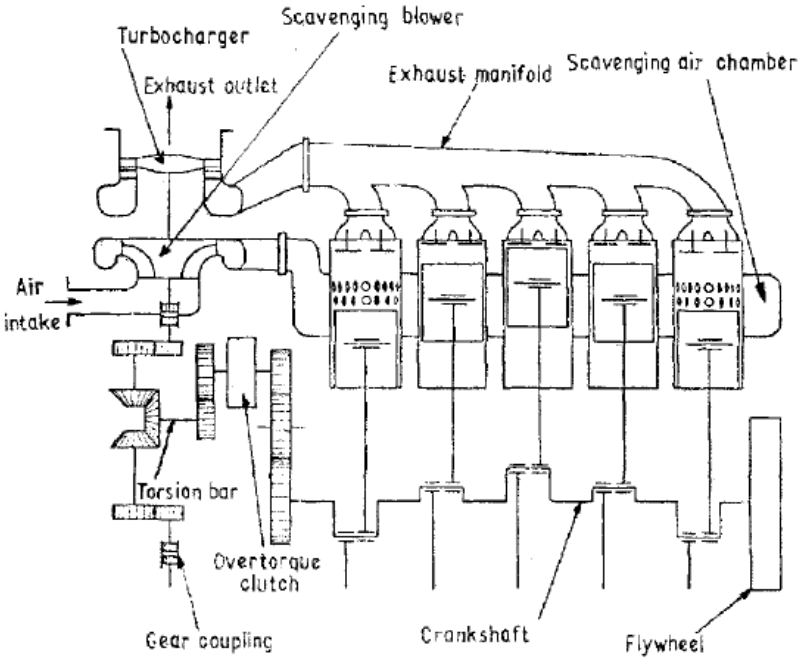

Figure 2.11. **Mitsubishi 10 ZF [139].**

Figure 2.11 illustrates the configuration of this system. The specifications of this engine was given in table 2.4. A number of uniquely designed components had been applied to this 10 ZF engine, including the uniflow system, to achieve a high scavenging efficiency. Besides, it was also featuring in great compactness and remarkable improvement in specific output. It was claimed that this engine was capable to produce a maximum gross output of 870 PS (858 hp) from 21.5 litre (131 in3) of cylinder displacement at the engine speed of 2200 rpm.

Table 2-4. Specifications of Mitsubishi 10 ZF.

Type	Two-cycle air-cooled turbocharged diesel engine
Cylinder number	10
Cylinder arrangement	90° V form
Bore	135 mm (5.32 in)
Stroke	150 mm (5.91 in)
Displacemen; volume	21 470 cm3 (131 in3)
Gross output	870 PS (858 hp) at 2200 rev/min
Mean effective pressure	8.29 kgf/cm2 (117.7 Ibf/in2)
Piston speed	11.0 m/s (2165.30 ftimin) at 2200 rev/min
Scavenging system	Uniflow with exhaust valves
Combustion system	Direct injection
Cooling fan	Two axial fans
Cooling power	I20 PS (118 hp)
Starting motor	25 PS (24.7 hp) 24 volt
Weight (dry)	2220 kg (4894 lb)
Overall dimensions : **Length** **Width, with cooling air duct** **without cooling air duct** **Height**	2220 kg (4894 lb) 1950 mm (76.8 in) 1800 mm (70.9 in) 1490 mm (58.7 in) 1095 mm (43.1 in)

Actually, because the turbo-compounding features to improve the fuel economy at high engine load, the most noticeable examples of turbo-compounding engines were still mostly found in maritime ships and air crafts that commonly tend to operate at constant high load for an extended periods of time [46]. With the modern technic level, maritime powertrains equipped with turbo-compounding can achieve an overall efficiencies greater than 50% [46]. During the next decade, between 1950s and 1960s, the interest in turbo-compounding began to spread to ground transportation [88]. But, because of the characteristic that it tends to improve fuel efficiency under high engine load, the most remarkable application of turbo-compounding engines were firstly found in train engines.

2.4.4 Differential compound engine

In the case of automotive engines, a traditional turbo-compounding usually adds a power turbine in series with the turbocharger turbine. The power turbine generates more work by harvesting the remaining energy from the exhaust gas downstream the original turbocharger

turbine. The power generated by the power turbine is then fed to the engine crankshaft in the form of mechanical work via a sophisticated transmission. It is different from a standard turbocharger as it does not have a compressor wheel to match with. Instead, the power turbine shaft is directly connected to the engine crankshaft via a gear set.

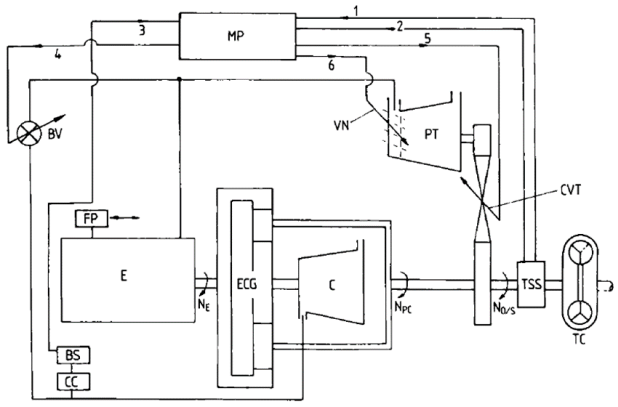

Figure 2.12. DCE layout: final version BV bypass valve; BS boost sensor; C compressor; CC charge cooler; E semi-adiabatic engine; ECG epicyclical gear train; FP fuel pump; PT power turbine; TC torque converter; VN variable turbine nozzles; TSS output torque and speed sensor; NE engine speed; No/s output shaft speed; Npc planet carrier speed; MP micropressor; Input signals: 1 torque transducer; 2 speed transducer; 3 boost transducer; Output signals: 4 bypass valve control; 5 CVT control; 6 nozzle control [66].

Figure 2.12 shows the layout of the differential compound engine which was firstly developed by Frank Wallace in 1973. This was a typical design for mechanical turbo-compounding. The inlet air was pressurised by the supercharger before it entered the cylinders. The exhaust from the engine was directed into the power turbine which was actually a variable geometric turbine (VGT). Mechanical power was then produced by the turbine and fed to the drive shaft via a continuously variable transmission (CVT) coupled with a torque converter. At the same time, the power turbine was also connected to the planet carrier of an epicyclical gear to provide power for the compressor which was connected to the centre gear. On the other side of the epicyclical gear, the engine crankshaft drove the outer ring. This boost pressure and the output shaft speed were monitored by a number of sensors. The collected data was feed into

a microprocessor. Optimum signal was then generated to control the VGT nozzles position, the CVT gear ratio and the output shaft speed.

According to the test results, the differential compound engine was able to achieve an overall thermal efficiency of about 36% under high load condition. A particularly good fuel economy was also realized with the extra turbine power feed to the engine crankshaft. However, under low load condition, this improvement in fuel consumption was seriously deteriorated due to the considerably lower efficiency of the Lysholm-type compressor. Besides, the excess air kept circulating in the bypass loop at low condition operation, which was simply a waste of the compressor power. Therefore, this design was given a four-star rating by the author comparing with the turbocharged engine who earned five stars in fuel economy. With respect to the torque output and transient performance, the deferential compound engine showed a particularly favourable character that none of the other engine types (turbocharged engine, gas turbine engine, two-stage Wankel engine and Stirling engine) was considered comparable. The detailed specification of the major components of this plant can be found in [48, 60, 61, 91]. During the 1980s, the attempts of applying turbo-compounding technology in heavy duty vehicles began to interest the automobile engine manufacturers [88]. One of the first turbo-compounding truck engines was developed by Cummins in 1981, which was known as the Cummins NH. It was typically a mechanical turbo-compounding equipped with a radial type power turbine. A fluid coupling was attached to the gear set connecting power turbine shaft and engine crankshaft to isolate the high speed gearing from the torsional vibrations from crankshaft. During the long distance (50000 miles) highway driving test in the United States, an average reduction of 4.7% in fuel consumption was achieved. Throughout the 1970s and 1980s, turbo-compounding engines were investigated in a number of military research programs such as Cummins V903 [138] which was firstly introduced in 1983 [88, 96, 104].

In 1986, Caterpilar equipped turbo-compounding to a 16.4 l heavy-duty engine. In this system, an axial power turbine was located after the radial turbocharger turbine. Under full load condition, fuel consumption could be reduced by up to 6% as claimed due to the high efficiency (up to 85%), low inertia, and low duct losses (no additional turns) of the axial turbine. However, the massive production of this system was then delayed by the difficulties

in designing an efficient and reliable high-speed gear set to feed the recovered energy (in the form of mechanical work) to the powertrain [89].

In 1991, the first commercialized turbo-compounding system was developed by Scania for their 6-cylinder 11 litre diesel engine which was known as the DTC 1101. It was claimed that fuel economy could be improved by 1-3% in real world driving test with this system. But, it was argued lately that this improvement in fuel efficiency was only achievable at high loads operation [46].

In 2004, Bowman Power Group [90] developed a turbo generator system wherein a high speed permanent magnet electric alternator was coupled to the power turbine downstream of the original turbocharger turbine. This system was of the feature of keeping the operating points within the region of high efficiency on the turbine map across a wide working condition, and thereby to increase the overall fuel economy further.

Other attempts for applying turbo-compounding include the 12 litre six-cylinder mechanical turbo-compounding engine from Scania and Cummins [89], the 21st century truck engine developed by Caterpillar in 1998 [138], the Ceramic IDI (2002) by Isuzu, D12-500TC (2002) from Volvo, and the Detroit diesel, which was known as the DD15, developed by Daimler in 2008 [89].

However, apart from the introduced practice in heavy duty trucks by Scania in 1991, the subsequent implementations of the turbo-compounding by other manufacturers were sporadic. It is partly due to the common sense that rising BMEP levels and reducing EGR rates in heavy duty engines could increase the suitability of turbo-compounding. Besides, the mainstream of the development in internal combustion engines now is downsizing and thus increasing BMEP which would drive the need for smaller power turbines. It increases the back pressure to the engine stroke as well as the challenge of matching the high turbine speeds to the engine.

However, the current study in [2] found that turbo-compounding could possibly recover 11.4% more exhaust energy on average and produce 3.7kW of extra power. If the system is mechanically coupled to the engine, it could increase the average engine power by up to 1.2% and improve the average BSFC by 1.9%, while in in an electrical turbo-compounding system,

a reduction of 8-9% in overall BSFC is possible for a turbocharger with relatively high efficiency. However, it has to face up to the issue that under low engine loading, there might be very little or even negative gain from the turbo-compounding system. Under partial load condition, the power turbine cannot work effectively due to the insufficient exhaust gas flow. Besides, it imposes higher back pressure to the exhaust and causes extra resistance to the engine breathing. In summary, as a typical energy saving system, the further implementation of turbo-compounding strongly depends on the future fuel costs and further development of the flow components, especially the turbine.

The history of turbo-compounding was summarised in table 2.5.

Table 2-5. History of turbo-compounding

1948: **Curtiss-Wright compound aircraft engine**	The first order for turbo compounding was issued by the US Navy to Wright Aircraft Engine Company. The first aircraft engine to be tested with a power-recovery turbine was the Rolls-Royce Crecy.
1950s: **Napier diesel compound aircraft engine**	Innovations in the aerospace industry lead to turbo compounding being adopted in aircraft engines by Lockheed, Canadair, Martin and Fairchild plane makers.
1968: **Mitsubishi 10 ZF**	Mitsubishi 10 ZF emerged as an early attempt to apply turbo-compounding for non-aero purpose.
1973: **Differential compound engine**	Differential compound engine was the first mechanical turbo-compounding engine designed for automotive
2004: **Electric Turbo Compounding (ETC) systems**	Bowman Power Group begins designing Electric Turbo Compounding (ETC) systems for the heavy truck industry with USDOE Funding.
2014: **1.6 litre turbocharged V6**	Formula 1 (F1) adopts ETC technology as part of new electric turbocharged engines; a new formula that uses turbo-compounding.

2.5 Exhaust energy availability

It is the belief nowadays that a global thermal efficiency higher than 42% is really difficult to achieve for an internal combustion engine. Typically, the efficiency of a spark ignition engine is within the range between 15 to 32% [140] because a big part of fuel energy is simply lost

through the exhaust to the environment. Generally, in a four-stroke engine, about one third of the combustion energy was wasted along with the exhaust. From the study in [3] the exhaust energy is proportional with the exhaust temperature. For an exhaust temperature of 600 °C, it may take up more than 30% of the combustion energy from the fuel, which is nearly the same as the amount of brake work in modern gasoline vehicles [3, 9, 65, 74, 83, 84, 92]. While in a two stroke engine, the proportion is about one fourth [93].

Generally, the exhaust energy availability greatly depends on engine type. Specifically, the maximum exhaust gas temperature of the gasoline engine is higher than that of the diesel engines. Besides, other factors such as engine speed, torque output and the load condition also have influence on the magnitude of waste heat. The exhaust temperature of different vehicle types are illustrated in table 2.6.

Table 2-6. Exhaust temperature of different vehicle types.

Vehicle type	**Exhaust temperature**
Light duty passenger car exhaust temperature	500 to 900 °C (with most may fall in the range of 600-700 °C)
Heavy duty vehicles exhaust temperature	400 to 650 °C
Naturally aspirated gasoline engine	450 to 800 °C
Two stroke engine exhaust temperature	250 to 500 °C

Typically, as the table shows, the exhaust temperature of two stroke engines is lower than that of the four stroke engines, even though it have high exhaust mass flow. It implies a significant potential for applying waste energy recovery system in four stroke engine. According to the second law analysis in [92] [94], the exhaust energy availability is high when the engine is operated close to its peak efficiency point, however, at the low load condition which covers the largest range of the driving cycle, the exhaust exergy is low. It has been identified in [140] that depending on the operating condition the exhaust energy in a SI engine varies significantly from 4.6 kW to 120 kW. When considering the efficiency of the waste energy recovery system, the most obtainable energy under ideal conditions roughly ranges from 1.7 to 45 kW.

As a popular approach to recover exhaust energy, the ideal P-V cycle of a turbo-compounding engine is shown in figure 2.13.

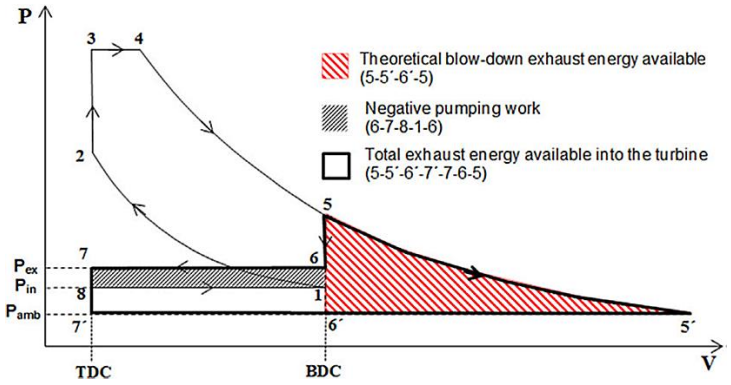

Figure 2.13. The ideal cycle of turbo-compounding engine and the energy availability into the turbine [136].

When the piston reaches the BDC at the end of power stroke, the exhaust valve opens to allow the piston pushing burnt gas to the power turbine which further expands the high temperature gas to the ambient pressure. During this process the energy available in the exhaust gas, which is known as the blow down energy, is converted into mechanical work by the power turbine. The maximum energy availability is as the triangular area (in red) shows. It should be noted that the energy losses from the blow down pulse will be reduced if the exhaust manifold pressure increases. Consequently, the energy recovery in turbo-compounding will increase. However, higher exhaust manifold pressure directly results in a negative pressure gradient between the intake and exhaust valves, which lead to the additional pumping working as shown in the grey rectangular area. Therefore, it is now the main topic to improve power output from turbo-compounding while limit the increasing in back pressure. Besides, the extended exhausting stroke may lead to extra losses of friction. So, it might also be an effective way to increase the net gain in fuel efficiency by shortening the stroke till intake valves open.

2.6 Typical turbo-compounding configuration

There are different ways of categorizing turbo-compounding engine. Generally, by considering whether the recovered energy is converted into mechanical or electric power, turbo-compounding engines can be divided into mechanical turbo-compounding and electrical

turbo-compounding.

In the last century, the mechanical turbo-compounding was considered as the standard technology worth further investigation, while the electrical turbo-compounding has not been widely investigated to the same extent despite of its superiority in flexibility of layout according to some vehicle manufacturer's statement. However, with the development in turbo-generator technology nowadays, the electrical turbo-compounding has also been increasingly studied considering its advantages in flexible arrangement and control strategies. The differential compound engine, as introduced in the History section, is a typical example of mechanical turbo-compounding. The specifications of this system, including the integrated engine transmission, was introduced in [60] and [61].

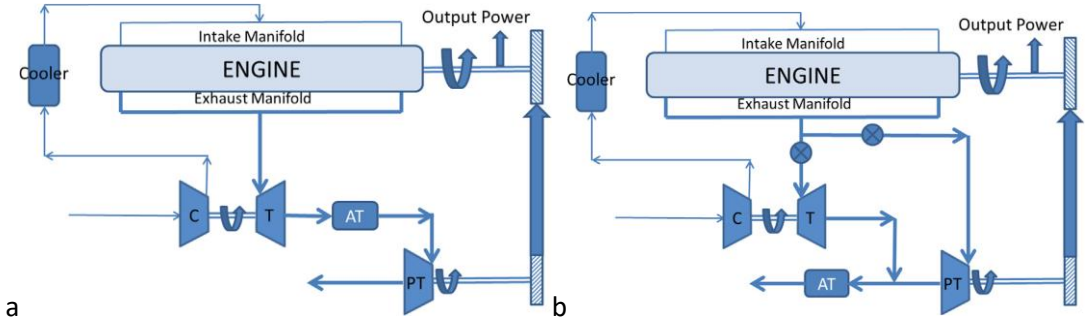

Figure 2.14. Mechanical turbo-compounding, series configuration. a, [141] and parallel configuration b, [148], exhaust after-treatment before power turbine; (T: turbine, C: compressor, PT: power turbine, AT: exhaust after-treatment).

In figure 2.14, two kind of mechanical turbo-compounding systems are illustrated. The layout in (a) is a conventional low pressure turbo-compounding in which a power turbine is attached after the turbocharger turbine. In this arrangement, the power turbine is exposed to the exhaust flow downstream the main turbine, and therefore operates with low pressure ratio. In figure (b), the power turbine is located in parallel with the main turbine. The inlet port of the power turbine is then directly linked to the exhaust manifold, which directs the exhaust gas with high temperature into power turbine. Because all of the exhaust energy extraction is occurring at exhaust manifold temperature (as opposed to the lower temperature that the power turbine in a serial turbo-compounding arrangement works at), the same amount of work can be extracted with lower overall expansion ratio (assuming same turbine efficiencies)

and hence lower backpressure. From this perspective, the parallel, also known as HP, configuration is better for turbo-compounding arrangement. Youssef Ismail et al have conducted a simulation work on the parallel turbo-compounding architecture and found that a power turbine that is well adapted to a series turbo-compounding is not necessarily suitable for a parallel one, since the turbines with higher pressure ratio and lower flow rates is able to provides better performance. By comparing with the series turbo-compounding they found that the parallel turbo-compounding has the advantage of producing lower harmful backpressure, however, the other shows a higher potential of energy recovery. This is mainly due to the reduction of the exhaust mass flow into the power turbine, which results in a lower energy availability and restricted turbine efficiency [120]. In his research, the power turbine is simulated by a converging nozzle. Only the diameter ratio of the nozzle is optimized, therefore, the mass flow rate splitting between the turbocharger turbine and the nozzle depends on the inlets geometry. Some other researchers, however, paid attention to the effectiveness that exhaust valve timing has on the turbo-compounding engine. By actively changing the exhaust valve timing, the exhaust flow is divided into blowdown and scavenging between two different exhaust manifolds. Consequently, the exhaust flow into the power turbine is able to be adjusted to minimize the losses caused by back pressure. These characteristics of this approach will be studied in the later section. For both system shown in figure 2.14, the power turbine is connected to the engine crankshaft mechanically, usually through an epicyclical gear set and/or a torque convertor.

By directly coupling a generator to the power turbine wheel, a turbo-generator is created. It is the key component of the electrical turbo-compounding engine [95-103], as shown in figure 2.15. In the electrical version, when the power produced by the turbine exceeds the power demand of the compressor, the surplus power will be converted into electricity by the generator and be stored in a battery or power bank. In other cases, when the power requirement of the compressor cannot be met, the electric motor will consume energy from the electricity storage to drive the compressor. The performance predictions indicated that the fuel economy can be improved by more than 2.5% over a wide range of working condition when compared with a mechanical turbo-compounding engine with the same displacement.

The most significant reduction in fuel consumption of 10.3% was achieved under full load condition.

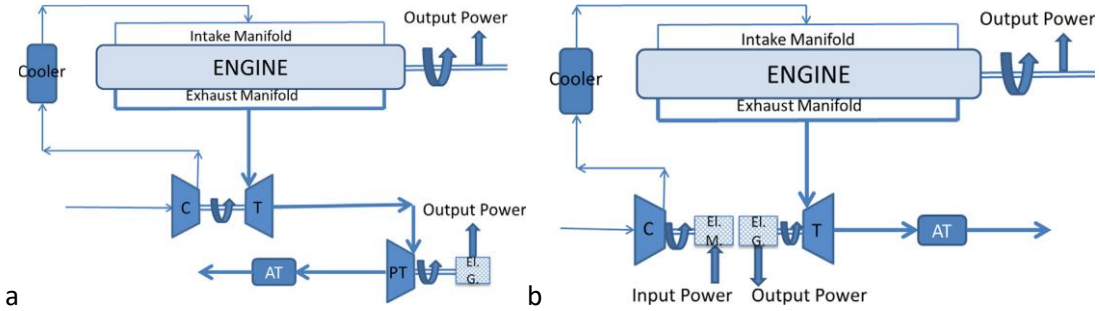

Figure 2.15. Electric turbo-compounding, LP configuration. A, [95, 105, 138], HP configuration. B, [105, 121, 122] (T: turbine, C: compressor, AT: exhaust after-treatment, El.G.: electric generator, El.M.:electric motor).

The layout of electrical turbo-compounding engine is shown in figure 2.15. Many studies has be carried out to evaluate the performance of this arrangement in different kind of internal combustion engines. Thompson et al has evaluated the performance of turbo-generator in a biogas engine through both actual engine tests and computer simulation [96]. The schematic of his study is shown in figure (a), wherein a generator was coupled to the low pressure power shaft which is located after the turbocharger turbine. The power turbine speed can be adjusted in this design to achieve the optimum efficiency. It was claimed that the fuel consumption could be reduced by 7.2% when compared to its mechanically compounding counterpart. The overall efficiency was improved to 45.3%. On the other hand, in spite of the high potential of improving the thermal efficiency, electrical turbo-compounding engines are still facing the challenges of developing suitable generator that is highly compact and able to operate at low speed. The ability to effectively reject the heat accumulated in the package is also required. In another popular design schemes, the high pressure turbine is separated from the compressor, as shown in figure (b). In other words, the turbocharger is removed. The power turbine is directly connected to the exhaust manifold. In this layout, exhaust gas with higher temperature and energy availability is expanded over the power turbine, so that higher mechanical power can be generated. The rotational power is transmitted to a generator mounted directly to its shaft. Similarly, the compressor is driven by an electric motor. Algrain M et al has included the design and analysis of the high pressure electrical turbo-compounding

serving a diesel engine in [107, 109]. Besides, the compressor speed in an electrical turbo-compounding engine is also fully adjustable, which allows a high flexibility of the engine power output independent of engine speed. Bo Hu et al has compared the performance of this design with a conventional turbocharged engine in a software environment. According to the results, under full load condition, the combination of a motor driven supercharger and an electrical turbo-compounding was able to increase the brake torque by 24% at low engine speed for a 2.0 litre gasoline engine, while the most significant improvement in fuel consumption was 8% being achieved at top engine speed.

2.7 The sensitivity of turbo-compounding engine to different variables

As mentioned above, the performance of turbo-compounding is highly affected by the engine types with different characteristics in gas exchange process and combustion phase. For example, an engine with longer expansion stroke could suffer from significantly higher friction loss, but it would increase the theoretical blow-down exhaust energy availability. Furthermore, the efficiency of power turbine and compressor are also extremely important, since they directly determine the waste heat harvesting and PMEP. Besides, other parameters including the compression ratio, ignition timing and valve timing are also detrimental factors for the load sharing among the reciprocating engine, turbocharger turbine and power turbine. And also, the combustion phase and essentially the knock onset will be changed accordingly. In terms of diesel engine, increasing the back-pressure will not influent the conventional diesel combustion and emission [150]. But, it will influent the low temperature combustion with a high EGR rate. Therefore, turbo-compounding is regarded beneficial for both high and low temperature combustion in a CI engine [9, 151]. In this section, the sensitivities of these parameters to the turbo-compounding engine performance will be reviewed.

2.7.1 Compressor pressure ratio

Mitsunori Ishii has performed a study on the optimization of a high pressure turbo-compounding diesel engine. It was stated that under full load condition a high compressor

pressure ratio is beneficial for improving the power output for both the engine and power turbine. Despite the increased power consumption by the compressor, the overall power output of the turbo-compounding engine is enhanced due to the increasing in air flow rate and exhaust energy. The results also indicated that increasing the compressor pressure ratio was able to shift the load allocation from power turbine to the engine, since a larger part of exhaust energy was consumed by turbocharger rather than the power turbine. It means that the rising in crankshaft output outweighs the sacrifice in power turbine output under full load condition. On the other hand, higher compressor pressure ratio unavoidably resulted in an excessive maximum pressure and temperature in the cylinders as well as the exhaust manifold. This means that the increases in the compressor pressure ratio should be confined from exceeding the upper limit of the mechanical strength and heat resistance of the engine. Under part load condition, it was concluded that there was an optimum value for the compressor pressure ratio, which is 1.5 for the specific diesel engine model in Ishii's research. As the boosting ratio increasing, the increasing rate of the driven power consumed by the compressor is larger than the growth rate of the crankshaft output since the operating of the turbocharger compressor deviated from the high efficiency region with low air flow rate. It means that the power consumption of the compressor could be more conspicuous comparing with the improvement of engine power under low load condition. This can also explain the phenomenon that the increasing rate of crankshaft output decreased as the inlet air pressure increasing. What is also notable is that for different compression ratio, there was an optimum expansion ratio for the power turbine to maximize the overall output and an optimum combination of compression ratio and the compressor pressure ratio that realizes the best fuel economy. More details will be given in the later sections introducing the impacts that the compression ratio and the expansion ratio have on the engine performance [121, 122].

2.7.2 Intake and exhaust valve timing

Variable valve timing (VVT) is a frequently studied area. A number of research showed that the pumping losses and the exhaust pollutions of an internal combustion engine can be significantly reduced with a properly designed variable valve actuation (VVA) and optimized control strategy. At the same time, the volumetric efficiency of the VVT engine can be

maximized. In a turbo-compounding engine, the adjusting in valve timing could additionally sweep the distribution of brake power between reciprocating engine and power turbine.

In an engine equipped with VVT, the intake and exhaust philosophies include:

1. Late intake valve closing (LIVC).
2. Early intake valve closing (EIVC).
3. Late intake valve opening (LIVO).
4. Early intake valve opening (EIVO).
5. Early exhaust valve opening (EEVO).
6. Late exhaust valve opening (LEVO).
7. Early exhaust valve closing (EEVC).
8. Late exhaust valve closing (LEVC).

As early as 1970s, Tuttle has conducted a research to couple a LIVC system to a single-cylinder SI engine [123]. According to the experiment results, the indicated thermal efficiency of LIVC engine is lower under part load condition comparing with the conventional engine with fixed compression ratio. It was believed due to the lower effective compression ratio since a part of the intake air was pushed back to the intake manifold. And also, LIVC resulted in a longer combustion duration which also contributed to the deterioration in combustion phase in the author's opinion. However, in terms of the brake thermal efficiency, the net specific fuel consumption was reduced by 6.5% because of the extreme reduction (about 40%) in pumping losses. Besides, the NOx emissions was reduced by 24% in the test.

Under full load condition, it was found that the penalty of the volumetric efficiency caused by LIVC was highly diminished. It was because of the higher momentum of the intake air flow at this operation. So that, fresh air was able to continuously fill up the cylinders even after the piston passes the bottom dead centre (BDC) [124].

Rabia and Kora [125] investigated the effects that the LIVC has on knock onset. It was found that in a LIVC engine, the risk of knock was increased at lower engine speed. According to their analysis, the reduced volumetric efficiency at lower engine speed leading to a lower air density and richer fuel-air mixture, which limited the flame speed, and thus increased the danger of knocking.

Since the intake valve closing is one of the most sensitive parameter influencing the pumping features of the engine, to fully exploit its advantage of achieving high volumetric efficiency at high engine speed and avoid the weakness of causing penalty in intake air charging and high knocking risk (especially at low engine speed), researchers [126, 127, 128] have suggested that variable valve actuation (VVA) and variable compression ratio (VCR) should be taken

advantage of.

From the analysis in [129], the exhaust timing should be carefully optimized as well. An improper exhaust valve phase, either an early or late timing, may have an unfavourable influence to the gas exchange process of the engine. Besides, considering the synthetic action, a shorter overlap between the exhaust and intake valve (LIVO and EEVC) also increases the pumping losses. On the contrary, a longer overlap (EIVO and LEVC) is beneficial for reducing the pumping losses, however, it causes penalty to the effective compression ratio and a loss in fresh charge. Except for acting as a dominating parameter for reducing the pumping losses, the exhaust valve timing also plays an essential role in promoting the internal EGR and alternatively balancing the power output between the engine and the power turbine. This is mainly due to its capability to change the effective expansion ratio of the engine and thus the exhaust energy availability to the power turbine [96, 103].

Specifically, in the case of EEVC with fixed lift duration, pumping losses is decreased from the perspective of exhaust stroke, which diminishes the expelling resistance. The indicated power generation from the engine decreases in this case due to the lower effective expansion ratio. Whereas higher energy is available from the exhaust flows into the power turbine and be converted into useful work. On the contrary, LEVC directly leads to a longer period of overlap. This results in back flowing of the burnt gases into the intake manifold during charging stroke and reduces the density of fresh air. For a conventional turbocharged engine or a naturally aspirate engine, LEVC is also able to reduce the pumping losses during the intake stroke as the charge pressure of the fresh air is higher than the exhaust gases [129], moreover, it is capable to diminish the compression of the burnt gas in cylinders at the end of the exhaust stroke. But, this is achieved at the cost of reducing fuel energy because the LEVC may lead to a sweep-over effect which expel the fresh air-fuel mixture to the exhaust manifold without burning. Therefore, Thompson et al [103] suggested that exhaust valve closure should be carefully optimized to achieve the best trade-off between reducing pumping work and fuel losses. On the other hand, EEVO is an effective way to prevent the loss of fresh air. By applying turbo-compounding, the deterioration of engine power (due to the reduction of effective expansion ratio, as introduced above) for this approach can be compensated by the power turbine at the

exhaust end.

Other innovative approaches include combining turbo-compounding engine with divided exhaust period (DEP). From previous studies, this concept reduced the fuel consumption and introduced a compromise between the turbine energy recovery and the pumping work in the engine optimization. It was concluded that the turbo-compounding DEP engine could improve BSFC by 0.5% to 3% at low engine speeds with the same cylinder head geometry, turbine efficiency and boost pressure of the original turbocharged engine being applied. The result also showed that increasing the size of the exhaust valves could improve the BSFC by about 0.5% at low engine speed. Besides, it also indicated that the changes in the diameters of the blowdown and scavenging ports had insignificant effects on BSFC. But the engine was more sensitive to the diameters of the exhaust valves at higher engine speeds.

2.7.3 Ignition timing

Many research has come to the conclusion that retarding the ignition timing is an effective way to reduce NOx emission for CI engines and prevent the occurring of knocking for SI engines [130]. However, for a conventional turbocharged engine, retarding ignition timing results in a reduction of power output of the engine because of the uncomplete combustion soon after the piston reaches TDC and thus lower maximum cylinder pressure. Besides, as mentioned above, increasing the boost pressure is helpful for improving the power output from engine crankshaft, but it also increases the risk of knocking onset. For the turbo-compounding engine, however, the boost pressure can be increased to promote the engine power output without warrying about knocking, since the ignition can be delayed accordingly to avoid the shock in combustion and reduce NOx emissions. This setting lead to a higher energy availability in exhaust gas. And then the remaining energy in the burnt gas will be recovered by the power turbine. So that the power losses resulting from retarding ignition can be compensated. Consequently, it is safe to say that there is an optimum ignition timing, which is usually retarded from the original setting, for the turbo-compounding engine to balance the trade-off between the engine power and turbine power. Shudo and Toshinaga has evaluated the effect of a large retardation of spark-ignition timing on the exhaust-gas thermal energy at steady operating conditions [131]. The results showed that a combination

of spark retardation and higher charging pressure could greatly increase exhaust energy with minimum deteriorations in engine efficiency. It was also effective in reducing pumping losses and in-cylinder heat transfer to the combustion chamber wall at high engine loads. Based on their research, it was also proposed that by combining spark timing retardation and large throttle percentage, the exhaust pressure and temperature in spark-ignition engines at idling and vehicle deceleration conditions could be significantly increased because of the higher volumetric efficiency, which is helpful for improving the operation of turbo-compounding under extremely low load condition.

Besides, early injection in diesel engine causes the burning gas working against the piston movement during the compression stroke while late injection did not make full use of the expansion ratio during the expansion stroke [2]. Therefore, it comes to the similar conclusion that there should be an optimum start time for combustion regarding the trade-off between the net engine power and the turbine power output.

2.7.4 Compression ratio

Gumbleton et al has conducted a study on the constraint of compression ratio setting regarding both the power output and emission [132]. The results proved that fuel economy of internal combustion engine could be improved by increasing compression ratio. However, the promotion in compression ratio resulted in higher cylinder pressure and pre-ignition temperature which require for higher octane to avoid knocking. It may leads to substantial energy losses for the petroleum industry to produce unleaded fuels with higher octane level. The overall effects turned out to be a non-significant fuel economy improvement could be achieved through promoting the fuel octane level to allow for the use of higher compression ratio.

Smith [128] and Ayala et al [129] has investigated the effects of compression ratio on the SI engine specifically. The results showed that the thermal efficiency of a SI engine with constant displacement increased with a decreasing rate as the compression ratio increasing. It was also found that the engine was more susceptible to the change in compression ratio when it was operated under low and medium load condition independent of fuel differences. Besides, Ayala also indicated the effect of increasing compression ratio on extending the air-fuel ratio

for peak thermal efficiency. More details will be given in the following section about lambda. Fanhua Ma et al has studied the effect of compression ratio on the performance of an HCNG (hydrogen enriched compressed natural gas) engine [135]. The results showed that the combustion speed and the heat release rate were significantly boosted by increasing the compression ratio. The early flame development and the combustion period were shorten as well. Consequently, the thermal efficiency as well as the brake power output were improved. But the improvement was weaken as the compression ratio rose, which indicated that an optimum was existing for the studied engine type.

In the works of Ishii [121, 122], study was conducted on the influence of compression ratio on the performance of a high pressure turbo-compounding light duty diesel engine. A conclusion was reached that an optimum combination was existing to minimise the brake specific fuel consumption (BSFC), even though the combination of a higher compressor pressure ratio and lower compression ratio was considered more favourable from the brake power perspective. It was suggested that the optimum engine compression ratio should be 19-20 with a turbine cross section ratio of 0.4 and a compressor pressure ratio of 2.2 for a single stage turbo-compounding operated under full load condition. Besides, for different compression ratio, the optimum turbine expansion ratio was varying to maximize the engine power output and thermal efficiency. This part will also be covered in the Power Turbine section. The general idea was that a higher compression ratio was beneficial for increasing the engine power output while reduce the exhaust energy availability for power turbine, and vice versa. In terms of better fuel economy, it also suggested the necessity to explore the optimum trade-off between reciprocating engine power outputs and exhaust energy availability through adjusting compression ratio.

2.7.5 Air-fuel ratio and EGR

Aghaali and Angstrom [136] have summarized the effects of air-fuel ratio on turbo-compounding engine performance based on their investigation on heavy duty internal combustion engines [87, 137]. It was found that pumping work and burn rate were two the most significant factor affecting the overall performance of turbo-compounding engine with a lean air-fuel equivalence ratio. A higher boost pressure was favourable for improving the

brake power in this case. For a richer air-fuel ratio, however, there was a need to reduce the boost pressure and thus the volumetric efficiency to avoid knock. The overall specific fuel consumption of the turbo-compounding engine is not greatly sensitive to the air-fuel ratio. However, it was found that the optimum air fuel ratio of a turbo-compounding engine is slightly lower than that of the turbocharged engine [87]. In fact, the exhaust back-pressure was optimized before the effectiveness of air-fuel ratio on turbo-compounding engine being investigated in the research. This suggested that the key parameter influencing the turbo-compounding engine believed to be back-pressure rather than the air-fuel ratio. Nevertheless, since it is impossible to vary air-fuel ratio in an engine without changing other parameters, a global optimization of all the relevant specifications are still in need.

From the study of Vuk et al [87, 138] a lower air-fuel ratio that was closer to stoichiometric equivalence ratio was favourable for improving the efficiency of a turbo-compounding engine due to the desired higher exhaust gas temperature and pressure. But, from Aghaali's study on a single stage turbo-compounding engine, the overall BSFC improvement was not significantly sensitive to the changing in lambda. Less than 1% fuel saving could be achieved from optimizing the equivalent ratio because of the trade-off among available waste heat and the lower specific heat ratio and higher heat transfer rate from the cylinder contents to the structure which are all detrimental to the overall efficiency. Besides, it should also be noted that the air-fuel ratio cannot be varied without affecting the optimum setting of other parameters. According to the conclusion in [121, 133] the optimum air-fuel ratio for highest thermal efficiency tends to increase when compression ratio is extended. The optimum percentage of turbine power in brake power will change accordingly. In the last, Aghaali also gave an ideal air-fuel ratio for the high pressure electric turbo-compounding diesel engine in his research to be 1.28.

When compare with a turbocharged engine, a turbo-compounding engine has higher EGR driving capability due to the higher exhaust pressure. Kruiswyk and Hountalas, has studied the effect of EGR on a heavy duty turbo-compounding diesel engine [9, 141] and indicated the benefits of EGR in reducing the NOx emission and pumping losses in turbo-compounding engine. However, Kruiswyk also pointed out the adverse effects caused by EGR, including

reducing the available energy into the power turbine and reducing the oxygen concentration into the combustion chamber. The conclusion from Kruiswyk was that the elimination of EGR could lead to an improvement of specific fuel consumption by up to 1.5%, but this improving rate decreased dramatically under part load condition.

2.7.6 Power turbine (expansion ratio, size and speed)

As mentioned above, in a turbo-compounding engine, the optimum expansion ratio of the power turbine increased with the growth in compressor pressure ratio. However, Ishii's research came to the conclusion that the optimum cross section ratio (the turbine inlet area divided by exhaust port area) remained approximately constant when he tried to optimize the performance of a high pressure diesel turbo-compounding engine [121]. Cross section ratio was one of the most important parameter determining the load allocation between power turbine and engine. Higher expansion ratio was usually correlated to a power turbine with a smaller cross section ratio. The turbine output would be increased accordingly in this situation. On the other hand, the reduction in cross section ratio could result in a sharp increasing in manifold pressure which might result in losses of crankshaft output. In other words, nonsignificant increasing in brake power output could be expected from increasing this parameter simply. It was stated by Ishii that the optimum cross section ratio for the power turbine for maximum brake power output were 0.1 and 0.4 for the partial and full load condition respectively no matter how much the boosting pressure was. It was also indicated that if the cross section was reduced further to about 0.1 under full load condition, power turbine would produce more power than the engine. The turbo-compounding engine system as a whole then became more dependent on the performance of the power turbine output. At this point, the overall thermal efficiency would be improved again. However, the temperature at the turbine inlet port would increase too much, which makes the operation much more difficult due to heat resistance and durability problems. Therefore, the mechanical strength of the turbomachinery must be taken into consideration when trying to improve the turbine output.

Thompson et al has investigated the character of a low pressure turbo-generator engine based on a validated 1 dimensional model [96]. From their simulating results, the power output from

the turbo-generator fell as the power turbine size being increased. This was mainly due to the reduction in pressure ratio and the temperature difference across it. However, the expansion ratio across the turbocharger turbine increased at the same time which enable the compressor to increase the air boosting for the engine. It was claimed that the increased mass flow rate was sufficient to offset the degradation in energy recovering of the power turbine. Brake power output from the engine crankshaft increased due to the higher volumetric efficiency. But, the authors also mentioned that the increasing in crankshaft power was not linear with the increasing in power turbine size. When the power turbine became too big, the rising tendency in brake power would be reversed. Therefore, it was believed that an optimum power turbine size was existing to enables the whole system to achieve a maximum power output. Moreover, when the turbocharger turbine size was increased, less power could be delivered to the compressor, which resulted in a lower mass flow rate. In this case, the power turbine would generate less power as well due to the reduction in available energy from exhaust gas. However, the engine power and the total power might be maximised because of the favourable trade-off between back pressure and boosting.

The efficiency of a conventional radial turbine reaches the peak with a velocity ratio around 0.7 [142, 143]. Weilin Zhuge et al [144] concluded that the efficiency of the power turbine became very low at low expansion ratio and high speed operating conditions. When the engine was operated under low load condition, the power turbine speed should be decreased accordingly, so that most of the operating points of the power turbine could be moved into the highest efficiency region. It was also found from their research that the engine efficiency at high load operation could be improved by adjusting the nozzle opening, but no appreciate improving was achieved under low load condition because of the flow losses across the nozzle. The efficiency of the variable nozzle turbine (VNT) turned out to be lower than the efficiency of the fix geometry turbine (FGT). Since the conventional mechanical turbo-compounding engine has the drawback that the power turbine is operated at a speed proportional to the engine speed due to the fixed transmission ratio, the power turbine unavoidably suffers from the deterioration in efficiency under low load condition. For this problem, Kruiswyk gave the solution to replace the gear connection between power turbine and engine shaft with a CVT

for, the BSFC of the turbo-compounding engine could be improved by 1-3% and 0-1% under low and full load condition respectively.

Furthermore, a research has been carried out by Rongchao Zhao et al to investigate the influence of the turbine geometry on the engine performance [144]. It was analysed that increasing the back blade angle or decreasing the blade height and blade mid-span radius was helpful to improve the power turbine expansion ratio. In addition, it would lead to a reduction in the expansion ratio of the turbocharger turbine, which caused lower intake air mass flow rate and higher exhaust temperature. The overall results turned out to be a larger proportion in load allocation for the power turbine.

A novel arrangement that combining turbo-compounding with a CVT supercharged 2.0 litre gasoline engine were examined by comparing its performance data with a conventional turbocharged engine of the same displacement and compressor characteristics. The simulation results showed that the CVT supercharger helped to increase the brake torque by up to 24% at 1500 revs/min. In the exhaust end, the turbo-compounding increased the brake torque evenly by 7% from 3000 revs/min and above. The BSFC was reduced by up to 8% at top engine speed. But the improvement descends as the engine speed slowing down and become vanished at 2000 revs/min because of the weakened power turbine function and the parasitic load imposed by the CVT supercharger. At low load condition, the turbine speed should be reduced (as the mass flow rate is much smaller) to move the operating point towards the high efficiency region of the performance map. This improvement in the turbine efficiency will lead to a further improvement in fuel economy [120, 145, 146]. By varying the power turbine speed in a LP turbo-compounding engine with a turbo-generator, a more constant boost pressure can be maintained, and the response time can be improved.

2.7.7 Power turbine type and location

According to the study in [108], an axial LP turbine stage or a nozzled radial turbine with divided housing are the feasible turbine options for LP turbo-compounding. The radial turbines that commonly used in turbochargers typically have their peak efficiency at a U/C at about 0.7. If the turbine peak efficiency point could be shifted to the lower U/C range, an improvement in exhaust energy utilization and engine thermal efficiency would be realized. A

mixed flow turbine with forward blades was introduced in [154] and was claimed capable to move the operating point of the maximum efficiency to lower U/C. On the other hand, according to the studies in [13] and [108], radial turbines or mixed-flow nozzled turbines with divided wall can also be considered as a proper turbine option for HP turbo-compounding.

It was found that the exhaust temperature after power turbine is below the light-off temperature for a light duty diesel engine under low load condition. Therefore, it seems that the power turbine should be bypassed or the exhaust after-treatment system should be placed upstream of the WER system [152]. In a diesel engine, placing DPF (diesel particulate filter) upstream of a WER system may also reduce the heat exchange fouling and alleviate some of the fuel penalty by recovering some of the energy released by exothermal reactions during catalyst regeneration events. Mamat et al concluded that placing the after-treatment system upstream of the power turbine provides the best compromise in terms of fuel consumption and engine performance [153]. About 1% BSFC improvement can be achieved with this placement at higher speed and loads, and less fuel penalty under low load condition. However, it is the general trend that adopting EGR and exhaust after-treatment to turbo-compounding engines will reduce the BSFC improvement of turbo-compounding.

2.8 Conclusion

The currently dominating technologies for waste energy recovery were summarized in this chapter. The working principles of Rankine cycle, Brayton cycle, thermoelectric generation and turbo-compounding were introduced in the beginning. In the later sections, this literature review particularly focuses on the comparison between each of these technologies in consideration of the thermal efficiency, effectiveness in recovering exhaust energy, size, weights and cost. It is believed that Rankine cycle, especially the organic version is much more effective in reducing fuel consumption of the overall engine system. At the same time, it imposes very little interference to the engine breathing. Turbo-compounding, on the other hand, is superior to its counterparts for compact size and lighter weight and better transient response. The Brayton cycle is mostly considered as an intermediate choice, since the effectiveness of it to harvesting waste heat is between the former two. And also, it still affects

engine breathing to a lower extent when comparing with turbo-compounding. The main drawback of Brayton cycle, however, is the high complexity of the system. Thermoelectric generation and heat insulation are less discussed in this chapter because of the low efficiency and high cost and limits in material technology.

The limits hindering the wide spread application of turbo-compounding include the added backpressure and thus high EGR rate, lower turbine efficiency under low load condition because of the dipping in exhaust energy and the sacrifice of engine efficiency due to the intervention of the bottoming cycle. Nevertheless, research has be carried out to explore the optimum setups for a variety of parameters that have important influence on the performance of the entire system, including boosting pressure, compression ratio, ignition timing, air-fuel ratio and so on. Based on these studies, it comes to the conclusion that higher compressor pressure ratio is preferable for the improvement in power output and thermal efficiency of turbo-compounding engine under full load condition, and the upper limit depends on the mechanical strength and heat resistance of the engine. While at part load operation, the optimum compressor pressure becomes lower. The intake and exhaust valve timing, as a sensitive parameter influencing the pumping features, should be fully exploited in order to achieve high volumetric efficiency and avoid the penalty in air boosting and knocking risk. It was also identified that the employment of turbo-compounding enables the engine to be operated with retarded ignition timing that helps to reduce the knock occurring. While the penalty in combustion efficiency can be compensated by increasing the boost pressure from the compressor. There is a significant compromise between the compression ratio and the compressor pressure ratio to achieve the lowest BSFC. Besides, the optimum turbine expansion ratio will also be varying for different compression ratio. Similarly, the air-fuel ratio of a turbo-compounding engine needs to be carefully adjusted to achieve the best compromise between pumping work and volumetric efficiency. When compare with a turbocharged engine, a turbo-compounding engine has higher EGR driving capability due to the higher exhaust pressure. It was stated that eliminating EGR could be conducive to enhance the energy availability to the power turbine and improve the fuel economy of a turbo-compounding engine. The turbine efficiency plays a significant role in reducing fuel

consumption in a turbo-compounding engine. The main challenge faced by commercially available radial turbines is that their peak efficiency is achieved at a speed ratio (U/C) about 0.7 where the energy in the exhaust pulse is starting to drop. Research aiming to shift the turbine peak efficiency to a lower U/C has been reviewed. Low pressure turbines that have higher efficiency when operating with lower expansion ratio and the mixed flow turbine with better swallowing capability are going to be included in the future research.

Chapter 3 – *Modelling methodology*

This chapter will present a modelling and calibration method as a foundation for the study in the following chapters. It mainly includes three sub-sections, namely engine modelling introduction and calibration for steady state and transient simulation and engine control theory and tuning.

3.1. Engine modelling

3.1.1. Introduction

Engine modelling is widely adopted in the engine design and development process. It can significantly enhance the efficiency of evaluating the conception of a specific technology and predict some engine parameters (such as the residual gas fraction and trapping ratio) that are difficult or impossible to measure in real test. Engine modelling approaches include black box model, mean value model, 1-D model, fast-running model and multi-dimensional model. These tools can be used for different objectives form a spectrum of computational time and prediction accuracy [148]. In this work, only the 1-D model will be introduced in detail.

Different from a mean value model that uses only simplified look-up tables to characterise the air flow and distribution of fuel energy without predicting the breathing and combustion processes, a 1-D engine code (such as GT-Power) solves the Navier-Stokes equations, as shown below (3.1-3.4). The equations are based on the conservation of continuity, momentum, and energy in one dimension piping system of the engine. Multivariate tools, such as simplified models, maps and look-up tables, are utilised to simulate critical parts like valves, turbochargers, cylinders and the friction and combustion process. It is a universal practice to make assumptions and extrapolation to the existing test data of the components when conducting a 1-D simulating. Thereby, the 1-D engine model usually requires extensive validation against the experimental data in real test [150].

$$Continuity: \quad \frac{dm}{dt} = \sum_{boundaries} \dot{m} \qquad \textbf{3.1}$$

$$Energy: \frac{d(me)}{dt} = -p\frac{dV}{dt} + \sum_{boundaries}(\dot{m}H) - hA_s(T_{fluid} - T_{wall}) \qquad \textbf{3.2}$$

$$Enthalpy: \frac{d(\rho HV)}{dt} = \sum_{boundaries}(\dot{m}\,H) + V\frac{dp}{dt} - hA_s(T_{fluid} - T_{wall}) \quad \textbf{3.3}$$

$$Momentum: \frac{d\dot{m}}{dt} = \frac{dpA + \sum_{boundaries}(\dot{m}u) - 4C_f\frac{\rho u|u|dxA}{2\quad D} - C_p\left(\frac{1}{2}\rho u|u|\right)A}{dx} \quad \textbf{3.4}$$

Where:

$\dot{m}$ **(g/s)**	Boundary mass flux into volume, $\dot{m} = \rho Au$
M (g)	Mass of the volume
V (mm^3)	Volume
P (bar)	pressure
p (g/mm^3)	density
A (mm^2)	Flow area (cross-sectional)
A_s(mm^2)	Heat transfer surface area
E (J/g)	Total internal energy (internal energy plus kinetic energy) per unit mass
H (J)	Total enthalpy, $H = e + \frac{p}{\rho}$
H (W/mm^2)	Heat transfer coefficient
T_{fluid} **(K)**	Fluid temperature
T_{wall} **(K)**	Wall temperature
U (mm/s)	Velocity at the boundary
C_f	Skin friction coefficient
C_p	Pressure loss coefficient
D (mm)	Equivalent diameter
dx **(mm)**	Length of mass element in the flow direction
dp **(bar)**	Pressure differential acting across dx

3.1.2. Combustion description and validation

Determining a well calibrated combustion model is the most critical step in 1-D modelling. It is usually the foundation to build up a predictive engine model. Two-zone combustion model is the most frequently used approach to almost all the combustion models in GT-Power, in which, the burned and unburned air-fuel mixtures are assumed to be trapped in the burned and unburned zones separately. Similarly, the temperatures in these two zones are computed separately, whereas the pressure distribution in the whole combustion chamber is considered as homogeneous. The energy equations in the two-zone model are different (as shown below), and are solved separately for each time step.

Unburned zone:

$$\frac{d(m_u e_u)}{dt} = -p\frac{dV_u}{dt} - Q_u + \left(\frac{dm_f}{dt}h_f + \frac{dm_a}{dt}h_a\right) + \frac{dm_{f,i}}{dt}h_{f,i} \quad \textbf{3.5}$$

Where:

m_u (g)	Unburned zone mass
V_u (mm^3)	Unburned zone volume
m_f (g)	Fuel mass
Q_u (J/s)	Unburned zone heat transfer rate
m_a (g)	Air mass
h_f (J)	Enthalpy of fuel mass
$m_{f,i}$ (g)	Injected fuel mass
h_a (J)	Enthalpy of air mass
P (bar)	Cylinder pressure
$h_{f,i}$ (J)	Enthalpy of injected fuel mass

Burned zone:

$$\frac{d(m_b e_b)}{dt} = -p\frac{dV_b}{dt} - Q_b - (\frac{dm_f}{dt}h_f + \frac{dm_a}{dt}h_a) \quad \textbf{3.6}$$

Where subscript 'b' denotes burned zone.

In terms of predictive, the combustion model in GT-Power can be divided into three types namely the non-predictive, semi-predictive and predictive models, which are believed to be best suitable for different situations specifically.

In a non-predictive combustion model, the burn rate is simply defined as a function of crank angle regardless of pressure or temperature or other conditions in the cylinder. This kind of model may be appropriate for the investigation of parameters that have little or no effect on the burn rate. For example, a non-predictive combustion model is usually prescribed in the spark-ignition engine simulation in the form of combustion profile or Wiebe model. In the following, the Wiebe model in a spark-ignition engine model is described, followed by the method of calibrating burn rate with measured cylinder pressure.

For most situations, the approach to predict SI burn rate with Wiebe function is precise enough when measured cylinder pressure is not available. The Wiebe equations are given below:

$$BMC = -\ln(1 - BM) \quad \text{Burned midpoint constant} \quad \textbf{3.7}$$

$$BSC = -\ln(1 - BS) \quad \text{Burned start constant} \quad \textbf{3.8}$$

$$BEC = -\ln(1 - BE) \quad \text{Burned end constant} \quad \textbf{3.9}$$

$$WC = \left[\frac{D}{BEC^{1/(E+1)} - BSC^{1/(E+1)}}\right]^{-(E+1)} \quad \text{Wiebe constant} \qquad \textbf{3.10}$$

$$SOC = AA - \frac{(D)(BMC)^{1/(E+1)}}{BEC^{1/(E+1)} - BSC^{1/(E+1)}} \quad \text{Start of combustion} \qquad \textbf{3.11}$$

Where:

AA (deg)	Anchor angle
D (s)	Duration
E	Wiebe exponent
CE	Fraction of fuel burned
BM	Burned fuel percentage at anchor angle
BS	Burned fuel percentage at duration start
BE	Burned fuel percentage at duration end

Burn rate calculation

$$Combustion(\theta) = (CE)\left[1 - e^{-(WC)(\theta - SOC)^{(E+1)}}\right] \qquad \textbf{3.12}$$

Where:

θ (deg)	Instantaneous crank angle

Calibrating burn rate from cylinder pressure trace is referred to 'reverse run' in this work, which uses the burn rate as an input to determine the cylinder pressure. The same equations described in the two-zone combustion methodology are utilised for both forward and reverse run calculations. In GT suite, two approaches are provided to calibrate the burn rate using measured cylinder pressure trace, namely the 'stand-alone burn rate calculation' and the 'three pressure analysis (TPA) burn rate calculation'.

The stand-alone burn rate calculation methodology essentially determines the burn rate by using only the cylinder pressure data which is either from a single cycle or an averaged parameters from a few cycle. This approach is advantageous in saving computational time comparing with the TPA discussed below. And also it can be cost-effective. However, this approach requires the estimation of some parameters, such as residual gas fraction and trapping ratio. In this work, the combustion calibration will be mostly based on this methodology, since the given 1-D engine models in this project are all of high-fidelity. Besides, at the time of writing, only the cylinder pressure trace is available from real test.

Instead, a TPA burn rate calculation requires for three measured pressure traces, including intake, cylinder, and exhaust - hence the name three pressure analysis. This approach uses a relatively detailed engine model, including the valves and ports, compared to the stand-alone burn rate calculation methodology; thus, there is no need to estimate the trapping ratio and residual gas fraction. It should be note that in a standard TPA model, it is desirable to reduce the magnitude of the fluctuations caused by reflections within the ports during the valve-closed period to make the predicted pressure behaviour within the port be closer to the measured behaviour [151]. It can be done by reducing the discretisation length, so that the unwanted noise in the pressure signal can be minimised.

Due to the shift of measured combustion phasing and the need of converting the measured signal into an absolute pressure in experiment, errors may occur when imposing the raw measured pressure data on the model described above. To correct the pressure phasing, a shift is often used to offset against the crank angle difference between the measured and calculated cylinder peak pressure. In terms of the cylinder pressure correction, it is recommended to set the cylinder pressure at IBDC equal to the average intake pressure.

It is often the case that the calculated cylinder pressure trace differs from the measured data when the measured and calculated cylinder pressure in the compression stroke is not overlaped, even though a standard calibration procedure is conducted. This might be due to the incorrect compression ratio in the given model, and the stack-up of the tolerances in each component (even if all of them are within specified tolerances). The cylinder heat transfer could also contribute to the inconsistency.

A semi-predictive combustion model is essentially a model using some significant variables such as the engine speed, intake manifold pressure and residual gas fraction as the inputs of a set of non-predictive burn rate. This allows changes of the burn rate in different operating conditions, without intensive central processing unit (CPU) penalty when compared to the predictive models. For a spark-ignition engine, if only full-load simulation is considered, the three terms of the Wiebe function (50% burn duration, 10-90% duration and exponent) will be interpolated from the look-up tables based on the engine speed. However, if a wider range of engine operating points is conducted, a representative set of data and an artificial neural

network may be required to train the behaviour of the engine characteristics.

Predictive combustion models will apprehensively take the cylinder's geometry, spark locations and timing, air motion, and fuel properties into consideration and require for an extensive calibration for model. Nevertheless, once the model is well-calibrated, the effects of cylinder geometry and spark timing on the combustion behaviour can be analysed based on the measured data.

Considering the engine hardware is available in this project, the burn rate could be calibrated the experimental data. And also, due to the fact that the control parameters only vary in a limited range, some non-predictive combustion models are utilised in this work to set up a semi-predictive combustion model.

3.1.3. Turbocharger modelling

Turbomachinery performance maps:

It is the common practice for some advanced 1-D gas dynamic engine simulation code like GT-Power to use zero-dimensional turbocharger performance maps in modelling. It is essentially a 'speed line' map composing of several sets of mass flow rate, pressure ratio, and thermodynamic efficiency, in which the data point with the lowest mass flow rate for each speed line of a compressor map is assumed to be on the surge line, while the peak efficiency data must be included at each turbine speed line so that the data can be fitted to a curve allowing the extrapolation of the test data (as detailed in the later section).

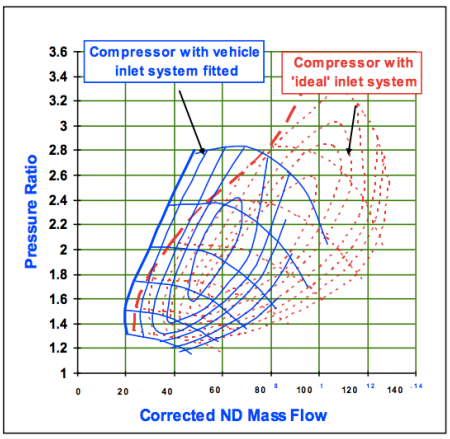

Figure 3.1. Corrected compressor maps with 'ideal' straight bell-mounted inlet and vehicle inlet system [183].

The compressor and turbine map data set must be corrected before using to account for the changes in temperature, pressure and compositions. A compressor map is usually corrected referring to the temperature and pressure of 298K and 1bar. The equations to correct the engine speed and mass flow rate are shown below:

$$RPM_{corrected} = {RPM_{actual}} \Big/ {\sqrt{\frac{T_{inlet-total}}{T_{reference}}}} \quad \textbf{3.13}$$

$$\dot{m}_{corrected} = \dot{m}_{actual} \times {\sqrt{\frac{T_{inlet-total}}{T_{reference}}}} \Big/ {\frac{P_{inlet-total}}{P_{reference}}} \quad \textbf{3.14}$$

Figure 3.1 shows a typical corrected compressor map with 'ideal' straight bell-mounted inlet and vehicle inlet system. This indicates that a shift of the compressor characteristic is highly possible when a dyno or vehicle inlet and charge air system is fitted, since it will affect the engine/turbocharger performance and the interactions between them.

As for the turbine maps, because of the significant difference in reference conditions, they are usually 'reduced' to clear the effects of the inlet temperature and pressure on performance, so that any two turbine maps could be compared then without looking at the reference conditions. The formula to reduce the turbine maps can be seen in the following:

$$RPM_{reduced} = \frac{RPM_{actual}}{\sqrt{T_{inlet-total}}} \quad \textbf{3.15}$$

$$\dot{m}_{reduced} = \frac{\dot{m}_{actual}\sqrt{T_{inlet-total}}}{P_{inlet-total}} \quad \textbf{3.16}$$

It might be worth noting that the ratios of specific heats and gas constants should be considered as well if exhaust gas with different compositions are passing through the turbine at different inlet temperatures. For example, when a spark-ignition engine is operating at large scavenging (i.e. rich air/fuel ratio), or a low-pressure turbine is considered, corrections for the ratios of specific heats and gas constants should be conducted by using the following terms multiplied by the reduced speed and reduced mass flow rate, respectively.

$$\sqrt{\frac{\gamma_R R_R}{\gamma_a R_a}} \quad \textbf{3.17}$$

Where:

γ_R	Reference ratio of specific heats
γ_a	Actual ratio of specific heats at the inlet of the turbine
R_R (J/mol·K)	Reference gas constant
R_a (J/mol·K)	Actual gas constant at the inlet of the turbine

Turbocharger shaft modelling:

In turbocharger modelling, turbocharger shaft is the component representing the total rotational inertia of the turbine wheel, compressor wheel and shaft itself. Thereby, this attribute has a larger effect on the transient response than the steady-state performance. However, in order to run the steady-state simulation with the least computing time, GT-Power allows an artificial manipulation to the turbocharger inertia. The recommended routine is to set a high inertia multiplier (usually around 100) for the first few engine cycles, so that the turbocharger speed does not experience a dip while the velocity in the manifolds is developing. After that, the inertia multiplier could be made very low (usually around 0.01) to allow the rotational speed to reach the convergence as quickly as possible within 10 to 15 engine cycles. And finally, the inertia multiplier should be returned to 1 for the rest of the simulation.

Although the mechanical efficiency of the turbomachinery could be adjusted in turbo shaft, most turbocharger suppliers tend to lump the bearing friction in the turbine efficiency map without explicit statement sometimes [149]. Since the turbine efficiency is calculated by dividing the isentropic enthalpy drop across the turbine multiplied by mechanical efficiency (see equation below) with the actual total enthalpy rise of the compressor in a recommended gas stand test procedure, the bearing friction has been included into the turbine isentropic efficiency map already. Thereby, this method is considered valid with the turbine inlet temperature close to that of the gas stand test. When the inlet temperature is significantly lower (at part load operation, for example), however, the effects of temperature change on the friction should be account for.

$$\eta_t = \frac{C_{P,comp} \times (T_{0,out} - T_{0,in})_{comp}}{\eta_{mech} \times \left(1 + \frac{1}{A/F}\right) \times C_{P,Turb} \times T_{0,in,turb} \times \left[1 - \left(\frac{1}{PR_t}\right)^{\frac{\gamma-1}{\gamma}}\right]} \quad \textbf{3.19}$$

3.1.4. Supercharger modelling

Supercharger modelling is similar to that of a turbocharger in GT-Power. The most significant difference lies in the way of computing the friction. As aforementioned, the shaft mechanical efficiency of the traditional turbocharger compressor is often lumped into the turbine efficiency map, while the supercharger compressor shaft mechanical efficiency should be explicitly modelled. It is usually done by imposing a power or torque template to extract the mechanical loss from the engine system or by estimating a mechanical efficiency (table). In the latest GT-Power version, a new compressor template is employed to include the total shaft power data in the compressor performance map to account for the mechanical losses in a supercharger system. This template is especially useful when an 'overblown' effect, wherein the inlet pressure is larger than the outlet, is investigated.

3.2. Control modelling and calibration

3.2.1. Control introduction

To create a proper control logic for the engine system is of great importance to achieve the required performance. For a gasoline engine, the most important variables defining the engine operating points are engine speed and load. The engine speed can be directly measured by a speed sensor, while the engine load can be expressed by throttle angle and thus the air mass flow (unlike diesel engines whose loads are regulated by fuel quantity) into the cylinder, since a full homogeneous mixture of fuel and air is required before combustion. Even though some models would consider intake pressure and temperature too.

In recent years, with the push for better fuel economy and higher emissions requirement and the development of the component technology, a number of actuators and engine control actions that can actively modulate the engine performance have emerged.

3.2.2. Feedback control

For automotive application, the most widely utilised control strategy is Proportional-Integral-Derivative (PID) control, because of the good understanding by the powertrain calibrators.

PID controllers are based around the process to minimise the error between a target value and a measured process variable by applying a correction to the system (see Figure 3.2). For

an automotive application, the derivative loop in a standard PID controller is usually not required for the following two reasons:

- It is usually the case for the function of a derivative loop being replaced by a feed-forward map control;
- Tuning of the derivative term can be quite demanding and an improper calibration will amplify the noise in the feedback that may cause oscillatory behaviour.

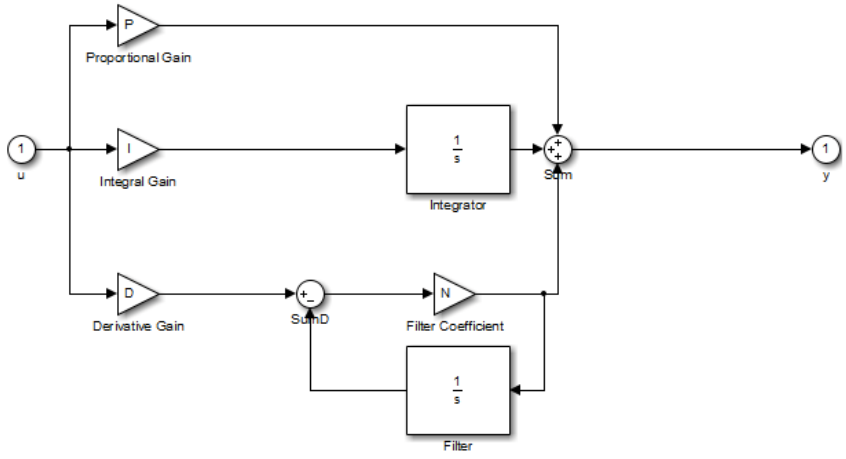

Figure 3.2. PID controller Simulink block

For an engine a model containing two or more PI controllers, some schedules for the regulated parameters are needed to avoid two controllers fighting each other and causing unstable operation of the engine. Also, an optimal PI controller setup that is ideal for one engine operating point might be not the case for another, which may result in slow convergence and oscillatory behaviour. A popular approach to deal with this is to alter the controller gains according to specific engine speed and load, which is known as gains scheduling.

Integral wind-up is also a problem in a PI controller, as shown in Figure 3.3. It is basically the scenario where the target is higher than the upper limit that can be achieved by the actuator. The integrator will then accumulate a significant error during wind-up and results in excess overshooting.

In order to avoid integral wind-up, both the back-calculation and clamping approach are used in this work. Figure 3.4 shows the back-calculation in PID controller block. An internal tracking loop is enabled to discharge the integrator output. Even though better dynamics are shown

in this approach, worse results are possible because of the difficulty in determining. As another widely utilised anti-windup method, clamping tend to set the integral path of a PID controller to zero when an integrator overflow being detected to avoid wind-up (see Figure 3.5). Compared to the back-calculation method, the clamping approach shows better stability.

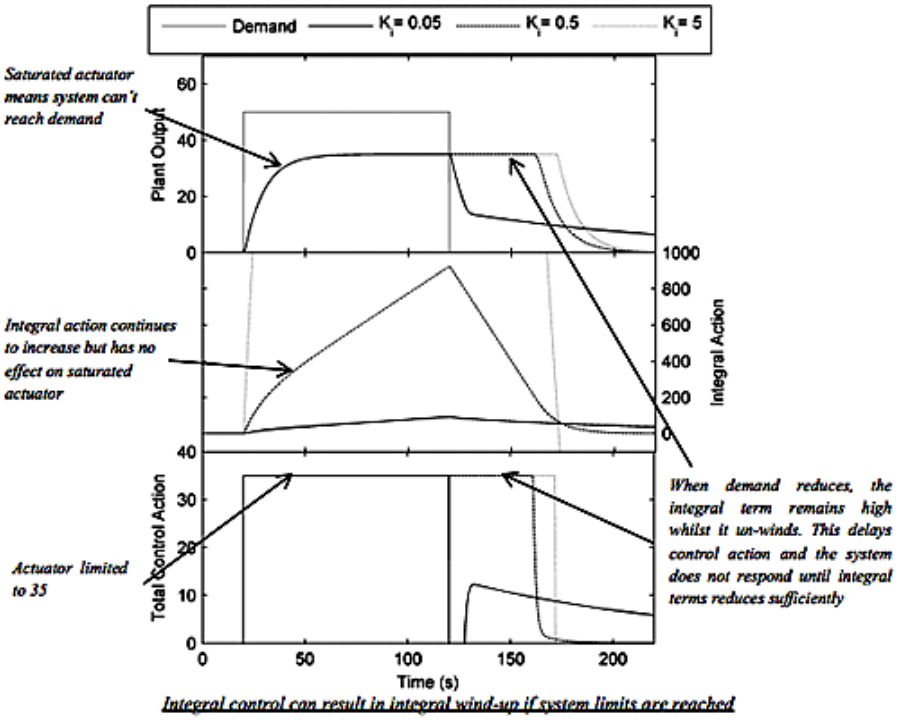

Figure 3.3. Integral wind-up for a PID control

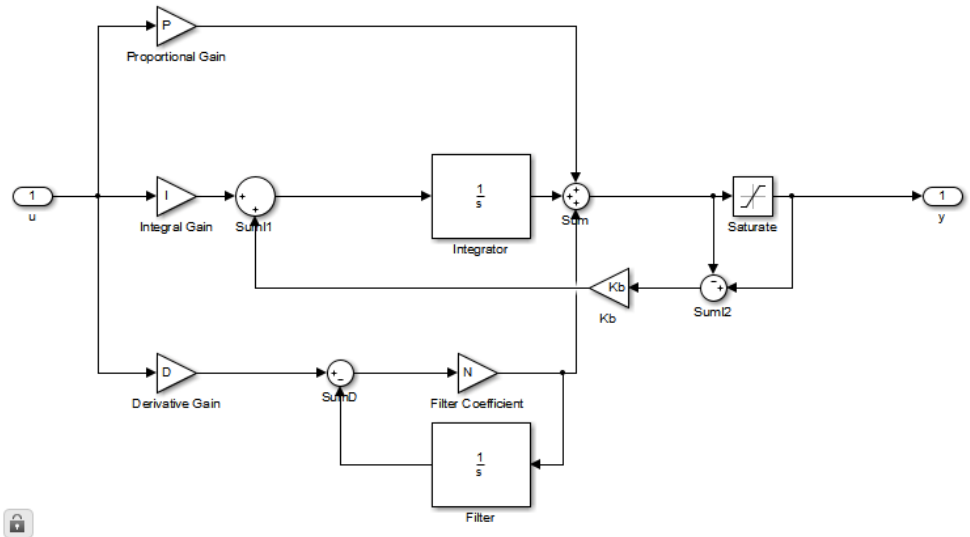

Figure 3.4. Back-calculation anti-windup method

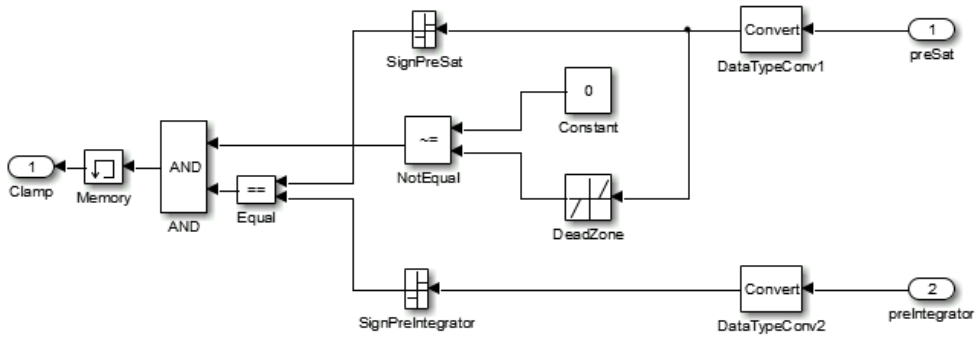

Figure 3.5. Clamping anti-windup method

3.2.3. Feed-forward loop

For an engine study, it is usually the requirement for fast and robust response behaviour, and adding a feed-forward loop to the existing feedback controller is the common practice to achieve that. This approach is basically implementing an optimized estimation of the controller action, and mapping this value against engine setups with direct control action. By doing this, the response time and the need for large feedback gains could be significantly reduced and the system could be more stable. A PID control demonstration with a feed-forward control is shown in Figure 3.6.

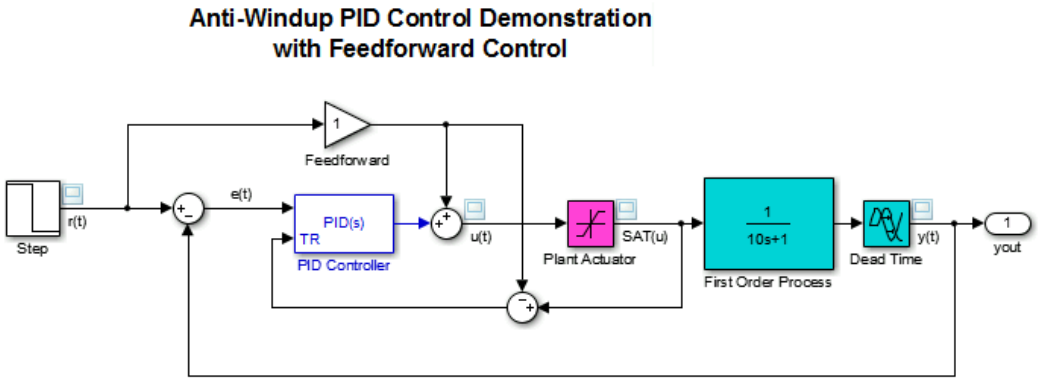

Figure 3.6. PID control demonstration with feedforward control

3.2.4. GT-Suite and Matlab/Simulink co-simulation

For the sake of convenience, it is a common practice in engine modelling where engine and powertrain are modelled in GT-Suite, while the electronic controllers are modelled in

Matlab/Simulink. By coupling GT-Suite models with the control modules developed in Matlab/Simulink Environment, a complete engine model is ready for desired operation and optimization. GT-Power provides two methods for GT suite and Matlab/Simulink co-simulation:

- Running a GT-Suite model from the Matlab/Simulink interface
- Compiling Matlab/Simulink models into .dll/.so files and importing them into a GT-Suite model.

For the co-simulation work in this thesis, the first option above was always utilised for convenience of setting up and tuning.

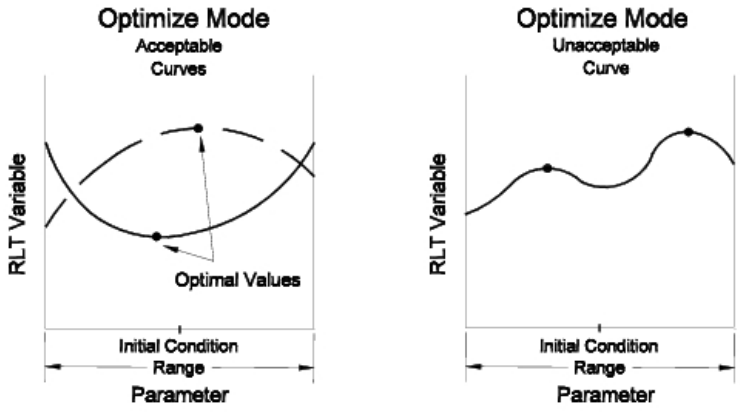

Figure 3.7. GT-Suite embedded optimization strategy

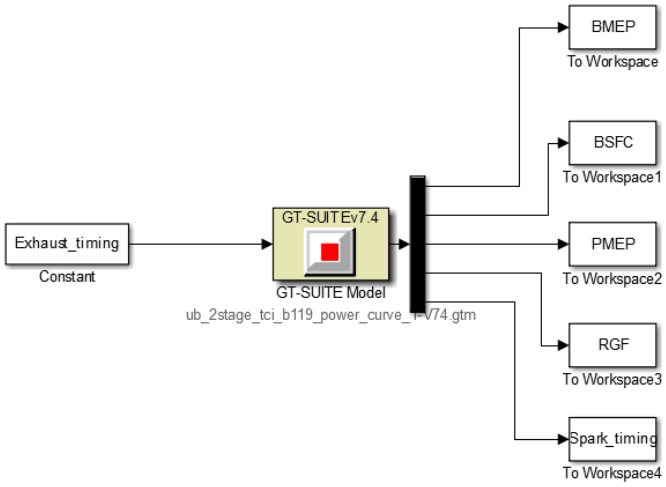

Figure 3.8. GT-Power engine model in Simulink interface

In GT-Suite, the embedded optimization tools requires the output variable to have a unique minimum or maximum, see Figure 3.7, in order to conduct a optimization to a non-linear engine system, while a genetic algorithm that can be realised in Matlab/Simulink can avoid the problems, and this is also the reason for employing co-simulation. Figure 3.8 illustrates the co-simulation between a GT-Suite engine model and a Simulink module.

3.3 Transient modelling and validation

3.3.1 Overview

Running an engine model in a transient mode (e.g. changing engine speed or load over time) requires attention to several areas that can be neglected when running a model steady state. In fact, every model is different and requires attention to different areas. A transient model should be set up and calibrated before running within the operating range.

3.3.2 Transient Running Modes

There are two different ways of running an engine model in GT-POWER.

- Imposing the engine speed and predicting the load (speed Mode).
- Imposing the load and predicting the engine speed (load Mode).

When performing a transient run where the engine speed is the dominant input of interest, it is recommended to perform the transient analysis in Speed Mode. A common scenario for this would be an acoustics test over speed transients. In speed mode, the engine speed can be imposed over time or period, using “ProfileTransient” or “ProfilePeriod” objects. When running in speed mode, the engine inertia in the Inertia folder could be ignored, since the indicated quantities (IMEP, etc.) will not be affected by the inertia. However, it is needed for the calculation of brake torque.

When running the engine model in load mode, a load may be imposed using a torque imposing module, such as “Torque” or “PowerRot”, connected to the crank train. With the load imposed on the engine, a value has to be entered for “Engine Effective Rotating Inertia” in the Inertia folder. A typical scenario for running a transient model in load mode would be a drive cycle simulation with an attached vehicle model requesting the load from the engine.

In this thesis, it is the speed mode that chosen for the transient evaluation of engine models.

3.3.3 Transient Model Inputs

Depending on the operating condition, all inputs have to be adjusted using either some form of look-up or a predictive model to account for the change.

Generally, for a gasoline engine attention should be paid to include the following:

- Turbocharger (Wastegate or VGT Rack position)
- Supercharger (clutching speed or CVT ratio)
- Cam timing and lift for VVT engine
- Air/Fuel ratio (especially SI engines)
- EGR Valve Control
- Coolant temperature (warm-up)

With the automatic interpolation and extrapolation of the turbocharger maps provided by GT-Suite, the turbocharger model is ready for transient runs. The quality of the extrapolation is especially important for transient runs with low engine speeds and loads that typically occur in drive cycle simulations.

The controller templates provided in the GT-SUITE controls library (e.g. “PIDController”, “ControllerEGRValve” module, etc.) are targeting controllers. To achieve a realistic behaviour in transient operation, the rate limits (Minimum and Maximum Output Rate) have to be set manually according to the physical system response speed. For example, the rate at which waste gate is opened or closed should be known and is required as an input to the controller.

3.3.4 Initialization

The correct initialization of the transient model is a very important input in transient simulation. It is different from the initialization approach taken for steady-state models. For steady-state, a value close enough to the actual operating value is used, to ensure a rapid convergence. The exact value is not important in this context. However, for transient runs, it is vital that the starting point is correct, and all parts of the model have to be initialized with the steady-state values of the starting operating point.

The recommended procedure for the initialization is to set up the first case of the model running the starting point as a steady-state operating point. Case 2 is then used for the actual transient run. To achieve the correct initialization, the flag Initialization State in Run Setup

should be set to “previous case”. Case 2 (the transient run) will then start with the result of case 1 (steady state starting point). Additionally, it is recommended to set the Wall Temperature Solver to steady for Case 1 (in order to speed up time for convergence) and transient for Case 2.

Another option is to initialize the transient model using results from the steady-state model previously run. This can be done by enabling the “Use RLTs” in the Initialization folder of “Run Setup” to initialize “user_imposed Cases” (Flow). For this option, only 1 case is specified (the transient run), and the initialization is done with results from the specified .gdx file.

For the work in this thesis, the first option was adopted.

3.3.5 Thermal Behaviour

Part of modelling transient engine operation is the wall-temperature change over time in pipes and flow splits as well as the cylinder. Since wall temperatures cannot be generally assumed to be constant with changing operating conditions, a wall temperature solver object should be specified in all pipes and flow splits. Also, since the wall temperatures of the cylinders will change with operating conditions, cylinder Wall temperature solver should be specified as Wall Temperature Object in Engine Cylinder.

The wall temperature solver has two operating modes, steady and transient. The flag can be set in Run Setup in the Thermal folder.

Charge Air Coolers that use imposed wall temperatures (directly, or via an effectiveness table) will change their wall temperature without delay, so they do not account for thermal inertias. In the absence of predictive models, a delay in the form of a First Order Filter should be used on the signal for the imposed wall temperature, to achieve a more realistic behaviours.

3.3.6 Transient calibration

The transients simulation studied in this thesis are load step type, which means that the engine speed is held constant while the load is increased rapidly.

As shown in figure 3.9 and 3.10, a non-calibrated transient engine simulation model cannot accurately predict the transient behaviour of the engine. One important reason is the thermal inertia of the engine, especially the hottest area. The model must be calibrated to accurately

model the building-up of temperature in the exhaust system during the transient operation. Besides, the combustion and AFR change during the transient must be altered to imitate this change during the load step. Lastly, since the turbine and compressor are produced through extrapolation based on a few measured points, the operating points of the turbo machinery during the transient are often far from any measured point and the results are often extrapolated with varying degree of accuracy, which may have to be corrected with efficiency multiplier. From the compressor map shown in figure 3.11, the region below the lowest row of measured points is extrapolated. A large part of the operating period of transient simulation is located in this area.

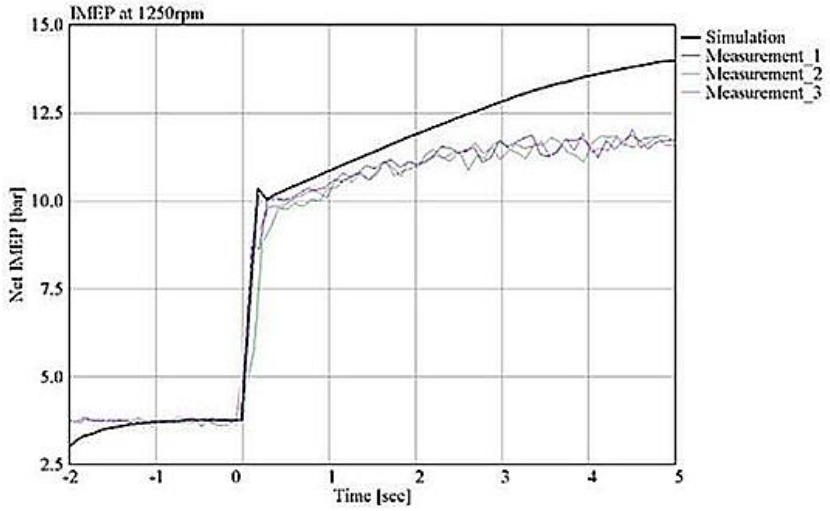

Figure 3.9. **Non-calibrated transient simulation [186].**

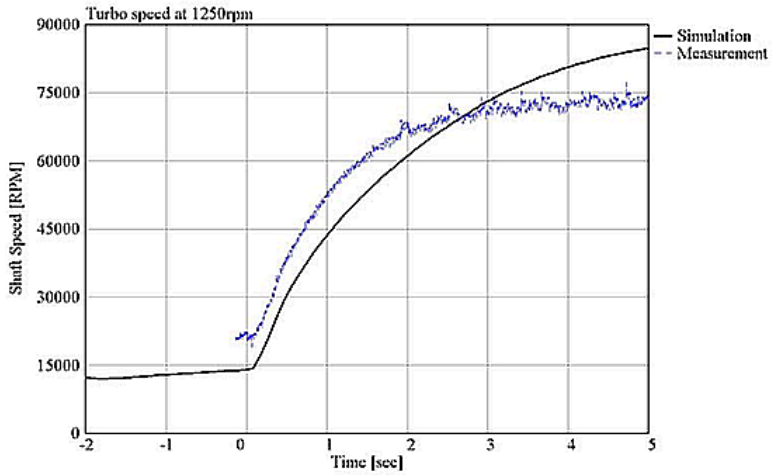

Figure 3.10. **Non-calibrated transient simulation [186].**

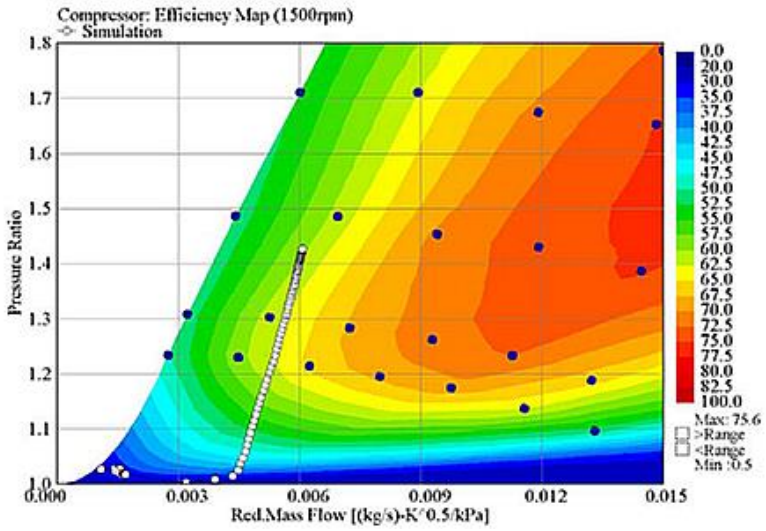

Figure 3.11. Compressor map with simulation (white dots) and turbo-manufacturer map points (black dots) [186].

3.3.7.1 Combustion calibration for transient simulation

The spark-Ignition Wiebe model imposes the combustion rate using a Wiebe functions with three inputs, namely the 50% burn point, the burn duration between the 10% and 90% burn points (see figure 3.12) and a Wiebe function exponent to shift the inputs in respect to each other. This model also needs measured data to imitate the combustion process.

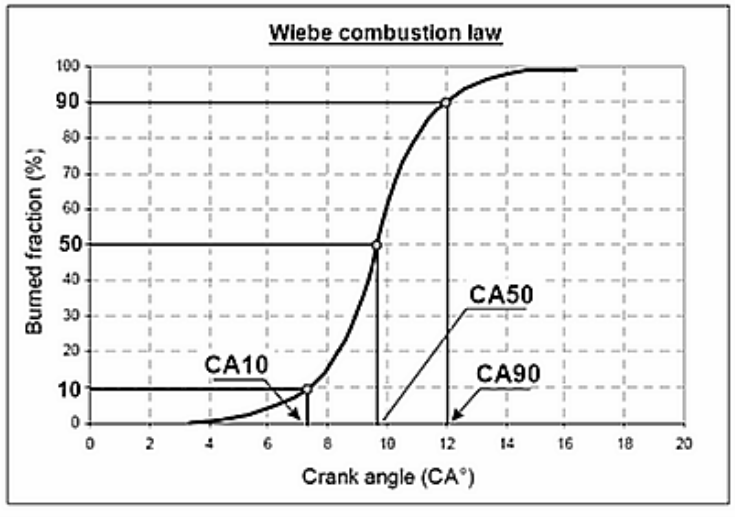

Figure 3.12. Wiebe function

3.3.7.2 50% burn point calibration

The calibration of the combustion process 50% burn point can be done by building up a map

of the 50% burned point (in the form of CAD after TDC) as a function of load and speed. Then the map is inserted in the EngCylCombSIWiebe model for transient simulation.

3.3.7.3 10-90% burn duration calibration

Calibration of the 10-90% burn duration is done in the similar way. The 10-90 burn duration is collected as a function of load. Data is then combined to engine speed to create a 2-D lookup table. This table is then inserted in the combustion model.

3.3.7.4 Air/Fuel calibration

As for AFR calibration, firstly, measurement data is collected from the ATI units, while the cylinder pressures are gathered through Dewetron. And then, a time resolved graphs were created for AFR and IMEP. Maps were then created from extracted data from these AFR/IMEP graphs for every speed. The AFR map was then inserted in the injector object in the model.

3.3.7.4 Turbocharger speed calibration

The turbocharger speed is one of the most important parameters for transient simulations, since it governs the mass flow, intake pressure and temperature etc. The calibration of the turbocharger speed usually starts from steady state condition at full load operation.

A PID controller is included to adjust the turbine efficiency multiplier allowing the turbocharger speed correlate to the target value for each engine speed and operating point.

When the turbocharger speeds are calibrated for each load and engine speed, the value of the turbine efficiency multipliers is inserted in a 2-D lockup table as a function of turbo and engine speed. The output signal value i.e. turbine efficiency multiplier (TEM) is sent to the turbine object. When this is done the turbocharger speed at the start and finishing points will correspond to the measurements, but deviations is still seen in the region between. Since the efficiency map only has two values for each engine speed at this point, so GT-power interpolated in the turbocharger speed range between these two values. Therefore, new turbocharger speed rows are needed ideally to accurately predict the turbocharger speed.

In practice, with the automatic interpolation and extrapolation of the turbocharger maps provided by GT-SUITE, the turbocharger model is ready for transient runs. However, the quality of the extrapolation is especially important for the accuracy of transient runs. Methods

to improve the fitting of the maps is introduced in [186].

As mentioned above, another important input for the turbocharger is the inertia specified in the ShaftTurbo. This value should be known from the supplier. Any inertia multiplier should be removed for transient runs.

Chapter 4 – System Optimization of variable drive supercharged engine system

The superchargers appearing on the market at present are mainly fix-ratio positive displacement types. Nevertheless, such charging systems have to face the challenges of fuel penalty because of the need for a bypass valve to recirculate the air mass flow under low load condition. Besides, a clutch is also necessary in this system to disconnect the compressor at high engine speed, which encumbers the transient response of the engine and may lead to Noise Vibration and Harshness (NVH) issues at transient operation.

CVT Supercharger is basically a centrifugal supercharger with variable driven ratio. This system is composed of a continuously variable transmission (CVT) and a centrifugal compressor which is developed by Torotrak for flexible and quiet boosting. Thanks to the wide transmission ratio range of CVT, the compressor is able be operated independent of engine speed to precisely meet the engine load. The active bypass valve in conventional supercharger system is replaced by a one-direction passive bypass eliminating the air recirculation, which bring about better fuel economy under partial load condition. The supercharger clutch were removed to trade for faster transient response in the cost of acceptable degradation of low load fuel efficiency. This chapter will compare the performance of turbo-super and super-turbo configurations to determine the location of CVT Supercharger. Optimization of pulley ratio and CVT ratio change rate will be presented. Control strategy will be further developed by examining the tip-in operation from different starting torque. The performance of the whole system will be evaluated by examining the fuel consumption at full load, part load and real world driving cycles.

4.1 Introduction

In spite of the emerging developments of alternative technologies, such as electric cars, internal combustion engines (ICE) is remain its predominance as the power source for automotive application at present. Therefore, it is essential to keep improving the ICE performance in either power output and fuel efficiency. At present, downsizing and down-

speeding are accepted as the most effective means to improve the fuel economy and CO_2 emission of passenger car SI (spark ignition) engine with extensive verifications in both experimental and real world environment [153][154], because of the capabilities of reducing pumping loss, improving heat transfer and bringing about lower friction of reciprocating piston ICE. Air charging systems, which are mainly superchargers and turbochargers, are now considered to be effective approaches to enhance the overall ICE performance at wide operation mode, instead of merely increasing the short-term peak power output. However, because of the inherent characteristics, challenges are faced by both of them. On the one hand, turbochargers are able to harvest exhaust energy which is almost free and make themselves self-sufficient. But, they struggle to provide enough low-end torque or satisfying transient response. On the other hand, although superchargers are able to provide sufficient boost at low engine speed with desired response speed because of their drive mechanism, they will unavoidably sacrifice the fuel efficiency to some extent in the form of parasitic loss. Therefore, the potential of gathering turbocharger and supercharger in one engine system to avoid the aforementioned problems has been investigated by a number of studies [1, 155, 156]. Promotions were demonstrated in both transient performance and power output over a wide engine speed range. Nevertheless, conventional fix-ratio superchargers, which are usually positive displacement compressors, are inevitably accompanied with active bypass valves to regulate air boost by circulating intake air across the compressor. And also clutches are needed to connect and disconnect the compressor from the engine shaft for different operating demand. Then, engine systems equipped with fix-ratio superchargers have to face the deterioration of fuel efficiency caused by air circulation, especially under mid-high load condition. And also, the response speed to tip-in will be restricted by clutching time. Besides, the efforts and costs spent on control strategy calibration to fit in active bypass valves are non-ignorable. Lastly, attenuation of NVH (Noise, Vibration and Harshness) is also one of the main challenges faced by fix-ratio positive displacement superchargers.

The CVT Supercharger system, however, allows a much more flexible control of the supercharger speed with the aid of a widely adjustable CVT. It, therefore, is capable of providing refined boosting to precisely and smoothly meet the engine demand. Furthermore,

elimination of supercharger clutch improves the transient response, and reduces the cost and difficulty in package. At the same time, NVH caused by the engage-and-disengage action of supercharger clutch is eliminated as well. Lastly, by replacing the active bypass valve with a passive valve which only allows air flow in one direction, the air circulation across the supercharger is closed. That helps to improve the fuel economy at middle and high load.

4.2 Scope and objectives

This chapter will firstly investigate two twin-charged engine configurations with different relative positions of supercharger and turbocharger to find the difference in performance. And then, the desirable configuration will be adopted for the optimization of pulley and epicyclic gear ratio trying to find the best trade-off between transient and part load fuel efficiency. After that, further regulation will be carried out for the CVT ratio change rate to avoid “dip” in brake torque which may affect the driving experience. The fuel economy of the refined model will be assessed by conducting a WLTP test in the final step. The overall performance, including full and partial load fuel consumption and response speed of the CVT Supercharger engine will be compared with a commercially available conventional supercharged counterpart which comprises a fixed ratio positive displacement (Roots) compressor, as shown in figure 4.1. Both engine systems are implemented in conjunction with a fix geometry turbocharger.

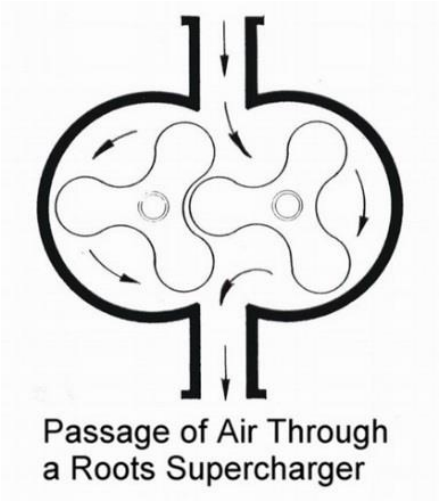

Figure 4.1. Positive-displacement supercharger (roots type for example)

4.3 CVT Supercharger and engine system configurations

CVT Supercharger system is essentially a variable drive ratio supercharger. As an alternative to conventional fix-ratio positive displacement supercharger, CVT Supercharger utilizes a centrifugal compressor driven by a CVT, which is developed by Torotrak, to couple with a fixed ratio step up pulley and epicyclic gear which have a speed ratio of 2.5:1 and 12.5:1 respectively. The CVT ratio thereby can be swept from 0.28:1 to 2.81:1, which means for the engine speed of 1000 rpm, the compressor speed can be varied from 8750 rpm to 88125 rpm. The detailed architecture of CVT Supercharger is shown in figure 4.2.

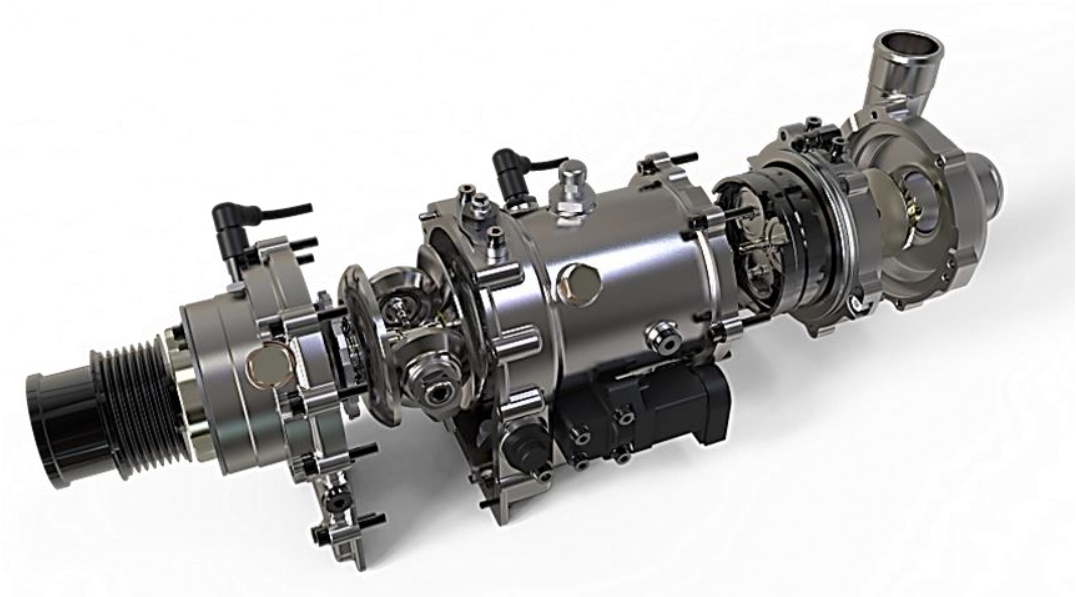

Figure 4.2. **CVT Supercharger variable transmission ratio supercharger.**

As mentioned above, it is a centrifugal compressor that is utilized to boost the intake air. This type of compressor is generally more efficient, compact and lighter for automotive application when comparing to their positive displacement counterpart. However, because of its inherent air flow characteristics, the boost is much lower at low rotational speed. It maybe not ideal for passenger car engines which usually works under part load condition for most of its service life. However, in this practice, the pressurization could be effectively remedied by the step-up transmissions (namely pulley and epicyclic gear set) which provide sufficient tip speed for the

compressor in the cost of additional mechanical losses within acceptable level. This will be explained in detail in the later paragraphs.

The baseline GT-Power engine model was supplied by Ford Aachen. It is a 1.0 litre turbocharged engine full-load model featuring a fixed-geometry turbocharger [157]. A fixed gear ratio of 7.03 was used for the supercharger, and an active by-pass valve was adopted to regulate the supercharger pressure ratio by recirculating the intake mass flow across the supercharger.

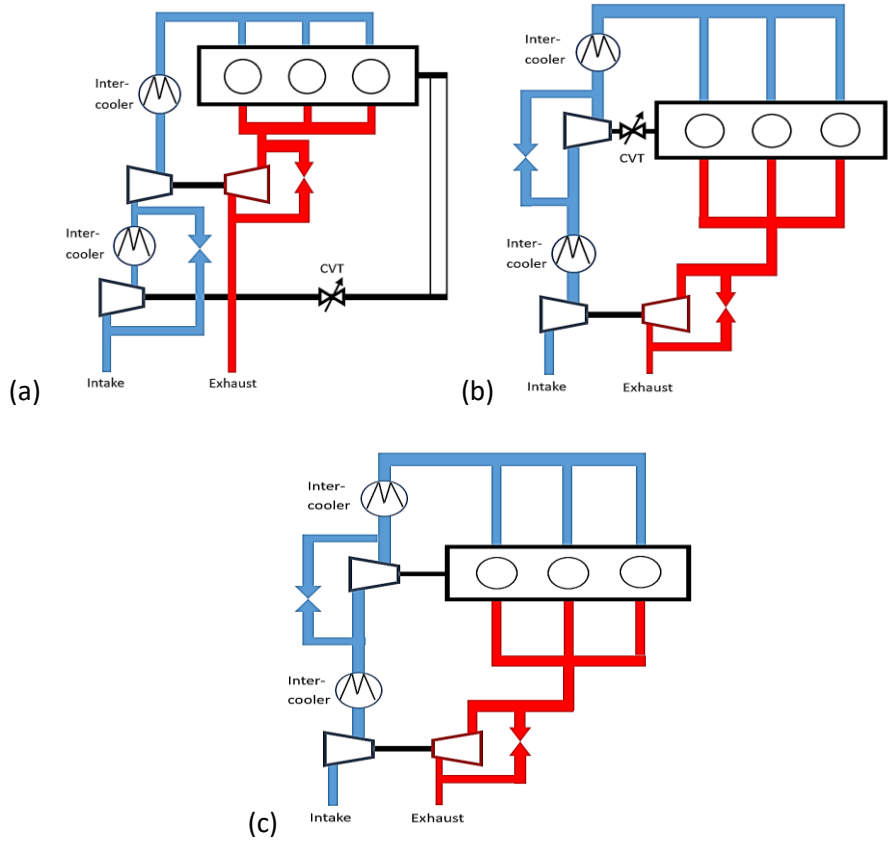

Figure 4.3. CVT Supercharger engine configurations. (a)Super-Turbo; (b) Turbo-Super

Figure 4.3 shows the Super-Turbo (a) and Turbo-Super (b) configurations with CVT Supercharger being located upstream and downstream turbocharger compressor respectively. The 1.0 litre three cylinders baseline engine is also illustrated in figure 4.3. Both of the novel configurations featuring the same turbocharger and CVT Supercharger systems. Intercoolers are located between and after the two boosting stages. The bypass valve parallel to CVT Supercharger is of passive type which only allows forward air flow and will be shut by reversed pressure drop.

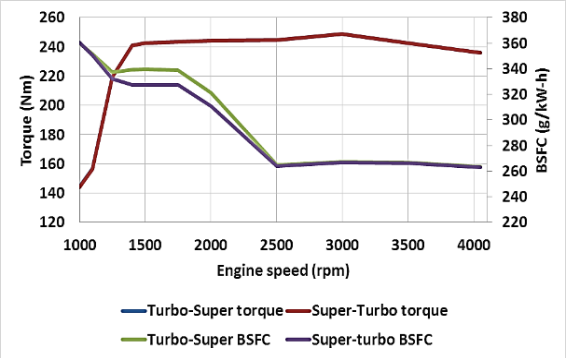

Figure 4.4. **Torque output and specific fuel consumption of two configurations.**

Figure 4.4 illustrates the torque performance and fuel consumption of the two configurations. For the simplicity of comparison, the same torque targets are set for the two configurations, which are also the stretched real test targets for this project. From this figure, the BSFC of the two models tended to coincide above 2000 rpm when CVT Supercharger was bypassed and running at lowest speed ratio. At 2000 rpm and lower engine speed, when CVT Supercharger participated in boosting the intake air, the difference in fuel economy began to emerge. The Super-Turbo configuration showed a fuel saving of up to 3.2% comparing with Turbo-Super model at 1750 rpm. It dues to the less power expenditure on CVT Supercharger of the super-Turbo layout, which can be explained by the following figures.

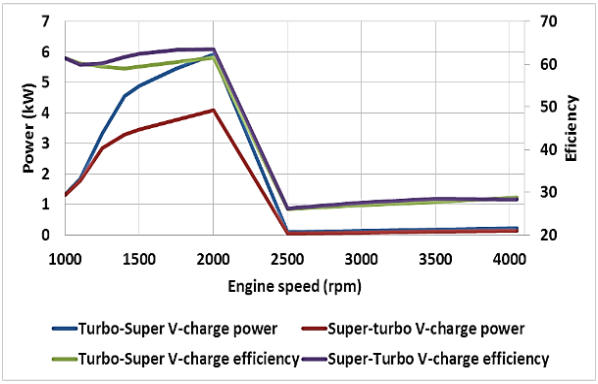

Figure 4.5. **CVT Supercharger efficiency and power consumption of both configurations.**

From figure 4.5, at 2000 and lower engine speed, the CVT Supercharger system in Super-turbo model had slightly higher efficiency and consumed much less engine shaft power. It is mainly because of the lower inlet air temperature to the CVT Supercharger compressor, as shown in figure 4.6.

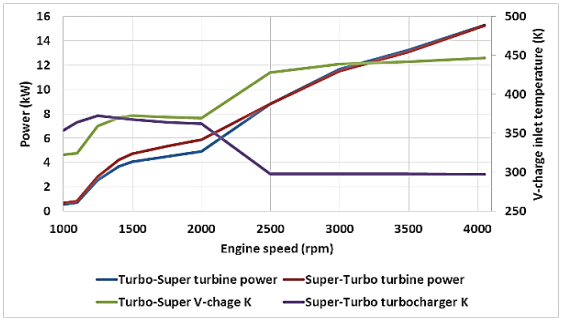

Figure 4.6. **Turbine power and inlet air temperature to CVT Supercharger and turbocharger compressors of both configurations.**

From figure 4.6, the air temperature at the inlet port of CVT Supercharger compressor was higher than 330 K in the Turbo-Super model. In the Super-Turbo model, it was close to the ambient temperature which is around 298 k. The lower inlet temperature enabled CVT Supercharger to provide about the same boosting level by consuming less driven power. On the other hand, the inlet air temperature for the turbocharger compressor was higher in the Super-Turbo model, which enhanced the potential of turbocharger to extract more exhaust energy. It could explain the turbine power difference between the two models.

It should be note that the margin in fuel consumption would be narrowed with a more efficient intercooler located between the two boost stages. It also suggests that, based on the analysis above, a two-stage intercooler would be necessary for the Turbo-Super layout, but optional for the Super-Turbo. Besides, Super-Turbo configuration was proven to be easier for packaging and pipework routing in real test. Therefore, the Super-Turbo version was chosen for the following studies.

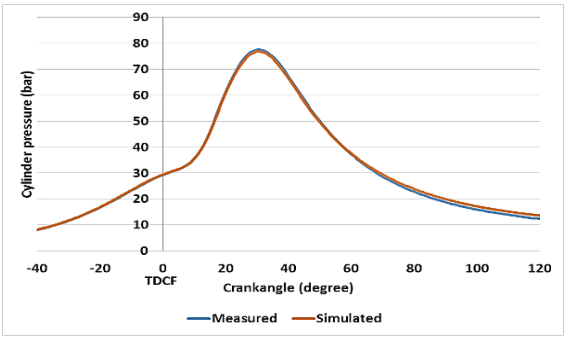

Figure 4.7. **Cylinder pressure from experiments and simulation.**

In order to ensure GT-power model to precisely predict the performance of the whole engine

system, a calibration was carried out to match the computed data from the simplified baseline engine model, in which the supercharger was de-activated, with the experimental testing. By comparing the cylinder pressure under full and partial load conditions, it indicated that the actual data and the calculation data matched fairly well in the qualitative tendencies, which confirmed the appropriateness of the combustion model. Figure 4.7 shows the full load cylinder pressure at 1400 rpm as an example. The results at other engine speeds showed the similar trend. The comparison of the simulated and tested in-cylinder pressure demonstrated a close match, as shown in figure 4.7. These results indicated that the model was of fairly acceptable level of precision to simulate the performance of the whole engine system based on the baseline model.

4.4 Optimization

4.4.1 Optimization for the pulley and epicyclic gear ratio.

For the conventional supercharger system in which a friction clutch is equipped, the parasitic losses from supercharger could be eliminated by disengaging the compressor. For the CVT Supercharger system, however, if no clutch was equipped, mechanical losses can be minimised by employing lower pulley and epicyclic gear ratio. Even though the losses cannot be eliminated completely.

To prove the prediction, a part load simulation has been carried out at the Brake Mean Effective Pressure (BMEP) of 2bar which output approximately 15Nm brake torque. In this simulation the epicyclic gear ratio was maintained at 12.67:1, while the pulley ratio was swept from 4:1 to 1:1.

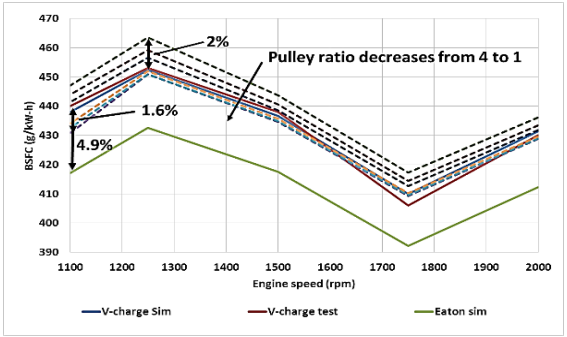

Figure 4.8. Low load (2bar BMEP) BSFC

Figure 4.8 shows the comparison of low load fuel consumption between CVT Supercharger and Eaton supercharger. The mechanical losses of the CVT Supercharger system was up to 4.9% (since the trend was the same for other load, only the results at 2bar BMEP were discussed in here) at the engine speed of 1100 rpm. It was mainly due to the losses of CVT, pulley and epicyclical gear. At higher engine speed, the deficit became smaller because the friction within the engine block (FMEP) occupied a higher percentage in overall mechanical losses, which overwhelmed the influence of CVT Supercharger system. At 1100 rpm, low load fuel consumption could be reduced by approximately 3.5% by turning down the pulley ratio from 4:1 to 1:1. At higher engine speed, for the similar reason mentioned above, the fuel saving became less prominent. Therefore, it suggested that it was a potentially effective way to reduce the mechanical losses of CVT Supercharger system by reducing the idle drive ratios of the pulley and epicyclic gear when the engine was running below boost line.

Unlike the positive displacement supercharger which is driven by fixed ratio, the CVT Supercharger system is able to meet the air boosting requirement with reduced pulley and epicyclic ratio relying on the CVT flexibility. However, a lower starting gear ratio would sacrifice the transient response since the maximum speed and acceleration of the supercharger will be reduced as well. The trade-off between the transient performance and the low load fuel economy will be investigated in the following paragraphs.

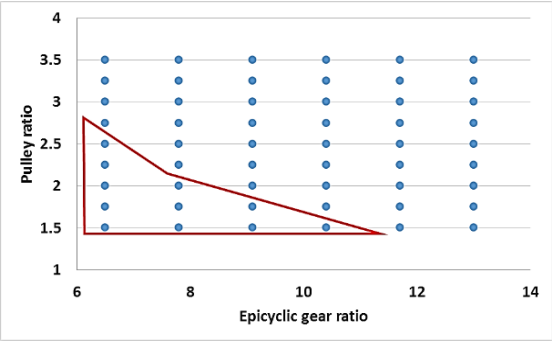

Figure 4.9. DOE data point of the drive ratio

A steady state simulation at 2 bar BMEP and a transient simulation have been carried out for a variety of pulley ratios and epicyclic gear ratios. As shown in figure 4.9, the sweeps for the two variables were from 1.5 to 3.5 and 6.5 to 13 respectively. A boundary limit for the DOE

(design of experiment) was set up for the compressor to provide sufficient boosting at full load steady state to fulfil the torque target. Therefore, the cases with the minimum pulley ratios and epicyclic ratios, as shown in the red polygon, were cleaned out.

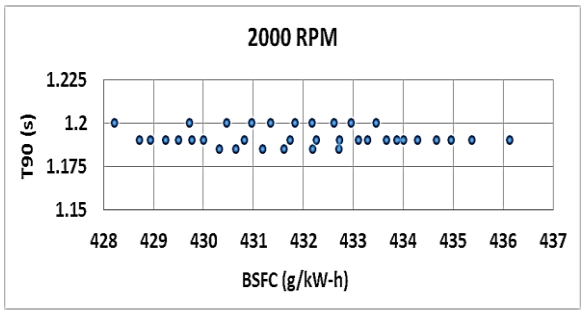

Figure 4.10. **The trade-off between T90 and BSFC at 2bar BMEP (2000rpm).**

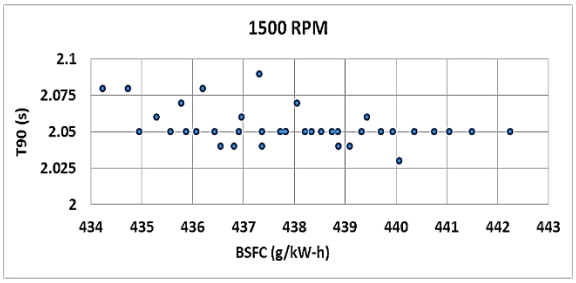

Figure 4.11. **The trade-off between T90 and BSFC at 2bar BMEP (1500rpm).**

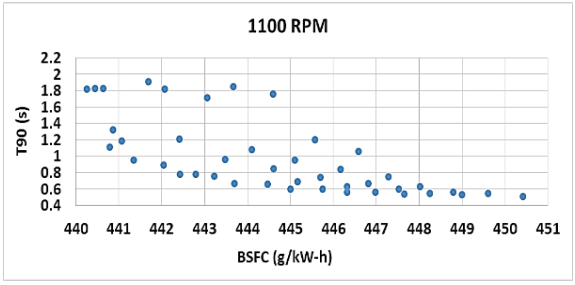

Figure 4.12. **The trade-off between T90 and BSFC at 2bar BMEP (1100rpm).**

The trade-off between T90 (response time of the engine system to raise brake torque from 0 to 90% of torque target) and BSFC at 2bar BMEP for different engine speeds (2000, 1500 and 1100 rpm) are illustrated in figure 4.10 to 4.12. By varying the drive ratios, a fuel consumption variation of approximately 2% could be found at all engine speeds in the simulation. At 1500 and 2000 rpm, the variation in T90 was smaller than 0.1 and 0.05 second respectively. At 1100

rpm, however, the response time varied in a much bigger scope sweeping from 0.5 second to 1.9 seconds.

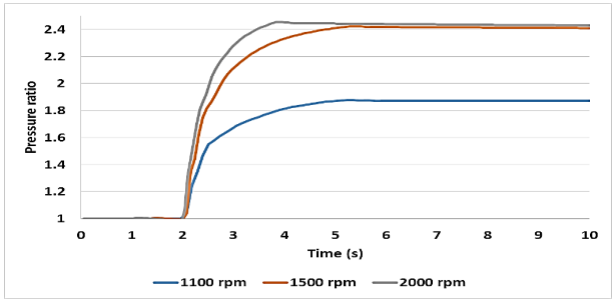

Figure 4.13. **Turbocharger responding time and pressure ratio.**

The larger variations of T90 at 1100 rpm were mainly due to the less contribution of turbocharger to air boosting. As figure 4.13 shows, turbocharger responded faster at higher engine speed providing higher boost pressure. It compensated the response delay to some extent and diminished the influence of CVT Supercharger drive ratio on T90 at the same time. Therefore, the trade-off between the low load fuel consumption and transient response existed mainly in the lowest engine speeds region particularly.

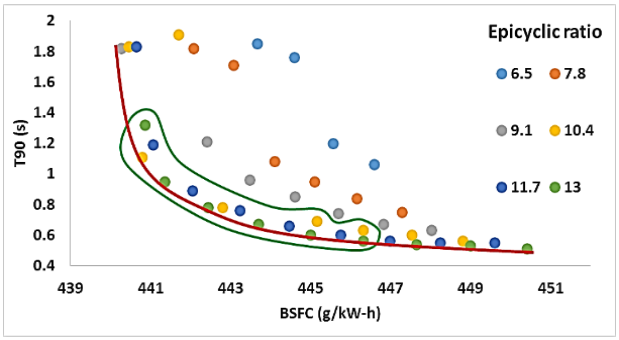

Figure 4.14. **Pareto front at 1100rpm.**

Figure 4.14 shows the Pareto front (the red curve) of the trade-offs between transient and fuel economy for the CVT Supercharger engine at 1100 rpm. The changes of epicyclic gear ratios were displayed in different colours. Operation points of each colour stand for the candidate pulley ratio, as shown in figure 4.9. The Pareto front was approximately a quadratic curve with decreasing slope stretching to larger fuel consumption. According to the fitting curve, the operating points in the green circle were regarded as the best compromising scenarios with respect to both T90 and low load BSFC. From the simulation results of the

chosen operation points, it generally cost 2% more fuel consumption at 2 bar BMEP to reduce T90 by 1 second on average. And also, it shows that the operations with higher epicyclic gear ratio, which took up most part of the Pareto front, were slightly more effective to convert fuel consumption into transient performance. In the end, it was decided to choose 12.57 and 2.4 for the epicyclic gear ratio and pulley ratio respectively for further research.

4.4.2 Optimization for Eaton clutch engagement time, CVT ratio and CVT ratio change rate

Before the transient simulations could be carried out for either the fix-ratio supercharger systems or CVT Supercharger systems, the engaging time for the friction clutch in Eaton supercharegr, and similarly, the maximum CVT ratio and change rate have to be regulated to shorten the response time of each system as much as possible without deteriorating the harshness. It should be noted that the combustion model were assumed to be the same as in the steady state simulation. Although this may not be realistic on real engine, the relative differences for the candidate systems were expected to be at the same level. In transient simulations, the engine load was kept to be about 10 Nm for 2 seconds before tip-in. For evaluation, response time to reach 90% of torque target (T90) was used as the metrics of transient performance. The comparison was based on the assumption that CVT Supercharger systems was not equipped with a clutch to disconnect the compressor for any operation. The compressor would be driven with the minimum CVT ratio, which is 0.28, when boosting is not needed. In this way, the control and packaging complexities were reduced while the transient performance of the whole system was expected to be improved. It, however, was at the cost of compromised fuel consumption at low load, which will be introduced in the later section.

In this study, the concept of “variator reaction torque” refers to the sum of input and output CVT torques. It was believed that, if a large spike appeared in the variator reaction torque curve (in terms of time), a dip would appear on the engine brake torque curve, which would eventually deteriorate the driveability. Therefore, the transient control strategy needs to be optimized to avoid violating that.

Specifically, if the spike of variator reaction torque appeared during the CVT was accelerating or the engine brake torque underwent a dip near the starting point, the CVT change rate should be reduced at that point. However, if the reaction torque exceeded after CVT reached

top speed or the dip appeared near the point of brake torque target, then the final CVT ratio needs to be reduced. This could be better explained by figure 4.15 and 4.16.

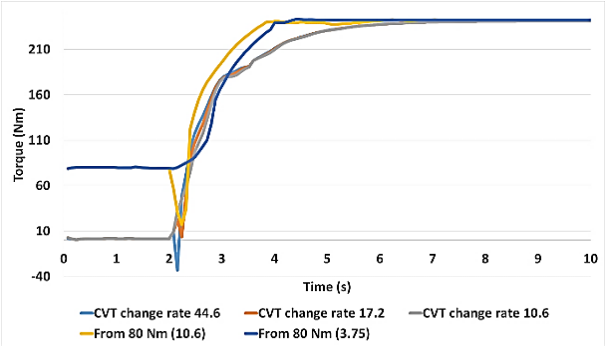

Figure 4.15. **CVT ratio change rate at 1500 rpm.**

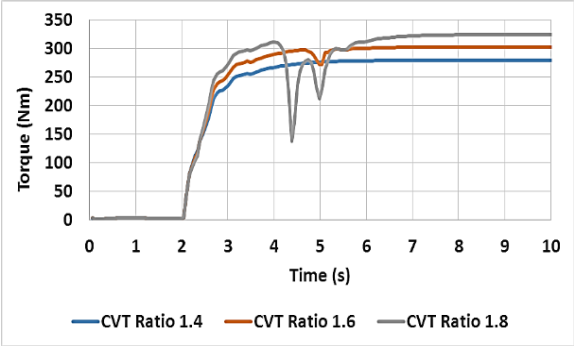

Figure 4.16. **CVT ratio at 2000 rpm.**

From figure 4.15, a dive appeared at the point when the engine brake torque started to increase from 10 Nm at 1500 rpm. By decreasing the CVT ratio change rate (refers to $|final\ CVT\ ratio - starting\ CVT\ ratio|/time$) from 44.6 per second to 17.2 per second and finally 10.6 per second, the dip was lightened and eventually flattened. It also shows that the magnitude of brake torque has not been affected since the final CVT ratio and thus the boost pressure were kept the same. The engine response speed showed a slight difference for different CVT change rate. However, because the transient was mainly dominated by turbocharger response which was much slower than throttle response and CVT Supercharger acceleration, the delay in final engine transient behaviour was almost imperceptible. It was also worth mention that the CVT ratio change rate should be further restricted for the tip-in operation from higher starting engine torque. For example, a severe dip was seen in the brake

torque curve when it started to shoot up from 80 Nm (40% throttle) with CVT change ratio of 10.6. It could be eliminated by decreasing the change rate below 3.75. This was because the faster throttle response could not be relied on to compensate the variator reaction torque in this case as it was already opened.

In figure 4.16, the dip was found near the target brake torque at 2000 rpm. It was filled up by decreasing the final CVT ratio from 1.8 to 1.4. Engine response was not affected while the maximum torque output decreased by approximately 50 Nm because of the reduction in CVT Supercharger boosting. It was worth mention that higher CVT ratios were allowed at lower engine speed because the parasitic load to engine was lower then.

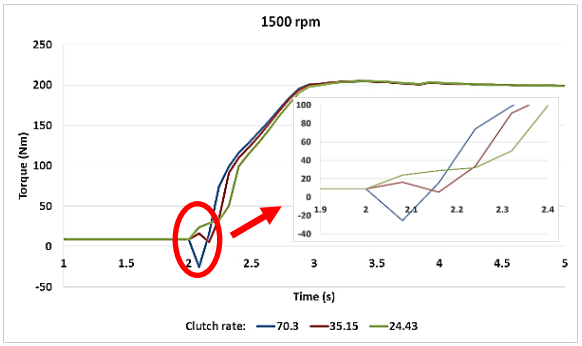

Figure 4.17. Clutch rate at 1500 rpm.

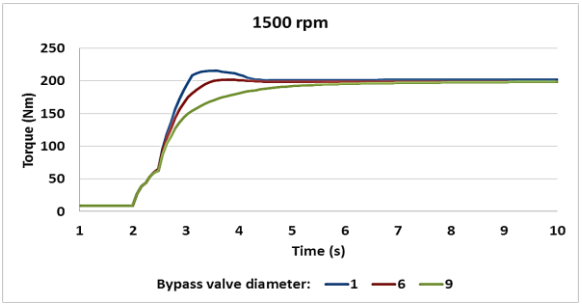

Figure 4.18. Bypass valve diameter at 1500 rpm.

The similar phenomenon was found in the Eaton system. At 1500 rpm, for example, higher clutch rate (refers to the supercharger gear ratio, which is 7.03, divided by clutching time) led to a descent of engine brake torque at the starting point of tip-in, as shown in figure 4.17. For a higher starting engine load, especially when the throttle was widely opened, those dips were more likely to appear, as the turbocharger could not accelerate fast enough to offset the

consumed brake torque. According to the simulation results, the highest clutch rate allowed was 24.43. Besides, optimization was also needed for the switching of the active bypass valve which was mounted parallel to supercharger. As figure 4.18 shows, a smaller bypass valve diameter would reduce the air circulation during boosting, and improve the response speed. At the same time, it might lead to overshooting in brake torque which was unfavourable to driveability. Therefore, a compromised diameter, which was 6 mm at 1500 rpm for example, needed to be determined.

Following the afore determined control strategy of the CVT Supercharger and Eaton system, the overall performance, including full load, part load and transient, of each engine system will be compared in the following section.

4.5 Results

4.5.1 Performance comparison between the CVT Supercharger and Eaton engine system

In this section, the influences of CVT Supercharger on engine performance, including full load, partial load and transient, will be analysed by comparing to the baseline fix-ratio supercharged engine. The study will focus on the low engine speed region below 2000 rpm. Actually, at 2000 rpm and above, turbocharger was able to provide sufficient boosting on its own for the engine to achieve the target BMEP. In order to minimise the mechanical losses, supercharger in Eaton system would be de-clutched, while the CVT Supercharger would be remain engaged but driven with the lowest CVT ratio. Consequently, the CVT Supercharger system might cause sacrifice to fuel economy at higher engine speed when comparing with Eaton counterpart, although the deficit was found minor (about 1%). Besides, as the engine is rarely running up to high speed in real driving, studies about the overall performance above 2000 rpm will not be included.

It also worth mention that, the CVT Supercharger system is able to raise the brake torque up to 240 Nm which is beyond the capability of the Eaton system. For the convenience of comparing the fuel economy of both, the torque target was limited to be 200 Nm for both systems.

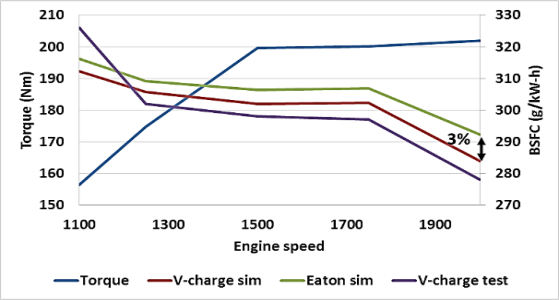

Figure 4.19. **Full load BSFC from simulation and real test.**

Figure 4.19 illustrates the full load fuel consumption of each system. It can be found that CVT Supercharger brought about 3% better fuel economy to the engine system when comparing with the positive displacement counterpart. It suggested that CVT Supercharger was capable to reduce the fuel consumption by eliminating the mass flow recirculation around the compressor, despite of the potentially higher mechanical losses of the integrated CVT.

The experimental results are also included in this graph showing a good correlation to the simulation data at 1250 rpm and upwards. The minor difference might come from the homogeneously over-predicted friction losses of the real engine. At the lowest engine speed, however, a greater divergence between test and simulation was found. It was speculated that it might be the combustion instability and turbo machinery inaccuracies at this challenging low flow conditions that cause the misfit. It suggests that the engine models may need further validation for better predictions of the real test at low speed. But, since the combustion model were assumed to be the same for both engine models, although this might not be realistic on real engine, it helped to keep the relative accuracy of the candidate systems at the same level, and made the simulation results comparable.

In addition, it could be predicted from the full load performance that the CVT Supercharger might embody further superiority in reducing fuel consumption at mid-high load operation when the supercharger is less needed to assist boosting. Furthermore, under “just boosted” condition, the greatest BSFC advantage over the fixed-ratio supercharged counterpart could be achieved since the CVT Supercharger was adjusted to approach the lowest speed at this point to provide the precise boost pressure as required and impose the least parasitic load to the engine. On the contrary, to provide the same boost pressure with the conventional

supercharger under this condition, the bypass valve must be wide opened to allow more circulated air flow, and thus causes much more losses. This prediction was proved by the results in figure 4.20. It shows that CVT Supercharger improves the fuel economy by up to about 40% at 16 bar BMEP when comparing with the conventional fix-ratio supercharged engine.

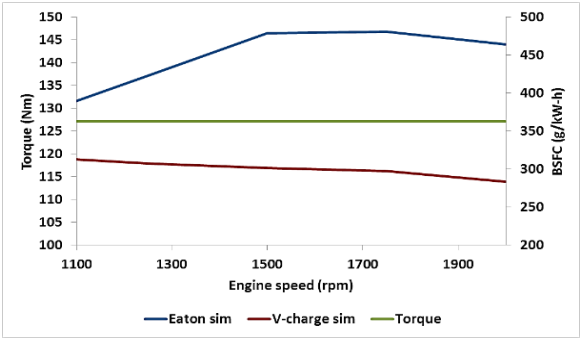

Figure 4.20. **BSFC at 16 bar BMEP.**

For the low load simulation, the fuel consumption of CVT Supercharger system was computed at 2 bar BMEP. The GT-Power models have been re-calibrated in accordance with the experiment data to make the comparison between the CVT Supercharger and the positive displacement supercharged model valid. For this operation, the CVT Supercharger system, which remained engaged, consumed more fuel than a de-clutched positive displacement compressor. As shown in figure 4.8, for the operation under extremely low load, CVT Supercharger consumed approximately 4.5% more fuel than the Eaton system did. Besides, as mention above, higher pulley ratio would worsen the fuel economy in a considerable scope (by up to 2%). Experimental data was also included in that graph, showing a better correlation with the calculated results. This could be explained by the less demanding on air charging devices, which diminished the erratic effects coming from turbine and compressor maps. The results suggest that a clutch might be needed for the CVT Supercharger system to regain the BSFC benefits at extremely low load operation. However, although the fuel consumption of CVT Supercharger would be reduced to the same level as the Eaton counterpart by adding a clutch, it will make the system less compact. The control strategy would become more complicated as well. Moreover, transient performance will be encumbered by the clutching

time. For the fix-ratio supercharged engine, actually, the supercharger usually needs to be engaged prior to tip-in to pre-boost the inlet air for better response speed, which will inevitably increase the system complexity and attenuate the advantages in fuel economy. It also should be noted that since the CVT ratio was remained the minimum for low load operation, CVT Supercharger imposed approximately the same parasitic load to the engine for any specific engine speeds. For higher load (but still turbocharged only), since the power consumption by CVT Supercharger took a smaller percentage of engine output, the BSFC deficit of CVT Supercharger system would descend further.

4.5.2 Driving cycle fuel consumption

For ease of analysis and comparison, the WLTP has been discretised into a number of steady-state 'Minimap' operating points. Each of these points represents a portion of the driving cycle, and holds a weighting equivalent to the proportion of the time that the engine is run at this speed, and load during the WLTP. In this section, the methodology of consolidated points was utilised to calculate the engine-level fuel consumption in WLTP driving cycle. Basically, this method reduced hundreds of operating points of the driving cycle into a dozen with least-squares method, as shown in Figure 4.21.

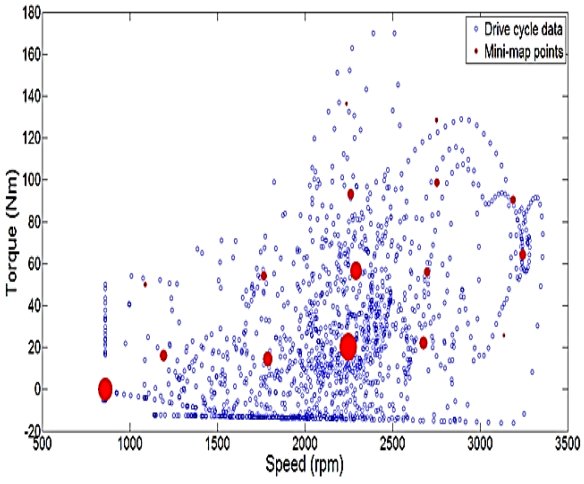

Figure 4.21. **Minimap for WLTC driving cycle.**

It has proved that the calculated fuel economy with this method showed satisfying correlation with the results from full driving cycle test with the computational efficiency being

significantly improved at the same time [159].

Table 4-1. **BSFC for WLTC driving cycle.**

Engine speed	CVT Supercharger BSFC (g/kW-h)	Eaton declutched BSFC (g/kW-h)	BSFC deficits	Eaton clutched (g/kW-h)	BSFC deficits	Weight (%)
1087	302.432	294.87	2.520738	345.89	-12.56	1
1193	462.918	440.43	4.937838	594.55	-22.13	4.8
1766	309.25	302.65	2.146536	372.46	-16.97	3.2
1787	498.268	474.37	4.872894	718.63	-30.66	8.2
2238	275.173	272.08	1.128246	303.72	-9.40	
2246	425.033	407.44	4.196151	609.35	-30.24	27.5
2261	275.896	271.43	1.625676	324.49	-14.97	5.3
2292	300.766	294.29	2.167047	370.81	-18.89	12.4
2677	432.261	414.51	4.162113	626.93	-31.05	6.1
2697	313.018	305.81	2.318934	395.69	-20.89	3.2
2749	277.882	274.40	1.257579	314.65	-11.68	2.2
2752	283.637	279.09	1.609935	335.04	-15.34	
3136	415.29	398.36	4.13184	582.13	-28.66	0.6
3189	291.274	286.11	1.782051	345.22	-15.62	
3244	310.694	303.62	2.29425	401.42	-22.60	3.7

The simulation results for WLTP driving cycle BSFC are shown in Table 4.1. 12 operating points were chosen for the simulation, representing 78.2% of the full WLTC driving cycle operation. It should be noted that because of the high divergence in fuel consumption, the idle condition was not take into account in this study despite of high weighting. From the results, the fuel consumption of CVT Supercharger engine was higher than the declutched fix-ratio supercharge system by up to 4.94% for WLTP driving cycle. When comparing with clutched fix-ratio supercharger, however, the fuel economy could be improved by up to 30.7%. By assigning weights to each of the operating points, the overall fuel economy of CVT Supercharger engine for the major part of the whole driving cycle was 2.74% worse than the disengaged positive displacement counterpart and 19.6% better than the engaged conventional supercharged engine.

4.5.3 Transient simulation

In terms of the transient simulation, the candidate models were started idling for 2 seconds

at 10 Nm brake torque for stabilization before the load demands were input. The experimental results were not included, because the specific control strategy adopted for boosting splits and thus the waste gate and CVT operation had significant effects on the transient characteristic which might result in unexpected discrepancies between simulation and test results. Moreover, since the objective of this project is to investigate the feasibility of CVT Supercharger as a candidate of better solution for engine downsizing, the investigation into the specifications of refinement and optimisation is out of the scope of this thesis. It is worth mention that the operation of the drive components in both systems, including CVT, pulley, epicyclic gear and clutch, were optimized based on the studies introduced in control strategy section.

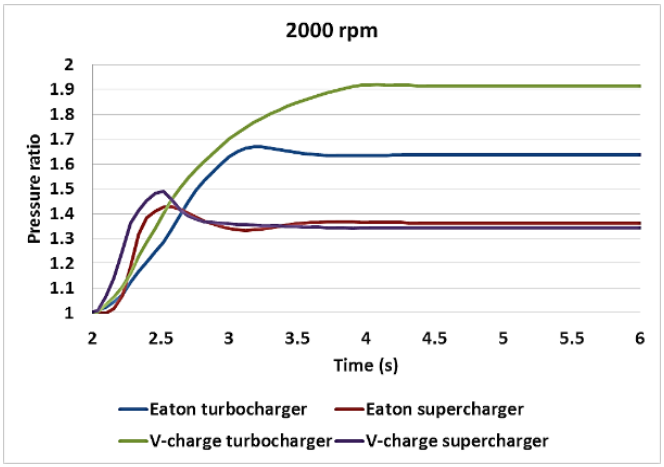

Figure 4.22. **Boosting response of the candidate systems at 2000 rpm.**

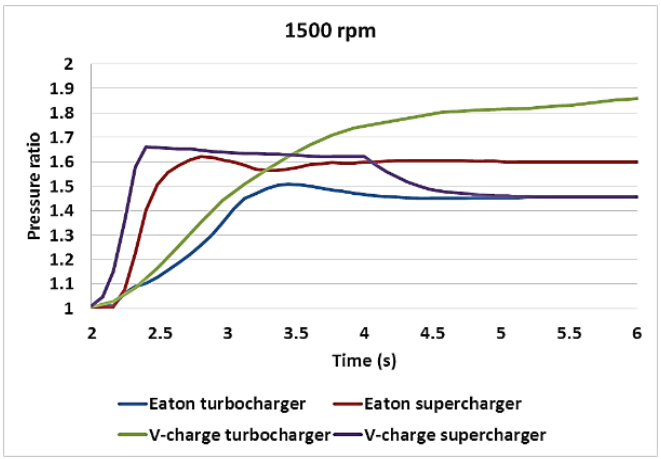

Figure 4.23. **Boosting response of the candidate systems at 1500 rpm.**

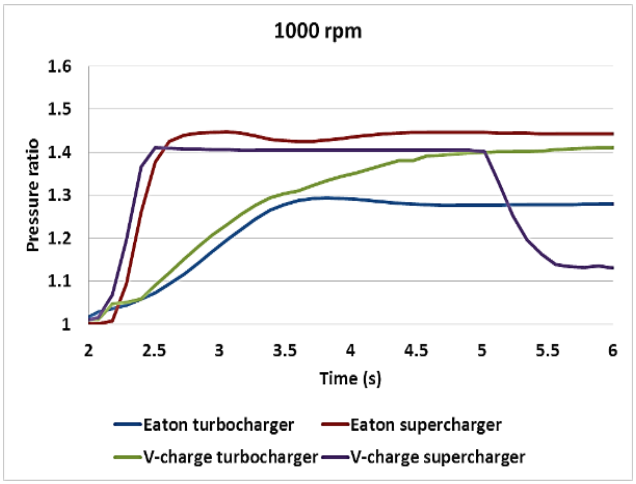

Figure 4.24. **Boosting response of the candidate systems at 1100 rpm.**

Figure 4.22, 4.23 and 4.24 illustrate the transient response of the air boosting devices of CVT Supercharger and conventional supercharger systems. It could be found that the responding time of CVT Supercharger system was about 0.15 second shorter than the fix-ratio supercharger. The faster increasing air mass flow from CVT Supercharger also helps to accelerate the turbocharger. That could explain the better response of the turbocharger in the CVT Supercharger engine. Besides, the pressure ratio of CVT Supercharger experienced an overshoot during the acceleration of turbochargers. As the turbochargers running faster, CVT Supercharger compressor decelerated gradually and handover the air boosting to the turbocharger without damaging the transient output, until the target load was achieved. At lower engine speed, CVT Supercharger was kept working with full power for longer time to help turbocharger to speed up, while at high engine speed when it was easier for the turbocharger to accelerate, CVT Supercharger handed over the boosting work sooner. This control strategy was to make full use of turbocharger and thereby to reduce the power consumed by supercharger. Besides, it could be found from charts 20 to 22 that the final CVT Supercharger pressure ratio was lower at higher engine speed since turbochargers take over more pressurization work. And also, because CVT Supercharger was able to slow down the compressor independently, the final pressure ratio of it is lower than that of the fix-ratio supercharger, especially at lower engine speed. This indicated that better fuel economy could be achieved by CVT Supercharger engine system.

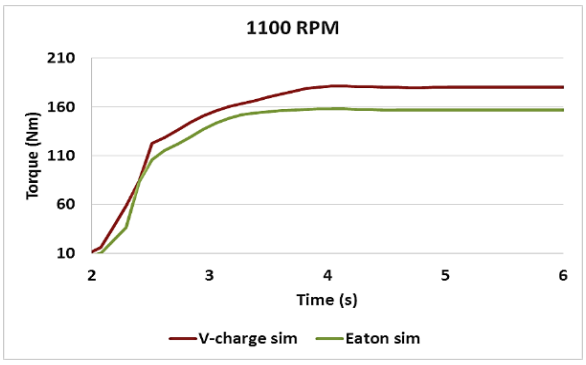

Figure 4.25. Transient performance at 1100 rpm.

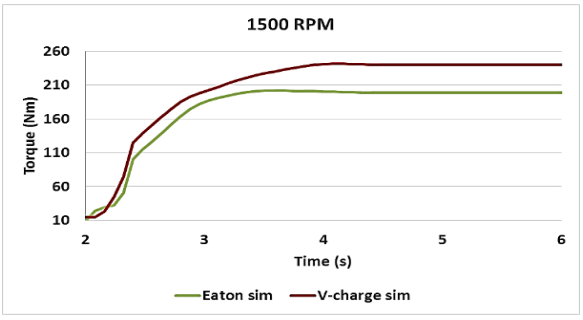

Figure 4.26. Transient performance at 1500 rpm.

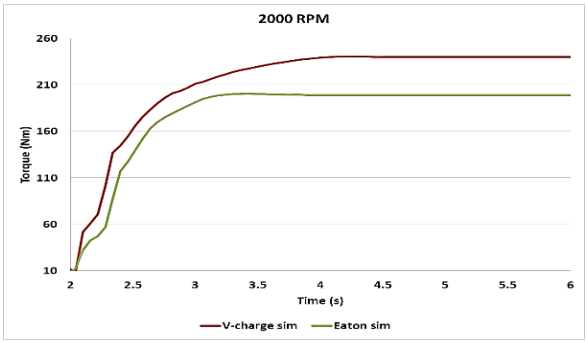

Figure 4.27. Transient performance at 2000 rpm.

Figure 4.25 to 4.27 demonstrate the transient performance of the whole engine systems at 1100, 1500 and 2000 rpm. From the results, the CVT Supercharger system enhanced the response speed of the baseline model by about 0.2 second at 1100 rpm. The results also show that the most significant improvement was found at higher engine speed. In the author's opinion, it is due to the higher level of participation of the turbocharger. The turbocharger in CVT Supercharger engine responded faster than that in conventional engine because of the

promotional impact of CVT Supercharger as mentioned above, the transient performance of the whole system is improved more with the synthetic effects from the two stage boosting.

4.6 Conclusion

This chapter compared the performance of turbo-super and super-turbo configurations to determine the location of CVT Supercharger compressor. Optimization of pulley ratio and CVT ratio change rate was presented regarding the tip-in operation from different starting load. The steady state performance of the whole system was evaluated by examining the fuel consumption at full load, part load and driving cycles. Transient performance was investigated by comparing to the baseline engine model.

1. Super-Turbo was proven to be a better configuration than the Turbo-Super counterpart for CVT Supercharger system in consideration of fuel economy, because the former imposed lower inlet temperature to the CVT Supercharger compressor. It also suggested that a two-stage intercooler was necessary for the Turbo-Super layout to achieve better thermal efficiency. Besides, the Super-Turbo configuration is proven to be easier for packaging and pipework routing in real test. Therefore, the Super-Turbo version is chosen in this study.
2. There was a trade-off between the low load fuel consumption and transient response at the lowest engine speed. For example, the engine would consume 2% more fuel at 2 bar BMEP to reduce the T90 by 1 second on average. Therefore, optimization has been done to determine pulley and epicyclic gear ratio to compromise the transient performance against fuel economy. The epicyclic gear ratio and pulley ratio was eventually determined to be 12.57 and 2.4 respectively for further research.
3. Because of the existence of variator reaction torque, the CVT ratio change rate and maximum CVT ratio of the CVT Supercharger system were restricted to avoid the dip in engine brake torque during tip-in operation. Similarly, the clutching speed and active bypass valve close rate of the conventional supercharger system were also limited to avoid the sharp decline and over-shooting in engine brake torque. Besides, a general trend

was found that the CVT change rate and clutching speed needed to be reduced further for higher starting load.

4. From the simulation results of the full load fuel consumption of each system, it was found that CVT Supercharger brought about 3% better fuel economy to the whole system when compare with the positive displacement counterpart. Furthermore, CVT Supercharger embodied further superiority at mid-high load operation when supercharger was less needed for assisting air boosting. At 16 bar BMEP, for example, CVT Supercharger was able to provide about 40% better fuel economy than the conventional fix-ratio supercharger did.
5. Under low load condition, when the CVT Supercharger is running with the lowest CVT ratio, approximately 4.5% more fuel is consumed than the Eaton system. Besides, it was consistent with the previous conclusion that higher pulley ratio will worsen the fuel economy in a considerable scope (by up to 2%).
6. A mini map was produced to imitate the WLTP driving cycle. From the results, the fuel consumption of CVT Supercharger engine is higher than the declutched Eaton system by up to 4.94% at extremely low load operation. When comparing with clutched fix-ratio supercharger, however, the fuel economy could be improved by up to 30.7%. By including weights to each of the operating points, the overall BSFC deficits for the major parts of all the operating points could be worked out that the fuel economy of CVT Supercharger engine was 2.74% worse than the disengaged Eaton and 19.6% better than the engaged Eaton system.
7. From the results of transient simulation, the CVT Supercharger system shorten the response time of the baseline twin charged model by about 0.2 second at 1100 rpm. It also demonstrates that the most significant improvement was seen at 2000 rpm because of the synthetic promotion from both CVT Supercharger and turbocharger.

Chapter 5 – System Verification of Variable Drive Supercharged engine System

As an alternative solution to the fixed ratio positive displacement supercharger, the CVT Supercharger variable ratio centrifugal supercharger utilizes a continuously variable transmission (CVT) coupled to a centrifugal compressor for near silent boosting. With a wide ratio spread of 10:1 and rapid rate of ratio change the compressor speed can be set independently of the engine speed to provide an exact boost pressure for the required operating points, without the need to recirculate the air through a bypass valve. A clutch and an active bypass valve can also be eliminated, due to the CVT capability to down-speed, thus improving the NVH performance. This chapter will present and discuss the experimental validation of CVT Supercharger technology on a GTDI Engine to achieve a better BSFC and transient response over the turbo only and the fixed-ratio positive displacement supercharger solution. The potential for the CVT Supercharger system to stretch the low-end torque and enable a down-speeding strategy is also discussed.

5.1 Introduction

In the simulation phase, as introduced in chapter 4, the CVT Supercharger variable ratio centrifugal supercharger was considered as an alternative to the fixed ratio positive displacement supercharger. This technology utilizes a continuously variable transmission (CVT) coupled to a more-efficient centrifugal compressor for near silent boosting. With a wide ratio spread of 10:1 and rapid rate of ratio change (within 360 ms) the compressor speed can be set independently of engine speed to provide the exact amount of mass flow for different engine operating points, without the need for wasteful recirculating of fresh charge. A clutch and an active bypass valve can also be eliminated, due to the CVT capability to down-speed which also mitigate the issues of cost, complexity and package and at the same time greatly improve the NVH situations [159]. From the simulation results, it comes to the conclusion that CVT Supercharger technology was effective in improving the low-end torque output and fuel economy (especially for middle high load operation). In terms of transient performance, it was

suggested that the CVT Supercharger system could provide faster response speed when compares with its fixed-ratio positive-displacement supercharger counterpart. It was especially true for the simulation at low engine speed.

Since the computational simulation results may not accurately reflect the real test performance, a test rig has been built to investigate the benefits that the CVT Supercharger system could actually achieve.

5.2 Scope and Objectives

In this phase, the novel boosting systems is applied to a 1.0 L turbocharged engine [169] aiming to achieve an enhanced target torque and power curve (see Figure 5.1).

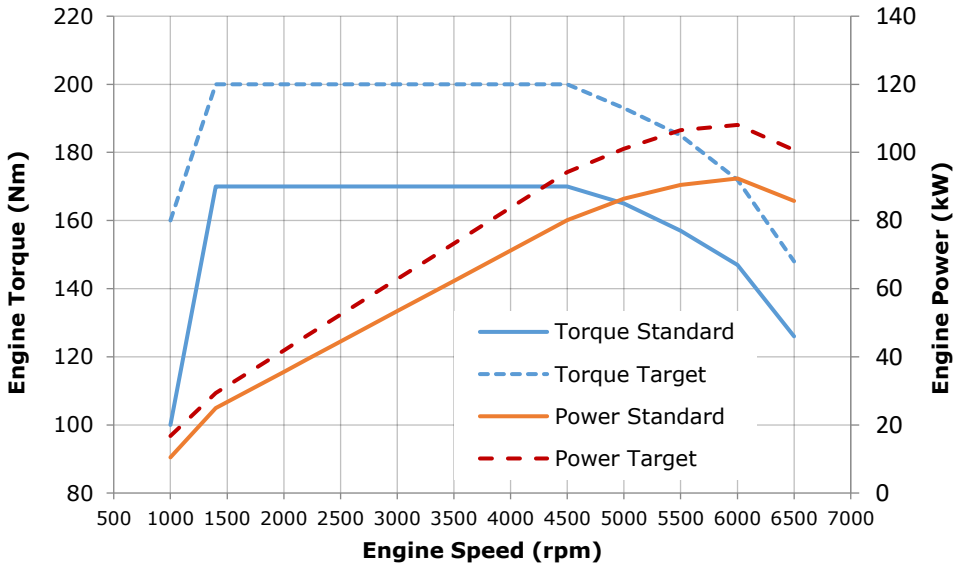

Figure 5.1. Original standard and targeted engine performance.

A larger Honeywell turbocharger is fitted to match the power at the high end, while the supercharger system is utilized to improve not only the transient performance but also the low-end torque, since a large torque difference exists between high and low engine speed which may cause a perceived turbocharger lag during vehicle launch even with adequate boost system response [174]. The objective in this chapter is to assess the performance of a centrifugal-type supercharger system which is driven by a Torotrak continuously variable

transmission. The results are compared against a fixed-ratio positive-displacement supercharger solution.

5.3 Control Strategy Implementation

The control strategy was also initially constructed in the simulation phase. In order to easily access the engine sensor measurements for use in the two-stage boosting control strategy, an aftermarket OpenECU was used in combination with the OEM development engine ECU.

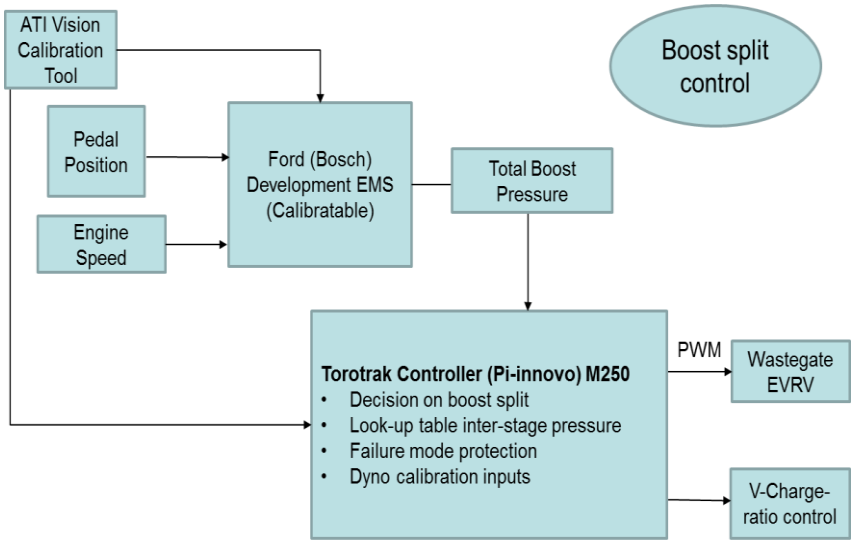

Figure 5.2. **Boost split control module.**

For the details of control sequence, as shown in Figure 5.2. The ECU will first receive the pedal position and engine speed signals from the driver to calculate the demand total boost pressure, and will then determine the boost split (feed-forward loop). Finally, a feedback control loop is required to correct the demand boost pressure to the target, under different boundary conditions (or, in other words, a different altitude) or component ageing.

Since the open ECU adopted in this project can be compiled in a Simulink environment, a near-to-complete control strategy was initially built in Simulink and transferred to the open ECU developer platform in the experimental phase.

The proposed CVT Supercharger speed control module (see in Figure 5.3) is made of several sub-systems, including a feedforward steady-state look-up table and a feedback loop on intake manifold pressure.

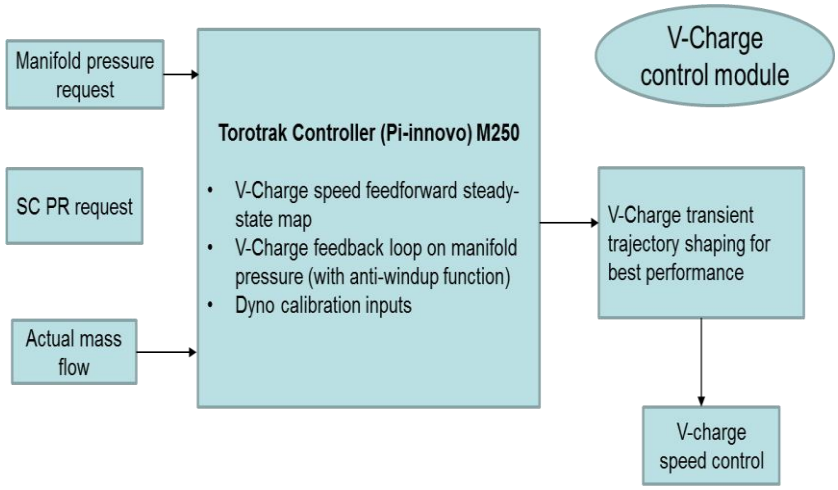

Figure 5.3. **CVT Supercharger speed control module.**

The feed-forward loop, which is basically a look-up table, is designed to help the controller to achieve the target boost split quickly and robustly. It might be noted that the control strategy currently adopted in this work is characterised of minimizing mechanical boosting in the interests of efficiency. It aims to achieve the highest possible utilization of the turbocharger, and the supercharger only assists when the turbocharger is unable to provide adequate flow at low engine speeds and during transient events.

The feedback control includes an anti-windup function and a gain scheduling strategy. The functions include adjusting the CVT Supercharger speed so that the total boost pressure can be achieved if the feed-forward loop is not working precisely (due to component ageing or different boundary condition) and detecting a transient signal in order for the supercharger to 'pre-boost' the engine system.

It might be worth noting that two look-up maps (i.e. upper and lower CVT Supercharger speed rate limiter) were used to optimize the transient trajectory shaping for the best CVT Supercharger performance, which was from the perspective of physical response behaviour, and also the driveability consideration. In according with the simulation results, it is found in test that the largest achievable CVT change rate might not be appropriate to implement during a transient event, due to the 'dip' phenomena (it is shown in section 5.4.2). Furthermore, whether the torque dip (if there is any) could be 'felt' by the driver is another question, which

also needs to take into consideration the damping effect of the whole powertrain system (and is thus beyond of the scope of this research).

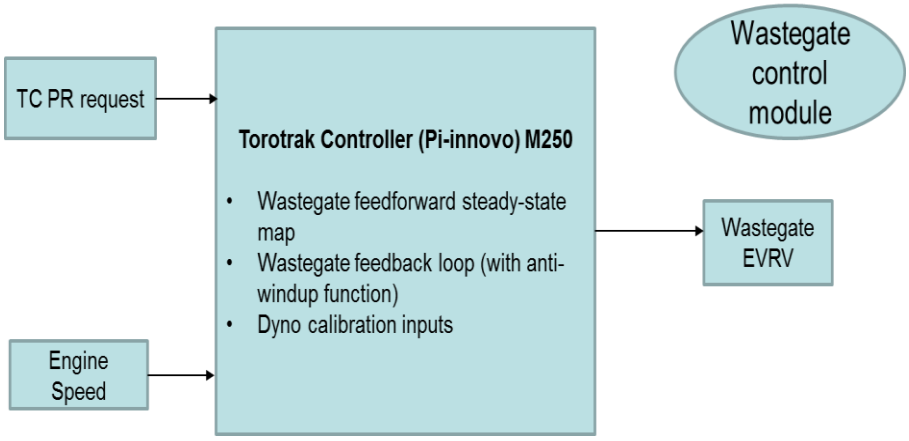

Figure 5.4. **Wastegate control module.**

In order to accurately control the boost split in the two-stage system, the standard closed-loop pneumatic mechanism was replaced by a 'smart' pneumatic wastegate mechanism with electronic control. Figure 5.4 shows the wastegate control module that was proposed for the CVT Supercharger project. It is, like the CVT Supercharger speed control discussed above, was comprised of two main sub-sections of controlling: feed-forward and feedback loop. There is also an anti-windup loop in the wastegate control module. Note that the PI controller input for the wastegate control is the turbocharger pressure ratio difference between the target and the actual, and that for the CVT ratio control is the total boost pressure difference between the target and the actual. This is for the purpose of avoiding the conflict between the two interdependent PI controllers.

5.4 Experimental Setup

The test was carried out in an engine test cell at University of Bath (see Figure 5.5). The system set up and measurement details are shown in Figure 5.6. In the facility, the ECU calibration software ATI Vision is communicated with the host system CP Cadet via an ASAP3 link for the easiness of record and monitoring. ATI Vision is also communicated with the ECU via a CAD Calibration Protocol (CCP).

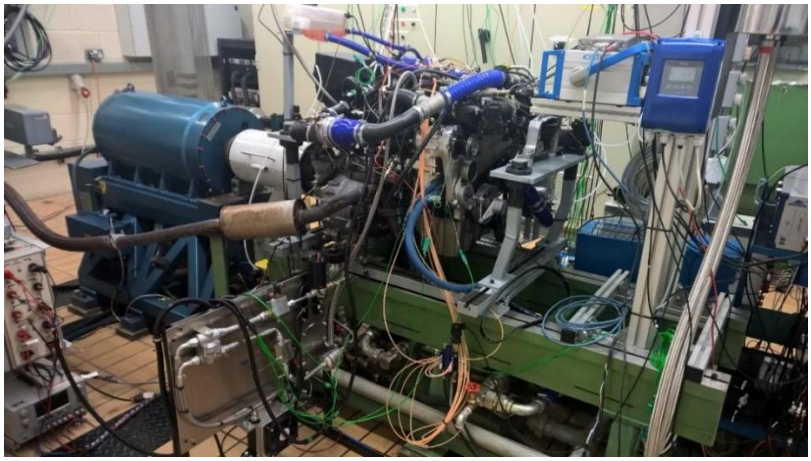

Figure 5.5. Test cell at University of Bath.

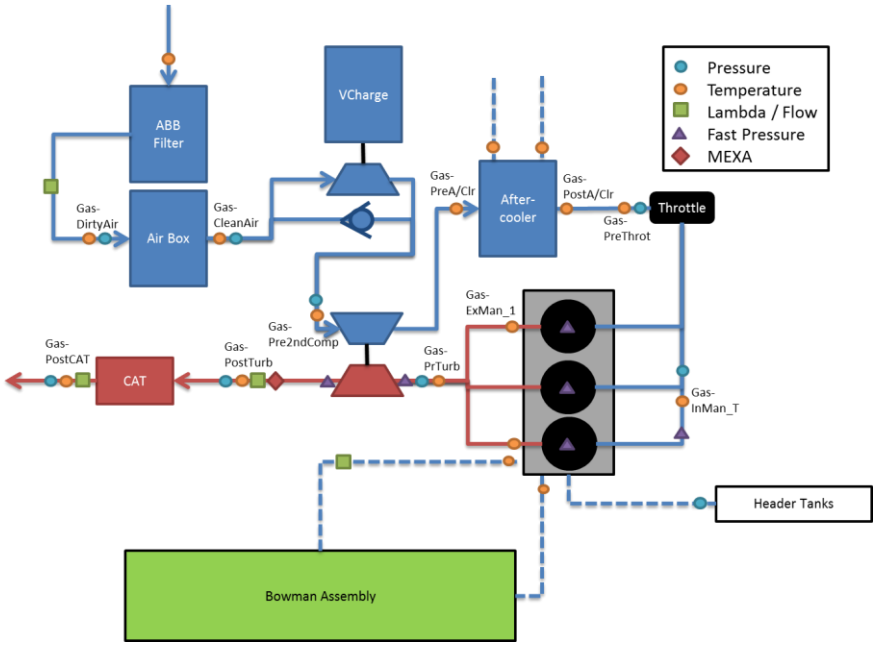

Figure 5.6. System schematic and measurement locations.

The experiments were conducted on a 1.0 L, three-cylinder, gasoline turbocharged direct injection (GTDI) engine with variable intake and exhaust-valve timing system [169]. The Torotrak CVT Supercharger system, which is comprised of a pulley step-up gear, a CVT mechanism and an epicyclic gear as shown in Figure 4.2, was directly connected to the engine crankshaft via a conventional micro-V belt, and in this proof of concept installation is achieved with a separate additional pulley. This is mounted alongside the standard fit FEAD pulley as shown in Figure 5.7. For a production integration the supercharger could be driven by an

upgraded FEAD belt, reducing the losses associated with an additional belt driven system.

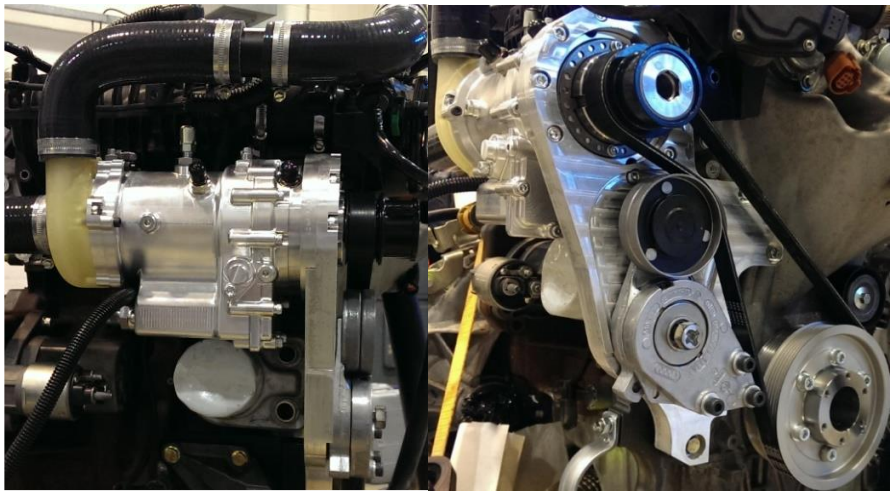

Figure 5.7. **CVT Supercharger system installation.**

Figure 5.8. **Check valve configuration.**

A check valve seen in Figure 5.8 was mounted around the CVT Supercharger compressor to act as a passive bypass valve in order to bypass the compressor when the CVT Supercharger compressor is not able to provide the required mass flow rate. It should be note that the rig for this work was built by the engineers of PVRC.

In order to have wide operating range and precise control of the engine boundary conditions, the cooling circuit for the engine coolant and oil were replaced with an external water-to-

coolant heat exchanger. In addition, an aftercooler was replaced by a water-to-air heat exchanger. Therefore the temperatures of the engine coolant, oil and engine intake air could be controlled by varying the water flow rate in each heat exchanger. In this test, before logging the test data, the engine coolant, oil and aftercooler temperature was kept around 90 degC, 100 degC and 45 degC.

5.4 Results and Discussions

5.4.1 Steady-state engine performance

The aim of this test was to understand how the CVT Supercharger may best influence engine performance and fuel economy and to build a robust control strategy using the steady-state experimental data. The work will focus on the low speed region which is considered most important a limiting in terms of maximum steady state BMEP and transient response.

5.4.1.1 Full Load performance:

The simulation and verification test activities have initially focussed on a modest increase of maximum steady state output torque, from circa 170Nm to 200Nm (see Figure 5.1).

In light of the pursuit of higher BMEP's to facilitate more aggressive downsizing and fuel economy benefits, an additional stretch torque target of 240Nm was specified, which reflects the output of the current 1.5 L 4 cylinder turbocharged engine. This steady state target for the 1.0L turbocharged engine equates to more than 30bar BMEP.

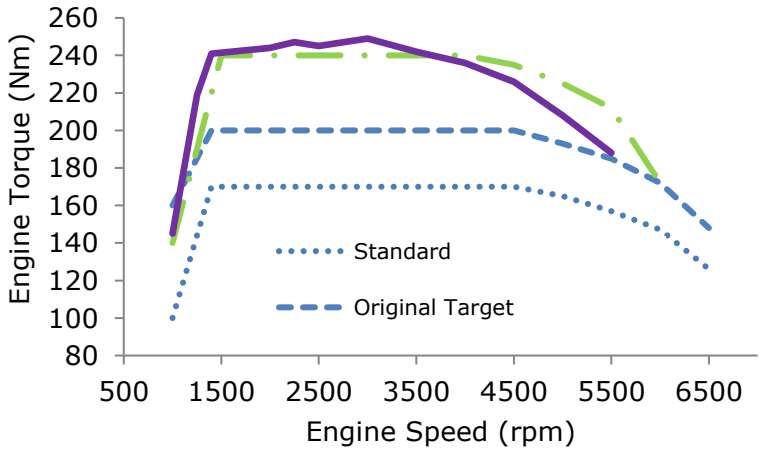

Figure 5.9. Engine torque output comparison.

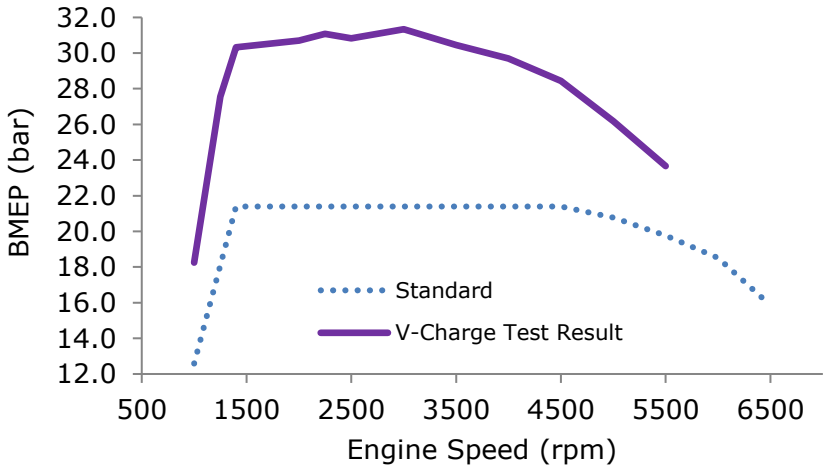

Figure 5.10. **Engine BMEP comparison.**

As can be seen in Figure 5.9 and Figure 5.10, the test results for the CVT Supercharger system demonstrates that the stretch torque target is achieved across much of the engine operating range. This is realised within safe combustion limits with headroom to potentially increase output further still.

The original target output at 1000rpm is not quite reached for steady state operation, with 145Nm achieved vs a 160Nm target. Transient torque capability at this speed is ~200Nm before falling back to 145Nm after a few seconds. This appears to be caused by the onset of turbocharger surge, which is always being monitored, and may be remedied by adopting a TurboSuper arrangement rather than the SuperTurbo configuration pursued in practical testing. Optimising turbocharger trim may also help with this limitation.

From approximately 4000rpm, there is a noticeable downturn in torque earlier than might be expected. This reduction corresponds with increasing post turbine back pressure, and is believed to be caused by the restriction of the original turbocharger exhaust downpipe and catalytic convertor, which are now being subjected to significantly higher exhaust flow rates. Reducing this restriction by a larger bore downpipe and converter is likely to realise more torque at higher speeds, and a reduced downturn characteristic.

It should be noted that the superior transient response of the CVT Supercharger equipped engine particularly at lower engine speeds will result in significantly improved driveability over

the standard 1.5L turbocharged unit, something that the steady state torque graph cannot reflect.

The level of engine brake torque achieved also alleviates the requirement of scavenging: a common approach to improve low-end torque of a direct inject turbocharged gasoline engine [176]. This will either aid minimising the engine-out emissions [175] or reduce catalyst exotherm when operating with stoichiometric exhaust [177].

5.4.1.2 Low load performance

The fuel consumption of CVT Supercharger system was tested under a low load condition of 2 bar BMEP. The GT-Power model has been re-calibrated in accordance with the experiment results to make the comparison between the CVT Supercharger and positive displacement supercharged models sensible.

It should be note that sources of inaccuracy do exist in this condition downgrading the calibration. It includes the lack of combustion and friction parameters of the engine and the fluctuation of the turbine performance at extreme low speed and pressure ratio.

The first target in this stage is to make the breathing of the engine model coincident with the test results. Specifically, the air pressure and temperature should be unified between simulation and experiment. There are a number of specifications, including intake valve timing, cylinder convection and friction factor and anchor angle, in GT-Power affecting the characteristics of the intake and exhaust gas.

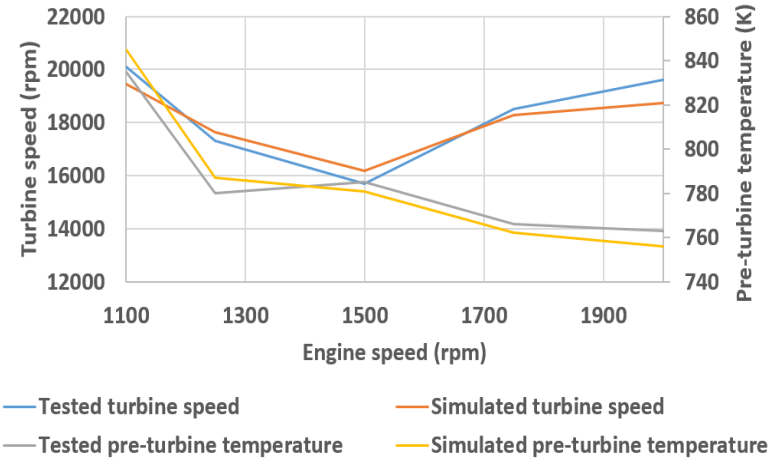

Figure 5.11. Tested and simulated turbine speed and pre-turbine temperature.

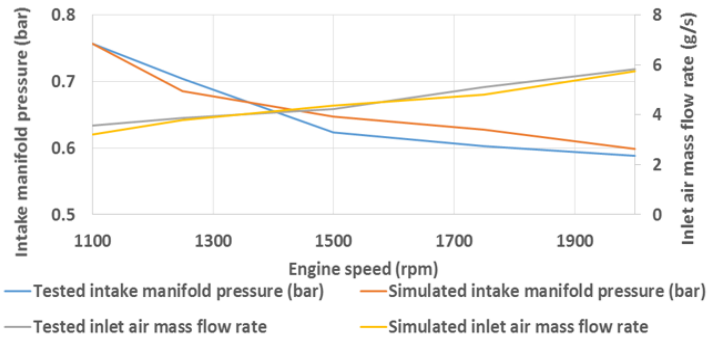

Figure 5.12. **Tested and simulated inlet air mass flow rate and pressure.**

From figure 5.11 and 5.12, the simulated inlet air pressure and mass flow rate and the exhaust temperature show good matching to the experiment results after validation. The maximum difference is found in the intake manifold pressure, which is less than 4 %.

The simulated and measured BSFC of the CVT Supercharger system shows good coherence as well with a maximum discrepancy less than 0.7%. Figure 5.13 also illustrates that the positive displacement supercharged engine is advantageous in fuel economy under low load. The specific fuel consumption declined by up to 4.9%, since the supercharger could be declutched to remove the mechanical losses. The influence of pulley ratio on the CVT Supercharger engine fuel consumption is also included in figure 5.13, which demonstrates that the fuel consumption increases prominently with higher pulley ratio setting, especially when the engine was operated at lower speed, or the pulley ratio was above 2.5.

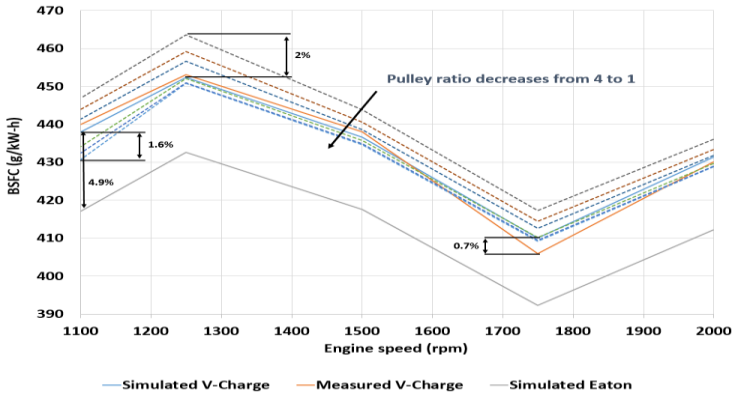

Figure 5.13. **Tested and simulated brake specific fuel consumption.**

5.4.1.3 WLTP driving cycle:

The compressor of the Eaton configuration usually needs to be disengaged at low load,

especially when a large drive ratio is installed. However, the CVT Supercharger system could trade some fuel efficiency at low load for better transient behaviour by constantly connecting the compressor to the engine crankshaft with its minimum ratio.

As there was a passive bypass valve installed, only one-way flow is allowed. If the CVT ratio is sufficiently low, there would be some pressure drop across it that force the bypass path to open, which will then results in the supercharger PR to be around 1.

According to the test data that sweeps the engine torque from very low to the largest within the NA line using the minimum CVT ratio, it can be seen that the supercharger PRs were all around 1 that indicates that at the minimum CVT ratio, the supercharger could not supply sufficient mass air flow without the assistance of the bypass valve. From the perspective of boosting, it also shows that the minimum CVT ratio could not generate a valid PR that boosts the intake air, consuming much power.

It is known that if the PR and the speed of a compressor is about the same, the power consumed to drive the compressor should also be similar. Thus, it is safe to say that for different engine operating points at the same engine speed, the parasitic losses are around the same. As there was no mass air flow sensor mounted in the supercharger path, the power consumed will be calculated in the validated simulation model in this work.

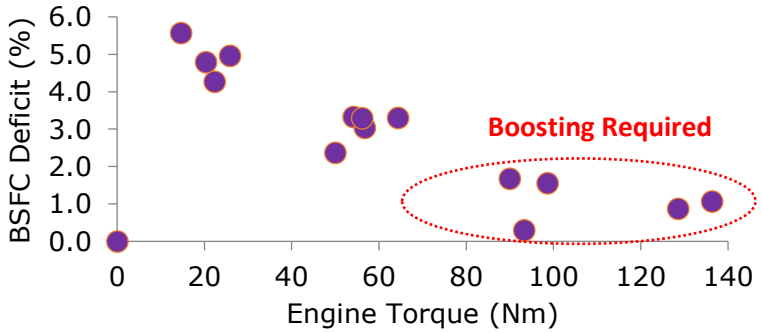

Figure 5.14. **WLTP driving cycle with Minimap.**

The simulation showed that at 1000RPM, only approximately 60W was wasted to constantly connect the supercharger compressor to the crankshaft, the ratio of the consumed power to the engine power being around 2% at low engine load (below 30N*m). At higher engine speed, a similar situation was observed. Figure 4.21 shows the engine operating points for a D-segment vehicle on a WLTP driving cycle with the calculated weighted Minimaps. The test results with these Minimap points can be seen in Figure 5.14, with the maximum BSFC deficit

around 5.5% and descending with higher engine torque. It should be noted that the BSFC deficit was calculated by the configuration of the CVT Supercharger with its minimum CVT ratio compared with the counterpart with the CVT Supercharger pulley off. The discrepancy of the simulation and test might be the underestimation of the pulley parasitic loss.

In order to reduce these parasitic losses, a novel approach was proposed that just takes the bypass valve out of the system. This so called 'wind milling' effect will force the PR of the supercharger to be below 1 at low loads, resulting in the energy flow to be reversed, in order to offset some of the parasitic transmission losses. However, if the CVT Supercharger control calibration is considered, the use of a passive bypass valve will be beneficial. This is mainly due to the fact that, at low load within the throttled region, the configuration with a bypass can constantly keep the CVT ratio at its minimum, while for the system without a bypass valve, the CVT ratio might need to be tuned to supply the required mass air flow (the parasitic losses will also be increased along with the durability of the CVT) [178].

Also it should be noted that compared to the standard engine configuration with a smaller turbocharger, the CVT Supercharger system, featuring a larger one, is potentially able to reduce its part load BSFC by approximately 2% due to its reduced backpressure [174].

Compared to the fixed-ratio positive displacement counterparts which often have to fit an active bypass (and a clutch) to reduce the parasitic losses at part load, the CVT Supercharger system only needs a passive bypass valve that can significantly reduce the control strategy calibration efforts and cost.

5.4.2 Transient performance:

Table 5-1. Control strategy calibration

VC operation / VC acceleration	Long	Medium	Short
Fast	**1**	2	3
Medium	**4**	5	**6**
Slow	7	8	9
Turbo-only			

After determining the boost pressure split and populating the control map, some transient

tests were conducted, with and without the assistance of CVT Supercharger system. Figure 5.15 to Figure 5.17 show the transient torque performance at 1100RPM, 1500RPM and 2000RPM respectively, under four distinctive control calibrations. There are two parameters that are used to define the CVT Supercharger speed trajectory in a transient: CVT Supercharger speed change rate and CVT Supercharger operation period. They are termed as VC acceleration and CV operation respectively in table 5.1. It might be noted that unlike the CVT Supercharger speed change rate which could easily be defined as a rate limiter in the control strategy, the CVT Supercharger operation period has to be determined by the transient behaviour of the turbocharger (thus an empirical turbocharger plant has been modelled). By advancing or delaying the turbocharger transient model, different CVT Supercharger operation period could be defined. In order to illustrate how different control calibrations work, test 1, 4, 6 and turbo-only in Table 5.1 corresponding to 'Fast VC with dip', 'Overlength VC operation with overshoot', 'Best time to torque' and 'Turbo only' were shown in the following.

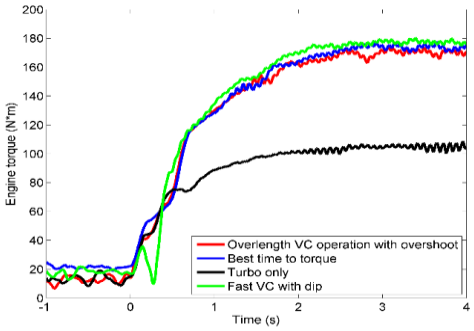

Figure 5.15. Transient torque performance at 1100RPM

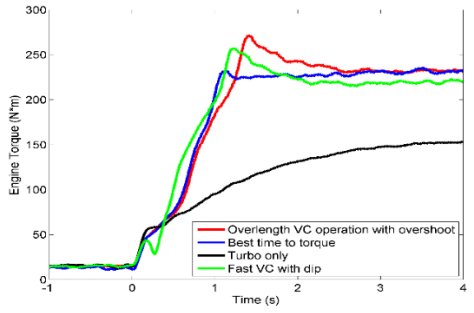

Figure 5.16. Transient torque performance at 1500RPM

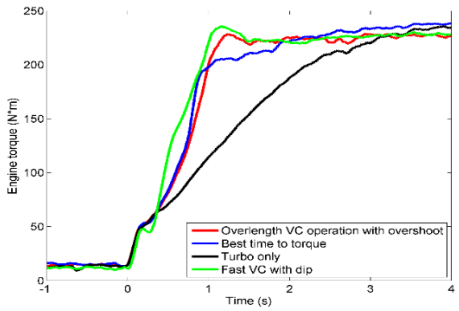

Figure 5.17. **Transient torque performance at 2000RPM**

It can be seen that compared to the turbo-only case, the system fitted with the CVT Supercharger system not only has the capability to enhance the final engine torque, but also characteristics significantly improved time-to-torque performance, although different control calibrations will result in different torque trajectory. In order to understand the interactions between the two boosting systems and the engine itself, a more detailed illustrations at a fixed 2000RPM tip-in from 10% pedal position was shown in Figure 5.18.

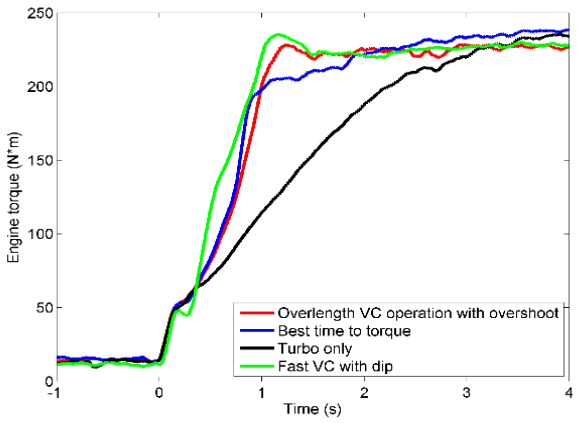

(a)

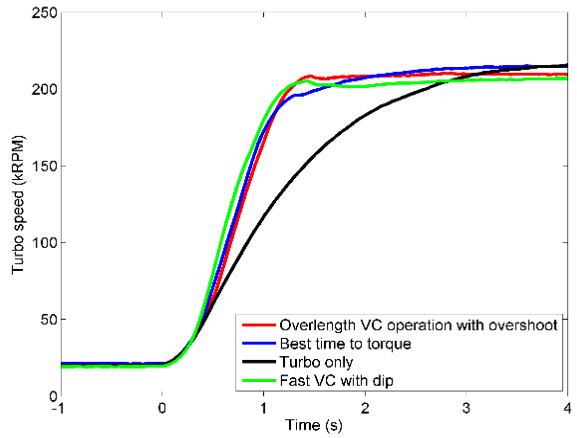

(b)

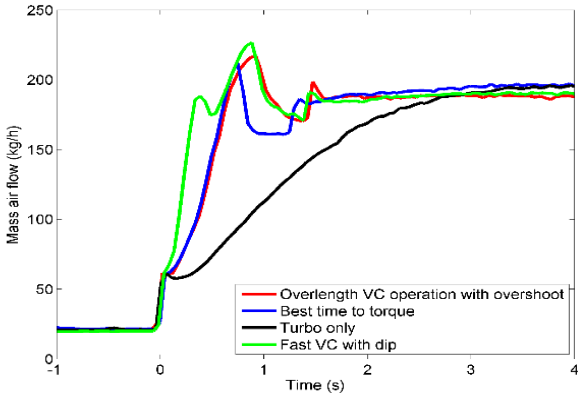
Mass air flow (kg/h)
Time (s)
Overlength VC operation with overshoot
Best time to torque
Turbo only
Fast VC with dip

(c)

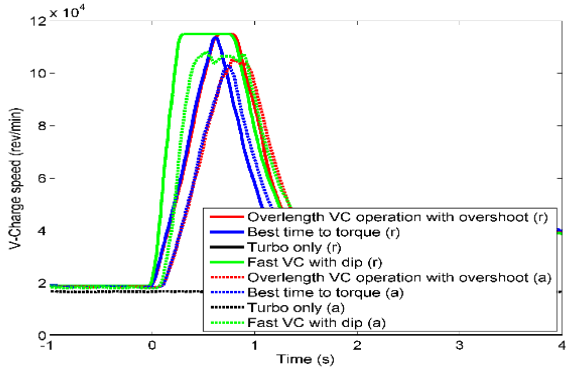
x 10^4
V-Charge speed (rev/min)
Time (s)
Overlength VC operation with overshoot (r)
Best time to torque (r)
Turbo only (r)
Fast VC with dip (r)
Overlength VC operation with overshoot (a)
Best time to torque (a)
Turbo only (a)
Fast VC with dip (a)

(d)

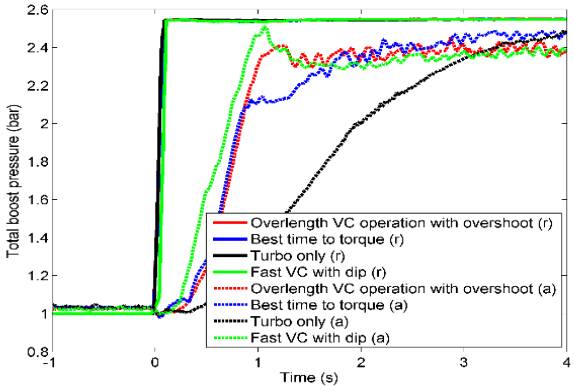
Total boost pressure (bar)
Time (s)
Overlength VC operation with overshoot (r)
Best time to torque (r)
Turbo only (r)
Fast VC with dip (r)
Overlength VC operation with overshoot (a)
Best time to torque (a)
Turbo only (a)
Fast VC with dip (a)

(e)

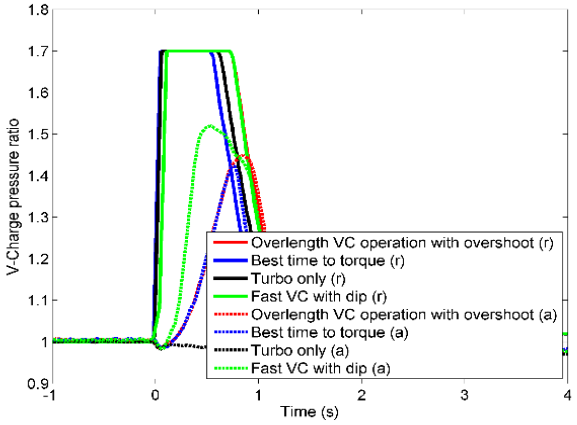
V-Charge pressure ratio
Time (s)
Overlength VC operation with overshoot (r)
Best time to torque (r)
Turbo only (r)
Fast VC with dip (r)
Overlength VC operation with overshoot (a)
Best time to torque (a)
Turbo only (a)
Fast VC with dip (a)

(f)

(g)

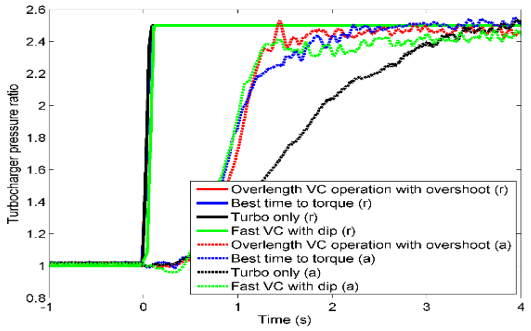

(h)

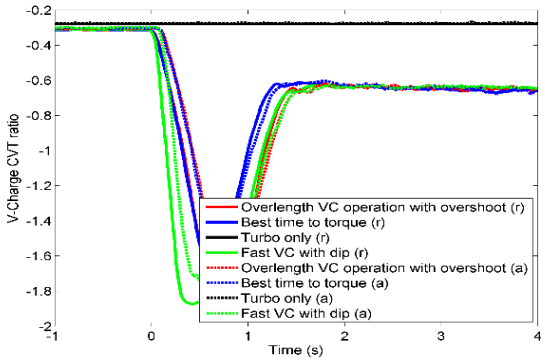

Figure 5.18. **Transient trajectories at a fixed 2000RPM from 10% pedal position:(a) Engine torque; (b) Total boost pressure; (c) Mass air flow; (d) Turbocharger pressure ratio; (e) Turbo speed; (f) CVT Supercharger pressure ratio; (g) CVT Supercharger speed; (h) CVT Supercharger CVT ratio**

From Figure 5.18 (a) (b) (c) it can be seen that the CVT Supercharger system, compared to the turbo-only counterpart, can improve the time-to-target performance by approximately 70%, making it behave more like a naturally aspirated engine. Compared to the other calibrations, the case with the fastest CVT Supercharger CVT ratio change rate characteristics an engine torque dip during the first phase of the transient which might influence the vehicle's driveability.

If test 4 (marked Overlength VC operation with overboost) and test 6 (marked Best time to torque) have been compared (see from Figure 5.18 (a) (f)), it can be seen that they do broadly the same thing when the CVT Supercharger is ramping on but test 6 is ramping off earlier. The result is a faster time to torque behavior and no apparent overshoot for test 6. There must be a point in the ramp where the CVT Supercharger takes more than it gives back during the end of the transient, due to the fact that mass air flow is increasing as manifold pressure builds so

CVT Supercharger uses more power to maintain pressure.

Figure 5.18 (d) (e) show the turbocharger compressor behavior during the transient. During the first phase of the tip-in, the turbocharger compressor pressure ratio of the 'Fast VC with dip' case was slightly below 1, due to the fact that the supercharger accelerates much faster than the turbocharger compressor (thus generating higher pressure ratio between the two boosting systems). This 'dip' pressure then helps the acceleration of the turbocharger compressor and makes its pressure ratio higher than the other two CVT Supercharger control calibrations and the turbo only setting. The supercharger's capability to enhance the turbocharger's power was also seen between the 'Best time torque' case and the 'Overlength VC operation with overshoot' case, where the turbocharger speed and pressure ratio was increased with the prolonged operation of the CVT Supercharger system during the end of tip-in.

The behavior of the CVT Supercharger system can be seen in Figure 5.18 (f) (g) (h). Compared to Figure 5.18 (d) (e), the boost split between the supercharger and the turbocharger during a transient can be illustrated: the supercharger pre-boost the engine at the start of a transient and then hands over the boost to the turbocharger while the turbocharger spools up.

It should be noted that the objective of this project is to demonstrate the CVT Supercharger's feasibility as an alternative solution to achieving a highly downsizing concept, thus the tuning of the control strategy which includes the refinement of the feedforward and feedback control is out of scope of this thesis The performance of the CVT Supercharger system could be further improved if a considerable effort of calibration was conducted.

Compared with the fixed-ratio positive displacement solution, due to the capability to be constantly connected with the engine's crankshaft, the CVT Supercharger system does not need a clutch resulting in significantly improved NVH performance during a transient. Also the necessity to disengage the supercharger for the fixed-ratio positive displacement configuration at higher engine speed (due to over-speeding) also affects the driveability consistency. Last but not least, the characteristics of the positive displacement compressor make it mandatory to include a noise attenuation device which is not necessary for the CVT Supercharger system.

It might worth noting that the optimized CVT Supercharger transient speed trajectory from different engine load should be set differently and the trend is that for a higher starting engine torque, a slower CVT Supercharger speed acceleration rate needs to be used, in order to avoid engine torque dip. This is mainly due to the fact that at low engine torque, after the tip-in, the engine torque that is used to accelerate the supercharger could be offset by the fast operation of the throttle opening, while for a higher engine load, especially above the naturally aspirated region, the torque extracted from the engine to accelerate the supercharger cannot be offset by the relatively slower operation of the turbocharger and an engine torque dip will be felt if a same supercharger acceleration rate is set.

5.5 Discussions

5.5.1 Driving cycle fuel efficiency improvement by further downsizing and down-speeding

From the test data above, it can be seen that both the steady-state full load performance and the transient behaviour for the CVT Supercharger system have been improved significantly compared with the counterparts with only turbocharger. This indicates that the same volume engine with the CVT Supercharger system fitted can drag a larger vehicle, realising downsizing to enhance fuel efficiency. In the meantime, due to the faster transient behaviour, an optimized transmission gear ratio or shifting strategy could be implemented, achieving down-speeding in order to improve fuel efficiency, shifting frequency and driveability [172, 179, 180].

5.5.2 The potential benefit of Miller cycle for CVT Supercharger system

The Miller cycle, usually achieved with an early or late intake valve closing, can achieve a longer expansion stroke than compression stroke, thus improving the engine's thermodynamic efficiency [181, 182]. In addition, for a gasoline engine, at part load Miller cycle can improve the fuel economy due to the reduced pumping losses and for the high load operation, the lowered end-of-compression temperature and pressure for the Miller cycle are able to enhance its anti-knock performance. However, a higher pressure ratio boosting system is required to regain the lost volumetric efficiency and maintain the target performance. The CVT Supercharger system with its superior low-end torque and significantly improved

transient behaviour may introduce more flexibility for optimizing the whole engine system with a Miller cycle concept, thus further enhancing its fuel economy.

5.6 Conclusions

Mechanically supercharging a passenger car engine is considered to be an alternative or a complementary approach to enable heavy downsizing to be carried out. The CVT Supercharger system, with the capability to enhance low-end torque, improve the transient driveability and reduce the low-load parasitic losses, is deemed to be a potential solution to address the fuel efficiency and driveability issues facing passenger car engines. After investigating, in both simulation and experiment, the CVT Supercharger system on a 1.0L GTDI, the following conclusions are drawn:

1: At steady-state, the CVT Supercharger system is able to significantly enhance an engine's low-end performance without crucially affecting its low load fuel efficiency. Further downsizing or Miller Cycle enabled by the enhanced engine performance could be used to mitigate the fuel penalty that is caused by the parasitic losses.

2: A ready-to-use control strategy at the engine's level has been built and calibrated using the steady-state engine test data. The influence of different control calibrations on the engine performance has been found and will guide the later control calibration tuning at the vehicle's level.

3: In transient, with its wide ratio spread of 10:1 and rapid rate of ratio change, the CVT Supercharger system can achieve significantly better transient performance in terms of time-to-torque compared with the turbo only configuration, and of NVH behavior in comparison to the fixed-ratio positive displacement counterpart with a clutch. Re-optimizing the transmission gear ratio or the shifting strategy, realizing further down-speeding, could further improve the engine's fuel efficiency in a real driving cycle, while maintaining a good driveability.

4: The CVT Supercharger demonstrator vehicle is expected to either achieve the goal of improving the vehicle's performance or enable an aggressive downsizing to achieve superior fuel economy.

Chapter 6 – Implementing full electric turbocharging (electric turbo-compounding) systems on highly boosted gasoline engines

From the perspective of engine energy flow, the copious amounts of wasted energy is habitually harvested by the turbine with low efficiency, subsequently the turbine power transmitted to the compressor is used solely to charge the engine. When this power for charging is excessive for the set engine operating condition, it either is consumed by throttling or is directly discharged through the wastegate, both as a pure enthalpy loss. To more efficiently harness the waste energy without deteriorating other engine performance parameters, a full electric turbocharging technology is provided by Aeristech Ltd. The system is composed of an electric turbo generator and an electric compressor connected only through electrical system. Without the constraint of a mechanical turboshaft, the compressor and the turbine can be operated at different speeds. The electrically driven compressor can be free floating when boost is not required and the motor can provide the boost promptly only when higher load is requested. Meanwhile, the electric turbine can be controlled by the generator to operate at any set speed, allowing maximum efficiency for energy harvesting. This chapter presents a simulation study of the capability of the decoupled eTurbocharging system to charge a highly boosted 2 litre gasoline engine. The simulation results have revealed that the two stage eTurbocharging system has the potential to reduce CO_2 emission in the proximity of 1 percent in different drive cycles compared to conventional wastegate turbocharger and the benefit would be much higher for future real world driving cycle.

6.1 Introduction

The electrification of the boosting system has been seen as a crucial enabler technology to achieve optimal drivability and CO_2 emission on highly boosted gasoline engines [183]. There are three main forms of boosting systems electrification: mechanical turbocharger assisted by a small ebooster, eTurbocharger with a shaft-mounted motor/generator and the mechanically decoupled eTurbocharger.

Out of the three options, the conventional turbocharger assisted by a small ebooster has been the most popular arrangement and has recently seen commercial application by Audi on Diesel engines with potential suppliers including all major turbocharger OEMs [184]. A study presented by FEV [185] has shown the benefit of such a system to both the emission control and performance enhancement with the aid of a 48V hybrid powertrain: increased EGR level enabled by eSupercharging can reduce the engine out NOx emission in the range of 50% during transient; adaptation of the size of base turbocharger has the potential to reduce fuel consumption up to 2% and downsizing and downspeeding of a eboosted engine can lead to the further reduction of 4-5%; furthermore, the expected low end torque improvement and transient response supported by an ebooster allows the mechanical turbocharger to charge the engine to higher power density.

The transient response improvement through the use of ebooster was discussed in more depth in a study presented by University of Ljubljana [186]. eBooster was shown to be superior to the integrated starter generator (ISG) in heavy duty Diesel vehicle application in terms of ratio of engine dynamics improvement to electric energy consumption.

Such comparison between ebooster and ISG was also confirmed by Continental [187], where a 2 litre TGDI engine was uprated from 220 to 250kW. While confirming the much improved transient performance through eboosting, it was stated that a 1.7kW electric energy invested on eboosting is equivalent to 20kW of ISG power input within a P2 mild hybrid architecture.

On the topic of extreme downsizing, Mahle and Aeristech [183] have managed to charge a 1.2litre engine to 33 bar BMEP, increasing the power rating of a demonstrator engine from 120kW to 193kW. The potential of turbocharging was greatly enhanced thanks to the ebooster which took over the engine boosting at low end.

An eTurbocharger with a shaft-mounted motor/generator has long been a novel turbocharging option. Back in 2000, Imperial College [188] has published theoretical study of a ‘hybrid turbocharger’ for both steady state and transient performance evaluation. Without considering emission due to the computational model limitation, the turbocharger can be resized and leading to a fuel economy improvement of 5-10%. Transient response was improved with various level depending on the power rating of the motor generator.

The transient simulation methodology was seen much improved a few years later in a study by University of Ljubljana [189], where a 0D simulation code calibrated by experimental data was used. Transient response was observed relating to both the power rating and inertia of the motor generator used; a typical torque tip-in has seen a more than 50% improvement through the use of electrically assisted turbocharger.

A more recent study [190] on the shaft-mounted motor/generator turbocharger has further demonstrated the flexibility of such a system to be used either to assist engine boosting or to harness energy to support on-board use. Fuel consumption benefit of 4.6% improvement in NEDC was reached on a highly downsized engine.

The mechanically decoupled eTurbocharger is gaining attention only in recent years. With the maturity of eboosting and turbo-compounding, such arrangements faces only the barriers of adequate control design and commercially viable cost-benefit ratio. A study by Clemson University [191] has presented a theoretical study of a boosting system comprised of an ebooster and an electric turbo-compounder. The study was supported by a comprehensive model built in AMESim, with dedicated physical model of the motor/generator and battery. An AFR based control strategy was proposed in the study and potential of positive energy balance from the boosting/turbo-compounding system and engine transient performance was demonstrated. Nonetheless, the controller oscillation has revealed the potential control difficulty of the system and the scope of the study did not include the practicality aspects such as engine full load condition, electrical system efficiency and motor/generator power rating.

To summarise the existing studies, the ebooster technology is a compact and cost-effective solution to support the turbocharged engines to improve the low end torque, rated power and transient performance. Fuel economy is improved mainly through the ebooster aided gas exchange process optimisation, turbo upsizing and engine downsizing. The technology will undoubtedly see popularity with the advent of universal hybridisation. On the other hand, the shaft-mounted motor/generator eTurbocharger technology adds in the advantage of energy harvesting without increased control complexity. However, it does not solve the problem of lack of low end torque in downsized engines due to the compressor surge. Finally, due to the complete independence of eCompressor and eTurbine speed, the decoupled eTurbocharger combines the performance augmentation of eboosters and the energy harvesting capability of electric turbo-compounders. However, the potentials and problems of such a technology are yet to be fully studied.

This study aims to find a viable solution of decoupled eTurbocharger for a highly boosted 2litre gasoline engine through simulation. The engine equipped with the novel boosting system should deliver a full load curve superior to the baseline setup. The potential of fuel consumption will be derived and the control strategy designed for the boosting system will be validated through improved fuel economy.

6.2 Modelling and simulation

6.2.1 Engine system

The engine model was implemented in the 1D wave dynamics modelling environment in GT Power. The baseline model has been calibrated for both full/part load steady state conditions as well as the transient operation. The combustion model was a test data calibrated Wiebe function matrix and could potentially create predictive errors when extrapolating above the baseline limiting torque curve or simulating transient operations, therefore care should be taken to use the exact numbers from such non-predictive combustion models.

The baseline engine was a 2.0litre production gasoline engine, charged by a conventional wastegated turbocharger, achieving a knee point torque of 340Nm at 1750rpm, max torque 350Nm at 3000rpm and max power 175kW at 5500rpm. The baseline model favoured transient performance and therefore has employed a relatively small turbocharger, raising low end torque at the expense of increased pumping work. With a novel boosting system, the full load torque was slightly optimised by advancing the knee point down to 1250rpm. Such optimisation will be the result of extra boosting from the ebooster.

Two eTurbocharger arrangements have been investigated as shown in figure 6.1 below. In the two stage boosting system the eTurbine can be placed either upstream or downstream of the mechanical turbine. eCompressor can also be placed upstream or downstream of the mechanical compressor, however simulation has shown that the performance of neither engine nor the boosting system was sensitive to the eCompressor location.

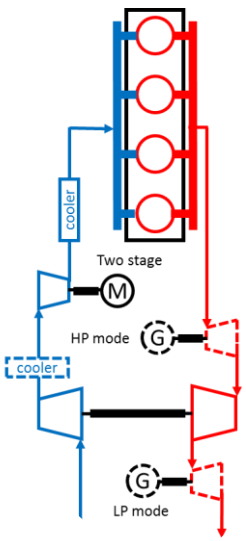

Figure 6.1. Two stage arrangement (HP and LP mode).

The simulation will aim to first achieve the full load torque target regardless of the eTurbocharger arrangements. Then the practical aspects such as the eTurbine power rating

will be discussed using the simulation results obtained. Following the full load simulation, part load simulation will cover the full area of the speed/torque map to evaluate the fuel economy and control strategy. Drive cycle fuel economy improvement will be calculated using minimap points with weighting for different drive cycles. Transient simulation at the end will further confirm the performance improvement.

6.2.2 Turbomachinery

The various compressors and turbines used in the simulations have been designed by Advanced Design Technology (ADT) Ltd specifically for the requirement of this study.

Figure 6.2. **Design of compressor wheel.**

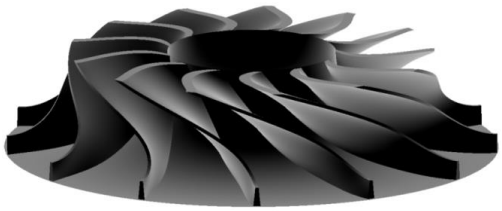

Figure 6.3. **Design of turbine wheel.**

The compressor design employed the inverse design method. The engine operating line at full load was first crudely generated using a scaled compressor map from the GT power library. Then the commercially developed mean-line design code TDpre was used to generate the meridional housing for the impeller wheel. Subsequently the design of impeller blade 3D shape was conducted in 3D inviscid design code TD1. ANSYS CFX was used to predict the performance map of pressure ratio and efficiency which iteratively supported the TD1 design practice until arriving at a satisfactory design when the full load operating line lay within a compressor map. Such method has the risk of predicting optimistic surge margin and stage efficiency and will be further evaluated experimentally in the following stage of the project.

The design of turbine wheel was a different process compared with conventional application since the turbine speed is independent of the compressor speed. Again, a mean-line method

is firstly used to find the combination of tip width and tip radius that can fulfil the requirement of both the highest and lowest mass flow conditions. The 1D results from TDpre was then sent into TD1 for 3D blade and nozzle shape design, with ANSYS CFX providing CFD calculation to support the design iteration. Without the constraints of compressor inertia and the shared turbomachinery speed, both turbine and compressor design seemed slightly different from the usual shapes of turbochargers for a similarly sized engine. A pair of compressor and turbine is shown in figure 6.2 and 6.3 (comparison not to scale).

6.3 Control strategy

The gas exchange system control strategy implemented in this study has been focused on optimal fuel economy. Whenever multiple solutions existed for the same target torque, a DoE simulation was always conducted to find the lowest BSFC.

For consideration of transient performance, the conventional mechanical turbocharger routinely 'overboosts' and throttles the engine at the same time in part load conditions, so that a torque transient request can be met with instant mass flow and a fast spinning turbocharger once the throttle opens up. An eboosted gasoline engine, on the contrary, can afford to charge the engine with the exact amount of boost pressure needed for the torque target, knowing that any transient request can be fulfilled by a responsive ebooster. Engine de-throttling through a boost control regime as such is a huge advantage for part load fuel economy.

Following the control philosophy of engine de-throttling, when throttling is necessary for the low load condition, it was better to throttle the engine using the eTurbine than the throttle, in that part of the throttling loss can be converted to electric energy. Depending on the eTurbocharger power system efficiency, such benefit disappeared at high mass flow, due to the fact that the pumping loss exceeded the energy recuperation.

The details of each controller can be explained as below.

Throttle

The throttle controller was a PID controller with feedforward and gain schedule targeting the BMEP at low to mid load. In the test environment the BMEP target can be substituted by a calibrated mass flow rate instead.

eCompressor

The eCompressor controller was a PID controller with feedforward targeting the BMEP. The controller was only activated at high load when extra boost was needed to achieve the torque

target or transient condition.

eCompressor bypass valve

The bypass valve opened by default and shuts completely when eCompressor was active.

Turbocharger wastegate

A large wastegate was necessary to bypass the mechanical turbocharger completely when boost was not needed at low to mid load. At mid to high load, the wastegate controller was a PID controller with feedforward targeting the BMEP.

eTurbine

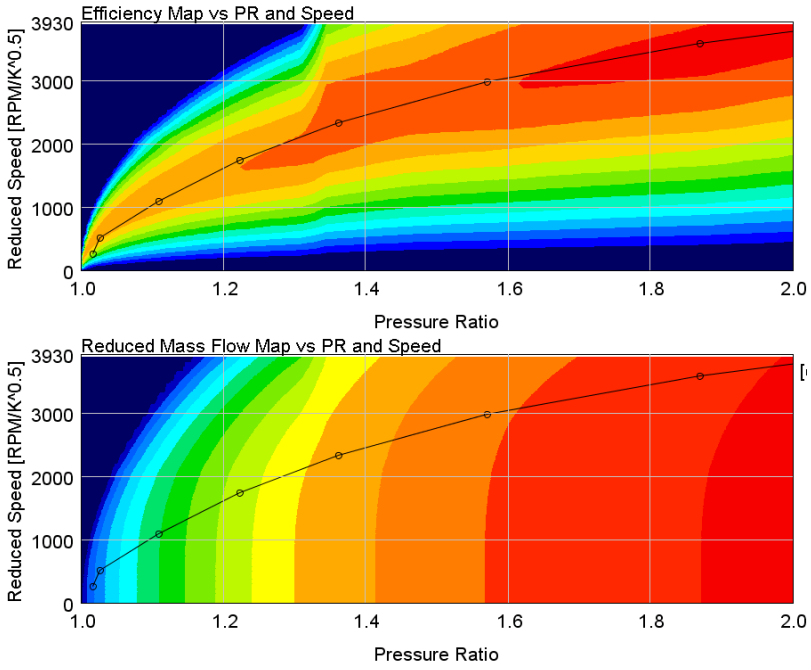

Figure 6.4. Speed control of eTurbine.

The eTurbine speed was controlled by changing the load on the motor/generator it was attached to. The target of the controller was to operate the turbine at its highest isentropic efficiency region. A polynomial model with pressure ratio as input was designed as shown in figure 6.4. A PID controller modulates the generator load to match eTurbine speed to the polynomial model output. A typical polynomial equation can be written as:

$$Speed_{target} = -4964 \times PR^{-1.585} + 5288 \quad \textbf{6.1}$$

eTurbine bypass valve

eTurbine bypass valve was the most complicated one. In test environment the controller would require heavy calibration effort. The controller is described as follows:

- At low load, map based binary control: fully shut to convert throttling loss to electric energy and fully open when not economical to do so at higher engine speed

- At low to mid load when throttle already fully opened, modulates engine back pressure through the involvement of eTurbine to target BMEP
- At mid to high load, the controller bypassed the eTurbine when wastegate starts to modulate BMEP.
- When eCompressor was active, the controller engaged the eTurbine to generate just enough energy to supply the eCompressor.
- Bypass valve controller also modulate the involvement of the eTurbine so that the power generated did not exceed the design limit of the motor generator (8kW in this study).

6.4 Simulation results

6.4.2 Two stage arrangement - eCompressor added

Steady state simulation results divided the engine speed/torque map into three regions as shown in figure 6.5.

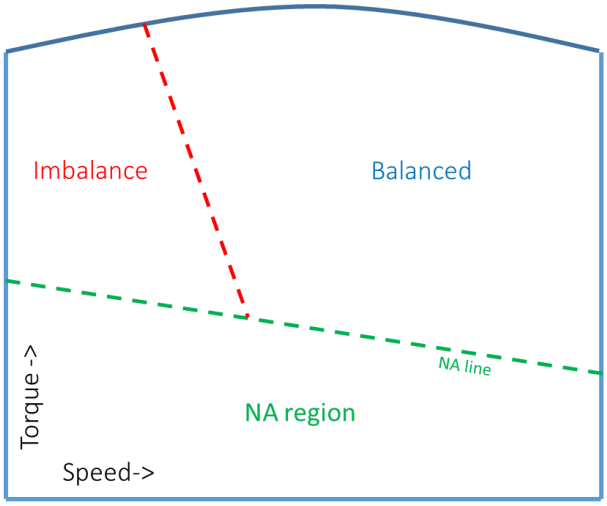

Figure 6.5. Division of engine speed and torque for steady state simulation.

For the two stage boosting engine system, the target BMEP at 1750 rpm and below was enhanced as shown in figure 6.6. As shown in figure 6.7, the mechanical turbocharger provided very little boost at low engine speed. At 1250 rpm, for example, the inlet air pressure was less than 1.28 bar for the baseline engine. By utilizing eCompressor, the inlet air was boosted up to 1.98 bar. As a result, the full load brake torque was increased from 225 Nm to 340 Nm at 1250 rpm. When the engine was operated above 1750 rpm, eCompressor was shut down and bypassed, imposing no effects on the power output from the engine.

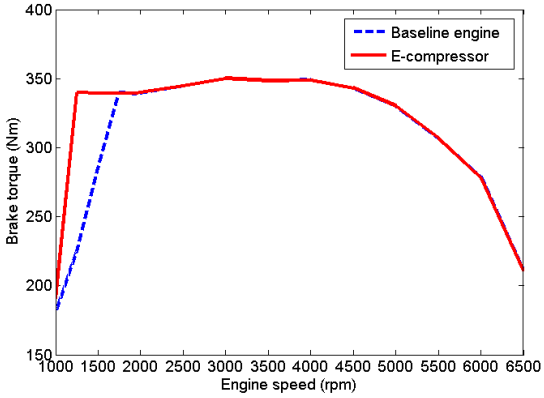

Figure 6.6. Performance target of two stage arrangement.

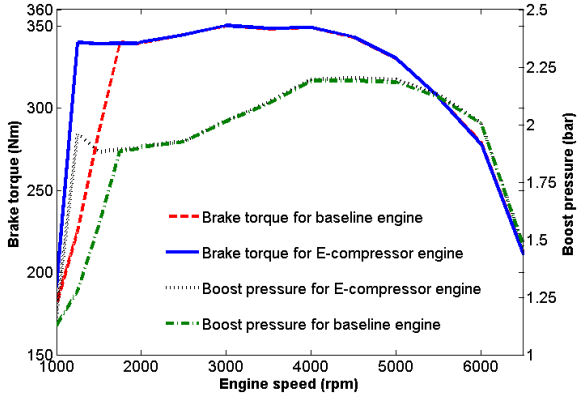

Figure 6.7. Brake torque and boost pressure for baseline and eCompressor engine.

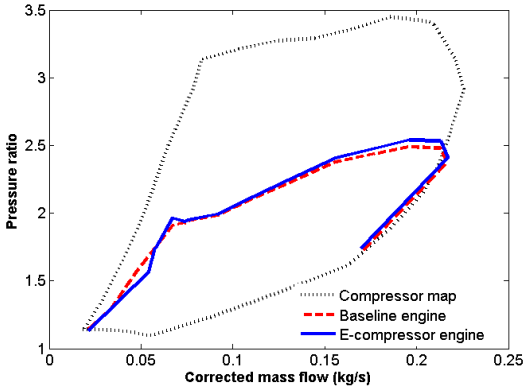

Figure 6.8. Lugline in the compressor map of baseline and eCompressor engine.

In figure 6.8, the operating points of the mechanical turbocharger compressor moved away from the surge line even though achieving higher torque at low end since the eCompressor shared part of the boost and helped to increase the inlet air mass flow. Such effect would

allow a larger compressor for the engine rated power, while avoiding low end surge. Above 1750 rpm, the bypass valve was fully opened to disengage the eCompressor from the air path. The lugline in this part coincides with the baseline setup.

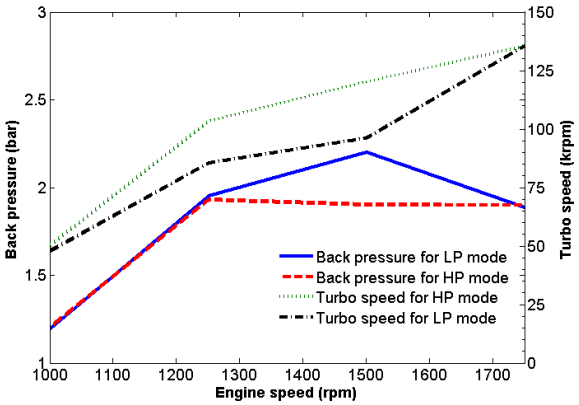

Figure 6.9. Back pressure and mechanical turbo speed for HP and LP mode.

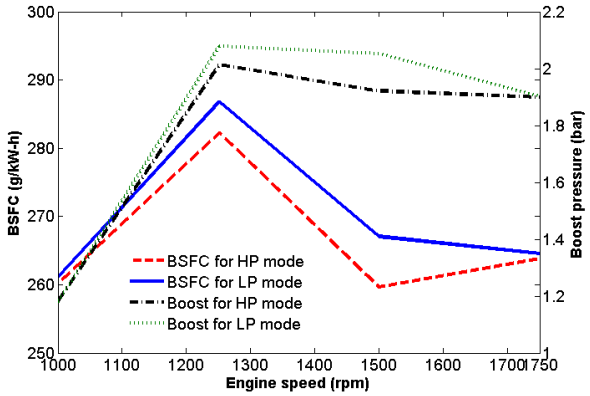

Figure 6.10. Full load BSFC and engine boost pressure for HP and LP mode.

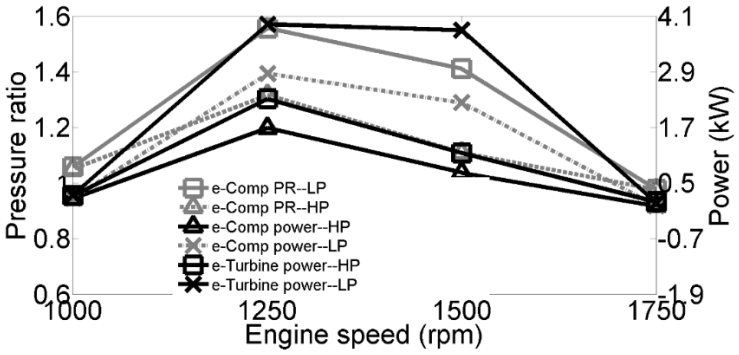

Figure 6.11. Electric E-turbocharger power and pressure ratio for HP and LP mode.

In order to decide the relative position of mechanical and electrical turbine, simulations were

carried out with the eTurbine being located upstream (HP mode) and downstream (LP mode) the mechanical turbine. From figure 6.9, mechanical turbine speed was lower in LP model, which indicated that the output from the mechanical turbocharger was reduced. Therefore, more power was consumed by eCompressor to make up for the deficit in mechanical boosting, as shown in figure 6.11. When the eTurbine was located downstream of the mechanical turbine, it generated more power than the HP mode because it shared more expansion ratio. Due to the smaller size of the eTurbine, it brought about higher back pressure in LP arrangement. Consequently, in order to achieve the full load target, higher boost pressure was required for the LP mode as well. It was the self-amplifying circle such as this that magnified the small advantage of HP mode into a large difference in performance. As shown in figure 6.10, the full load BSFC is lower (by up to 2.7% at 1500 rpm) when eTurbine was located upstream the mechanical turbine (HP mode) because of the lower back pressure and less power consumption by the eCompressor as aforementioned. However, when considering the exhaust temperature at the inlet port of eTurbine, the LP mode was more preferable to retain greater margin to the limit, which was beneficial to prolong the life cycle of the electric turbine.

In addition, the eCompressor efficiency was nearly the same for both configuration, while the operating points of mechanical compressor in the LP model shifted away from the surge line to the higher efficiency region, as shown in figure 6.12 and 6.13. Based on synthesized considerations, it was decided to locate the eTurbine downstream the mechanical turbine (LP configuration) in this model for further studies.

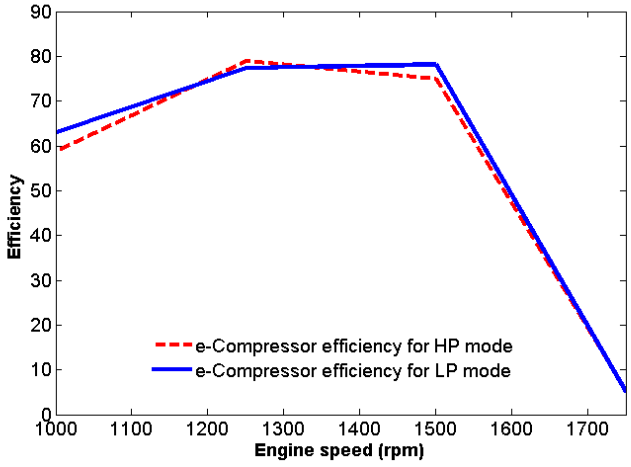

Figure 6.12. eCompressor efficiency for HP and LP mode.

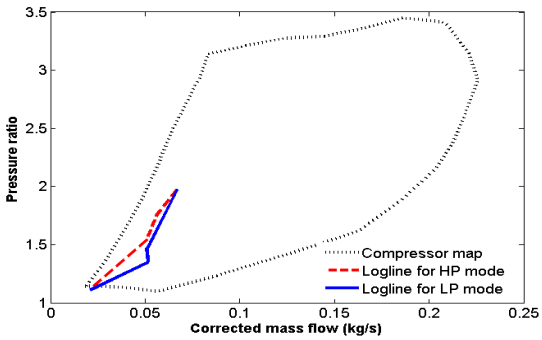

Figure 6.13. Luglines in mechanical compressor map for HP and LP mode.

6.4.3 e-Turbine performance for LP mode

In order to locate the operation points in the region of highest thermal efficiency, the eTurbine speed was regulated. Specifically, a favourable line of reduced turbine speed was calculated for a set of pressure ratios according to the polynomial equation 6.1.

In the control module, expansion ratio of the eTurbine was used to calculate the desired eTurbine speed. A PI controller then modulates the load to the eTurbine to achieve the target speed.

In figure 6.14, power output from the eTurbine was multiplied by an overall conversion efficiency of 67% to indicate the power availability to the eCompressor. The results showed that there was a minor shortage at 1250 rpm. Such deficit would need to be provide by the battery which was a manageable power level. The power requirement of the eCompressor at other engine speeds can be satisfied without imposing parasitic load to the engine.

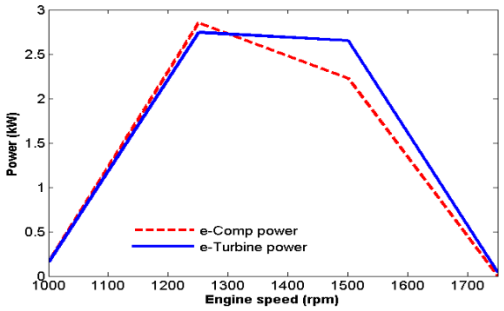

Figure 6.14. eTurbine power vs eCompressor power.

6.5 Simulation results

The fundamental principle of the control strategy for partial load simulation is to explore as much potential of the eTurbine as possible for all the engine loads to reduce throttle losses

and the exhaust energy expelled through the wastegate as long as it was economical to do so. The simulation results were shown in figure 6.15 to figure 6.22 respectively for a variety of partial load conditions.

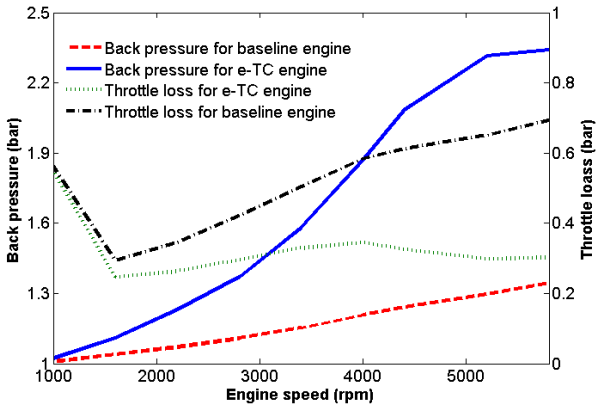

Figure 6.15. Back pressure and throttle loss of baseline and E-TC engine at 20% load.

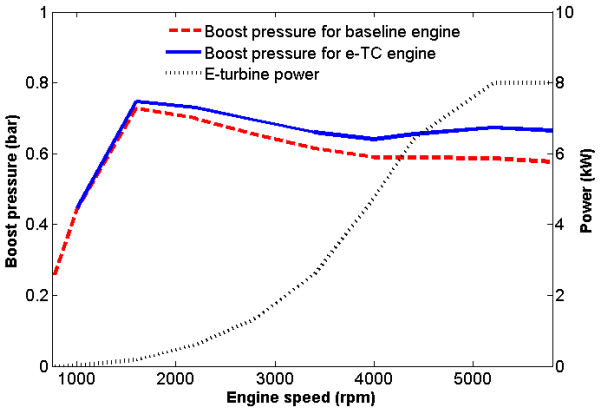

Figure 6.16 Boost pressure and eTurbine power for baseline and E-TC engine at 20% load.

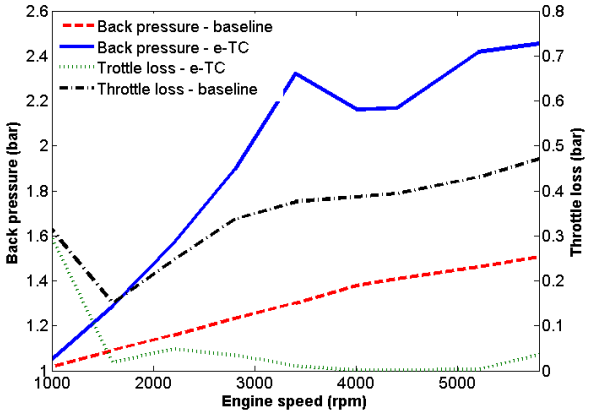

Figure 6.17. Back pressure and throttle loss of baseline and E-TC engine at 40% load.

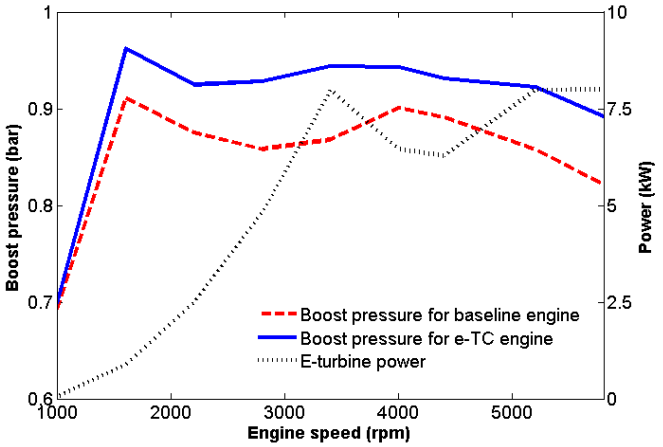

Figure 6.18. Boost pressure and eTurbine power for baseline and E-TC engine at 40% load.

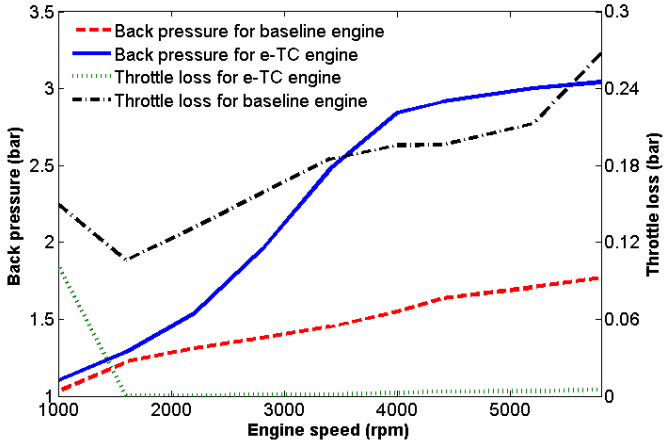

Figure 6.19. Back pressure and throttle loss of baseline and E-TC engine at 60% load.

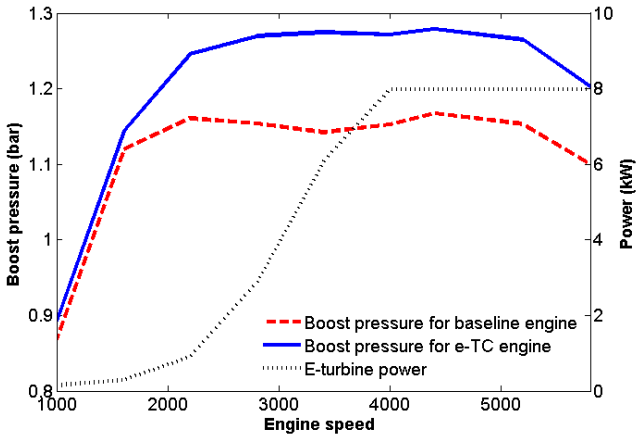

Figure 6.20. Boost pressure and eTurbine power for baseline and E-TC engine at 60% load.

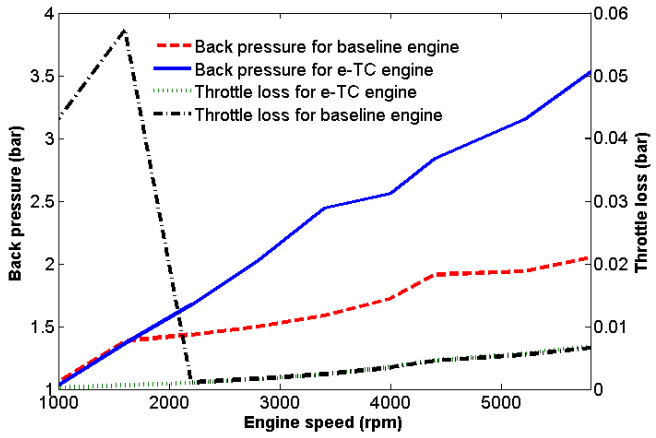

Figure 6.21. Back pressure and throttle loss of baseline and E-TC engine at 80% load.

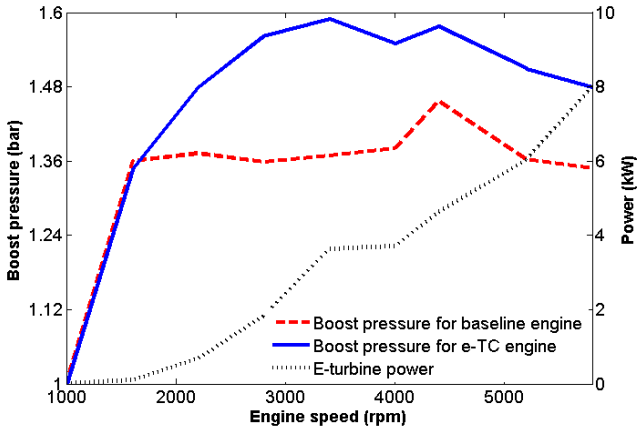

Figure 6.22. Boost pressure and eTurbine power for baseline and E-TC engine at 80% load.

6.5.1 Partial load simulation

From the results, it was a general trend that the intervention of eTurbine increased the back pressure and the boost demand for the engine system. At the same time, since the engine breathinging could be regulated by adjusting the eTurbine bypass valve as an alternative, throttle angle was less closed. It was effectively to move the throttle loss to the eTurbine where the losses could be harvested. At 20% load, for example, back pressure increased by up to 1 bar at 5800 rpm, while the pressure drop across the throttle body was reduced from 0.7 bar to 0.3 bar. And also, at lower engine speed when the exhaust mass flow decreased, electric turbine imposed less effects on air scavenge. The effect of de-throttle became less significant. The demand for boost pressure at 20% load was higher in the case of the eTurbocharged engine, which suggested the mechanical turbine was pushed harder by the additional turbine. The similar trend was seen in the results of 40% and 60% load. But, it is

worth noting that it was possible to eliminate throttle loss at 40% load and higher, and merely rely on electric turbine to regulate the air flow. At 80% load, the pressure drops across the throttle body were especially low for both baseline and eTurbocharged engine. The difference in boost demand between baseline and eTurbocharged engine models stayed around 0.2 bar, as the magnitudes of the increments in back pressure were about the same, which was around 1 bar.

The control strategy for the eCompressor was relatively simple, since it was only needed in a small region at upper left corner on the engine map when the mechanical turbocharger could not provide enough boost. In the partial load points simulated, the electric compressor was completely bypassed.

6.5.2 Engine Part load BSFC map

Although the eTurbine was able to generate useful work from the otherwise wasted exhaust energy and reduce the throttle losses, it increased the back pressure and thus the boost demand for the same BMEP target. It was therefore not always advised to use the eTurbine harnessing mode. The BSFC map in figure 6.23 has shown an 'eTurbo enclosure' line where inside the dashed-line region eTurbine operation can achieve a positive balance.

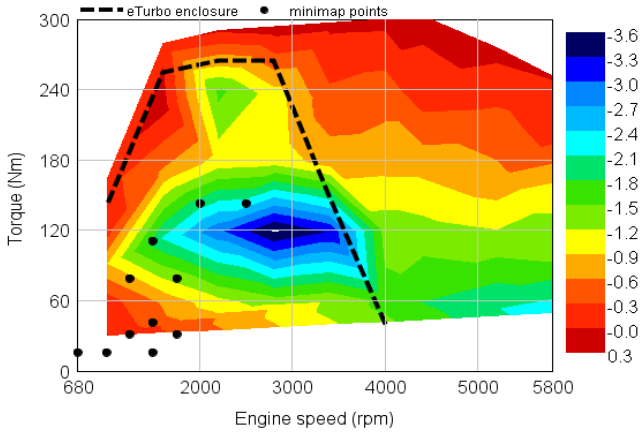

Figure 6.23. Delta BSFC for the whole system.

Meanwhile, since the eCompressor is expected to support improvement in transient response and increased surge margin, the mechanical compressor was allowed to be a 20% larger device. The avoidance of over-boosting as in a conventional turbocharged engine was also showing fuel economy benefit as in the region outside of the 'eTurbo enclosure' line.

In the part load simulations, the excessive eTurbine power was converted into electricity and then fed back into to the crankshaft with a conversion efficiency of 85%. Practice as such reduced the IMEP of the engine for the same torque generation, which moved the engine to

its less efficient region. In spite of this, it was found that the integration of eTurbocharging system brought about a promising improvement in fuel economy. The BSFC was reduced by up to 3.6% in the middle of the engine speed/torque map. Nevertheless, under extremely low load conditions, a negative effect was seen because of the poor efficiency and little power output of eTurbine. At the highest engine speed and WOT operation, on the contrary, even though the eTurbine was more efficient in harvesting exhaust energy, it created too much back pressure to be remedied by the power provided by itself. Therefore, the fuel economy of the whole system deteriorated by about 0.3%.

6.5.3 Driving cycle fuel consumption

Minimap point simulations with weightings for different drive cycles were conducted using the points as in figure 6.23. The results in Table 6.1 demonstrated the improved fuel economy for the operation under a variety of driving cycles when comparing with the baseline turbocharged engine. However, the magnitudes in BSFC reduction were relatively lower than that of the full and partial load simulation. It was due to the fact that the operation points of driving cycles mainly resided in the region of extremely low load when the eTurbine could not work effectively to recover waste heat, as illustrated in figure 6.23. A few points having negative impact on fuel economy took up more than 50% of the weighting. As a result, the HiWay driving cycle, which had larger weighting in the mid-high load region, showed better potential of the novel technology, while fewer benefits were seen in NEDC. It was expected that the eTurbocharger will provide larger benefits in real world driving cycle with a much wider speed and load region covered.

Table 6-1. **Fuel saving in driving cycles.**

Driving cycles	BSFC reduction
NEDC	-0.4%
FTP	-0.5%
HiWay	-0.8%
WLTP	-0.7%

6.6 Conclusions

This chapter compared the performance of a conventional turbocharged engine model with a two-stage boost engine model equipped with a decoupled electric turbocharger. A carefully designed control strategy was designed for the electric turbocharger for a variety of engine

speed/load conditions. The steady state performance of both systems was evaluated by examining the fuel consumption at full load, part load and minimap based driving cycles. The total boost pressure, back pressure of both the baseline and novel models were compared to seek out the origin of the difference in fuel economy. Power consumption of the eCompressor and power generation of the eTurbine was analysed to indicate the effects that they have on the performance of the overall system.

1. As for the location of eTurbine, LP mode was selected for the lower eTurbine temperature for the thermal protection although HP mode would be a more economical solution.

2. At full load condition, eCompressor was expected to provide extra boost at 1750 rpm and below to enhance the low end torque by up to 115 Nm. It was beneficial for improving the driveability of the engine system. Above 1750 rpm, when the mechanical turbocharger was able to provide sufficient boost on its own, eCompressor was totally bypassed. At the same time, electric turbine was harvesting exhaust energy independently. The power output from the eTurbine was sufficient to satisfy the power consumption of the eCompressor.

3. At partial load condition, mass flow could be regulated by adjusting the eTurbine bypass valve as an alternative to throttle, so that throttle was less shut. It helped to reduce the throttle loss. At 40% load and higher, the pressure drop across the throttle body was nearly eliminated. Besides, eTurbine was able to harvest up to 8 kW power from the exhaust energy, which could be converted into useful mechanical work. However, similar with the case in full load condition, back pressure and requirement of boost was increased because of the employment of eTurbine. The tendency to knock due to higher back pressure should be further investigated in the experimental phase of the study.

4. Across the part load map the BSFC was reduced by up to 3.6%. At the high engine load, fuel consumption will increase because of the high back pressure as a result of eTurbine trying to harness energy to support eCompressor.

5. The minimap points of driving cycles were located mostly in the lower left region of engine load. A few load points with small or even negative impact on fuel economy took large weighting in the calculation. That made the improvement to the fuel economy less remarkable. From the results, the largest reduction in BSFC was seen in HiWay driving cycle, which is 0.8%. In NEDC, the number decreased to 0.4%. The upcoming RDE cycle will be investigated in future works and the eTurbo technology is expected to achieving larger fuel economy benefit due to the higher load/speed of the real world drive cycle.

Chapter 7 – *Modelling the HP Turbo-Compounding Concept*

For the LP turbo-compounding system with power turbine being located in series with the main turbine, power losses are incurred due to the higher back pressure which increases the pumping losses. This chapter evaluates the effectiveness that the turbo-compounding arrangement has on a 2.0 litre gasoline engine and seeks to draw a conclusion on whether the produced power is sufficient to offset the increased pumping work. Furthermore, since the baseline engine model in this part is not a heavy-duty diesel engine that is more appropriate to the turbo compounding mechanism for automotive application, but a 2 litre gasoline engine. This chapter also aims to explore a potential methodology for extending the operating range of the turbo compounding in light-duty petrol engine over its entire speed range under full load condition. Besides, this system will be further investigated considering the fuel consumption under part load condition as well as the transient performance. The CVT drive ratio and thus the pressure ratio of the compressor will be further optimized to achieve the best fuel economy and drivability. The system model in this chapter was also built in GT-Power which is a 1 dimension (1-D) engine simulation code. Simulation results show that with the assistance of a variably driven supercharger, the output torque of the engine system is much larger (up to around 24%) at lower engine speeds. The fuel economy is also improved by up to about 8%.

7.1 Introduction

By now, the most frequently utilized technology in exhaust heat recovery is the turbocharger which extracts the kinetic energy from the exhaust flow to drive the compressor. However, the benefit for turbocharged engine always comes along with the drawbacks in transient response and over-boost risk at high engine speed Specifically, a large turbocharger can offer the power at high speed, but suffers from poor efficiency and delayed transient response at lower engine speed due to the lack of exhaust gas flow to overcome the inertia of the system. On the contrary, a small turbocharger is able to provide improved boost pressure and transient response at lower engine speed due to the reduced inertia. However, as the engine speed rising, it would need the bypassing valve, typically through a waste gate, to prevent the turbocharger from over speed which may otherwise leads to over boost.

Besides, the power produced by the main turbine of a turbocharger unit has to be totally consumed by the compressor, which means the capability as well as the efficiency of the turbine is limited by the power demand of the compressor and substantially the air demand of the engine. When the extracted energy from the exhaust is excess, a waste gate is needed to bypass the redundant exhaust gas, otherwise the inlet air to the engine will suffer from over boost which causes damage to the cylinders. If the engine is equipped with the turbo compound arrangement, however, the power produced by the power turbine will be feed back to the engine crank shaft mechanically or converted into electricity. In this way, the waste energy recovery is only limited by the inherent specification of the power turbine such as inertial and isentropic efficiency.

The main disadvantage of turbo-compounding technology lies in the fact that it increases the backpressure of the engine and the pumping losses that results in reduction of the net engine power. Especially in a light duty transport or when the engine is running under part load condition or at low engine speed, the power produced by the power turbine is even not enough to offset the increased pumping losses [192, 193, 195]. For this reason, it is widely accepted that the turbo-compounding engine is only suitable for heavy-duty vehicles or the transports that are consistently operated under high-load condition.

7.2 Methodology

In order to diminish the aforementioned negative effects of the turbocharging and to catch up with the drivability of a comparable naturally aspirated unit, a number of solutions, such as the variable geometry turbocharger (VGT), twin and double turbine scrolls and multi-stage turbocharging[197] has been explored. Although the average efficiency and the transient response of these systems unit are improved to some extent, they still rely on the build-up of exhaust flow rate and thus the availability of the exhaust gas energy [198]. Consequently, none of them completely solves the problem of low speed transient response. In the last few years, a new design called continuously variable supercharger (CVT Supercharger) was presented [60]. It is a combination of a supercharger and a continuously variable transmission drive (CVT) which is able to effectively shorten the response time of the booster and minimize the parasitic losses at high engine speed, in other words, this arrangement enables the performance of the supercharger to be fully exploited over the entire engine speed range.

As for the other aspect of the problem, the back pressure and the resulted pumping losses have to be minimized. The solution is to diminish the number of the turbine in series.

Therefore, the original turbo-machinery was no longer used in the charged scheme, which makes the inlet air boosting totally relies on the CVT Supercharger; and the power turbine becomes the only component to recover exhaust gas energy. The size of the power turbine was carefully designed based on optimization technique.

It can be assumed that as the engine speed increases, the exhaust gas pressure will be increased rapidly leading to reduced, or even negative, pumping pressure. For this reason, the volumetric efficiency of the engine will decrease at high engine speed. The turbo-compounding engine, as the turbine waste gate will be closed over the entire speed range, will suffer from larger back pressure and poorer volumetric efficiency at high engine speed. However, the power turbine is capable of recovering energy from the exhaust gas and feeding it back to the engine crankshaft. The recovered energy may be able to offset the pumping losses.

The increased back pressure is also seen in the turbocharged engine causing the similar drawbacks. Besides, the energy recovery in turbocharged engine is in an indirect way. The reclaimed energy by turbocharger is consumed by the compressor which boosts the inlet fresh air for the engine to enhance its volumetric efficiency. Its thermodynamic calculation is presented in [46]. In order to prove the advance of turbo-compounding engine over its turbocharged competitor, the brake torque as well as the specific fuel consumption of these two waste energy recovery arrangements will be compared with each other in the following section.

7.3 Modelling and simulation

The original compressor from the baseline turbocharged engine was retained to make the results comparable.

Table 7-1. Engine specifications

Engine type	4 stroke
Number of cylinders	4
Capacity	1.99 litre
Bore	86 mm
Stroke	86.07 mm
Compression ratio	9.5
Maximum power	160 kW
Maximum torque	472 Nm

The baseline engine is a 2.0 litre four-cylinder inline turbocharged intercooled gasoline engine. Its specification is shown in Table 7.1.

As Figure 7.1 shows, the maximum produced torque of the turbocharged engine is 472 Nm at the engine speed of 2500 rpm; accordingly, the maximum brake mean effective pressure (BMEP) in the cylinder is 29.7 bar. The maximum power is 164 kW generated at 4000 revs/min.

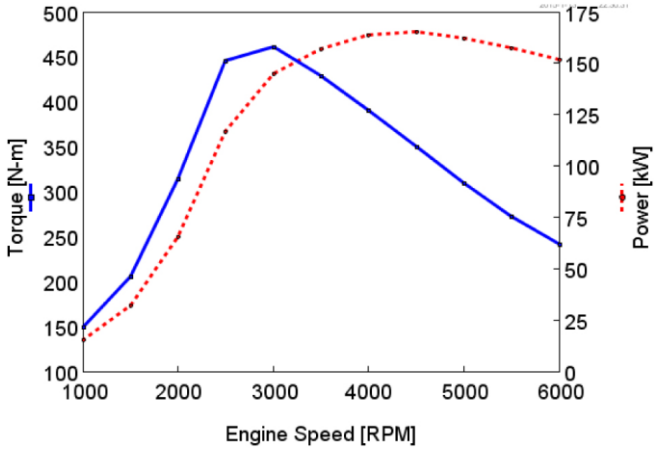

Figure 7.1. **Engine performance characteristics.**

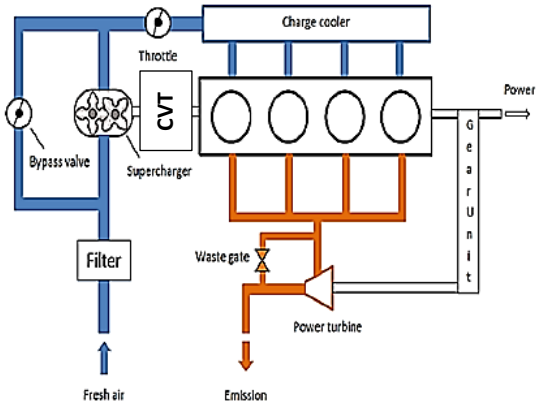

Figure 7.2. **The overall arrangement of the CVT Supercharger Turbo-compounding engine.**

The overall layout of the CVT Supercharged turbo-compounding engine is shown in Figure 7.2. The fresh air from the filter is compressed by the supercharger which is driven by the crankshaft via a CVT before it enters the inlet manifold of the engine. At the other end, the exhaust from the manifold enters the power turbine directly. The energy is extracted by the power turbine and converted onto mechanical power and feed back to the output crankshaft through a set of gears.

During the simulation process, the engine speed was changed in increments of 500 rpm in the range between 1000 and 6000 rpm. The air fuel ratio is considered as a constant of 14.5 for simplicity.

Table 7.2 shows the specification of currently popular CVT types. As the table lists, the overall CVT ratio ranges of the full & half Toroidal CVT and the belt drive CVT are between 29.3 to 175.8 and 28 to175 respectively. They are both qualified for the transmission between the compressor and the engine shaft.

Table 7-2. CVT specification [163].

Parameters	Milner CVT	Full & half Toroid CVT	Belt drive CVT
Input speed limit (rpm)	10000	10000	6000
Input drive ratio	3.5	3.5	2
CVT ratio range	4.5	6	6
Min CVT ratio	2	0.41	0.4
Max CVT ratio	9	2.45	2.5
Step-up ratio	5.6	20.5	35
Min overall ratio	39.2	29.3	28
Max overall ratio	176.4	175.8	175

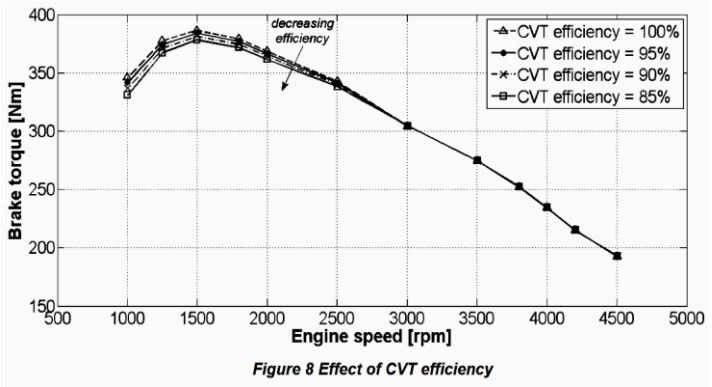

Figure 7-3. The effect of CVT efficiency on engine performance [74].

Since the current object of this project was to investigate the potential of the general concept rather than constrain to a specific type of CVT, therefore, the CVT efficiency in this phase was assumed to be 100% to simplify analysis. Furthermore, based on the investigation in [60], the CVT efficiency value has little influence on the overall performance of the entire system. The peak torque was only decreased by 2% when the CVT efficiency was reduced to 85%.

However, before moving to the partial load and transient simulation stage, further optimization was carried out for the CVT ratio and turbine speed to achieve the best power output under full load condition. The results of rated power output will be employed as the upper limit of the power criterion in the following transient performance simulation.

Under partial load condition, the compression ratio would also be verified depending on the CVT driving ratio in order to find the best combination for the benefit of reducing specific fuel consumption. And then, the influence of these parameters on the fuel economy of the entire system would be summarized.

For the full load simulation, the engine speed was varied from 500 to 6000 rpm in the increments of 500 rpm, which was the same as the case setup in the first report. For the partial load operation, brake mean effective pressure (BMEP) was kept at 2 bar over the engine speed range from 500 to 3000 rpm. During evaluating the transient performance of the system, the duration that was taken by the engine BMEP to climb from 2 bar to 90% of the rated value was measured. Similar to the operation in the first report, the air fuel ratio was considered as a constant of 14.5 for all the engine speed and working condition for simplicity. Besides, as this investigation was to assess the potential of the concept, the original turbine and compressor machineries were retained for the convenience of comparison.

7.4. Optimization on the CVT Ratio, Compression Ratio and Turbine Speed for Full Load Operation

In an earlier paper investigating the performance of the continuously variable supercharger in a diesel engine [8], Adam Rose et al applied DoE (Design of Experiment) techniques to optimize the scaling factor of the supercharger and stated that the compressor size should be reduced to provide the required boost pressure at lower engine speed (and thus low mass flow rate) without exceeding the surge limits, while the turbocharger compressor should be increased in geometry size to satisfy the increased mass flow rate at high engine speed. However, it should be noted that it was a twin-charge system that was included in that model, which means the intake boosting would be “handed over” to the turbocharger at high engine speed by declutching the supercharger, therefore, the turbocharger did not need to accommodate for the pressure ratios that was normally required at low speed. On the other hand, the model in this chapter was expected to satisfy the boost requirement of the engine at all the operation regions because of the absence of the turbocharger devices. Therefore, the original compressor was kept in this model for the convenience of matching the intake air flow characteristics under different working condition.

In this chapter, the optimization of the turbine speed was the key factor to consider to

achieve the maximal power output and the best fuel economy. However, optimum performance could not be realized by merely adjusting the turbine speed. The compression ratio, as one of the most important factors determining the allocation between engine power and turbine power should be taken into consideration as well. Besides, the CVT ratio that directly determined the boost pressure across the compressor should also be optimized accordingly for the highest overall efficiency of the entire system. Therefore, a formal approach was needed to optimize the complex interdependence of each of the parameters over the whole engine speed range (500 RPM to 6000 RPM).

The constraints imposed upon the simulation process in the first report were also retained, which included limiting the maximum cylinder pressure below 80 bar and the maximum compressor speed lower than 200000 revs/min. The ranges for the design of experiments factor were listed in table 7.3.

Table 7.3. **Design of experiment factors and ranges.**

Parameters	**Minimum Value**	**Maximum Value**	**Ranges**
Turbine Speed (RPM)	10000	600000	15
CVT Ratio	20	100	8
Compression Ratio	8	11	6

The optimized value for each parameter were specified in table 7.4.

Table 7-4. Parameter optimization.

Factors Speed	**Turbine Speed (RPM)**	**CVT Ratio**	**Compression Ratio**
500	13451.2	16.7	9.5
1000	60498.0	60.8	9.5
1500	137184.0	90.2	9.5
2000	182589.0	77.7	9.5
2500	200770.0	74.3	9.5
3000	200351.0	66.6	9.5
3500	200379.0	57.1	9.5
4000	200867.0	50.0	9.5
4500	200434.0	44.4	9.5
5000	200095.0	40.0	9.5
5500	200153.0	36.3	9.5
6000	185453.0	33	9.5

For a radial turbine with fixed geometry, the peak efficiency is typically found at the velocity ratio (U/C) of about 0.7, where U is the blade tip speed; and C is the isentropic velocity resulting from an ideal expansion of the gas at the same expansion ratio as in the turbine [199]. Therefore, the turbine speed was adjusted to shift the velocity ratio close to 0.7, so that the operating point would move towards the high efficiency region of the performance map.

From Mitsunori Ishii's study on a high pressure turbo-compounding diesel engine, it was concluded that a higher compressor pressure ratio was beneficial for improving the power output for both the engine and power turbine [198]. The increased power consumption by the compressor was well compensated, and the overall power output of the whole system was enhanced. Consequently, the optimization for the CVT driving ratio in this report was quite straightforward as it suggested. It was sensible to drive the compressor at a rotation speed as high as possible to provide the rated boost pressure at full load operation. However, considering the limits of mechanical strength, heat resistance as well as the surge line of the compressor, the CVT ratio was kept below a ceiling of 90.1. The compression ratio was also reduced to prevent the maximum cylinder pressure from rising too high.

7.5 Results and discussions

First of all, it should be note that the CVT efficiency was assumed to be 100% during the simulation to simplify the analysis. The basis for making this simplification lies in two aspects: firstly, the main object of this project at this stage was to investigate the potential of the general concept of combining a CVT supercharger with turbo-compounding rather than specifying the CVT component to a constraint type; secondly, According to the work in [60], a CVT efficiency of 85% results in 2% reduction in peak torque compared to the performance of an twin-charged engine with an ideal CVT drive. Figure 7.3 shows the influence of the CVT efficiency on the torque curve of the twin-charged system, indicating that the deterioration in CVT efficiency has very little impact on the overall performance of the entire engine system.

7.4.1 Full load brake toque

In order to indicate the advantage of the CVT supercharger over a conventional turbocharger, the compressor from the original turbocharged engine was retained. The effect of this arrangement can be detected from the engine brake torque curves in figure 7.4 in which the peak torque produced by the CVT supercharged engine and the turbocharged engine are

about the same. The reason of it is that the compressor reached its operating limit at this point, which means further increases in compressor speed and boost pressure were not allowed. Consequently, the CVT drive is of little effect to enhance the maximum brake torque.

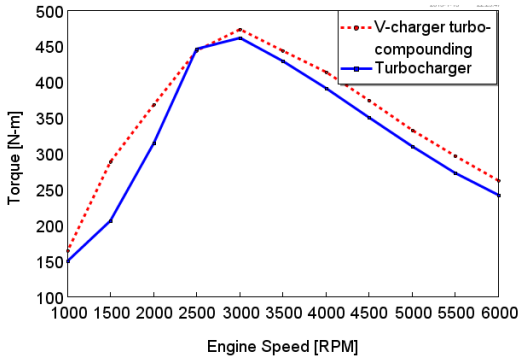

Figure 7.4. Engine brake torque.

However, at the lower speed range before the submit point, a remarkable increase in the brake torque generation can be found. Especially at 1500 rpm, the CVT Supercharged engine produces 24% more torque. But when the engine speed fells to 1000 rpm, its performance superiority became less evident because the speed and thus the pressure ratio of the inlet air was extremely restricted by the surge line. From the peak point afterwards, the CVT Supercharger turbo-compounding engine is again of advantages. As the figure shows, the torque output was enhanced by around 7% above 3000 rpm. This is due to the intervention of the power turbine. Within this range, the power turbine was fully engaged to recover energy from the exhaust gas and feed back to the crankshaft with no need to open its wastegate to bypass exhaust flow to prevent the compressor from over speed as the turbocharger did.

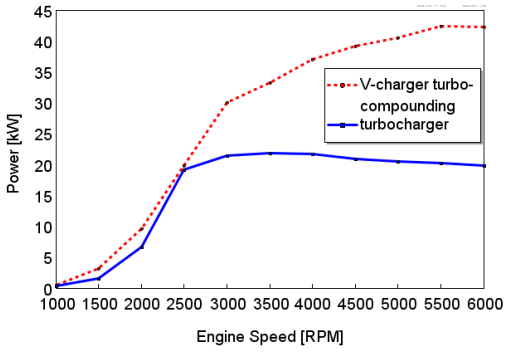

Figure 7.5. Average power recovery by the main turbine and power turbine.

The energy recovered by the main turbine of the turbocharger and the power turbine is illustrated in figure 7.5. The wastegate of the main turbine of the turbocharger was partially

opened after the engine speed reaches 2000 rpm to keep its speed within the operating limit of the connected compressor; the power turbine in a turbo-compounding engine, on the other hand, was allowed to have its wastegate closed completely over the entire engine speed range. Consequently, the recovered energy by the power turbine is far exceeding that from the main turbine at high engine speed range.

From figure 7.6, the turbine efficiency reached its peak at the engine speed of 2500 RPM and declined slightly at higher or lower engine speed. But overall, the turbine efficiency was kept above 70% when the crankshaft was running above 1000 RPM. At 500 RPM, the turbine efficiency saw a sharp decline due to the drastic decreasing in gas flow rate.

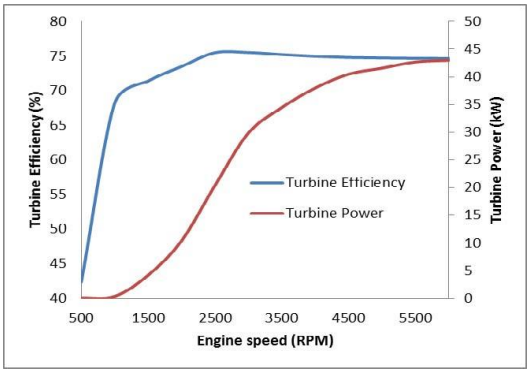

Figure 7.6. Power turbine efficiency and power output under full load condition.

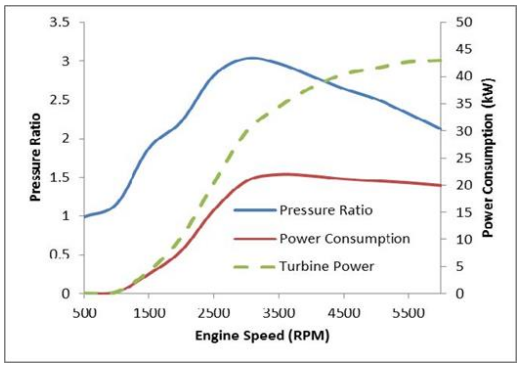

Figure 7.7. Pressure ratio across the compressor vs. the power consumption by the compressor

By comparing figure 7.6 and figure 7.7, it could also be indicated that the power output from the gas turbine was higher than the power consumption by the supercharger, which means extra useful work could be converted from waste heat and fed to the engine crankshaft. Especially when the engine was operated at high speed (above 2500 RPM), the power

consumption by the compressor became horizontal due to the speed limit that prevents the operated point from exceeding the surge line, while the power generation from the gas turbine kept growing, with a decreasing rate, though, resulting in greater power surpluses within this speed range. On the other hand, at 1500 RPM and lower engine speed, the margin descended significantly because of the reduction in mass flow rate. Thereby, even though more power was consumed by the supercharger, it was considered favourable to maintain the boost pressure at high level at this operation point as the engine would benefit from the enhanced scavenging efficiency and wasted heat recovery rate.

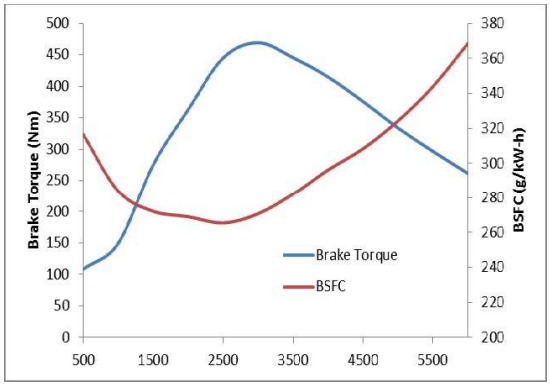

Figure 7.8. Brake torque and brake specific fuel consumption of the whole system at full load operation.

The brake torque and brake specific fuel consumption was illustrated in figure 7.8. The results suggest that the variation in turbine speed make little difference to the engine performance under full load condition comparing with the effects of changing the CVT driving ratio. Therefore, it could be speculated that the optimization of the turbine speed might be even less relevant at low load operation when the gas flow rate became gravely insufficient, because the power turbine contributed fewer to the overall power generation then.

From the work in [60], it can be predicted that a positive displacement compressor will be much better at boosting the engine power at low speed. However, as is stated above, the object of this phase is to investigate the potential of the concept and evaluate its advantage over conventional turbocharged engine; the typical arrangement with positive displacement compressor was not discussed further.

7.4.2 Full load brake specific fuel consumption

As figure 7.9 illustrates, the CVT Supercharger turbo-compounding engine shows a significant reduction in fuel consumption when the engine speed reached 2500 rpm and above. The improvement in fuel economy grew continuously as the engine speed rising and reached the

maximum percentage of 8% at 6000 rpm. It is because the power turbine provided the engine with more recovered energy at high engine speed. Even though the pumping mean effective pressure (PMEP) is lower in turbo-compounding engine (there will be further description later) the overall effect is positive. However, when the engine speed is below 2500 rpm the CVT Supercharger turbo-compounding engine has very little advantage in fuel economy. This is due to the rapidly decreased power generation of the power turbine. As the engine decelerated, the exhaust mass flow rate decreased. The energy extraction from the waste became much lower.

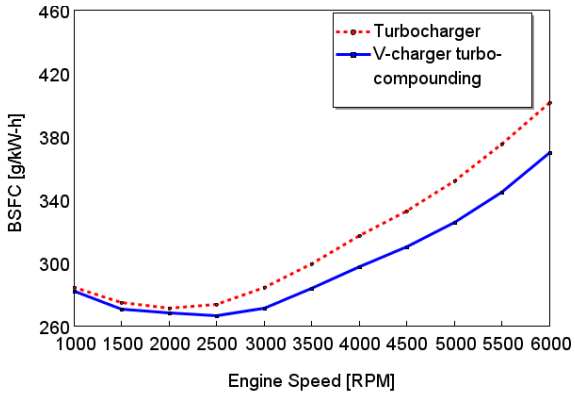

Figure 7.9. **Brake specific fuel consumption.**

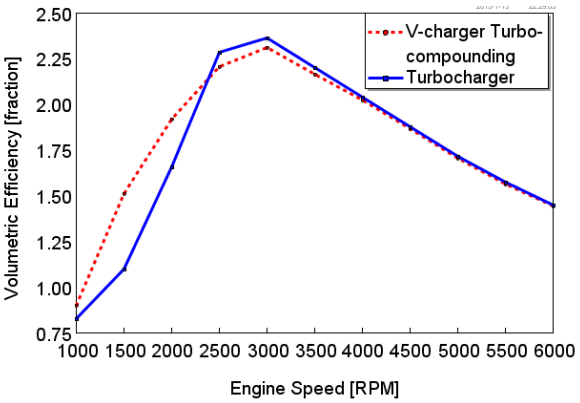

Figure 7.10. **Volumetric efficiency of the engine.**

At the other end, the engine must provide power for the compressor to overcome the imposed parasitic load, which increased the fuel consumption further. The PMEP of the CVT Supercharger turbo-compounding engine was greater than the turbocharged engine within lower engine aped range (from 1000rpm to 2000 rpm), but it made little difference to the brake specific fuel consumption (BSFC). The small reduction in BSFC indicated at 1500 rpm is

basically due to the better volumetric efficiency of the engine as shown in figure 7.10.

From figure 7.10, the volumetric efficiency of the turbo-compounding engine at high speed range is even slightly smaller than that of turbocharged engine (become identical at top engine speed). This is because the power turbine brought about slightly higher back pressure and increased the pumping losses. It also proofs that the lower specific fuel consumption was mainly achieved by the energy recovered by the power turbine. At lower engine speed, the CVT supercharger effectively increased the inlet air density which enhanced the volumetric efficiency significantly.

7.4.3 Pumping mean effective pressure and turbine efficiency

Another important influence that the turbine has on engine is the pumping means effective pressure (PMEP) which directly leads to the pumping losses and deterioration in fuel efficiency.

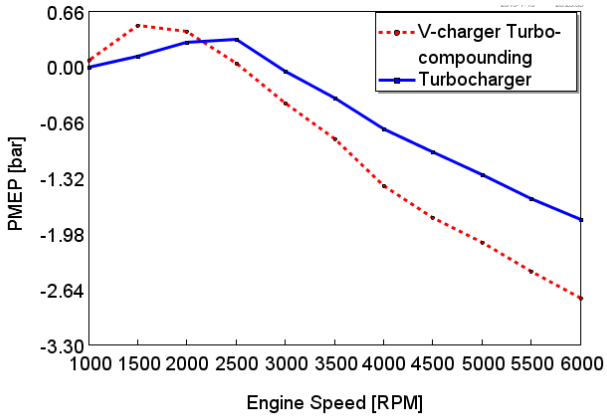

Figure 7.11. **Pumping mean effective pressure.**

From Figure 7.11, the PMEP for both engine systems are positive at 2500 rpm and below and decrease rapidly at higher engine speed. This is because the exhaust gas mass flow rate was smaller at low speed and the temperature was lower. Thus, the average pressure in the exhaust manifold was lower than the intake pressure. At high engine speed, however, the exhaust gas pressure increased dramatically, which created negative pumping pressure.

The installation of power turbine considerably reduced the pumping pressure comparing with the original turbocharged engine. It is due to the wastegate position in the power turbine which was kept closed bringing about higher back pressure to the exhaust manifold, while in the main turbine the wastegate was partially opened at high speed to bypass some of the exhaust flow reducing the back pressure. Nevertheless, from the abovementioned results, the losses in pumping work are remediable by the power recovered from the exhaust.

When the engine speed was below 2250 rpm, however, the wastegate for both turbines were completely shut, but thanks to the more efficient work of the CVT supercharger, the pumping mean effective pressure in CVT Supercharger Turbo-compounding engine regained advantage over the turbocharged engine.

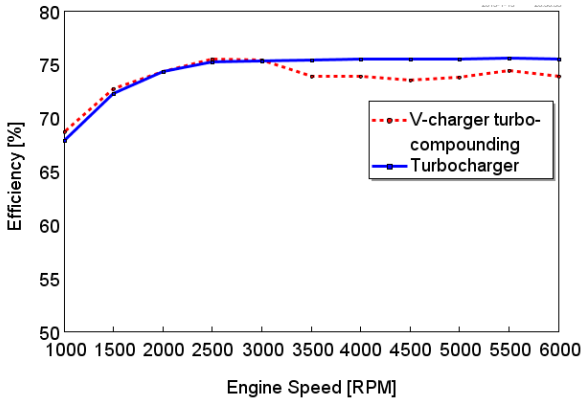

Figure 7.12. **Turbine efficiency.**

As for the power turbine, the GT-Power software allows it to be 'scaled' to have a different size, but with similar flow characteristics. Specifically, the code calculates the instantaneous expander ratio and speed of the power turbine and then looks up its mass flow rate according to the turbine map. Afterwards, the mass flow rate times the scalar before it is imposed. Similarly, it is also possible to use differently scaled compressor for further improvements. In this project, however, the compressors for the turbocharged engine and the CVT Supercharger turbo-compounding engine are of the same size. As figure 7.12 shows, the efficiency of the power turbine is a little below that of the main turbine above the engine speed of 3000 rpm. But the difference is acceptable. Besides, the overall efficiencies for both turbines are above 70%, therefore the slight drop makes little difference to the engine performance.

7.4.4. Part load fuel consumption

As figure 7.13 illustrates, the fuel consumption presented a very small change according to the variation in turbine speed. As mentioned above, it is the inherent characteristics of a centrifugal turbine to reach the peak efficiency at a velocity ratio (U/C) around 0.7. This could explain the rapid decline in turbine efficiency as the turbine speed rising. Although an uptrend (towards the higher turbine efficiency end) in fuel economy could be seen from the plot, the improvement was less than 0.1%, because very little useful work could be extracted from the power turbine (less than 0.008 kW) under this specific working condition.

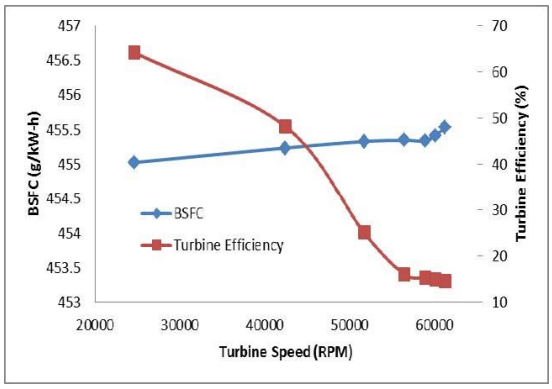

Figure 7.13. **Turbine efficiency and the corresponding engine fuel consumption under load condition (1500 RPM, 2bar) at different turbine speed.**

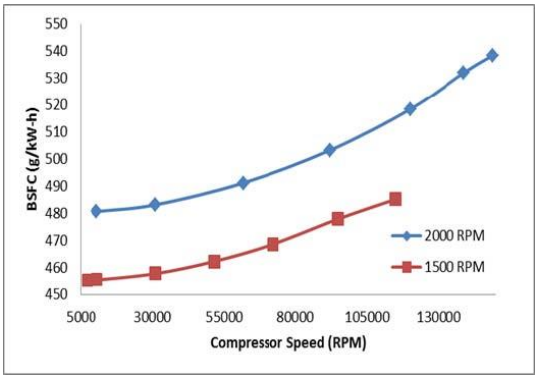

Figure 7.14. The brake specific fuel consumption of the engine vs. compressor speed at 2000 RPM and 1500 RPM (2 bar) respectively.

Figure 7.14 shows the influence that compressor speed has on system fuel economy under partial load condition. The curve started at the minimum required compressor speed for each engine speed, which means a lower compressor speed would not satisfy the BMEP requirement. From the plot, the fuel consumption saw a monotonically increasing with high compressor speed. At the lowest compressor speed, the compressor consumed the least amount of energy. Meanwhile the least pumping work was expended for the intake stroke as the throttle valve was full opened. As the compressor speed rising, the energy spent on the supercharger to boost the intake air was simply wasted across the closing throttle body to meet the low load requirement.

The simulation results suggested that the throttle losses could be eliminated by adjusting the CVT driving ratio at low load operation. But, it also means that the transmission ratio range needed to be significantly extended. Table 7.5 shows the CVT driving ratio demand under

partial load condition as well as the extended ratio ranges for engine speed from 500 RPM TO 3000 rpm.

Table 7-5. Extended CVT driving ratio ranges.

Engine Speed (RPM)	CVT Driving Ratio at Full Load Operation	CVT Driving Ratio at Partial Load Operation	Ratio Ranges
500	16.7	5.5	3.0
1000	60.8	5.4	11.3
1500	90.2	5.3	17.0
2000	77.7	5.0	15.5
2500	74.3	4.7	15.8
3000	66.6	4.7	14.2

Taking the full load CVT driving ratio at high engine speed (from 3500 RPM to 6000 RPM) into consideration, the overall CVT ratio was 19.2.

It should also be noted that the power consumption by supercharger was negative at low load operation when the least compressor speed was applied. The following graph shows the minimum power consumption by supercharger at low load.

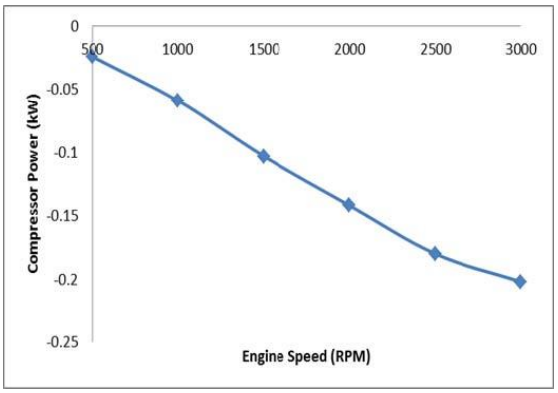

Figure 7.15. **The lowest compressor power consumption at 2 bar BMEP.**

From figure 7.15, a negative value was observed at medium and low engine speed as the intake air blew through the compressor. It means that this power, resulting from windmilling effect, could be transmitted back to the engine crankshaft depending on the working mode of the clutch. If a one way clutch was coupled between the CVT and the crankshaft, the power from the supercharger would simply lost in the form of mechanical and heat losses. Otherwise, the power could be reused to enhance overall efficiency of the engine system. It is demonstrated from the following diagram.

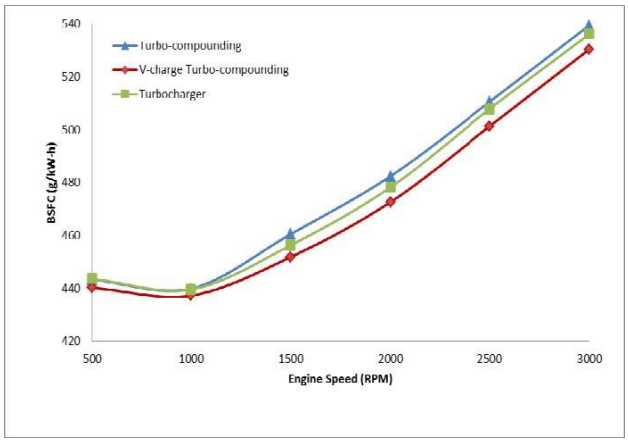

Figure 7.16. Comparison of the fuel consumption (at 2 bar BMEP) between CVT supercharged turbo-compounding engine and traditional turbocharged and series turbo-compounding engines.

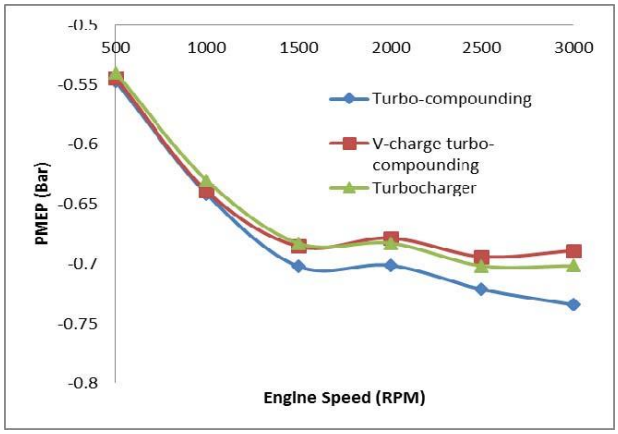

Figure 7.17. Pumping mean effective pressure (at 2 bar BMEP) of CVT supercharged turbo-compounding engine, turbocharged engine and series turbo-compounding engine.

At partial load operation (2 bar BMEP), the exhaust mass flow was extremely low (smaller than 0.002 kg/s). Very little exhaust energy was available for the power turbine. The power turbine efficiency was lower than 20% and the power output was lower than 0.1 kW under this condition. However, a small improvement was still realised by the novel configuration. From figure 7.16, the specific fuel consumption (at 2 bar BMEP) of CVT supercharged turbo-compounding engine was slightly lower than that of the traditional turbocharged engine by up to 0.9%. It should main attributed to the power output from the power turbine and the supercharger as analysed above. Moreover, the waste gates for both the turbocharger turbine and the power turbine were fully closed in this simulation. Without the parasitic load from the compressor, the power turbine was able to spin at higher speed, resulting in higher

pumping mean effective pressure for the engine system, which can be seen from figure 7.17, and thus less pumping losses at medium engine speed. It also contributed to the better fuel economy in CVT supercharged turbo-compounding engine.

By comparing the PMEP (at 2 bar BMEP) of CVT supercharged turbo-compounding engine with the series turbo-compounding engine, it could be found that the pumping losses was significantly reduced in the former design. This could explain the difference in fuel consumption between them.

7.4.5. Transient response

The ability to respond rapidly to transient operation is an important aspect to evaluate the performance of an air handling system. In this section, an investigation was carried out to predict the response speed of CVT supercharged turbo-compounding engine to a tip-in manipulation by comparing the results with a turbocharged and a series turbo-compounding engine. A linearly interpolated lookup table was constructed for the boost demand and corresponding CVT ratio based on the simulation results from the full load steady state results. The changing rate of CVT ratio was controlled in a linear mode and limited by a limiter template. In [8], the upper limit for the rate of change was decided to be +/- 320 per second, which allowed the rated CVT ratio range 200:1 – 40:1 could be achieved in 0.5 second. For the CVT employed in this chapter, the transmission ratio was linearly varied from 10 to 100 within 360ms [201]. This was a simple and crucial controlling module, but was deemed competent for the purpose of this study. However, a test platform is more preferable to carry out this investigation in the future.

When the engine speeds was below 3000 RPM, the difference in transient brake torque response between the CVT supercharged turbo-compounding engine and turbocharged engine was distinct as shown in figure 7.18.

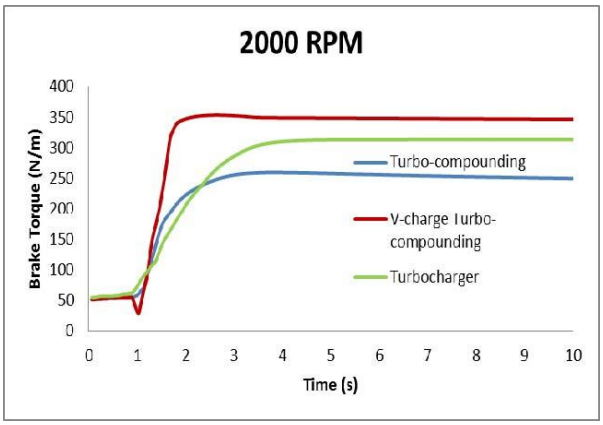

Figure 7.18. Transient brake torque response at 2000 RPM.

It can be seen from figure 7.18, the CVT supercharged turbo-compounding engine was able to achieve the rated torque output within 0.7 seconds, which was 0.3 second faster than the turbocharged engine.

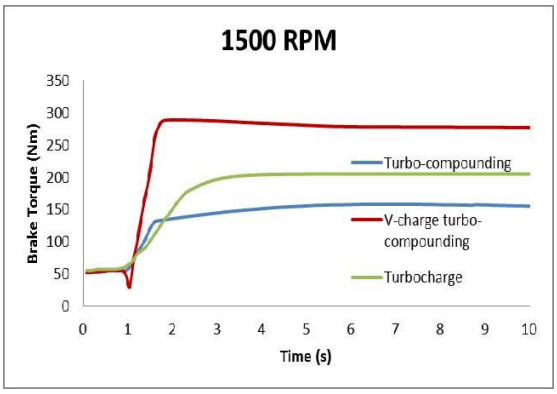

Figure 7.19. **Transient brake torque response at 1500 RPM.**

As the engine speed decreased, the gap between the models was significantly widened, as shown in figure 7.19. At 1500 RPM, the response time for the CVT supercharged engine model to reach the target torque output approximately remained the same, while the turbocharged engine model took much longer time (about 1.7 seconds) to build up the turbine speed and thus the required boost pressure. This could be better demonstrated by the following transient boost pressure plots.

Figure 7.20 illustrates the boosting response at 2000 RPM. As it shows, the CVT driven supercharger takes shorter time to build up the required boosting pressure. While the response of the turbocharger was significantly delayed by the lower acceleration rate of the turbine. At lower engine speed, because of the decreasing in gas flow rate, fewer energy was available for the turbocharger turbine. Therefore, it became more difficult for the turbocharger to speed up and generate desired intake pressure for the engine.

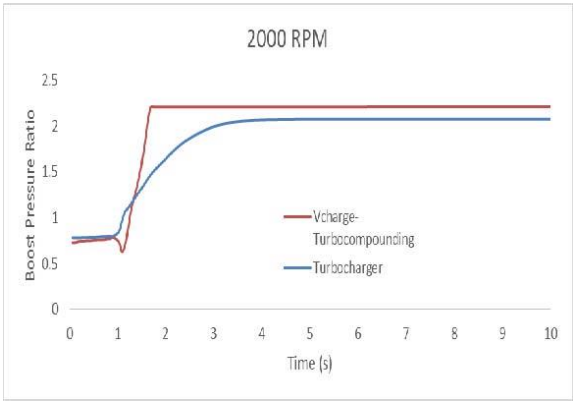

Figure 7.20. **Transient boost pressure ratio response at 2000 RPM.**

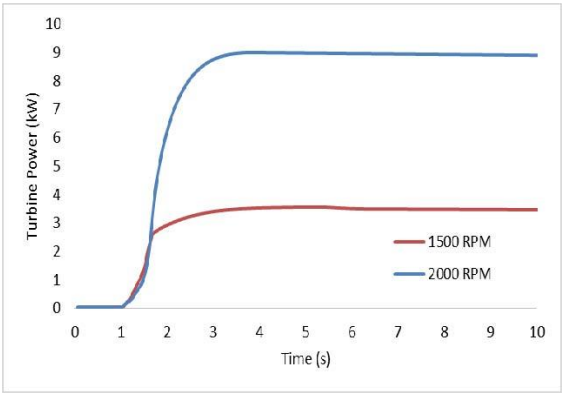

Figure 7.21. **Transient turbine power response at 2000 and 1500 RPM.**

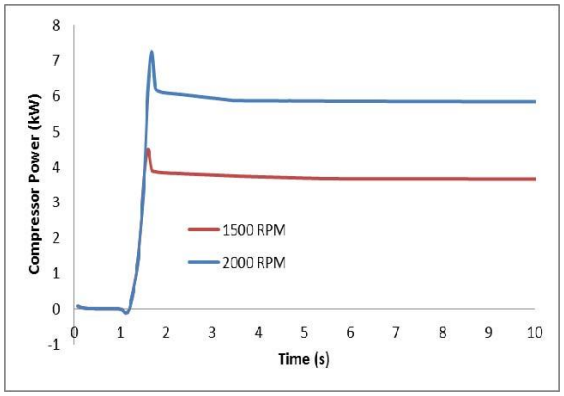

Figure 7.22. **Transient supercharger power consumption response at 2000 and 1500 RPM.**

On the other hand, the CVT supercharger compressor was mechanically driven by the engine crankshaft, which allowed it to keep a relatively constant response rate independent of engine speeds.

However, it is worth noting that a small diving was existing at the starting point (around 1 second) of the brake torque curve for the CVT supercharged turbo-compounding engine, as shown in figure 7.21 and 7.22. It demonstrates the torque extracted from the engine crankshaft to overcome the inertial of the compressor as well as the CVT drive. From the following plots, the power output from the power turbine was slightly higher than the power consumption of the supercharger at 2000 RPM, but slightly lower at 1500 RPM. More importantly, power generation from gas turbine was much slower than the consumption rate of the supercharger, which means extra torque needed to be extracted from the crankshaft to drive the compressor. This, in turn, resulted in the diving in the brake torque output.

The magnitude of this torque is proportional to the inertia and acceleration of the

supercharger system. The inertia of the CVT would depend on the particular CVT system applied. In this chapter the inertial of CVT and the belt pulley was determined to be 0.00078 and 0.00029 kg·m^2 respectively. It is suggested that an appropriate calibration for the transmission ratio control system would be needed to rectify this and improve the drivability.

7.5 Conclusion

The effect that a turbo-compounding has on a 2.0 litre gasoline engine and the benefit of coupling a CVT to the supercharger were examined by comparing its performance data with a conventional turbocharged engine of the same displacement and compressor characteristics. In this project, both the power recovery by the power turbine and the pumping losses resulted from the higher back pressure were considered. The CVT supercharger in combination with the turbo-compounding contributed to improve the engine performance at lower engine speed range. The simulation results proved the practicability of this concept. The CVT Supercharger helped to increase the brake torque by up to 24% at 1500 revs/min. In the other end, the turbo-compounding increased the brake torque evenly by 7% from 3000 revs/min and above. The BSFC was reduced by up to 8% at top engine speed. But the improvement descends as the engine speed slowing down and become vanished at 2000 revs/min because of the weakened power turbine function and the parasitic load imposed by the CVT supercharger.

Under partial load condition, very little improvement was gained from adjusting the turbine speed due to the significant decrease in turbine power output. On the contrary, the CVT driving ratio for the compressor needed to be carefully optimized as it helped to reduce the power consumption by the supercharger, and more importantly, improve the fuel economy of the whole system. The improvement in specific fuel consumption of the CVT supercharged turbo-compounding engine, when comparing with traditional turbocharged engine model, was believed due to the windmilling effect of the compressor and the reduced pumping losses.

For the transient performance evaluation, the CVT supercharged turbo-compounding engine was able to provide the rapidest response of boost pressure and torque output due to the mechanical connection between the supercharger and the engine crankshaft. A diving in brake torque was seen as the compressor starting to accelerate. These torque losses was proportional to the inertial of the supercharger and the transmission ratio. A proper calibration was needed to rectify this in order improve the drivability.

Chapter 8 –Comparison between inverted Brayton cycle and CVT Supercharger turbo-compounding

The application of turbo-compounding and Brayton cycle in small automotive power plants has been relatively less explored because of the inherent difficulties, such as the detrimental backpressure and higher complexity imposed by the additional devices. Therefore, research has been conducted, in which modifications were made to the traditional arrangement aiming to minimize the weaknesses. The turbocharger of the baseline series turbo-compounding was eliminated from the system so that the power turbine became the only heat recovery device on the exhaust side of the engine, and operated at a higher expansion ratio. The compressor was separated from the turbine shaft and mechanically connected to the engine via a CVT. According to the results, the backpressure of the novel system is significantly reduced when comparing with the series turbo-compounding model. The power output at lower engine speed was also promoted. For the pressurized Brayton bottoming cycle, rather than transferring the thermal energy from the exhaust to the working fluid, the exhaust gas was directly utilized as the working medium and was simply cooled by ambient coolant before the compressor. This arrangement, which is known as the inverted Brayton cycle was simpler to implement. Besides, it allowed the exhaust gasses to be expanded below the ambient pressure. Thereby, the primary cycle was less compromised by the bottoming cycle. The potential of recovering energy from the exhaust was increased as well. This chapter analysed and optimized the parameters (including CVT ratio, turbine and compressor speed and the inlet pressure to the bottoming cycle) that are sensitive to the performance of the small vehicle engine equipped with inverted Brayton cycle and novel turbo-compounding system respectively. The performance evaluation was given in terms of brake power output and specific fuel consumption. Two working conditions, full and partial load (10 and 2 bar BMEP) were investigated. Evaluation of the transient performance was also carried out. Simulated results of these two designs were compared with each other as well as the performance from the corresponding baseline models. The system models in this chapter were built in GT-Power which is a one dimension (1-D) engine simulation code. All the waste energy recovery systems were combined with a 2.0 litre gasoline engine.

8.1 Introduction

8.1.1 Exhaust energy recovery technologies

As mentioned in **chapter 2**, there are a number of methods to capture the exhaust energy from the internal combustion engine and convert it into useful power. Currently, the dominating technologies include bottoming cycles, such as the Rankine cycle and the Brayton cycle, and turbo-compounding technologies. Amongst these technologies, Rankine cycle, especially the organic Rankine cycle, has the greatest potential to elevate the overall systematic efficiency without interfering with the engine working condition [20, 205, 206].

Despite the relatively low potential for heat recovery of the turbo-compounding and the Brayton cycle comparing with the Rankine cycle, the appeal of these two approaches mainly consisted in the simplicity and compactness in construction and the capability of directly utilizing commercially available radial turbomachinery devices. Besides, they are also different from Rankine cycle, which has to include a heat exchanger to transfer thermal energy from the exhaust gases to the working fluid before convert it into mechanical work, that the working medium for pressurized Brayton cycle is air, whilst the turbo-compounding or the inverted Brayton cycle even can directly use the exhaust gas as the working fluid which further simplifies the implement.

8.1.2 The purpose of proposing the novel schemes

Simulation results shows that the combination of supercharger and continuous variable transmission drive (CVT) could effectively shorten the response time of the booster and minimize the parasitic losses of the supercharger at high engine speed. In other words, the addition of CVT enables the operation of the supercharger to be fully optimized over the entire engine speed range. Because all of the exhaust energy extraction is occurring at exhaust manifold temperature (as opposed to the lower temperature that the power turbine in a serial turbo-compounding arrangement works at), the same amount of work can be extracted with lower overall expansion ratio (assuming same turbine efficiencies) and hence lower backpressure. In the novel arrangement, the original turbocharger was no longer used as the foundation for the charged scheme, which means the inlet air boosting totally relied on the CVT supercharger while the power turbine becoming a monofunctional component to recover exhaust gas energy. Modification was also made to the Brayton cycle. The waste energy recovery unit in the original system was inverted, which means, rather than absorbing the exhaust thermal energy with pressurised air, the exhaust gas would be firstly directed

into the power turbine to generate mechanical power before it was cooled and boosted back to atmospheric pressure. Detailed introduction about the schematic of these two novel designs will be given in the following section. This chapter aims to provide a back-to back comparison to between these two novel systems on the same baseline engine.

8.2 Modelling Description

The baseline engine is a 2.0 litre four-cylinder inline turbocharged intercooled gasoline engine which is the same to **Chapter 7**.

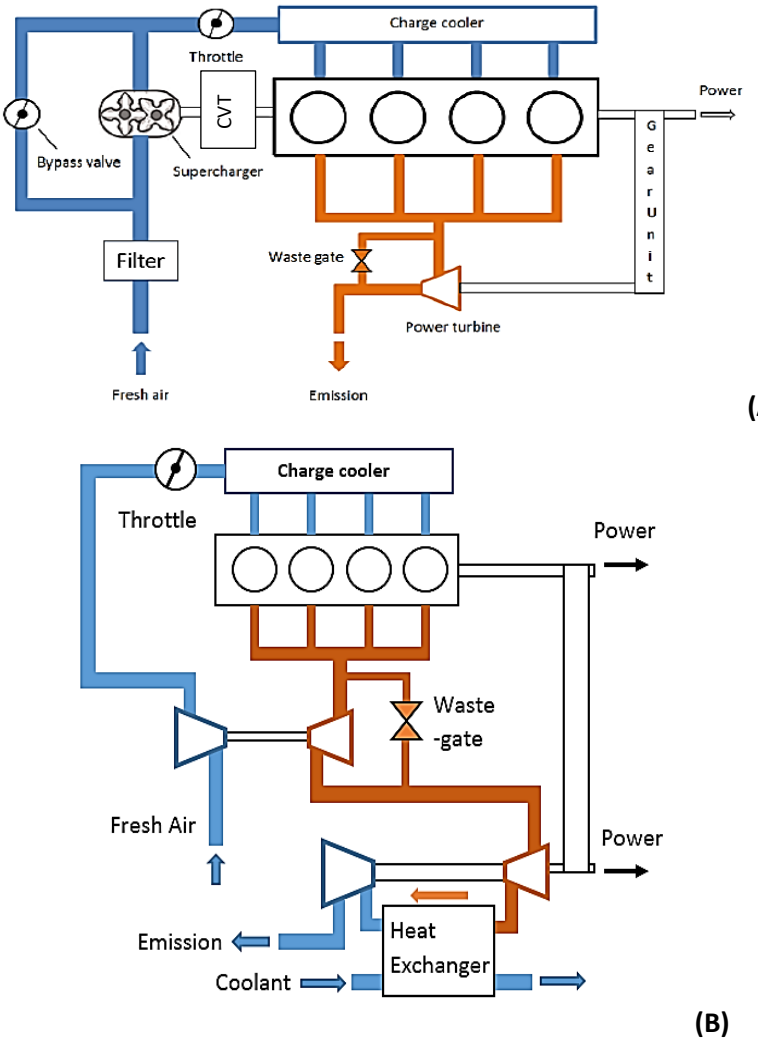

Figure 8.1. **Schematic diagram of (A) CVT supercharged high pressure turbo-compounding engine and (B) the inverted Brayton cycle engine.**

The layouts of the high pressure turbo-compounding engine equipped with the CVT driven supercharger and the inverted Brayton cycle engine system are shown in Figure 8.1. For the

top diagram, fresh air from the filter is boosted by the supercharger which is mechanically connected to the crankshaft via a CVT before it enters the inlet manifold of the engine. On the exhaust side, the burnt gas from the manifold directly enters the high pressure power turbine. Exhaust energy is extracted by the power turbine that converts it onto mechanical power which is in turn routed to the engine crankshaft via mechanical gear. As mentioned above, the compressor speed can be adjusted according to the engine load and speed to explore the optimal trade-off between satisfying the boosting requirement and imposing parasitic power consumption to the engine.

The diagram on the bottom illustrates the schematic of the engine model equipped with the inverted Brayton cycle. Substantially, this cycle can be regarded as an extension to a series or low pressure turbo-compounding unit with an exhaust air cooler and a power turbine driven compressor to make up a Brayton cycle [51]. The addition of compressor in the bottoming cycle allows the expansion of the exhaust gases below atmospheric pressure, while the heat exchanger gives rise to the power margin between power turbine and compressor.

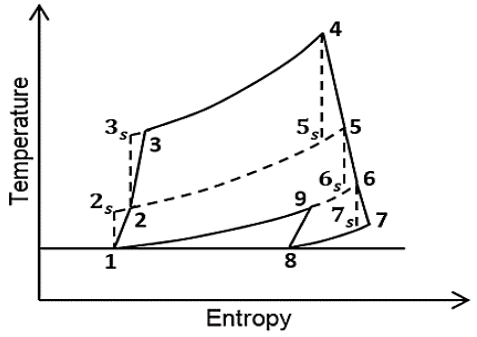

Figure 8.2. **Temperature and entropy diagram of a turbocharged engine with single stage of the inverted Brayton cycle compression.**

A T-S plot is also shown in figure 8.2 to clarify the stages within the cycles. A standard Otto cycle is made up of an isentropic compression process $\mathbf{2 \rightarrow 3}$, a constant volume heat addition process $\mathbf{3 \rightarrow 4}$, an isentropic expansion process $\mathbf{4 \rightarrow 5}$ and a constant volume heat rejection process$\mathbf{5 \rightarrow 2}$. In a supercharged turbo-compounding engine, on the other hand, the high temperature exhaust gas at state 5 was expanded through the power turbine before it left state 6 and further released heat to state 1. With the addition of the inverted Brayton cycle, the exhaust at state 6 would be over-expanded by the next stage turbine to state 7 from where the subatmospheric gas was directed through an intercooler and a compressor in

series to be pressurised back to atmospheric pressure. The dashed line in this plot represents the idealized isentropic process where the irreversibility was not considered.

Comparing with the turbo-compounding set-up, the inverted Brayton cycle is of the advantage of increasing the potential to draw energy from the exhaust gas and leaving the primary cycle less affected. However, in this arrangement, because a high entering pressure is preferable for the power turbine to generate higher kinetic power, the engine performance will also compromise due to the raised back pressure. Therefore, the exhaust pressure between the main and power turbine needs to be carefully optimised in this research.

The major challenge with electric turbochargers is the difficulty to reject the heat developed within the constrained physical size of the motor/generator [83]. Besides, most electrical generators run at low speeds are relatively large and heavy, while the generators utilised in electrical turbo-compounding technology need to be very compact, high speed and high efficiency and can be added directly to the high-speed turbine shaft. The energy storage device can be a battery, a super-capacitor bank (specifically, the DC applications requiring many rapid charge/discharge cycles and short term compact energy storage and lower cell voltage are more favourable) or a combination of both [208].

Exhaust can be placed after the second turbine or between the turbocharger turbine and the power turbine in LP configuration. Placement of an after-treatment unit upstream of a WER system would reduce the heat exchanger fouling and alleviate some of the exhaust after-treatment fuel penalty by recovering some of the energy released by exothermal reactions during catalyst regeneration events. If the exhaust after treatment is located upstream of the power turbine, then the power turbine expansion ratio will be applied to a lower outlet pressure and thus the expansion ratio will be slightly higher. This may help the turbine to work more efficiently. Mamatetal [46] concluded that locating the exhaust after-treatment upstream of the power turbine would provide the best compromise in terms of fuel consumption and engine performance. On the other hand, as reported by Kruiswyk [134], this placement may limit the options of hardware. In general, this placement is able to result in an incremental 1% BSFC improvement at higher speeds and loads, and less fuel penalty under very low load conditions.

In terms of the compactness, the added weight of a turbo-compounding system of a Scania production engine that uses an electric turbo compound device is in the order of 80 kg (Scania press release) whereas a comparable Rankine cycle secondary fluid power system would weigh around 100 kg. The weight of a mechanical turbo compound drive of a Caterpillar engine would also be in the same order [29].

Lastly, according to the investigation in [57], the turbo-compounding system has a significant price advantage over other alternate power cycles. The incremental difference between the turbo-compounding and Brayton cycle system is more than $4000 for the equal power level.

8.3 Methodology

In order to simplify the modelling process, the gear units between the power turbine and the crankshaft was replaced by a “load” and a “power rot” unit to remove mechanical power from the turbine and add it to the engine. The turbine speed could be varied by changing the imposed load. In the same way, the optimization to the power turbine speed was also carried out through varying the imposed load. The CVT efficiency was assumed to be 100% during the simulation to simplify the analysis. According to the work in [60], a CVT efficiency of 85% results in 2% reduction in peak torque compared to the performance of a twin-charged engine with an ideal CVT drive. Therefore, it was supposed that the assumed CVT efficiency would satisfy the precision requirement of the study in current stage

This chapter aimed to analyse and optimise the parameters (including CVT ratio, turbine and compressor speed and the inlet pressure to the inverted Brayton cycle) that are sensitive to the performance of the small vehicle engine equipped with the inverted Brayton cycle and novel turbo-compounding system respectively. In order to evaluate the performance of the whole engine system, both the operation under full and partial load (at 10 and 2 bar BMEP) condition were investigated in terms of brake torque output and specific fuel consumption. Evaluation of the transient performance was also carried out. Simulating results of these two modified system were compared with each other and the computation results from the corresponding baseline turbocharged engine models.

In the previous studies, Mitsunori Ishii et al [199], stated that higher compressor pressure ratio was beneficial for increasing the power output of both the power turbine and the reciprocating engine in a turbo-compounding engine system. It was indicated that the increased parasitic power consumption of the supercharger resulted from enhanced compressor pressure ratio could be well compensated by the improvement in engine power output. Therefore, as it suggested, when a high pressure turbo-compounding engine was operated under full load condition, the upper limit of the mechanical strength and heat resistance of the system became the only confine for the compressor pressure ratio. Moreover, because a radial compressor was employed in this research, the operation of the booster should be carefully controlled within the surge limits. On the other hand, it was also

indicated that an optimum value existed for the boost pressure, which it was 1.5 for the engine model in Ishii's research, at partial load operation. This was because the power consumption of the compressor was more conspicuous than the benefit it bringing to the overall power output of the system. It means that a proper optimization of the boost pressure and essentially the driving speed of the compressor are necessary for the improvement of the overall efficiency of the whole system under low load condition. Besides, it was determined by the inherent characteristics that the highest centrifugal efficiency was realised at a blade-to-gas ratio of about 0.7 which means for different working condition, there was an optimum spinning speed and thus expansion ratio for the power turbine to maximize the overall thermal efficiency. Efforts should also be made to explore the trade-off between compression ratio and the compressor pressure ratio to realize the most optimal allocation between engine power and turbine power output for the highest overall efficiency, and more importantly, prevented the in-cylinder pressure from exceeding the upper limit. As aforementioned, the performance of CVT supercharged turbo-compounding engine was optimized by adjusting the compressor boosting and the expansion ratio of the power turbine. As a matter of experience, the best fuel economy was achieved with maximum power output if the overall thermal efficiency was defined by brake specific fuel consumption. Thereby, the system optimization at full throttle operation concentrated on improving the power output of the whole system.

Based on the work in [51] and [207], it could be concluded that there are a variety of aspects that affects the improvement in the bottoming inverted Brayton cycle (IBC) performance. It includes the inlet temperature and pressure to the power turbine, the isentropic efficiency of the turbomachinery, the number of compression stages and the effectiveness of the heat exchanger. Theoretically, the IBC performance can be improved by increasing the compressor stage in the bottoming cycle. However, taking the system complexity and package into consideration, one stage compression could thus be regarded as the most sensible configuration for automotive application. In this research, the inlet pressure into the power turbine was adjusted by changing the turbine size. The utilized simulation code allow the turbine map to be scaled while maintain the similar mass flow characteristics. The compressor mass multiplier can be changed in the same way. The turbine speed can be adjusted by changing the load imposed on the turbine shaft in simulation, while in real test, it can be realised by changing the transmission ratio between turbine and engine shaft instead. Unlike the turbo-compounding devices that rely on a relatively high back pressure to operate effectively, the IBC system causes less deterioration to the engine performance.

However, there is a minimum requirement of the inlet temperature and turbomachinery efficiency for IBC to ensure positive work to be produced. In other words, the high performance of the turbomachinery and the heat exchanger is necessary for the bottoming cycle to deliver its full potential.

8.4 Simulation and Results

In order to ensure the capability of the GT model to precisely predict the performance of the whole engine system, a calibration was carried out to compare the data from the baseline turbocharged engine model with the experimental testing. By comparing the cylinder pressure under full and partial load conditions, it indicated that the actual data and the calculation data matched fairly well in the qualitative tendencies which confirm the appropriateness of the combustion model, etc. The comparison of the heat release rate and in cylinder pressure also demonstrated a close match, as shown in figure 8.3 and 8.4. These results indicated that the model was of fairly acceptable level of precision to simulate the performance of the whole engine system based on the baseline model.

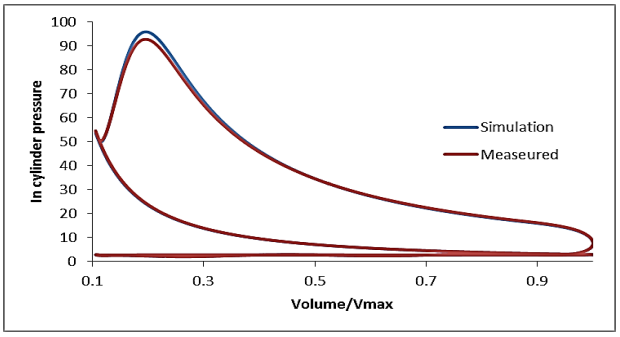

Figure 8.3. Comparison of simulated and measured P-V diagrams.

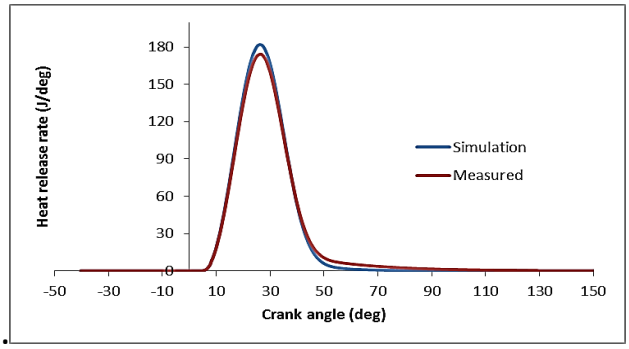

Figure 8.4. Comparison of simulated and measured heat release rates.

Unlike the CVT supercharged system [167] that will “hand over” the intake boosting to the

turbocharger at high engine speed, so that the supercharger only needs to accommodate for the pressure ratios that was normally required at low speed, the novel engine model in this chapter expects the supercharger to satisfy the boost requirement of the engine at all operation points because of the absence of the turbocharger devices. Therefore, the original compressor from the baseline turbocharged engine model was kept for the convenience of matching the intake air flow characteristics.

In this chapter, the compressors are of the same size and mass flow characteristics as that of the baseline turbocharged model. The power turbine in the turbo-compounding model is also the same as the turbocharger turbine in the original and the inverted Brayton cycle engine models.

The simulation process was constrained by two performance limits. Firstly, the maximum cylinder pressure should not exceed 110 bar; secondly, the maximum compressor speed should be kept below 200000 rpm, and certainly, the operating point should not move beyond the surge line. The power turbine speed was varied up to 300000 rpm.

Optimization was firstly carried out for the CVT ratio and turbine speed in the turbo-compounding engine to achieve the best power output under full load condition followed by the tuning of the bottoming cycle in IBC. The results of rated power output would be employed as the upper limit of the power criterion in the following transient performance simulation.

For the CVT supercharged turbo-compounding engine, similar to Chapter 8, the power turbine speed as well as the CVT ratio were determined by the DoE optimization according to different working condition.

Under partial load condition, the CVT driving ratio would also be verified in order to find the best setups for the benefit of reducing specific fuel consumption. In this chapter, the BMEP has been set to 10 and 2 bar to represent the partial load operation.

In the following section, the influence of these parameters, namely the compressor and power turbine speed, on the fuel economy of the CVT supercharged turbo-compounding engine would be summarised.

For the full load simulation for all the models, the engine speed was varied from 500 to 6000 rpm in the increments of 500 rpm. For the partial load operation, two setups of brake mean effective pressure (BMEP), 2 bar and 10 bar, were examined over the engine speed range of 500-3000 rpm and 1000-6000 rpm respectively.

During evaluating the transient performance of the system, the duration taken by the engine BMEP to climb from 2 bar to 90% of the rated value was measured. The air fuel ratio was

considered as a constant of 14.5 for all the engine speed and working condition for simplicity. This chapter also aims to assess the systematic benefit from adding an inverted Brayton cycle to a turbocharged Otto cycle. The turbine size in the bottoming cycle was scaled trying to optimize the inlet pressure to the power turbine. Design of experiments factors and ranges for the turbine size in the inverted Brayton cycle was given in table 8.1.

Table 8-1. Design of experiments factors and ranges for the turbine size in the Brayton cycle.

Parameters	Minimum Value	Maximum Value	Ranges
Turbine Size Multiplier	0.2	3	15

In the following section, the influence of the inlet pressure on the inverted Brayton cycle will be introduced in detail.

8.5 Results

Firstly, it should be indicated that the shown values for engine power and torque in this section are all brake values.

8.5.1 Optimization under full load condition

Figure 8.5 shows the influence that supercharger speed has on power output and fuel economy of the whole system under full load condition at 3000 rpm. The curve starts at the compressor speed of about 100000 rpm and ends at the upper limit for the supercharger speed which is 200000 rpm.

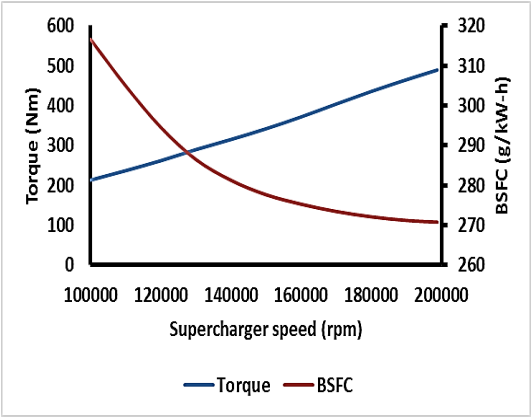

Figure 8.5. CVT supercharged turbo-compounding engine torque and BSFC vs supercharger speed at 3000 rpm.

From the plot, the fuel consumption decreased monotonically as the compressor speed

increased, along with an almost linear increasing in brake torque. It should mainly thank to the improvement in turbine power and volumetric efficiency of the engine.

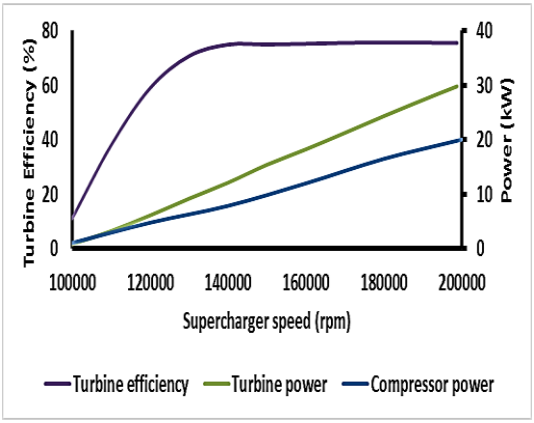

Figure 8.6. CVT supercharged turbo-compounding turbine efficiency and power vs supercharger speed at 3000 rpm.

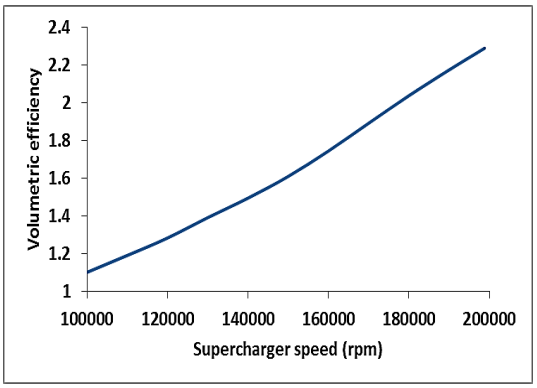

Figure 8.7. CVT supercharged turbo-compounding volumetric efficiency and power vs supercharger speed at 3000 rpm.

As shown in figure 8.6 and 8.7, the power turbine efficiency and volumetric efficiency kept rising as the supercharger running faster. Even though the power efficiency reached a plateau at 140000 rpm, the power output from the turbine increased continuously (up to 30 kW) due to the increasing flow of exhaust gas and thus the energy availability. Moreover, the improvement in volumetric efficiency played a very important role in reducing the fuel consumption of the engine. Generally, at full load operation, higher supercharger speed was beneficial for improving the power generation and fuel economy of the whole system. The examination was also conducted for other engine speed, and similar results were obtained. On the other hand, when the engine was operated under low load condition, results were just the opposite.

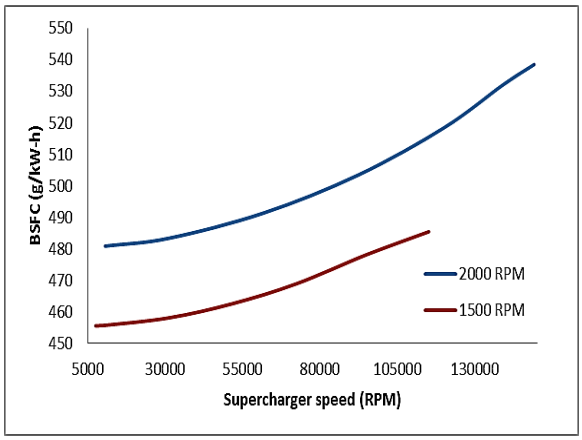

Figure 8.8. **CVT supercharged turbo-compounding engine BSFC vs supercharger speed under Low load condition.**

Figure 8.8 illustrates the fuel consumption trend along with the change in supercharger speed when the engine ran at a low load of 2 bar BMEP. From the plot, both the specific fuel consumption at 1500 and 2000 rpm increased at higher supercharger speed.

It could be explained that at the lowest compressor speed, the compressor consumed the least amount of energy. At the same time, less pumping work was expensed by the intake stroke as the throttle valve was more widely opened. As the compressor speed rising, the energy spent on the supercharger to boost the intake air was simply wasted across the closing throttle body which has to reduce the inlet air pressure to meet the load requirement. The simulating results also suggested that the throttle losses could be eliminated by adjusting the CVT driving ratio according to different working condition. But, it also means that the transmission ratio range needed to be significantly extended in that case.

It should also be noted that the power consumption of the supercharger was negative at low load operation when the lowest compressor speed was applied, which means the compressor was working in a “windmilling” mode. The generated power, despite its magnitude was smaller than 0.3 kW, could be transmitted back to the engine crankshaft depending on the working mode of the clutch. If a one-way clutch was coupled between the CVT and the crankshaft, the power from the supercharger would simply lost as mechanical and heat losses. Otherwise, the power could be received by the engine to enhance the overall efficiency of the whole system.

Figure 8.9 shows the turbo-compounding engine torque and fuel consumption at different turbine speed. The CVT ratio was kept constant to be 66.6 when the turbine speed was swept. As the curves illustrate, when then engine ran at 2000 or 3000 rpm, the brake torque increased significantly as the power turbine speed rising. The specific fuel consumption was

reduced accordingly. This is due to the increased turbine efficiency and reduced pumping work. At higher engine speed, however, the growth trend slowed down, while the plateau appears earlier. This is because of the inherent characteristics of a centrifugal turbine to reach the peak efficiency at a velocity ratio (U/C) around 0.7.When the mass flow rate decreased at high engine speed, the power output and the optimum speed of the power turbine decreased correspondingly.

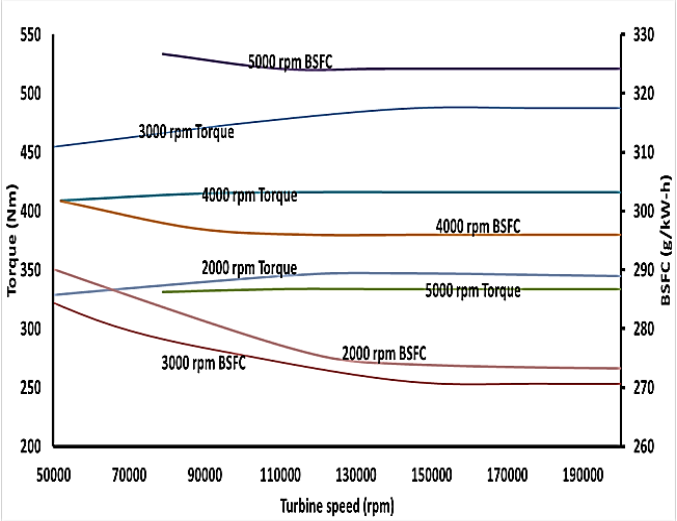

Figure 8.9. CVT supercharged turbo-compounding engine torque and BSFC vs turbine speed.

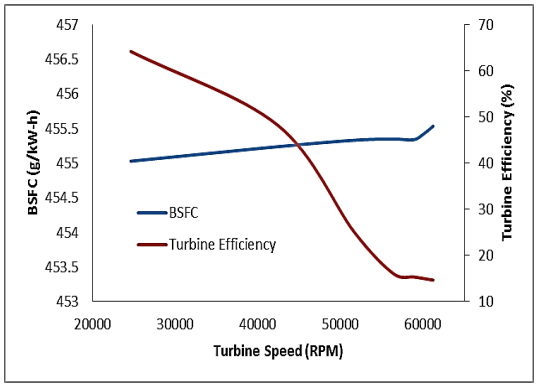

Figure 8.10. CVT supercharged turbo-compounding engine BSFC and turbine efficiency vs turbine speed under low load condition.

At low load operation when the mass flow was extremely small, the power turbine efficiency decreased rapidly as the running speed increasing, as shown in figure 8.10. However, the performance of the power turbine had very little influence on the overall engine system. It could be found in the graph that less than 0.1% extra specific fuel consumption was added by the deep diving in turbine efficiency. The reason was that the exhaust energy was very

low under low load condition, so that the power output from turbine was too small to affect the overall performance of the entire system.

8.5.2 Optimization of the inlet pressure before the inverted Brayton cycle

Figure 8.11 illustrates the effects that the inlet pressure to the IBC has on the brake torque and BSFC of the engine system under full load condition.

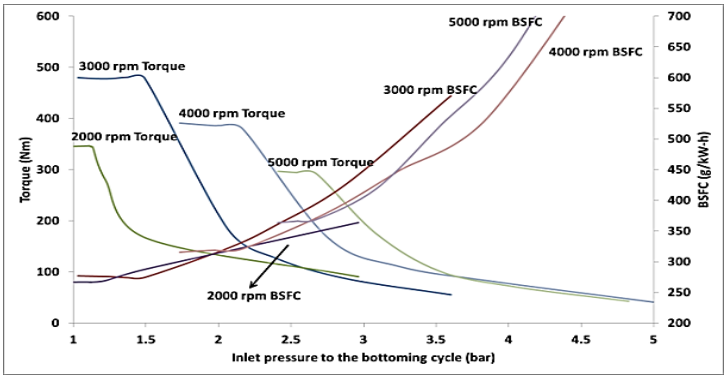

Figure 8.11. **IBC engine torque and BSFC vs inlet pressure to the bottoming cycle.**

Within the speed range between 2000 rpm and 5000 rpm, it was a common trend that the engine performance rapidly deteriorated with increased pressure before the bottoming cycle. In the author's opinion, the reason was that both the engine performance and the exhaust gas mass flow rate were very sensitive to the back pressure at high load operation. Because of the increasing in pre-IBC pressure, more pumping load was imposed to the scavenging process, at the same time, the exhaust mass flow rate decreased significantly, which reduced the energy availability to the bottoming cycle. At 3000 rpm, for example, the torque output from the power turbine was maximised with the inlet pressure of 1.4 bar. However, the magnitude was about 1.5 Nm, which was much smaller than the engine brake torque. This could explain the flat trend below a certain inlet pressure when the scavenging of the stroke was very little affected by the back pressure.

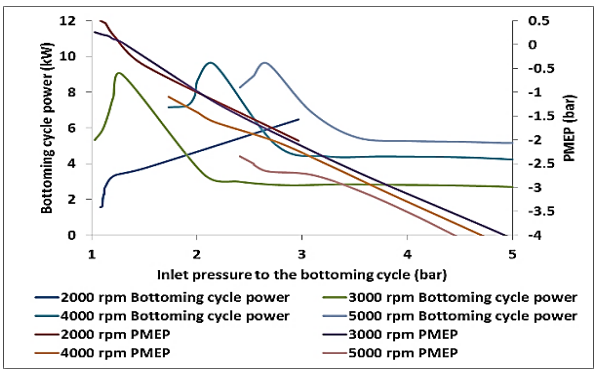

Figure 8.12. **IBC power and PMEP vs inlet pressure to the bottoming cycle.**

As shown in figure 8.12, PMEP plummeted down when the back pressure increased, which brought about a rapid decline in the bottoming cycle power output.

Figure 8.13 shows the IBC power output and BSFC against the sweep of heat exchanger effectiveness from 0.3 to 0.9. From the results, the net power outputs from the IBC bottoming cycle reached the maximum at all engine speeds. But, they were not linear increase. Slight dips can be found with a particular heat exchanger effectiveness at each engine speed. These low points should be ascribed to the compromise between the power generation from the IBC turbine and the working load imposed to the compressor. Specifically, on the one hand, the bottoming power turbine is able to expand the exhaust gas to lower pressure and extract more energy from it with higher heat exchanger effectiveness. On the other hand, the compressor has to consume more power to pressurise the exhaust gas above atmospheric pressure. Therefore, it should also be noted that, although the overall thermal efficiency of the bottoming cycle, especially the compressor efficiency, is higher with more effective heat exchanger, it may not have direct effects on the power output. However, it is also illustrated in figure 8.13 that the fuel consumption of the whole engine system is continuously reduced by enhancing the heat exchanger effectiveness. It mainly benefited from the decreased back pressure imposed by the bottoming cycle. As mentioned above, the outlet pressure from the IBC turbine is lower with higher heat exchanger effectiveness. It allows the compressor to pressurize the exhaust gas to a lower pressure level, above atmospheric pressure though.

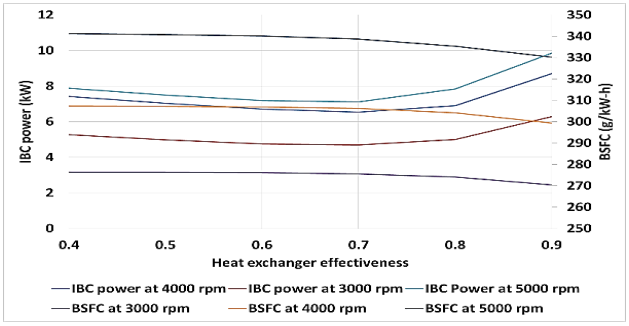

Figure 8.13. **IBC power and BSFC vs heat exchanger effectiveness.**

8.5.3. Part load performance

Figure 8.14 illustrates the fuel consumption of IBC and CVT supercharged turbo-compounding engine at partial load operation. From the results, the specific fuel consumption of these two arrangement were very close at 2 bar BMEP as the air flow through the engine was very low and almost immune to the changes in the layout of the exhaust system in this condition. Besides, due to the rarefied exhaust gas, these two waste energy

recovery technologies made very little contribution to improve the engine performance. When the engine load went up to 10 BMEP, however, the difference between them began to emerge. From the plots, at lower engine speed, the IBC engine had more advantages over the other in fuel economy, while the turbo-compounding engine offered better performance at high engine speed (above 2000 rpm).

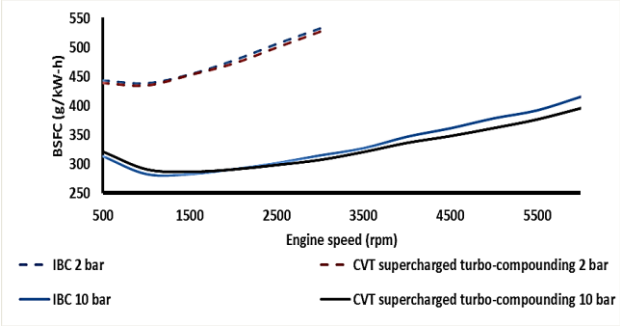

Figure 8.14. Comparison of the fuel consumption between IBC and CVT supercharged turbo-compounding engine under partial load condition.

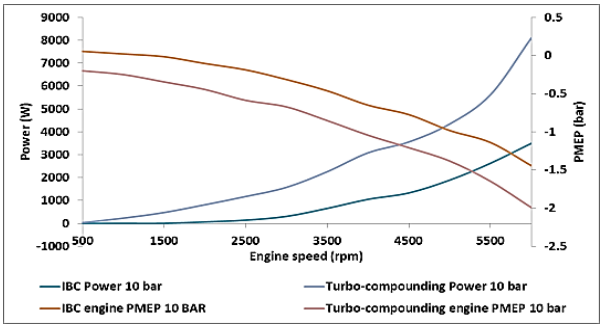

Figure 8.15. IBC and turbo-compounding power output and PMEP.

This could be explained with the results shown in figure 8.15. When the engine was running at lower speed, the energy recovery systems provided very little power. The overall efficiency was more affected by the pumping losses. The IBC engine, consequently, was able to embody the superiority in fuel consumption with higher PMEP. When engine ran faster, the power output from the turbo-compounding system gradually offset the disadvantage in pumping losses and provides better fuel economy.

8.5.4 Full load performance

Figure 8.16 shows the performance of the novel arrangements and conventional turbocharged engine under full load condition. From the results, both the waste energy recovery technologies helped to improve the engine brake torque and fuel economy over the entire speed range when comparing with the baseline turbocharged engine. Specifically, the

IBC engine provided up to 100 Nm more torque and nearly 9% lower fuel consumption. While the CVT supercharged turbo-compounding engine, in addition to the enhanced engine performance at middle and high engine speed, offered impressively higher torque at 1500 rpm thanks to the higher boost pressure from the CVT driven supercharger, and this was very useful for improving the driveability.

Based on the similar logic, the difference in fuel consumption could be explained by the shift in bottoming cycle power output and PMEP. As shown in figure 8.17, the turbo-compounding engine showed better exhaust energy recovering ability at high engine speed while suffers from more pumping losses at low speed. Therefore, it offered better fuel economy at high engine speed but was inferior to the IBC engine at lower engine speed. It also suggested that the IBC engine was less susceptible to the working condition of the engine. And also, the engine performance was less compromised by the inverted Brayton cycle.

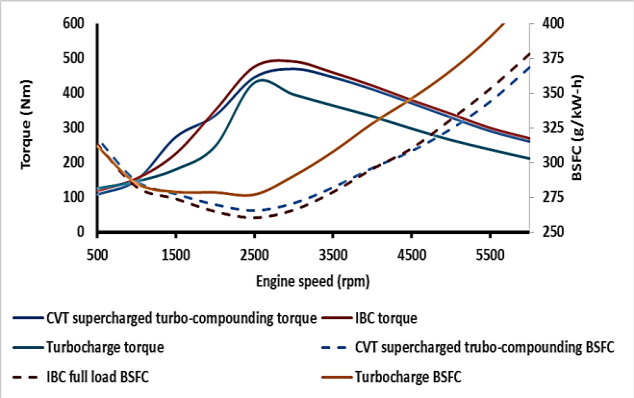

Figure 8.16. Full load performance comparison between IBC and CVT supercharged turbo-compounding engine.

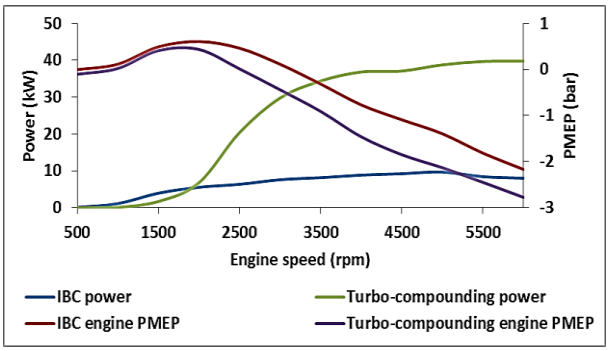

Figure 8.17. Power generation of the waste energy recovery devices and the PMEP of the whole system.

8.5.5 Transient performance

Figure 8.18, 8.19 and 8.20 demonstrate the transient response of each arrangement at

different engine speed. It was evident that the CVT supercharged turbo-compounding engine achieved the torque demand much more quickly comparing with the other two, while the IBC engine was the worst in terms of transient performance. At 2000 rpm, the turbo-compounding engine equipped with CVT driven supercharger was able to achieve the target power output in less than 1 second which was about 4 and 3 seconds faster than the IBC and turbocharged engine respectively. This was due to the rapid acceleration of the CVT driven supercharger. The turbocharger, on the other hand, had to wait for the accumulation of the exhaust energy before it built up the spinning speed.

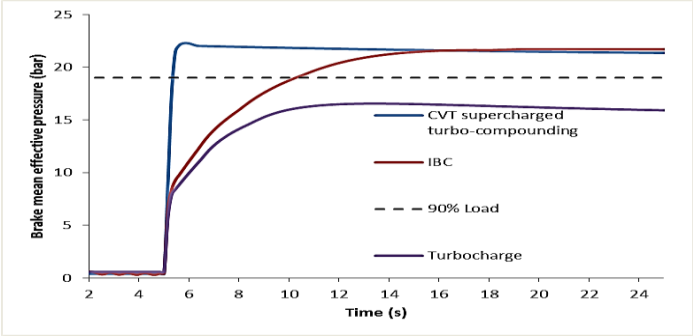

Figure 8.18. Transient performance between IBC and CVT supercharged turbo-compounding engine at 2000 rpm.

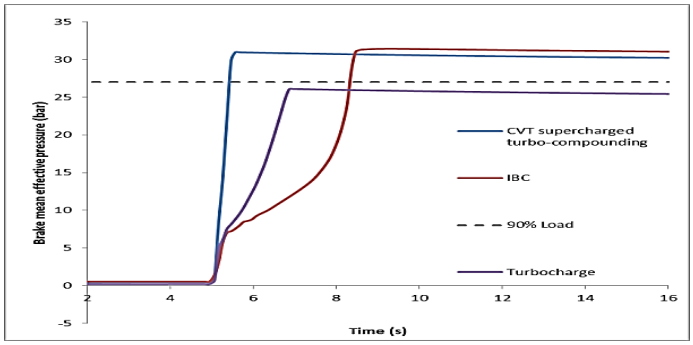

Figure 8.19. Transient performance between IBC and CVT supercharged turbo-compounding engine at 3000 rpm.

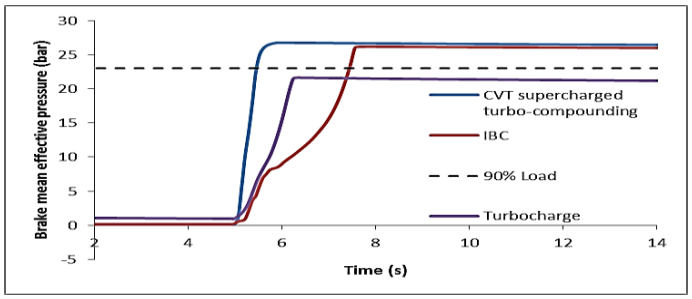

Figure 8.20. Transient performance between IBC and CVT supercharged turbo-compounding engine at 4000 rpm.

Besides, figure 8.18 also shows that the response speed of the Brayton cycle engine is also faster than the turbocharged engine at 2000 rpm. Because the Brayton cycle allows the exhaust gas to be expanded below atmospheric pressure, the bottom cycle imposed a lower pressure to the outlet port of the upstream turbine. According to the simulation results, the outlet pressure of the Brayton cycle engine main turbine was about 0.19 bar lower than the baseline engine turbine (1.22 bar vs 1.03 bar), which resulted in a bigger expansion ratio (2.21 vs 1.63). Therefore, the efficiency of the turbocharger and thus the mass flow rate in the Brayton cycle engine were both higher. This in turn improved the transient performance of the novel model. When the engine speed increased, however, the operating point of the turbocharger in the baseline engine was closer to the high efficiency region, whereas the Brayton cycle engine suffered from higher back pressure and much bigger rotation inertia which encumbered the response speed, which can be seen in figure 8.19 and 8.20. At 3000 and 4000 rpm, the performance deficit between these three models decreased gradually because of the increasing in exhaust mass flow rate. The response time of the IBC engine was reduced by about 1.5 and 2.5 seconds at 3000 and 4000 rpm respectively, and a similar improvement was seen from the turbocharged engine. The CVT supercharged engine, however, was almost unaffected by the change in engine speed. Furthermore, it could be seen from the graphs, the BMEP of the novel models was also greater than that of the baseline turbocharged engine in final magnitude. This was mainly due to power generation from the bottoming cycle and the lower back pressure.

Brands et al [24] have also reported the good driveability of a mechanical turbocompound diesel engine in a real driving cycle, but stated that as the output of the engine was increased the turbocharger match was compromised and driveability suffered.

8.6 Conclusion

This chapter demonstrates the potential of the Inverted Brayton cycle and high pressure turbo-compounding for the augmentation of the power output and fuel economy of conventional turbocharged engine. A 2 litre turbocharged gasoline engine was employed as the foundation for the novel scheme in the simulation. The compressor and turbo machinery from the baseline model was inherited by the new arrangement as the charging system for the simplicity of matching with the air flow characteristics of the engine.

8.6.1 Optimization

Design of experiments techniques was used to optimise the compressor and power turbine speed of the turbo-compounding engine and also the size of the turbo-machinery in IBC

aiming to achieve the optimal performance of the whole system. It was found that both the brake torque and BSFC of the CVT supercharged turbo-compounding engine were continuously improved along with the acceleration of the supercharger under full load condition. Among the reasons, the promotion in volumetric efficiency and the turbine power output made the biggest contribution. At partial load, however, a lower supercharger speed was more preferable considering the power requirement by the compressor and the throttle losses. Besides, when the engine was operated at middle and low speed, the power output and fuelling efficiency increased significantly with higher turbine speed, while at high engine speed the growth rate was smaller and the plateau appeared sooner. When the throttle was partially closing, the influence of the power turbine speed on the overall engine performance was weakened. By adjusting the size of the power turbine in the inverted Brayton cycle, the inlet exhaust pressure to the bottoming cycle was scaled. Within the engine speed range from 2000 to 5000 rpm, it was found that the IBC engine performance deteriorated rapidly with higher inlet pressure. It was believed resulting from the plummet in PMEP and thus the deterioration of the scavenging process.

8.6.2 Steady state performance

When the engines were operated at lower load, the difference in fuel consumption between those two novel models was narrowed. The general trend was that the IBC engine offered better fuel economy at lower engine speed (below 2000 rpm, typically), while the CVT supercharged turbo-compounding engine took over the advantages at higher speed. It was the similar trend that applied to the performance under full load condition. This result should be attributed to the proportion between the effects of PMEP and power generation from the energy recovery system. Specifically, the IBC engine benefited from imposing less back pressure to the engine when it was running below 2000 rpm. At higher speed, the turbo-compounding engine was able to regain the priority by compensating the pumping losses with recovered energy from the power turbine. It was also worth noting that the power generation and the fuel consumption from the novel system were both significantly better than the baseline turbocharged model. Furthermore, the low speed torque from the turbo-compounding engine was enhanced impressively with the assistance of CVT.

8.6.3 Transient performance

During the evaluation of the transient performance, CVT supercharged turbo-compounding engine showed the fastest response speeds, while the IBC which was delayed by building up the turbine speed took the longest time to achieve the required BMEP.

Chapter 9 – Modelling the Divided Exhaust Period Concept for a Turbo-compounding Engine

Turbo-compounding, as one of the most compact waste energy recovery technology with lower cost and complexity, has been proven to be effective in improving fuel economy. However, issues such as high back pressure and poor turbine efficiency at specific working condition are hindering the wider application. The Divided Exhaust Period (DEP) is a novel gas exchange concept, which has been proved to be capable of significantly reducing the back pressure of turbocharged engine and keeping the operating points of the turbine machinery in high efficiency area.

This study was carried out on a 1-D baseline model of a highly boosted gasoline engine. In the novel model, a scaled power turbine was added in parallel to the main turbine of the turbocharger as a waste energy recovery device. The DEP concept features two exhaust valves that function independently. The blow-down valve evacuates the first portion of the exhaust gas to the main turbine as a traditional turbocharged exhaust valve does. The scavenge valve directs the latter portion into the power turbine which converts the remaining energy in the exhaust gas into useful power. By separately optimizing the two exhaust valve timing and lift parameters, it is expected that the novel system could achieve better breathing characteristics and thus better performance and fuel economy than the baseline model over a wide engine speed range. Furthermore, the parameters that are of the greatest interests to the fuel economy will be optimized simultaneously using genetic algorithm after the effects of exhaust valve timing, lifts and size having on the engine performance being summarized separately. This work was carried out by co-simulation of GT-power and Simulink.

9.1 Introduction

The base of DEP (Divided Exhaust Period) concept can be traced back to 1924. In a British patent [208] it was first mentioned as an approach to improve the thermal efficiency of an internal combustion engine. From then on, patent claims have been made by several companies, including Deutz AG [209], Fleming Thermodynamics Ltd. [210] and Saab Automobile AB [211]. The investigation was commonly carried out on a passenger car SI

engine with variable camshafts phasing for the exhaust valves. This is probably due to the inherent problems, such as throttle losses, larger portion of residuals, spark timing and compression ratio limitations, which make DEP implementation on SI engines more effective. In recent years, researchers start to pay attention to the application of DEP in turbocharged engine. Because the exhaust energy contains about 35% of the total fuel energy. Turbocharger is an efficient way to extract a part of this energy and eventually to improve the engine performance greatly. BorgWarner have explored the potential of utilising DEP to improve the flow characteristics of a turbocharged SI engine with both simulations and engine tests for with different EGR routing. [212, 213]. Results from that study showed an improvement in fuel efficiency of 1.5-5.5 % due to the improved pumping work. Furthermore, by reducing the backpressure via valve overlap, the residual gas fraction was reduced as well. It led to an advance of spark timing by up to 17° which in turn was able to improve the fuel efficiency further for 12.3%. Besides, the reduced residuals also made it possible to increase the compression ratio without violating the knock limits. As the authors claimed, the compression ratio could be increased by 2-3 for better fuel economy over the whole operating range.

The results in [214] showed that the turbine mass flow and pressure ratio of the DEP system vary within the high efficiency range of the turbine map due to the less flow. On the contrary, the turbine mass flow and pressure ratio of the baseline turbocharged engine vary widely in the turbine map due to the highly pulsatile exhaust flow, which deteriorate the turbine efficiency. The author also suggested that if only the high pressure blow-down pulse is directed to the turbine, the flow will be less pulsatile, but the peak pressure of the exhaust flow will be maintained. With a proper valve timing strategy it is possible to control the exhaust mass flow and pressure to make the turbine operate within a high efficiency area for a wide operation, meanwhile provide the same amount of power.

In [215], the BSFC behaviour of a highly downsized SI engine equipped with DEP was investigated for different scavenge valve profile. It was summarised that BSFC behaviour at higher engine speed was more sensitive to the change of the scavenge valve profile than that of low speed. Because the back pressure was significantly higher at high speed, DEP was more prone to reduce the working load on the pistons by decreasing the backpressure and eventually improve the fuel efficiency. On the other hand, the study in [216] showed the different results. It was stated that the mass flow in a DEP engine was more likely to suffer from choking at high engine speed since only one exhaust valve (either blow down or scavenging valve) was opened for different portion of exhaust gas, which led to additional

pumping loss. Besides, in a DEP engine system, it was the general trend that high lift is beneficial for decreasing residual gas fraction leading to an advance of spark timing which is beneficial for fuel saving. However, some fresh charge will flow out of the cylinder due to the blow through effect in this case, which would significantly increase BSFC. Severe choking is also a weakness for higher lift as the accompanying scavenge valve retards causes more time with only one valve involved. The similar trend was found for the sweep of scavenge valve duration. It suggests that the profile of the exhaust vales should be carefully optimised in order to achieve the desirable fuel economy. But, the main challenge is that the exhaust valve profile cannot be adjusted in isolation. It is strongly interrelated with other parameters such as intake valve timing, turbocharger sizing and combustion phasing. In [217], the authors provided an approach to test all parameters against each other with genetic algorithm, which is able to significantly reduce the simulating matrix and time.

By reviewing the recent studies on DEP concept, it was mainly applied to turbocharged SI engine, either single stage or two stage. It was utilised to reduce the backpressure and thus the pumping loss by regulating the exhaust flow and reducing pulsation interference. In fact, turbo-compounding engine is more prone to suffering from high back pressure, especially when a power turbine was located in series with the turbocharger turbine to harvest waste heat energy. This chapter will explore the potential of DEP in reducing the back pressure of series turbo-compounding engine. The effects that exhaust valve profile and phasing have on the overall engine performance will be given. Genetic algorithm will be employed to explore the optimal fuel economy of the whole system.

9.2 Methodology

For the simulation work presented in this chapter a validated 1D model of a highly downsized two stage SI engine detailed in table 9.1 was used as a starting point. The engine had a BMEP designed to facilitate a 60% downsizing ratio when compared with an equivalent NA engine [218]. Noted here that the supercharger was connected to the crankshaft via a CVT, so that the supercharger speed could be adjusted independently. It was beneficial for improving the fuel efficiency at mid-high load operation as well as the response speed. In order to implement the DEP functionality to the engine system, the exhaust pipes were re-routed as shown in figure 9.1, in which the blow-down and scavenge valves were actuated by two unique cam profiles. The concept was that the exhaust gas from the blow down valves with higher pressure and temperature would be directed to the turbocharger turbine to provide

power for air boosting, while the other portion of exhaust from the scavenge valves would be expanded in the power turbine to convert the waste heat into mechanical power which was fed back to the crankshaft. The wastegate function of the conventional fixed geometry turbocharger was replaced by adjusting the timing of the scavenge valve to maintain or exceed the target BMEP.

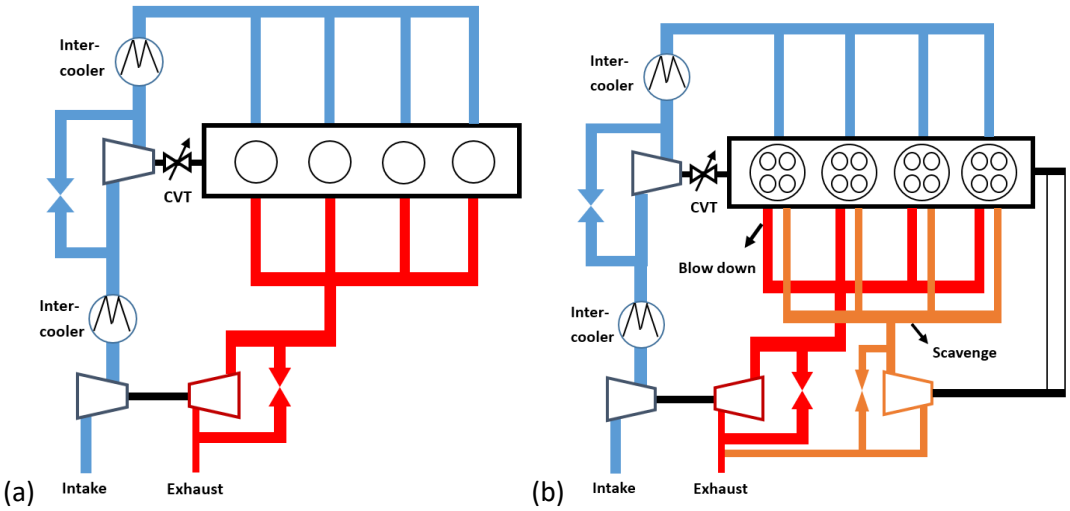

Figure 9.1. Engine model arrangement. (a) baseline; (b) DEP.

Table 9-1. Engine specifications.

Parameter	**Specification**
Engine type	Inline 4 cylinder
Capacity	1991 cc
Bore	83 mm
Stroke	92 mm
Compression ratio	9.0:1
Firing order	1-3-4-2
Combustion system	Gasoline GDI
Valvetrain	DOHC, cam phasers and cam profile switch on intake and exhaust camshafts
Specific power	142@ 6500 kW/l @ rpm
Specific Torque	255@ 3500 Nm/l @ rpm
Maximum BMEP	35 @ 3500 (25 @ 1000 and 6500) Bar @ rpm
Air charging system	HP: Eaton R410; LP: Honeywell GT30

It was expected that DEP could help to reduce the back pressure of turbo-compounding engine through a careful optimization of the exhaust flow to the main and power turbine. However, as mentioned in the review of the previous studies, it was concerned that the exhaust valves in DEP engine might suffer from choking. Besides, the volumetric efficiency

might be changed because some of the fresh charging might swept out of the cylinder without involving into combustion. Therefore, parameters, such as the exhaust valve timing, lift, duration, turbo size and intake valve timing would be investigated one by one to give a general trend of the effects to the engine performance before the genetic algorithm being utilised to explore the global optimal solution.

9.2.1 Knock model

In this study, the Douand and Eyzat knock model was employed to showcase the potential of the DEP system to improve the combustion phasing. The basic principle of this model is to compare the knocking behaviour of commercial fuel in a cooperative fuel research engine (CFR) with that of the primary reference fuel (PRF) for which the octane number (the mixtures of isooctane and n-heptane) is already known. In this method, the occurrence of knock of PRF was determined based on induction time correlations representing the autoignition delay as shown in formula 9.1.

$$\mathrm{I}(\alpha) = \frac{1}{6(rpm)} \int_{-100}^{\alpha} \frac{1}{5.72\times10^{6} M_1 (\frac{ON}{100})^{3.402} p^{n} \exp(\frac{3800}{M_2 T})} d\alpha \qquad \textbf{9.1}$$

where I is the induction time integral, α is the crank angle, rpm is engine speed, ON is the fuel octane number, p is the instantaneous cylinder pressure (Pa), T is the instantaneous unburned gas temperature (K), n is the pressure coefficient, M_1 is the knock induction time multiplier, and M_2 is the activation energy multiplier. With the "Four-Octane-Number Method" developed by A. M. Douaud and P. Eyzat [219] for Predicting the Anti-Knock Behavior of Fuels and Engines, the coefficient M_1, M_2 and n can be worked out with four reference fuel conditions being provided. And then this empirical formula can be generalized for all engines and fuels to forecast the knock behaviour.

The knock index (KI) is a phenomenologically based parameter developed by Gamma Technologies. It can be scaled to the loudness of knock using the KI multiplier. The KI is defined as a time-dependent value as follows [220]:

$$\mathrm{KI} = 10000\mathrm{Mu}\frac{V_{TDC}}{V}\exp\left(\frac{-6000}{T}\right)(\max(0, 1-(1-\varphi)^2))I_{avg} \qquad \textbf{9.2}$$

In which KI is the knock index, M is the KI multiplier, u is the percentage of cylinder mass unburned, V_{TDC} is the cylinder volume at TDC, V is the cylinder volume, T is the bulk unburned gas temperature (K), φ is the equivalence ratio of the unburned zone, and I_{avg} is the induction time integral, averaged over all end gas zones.

A Wiebe combustion model was adopted in the engine model, in which a reference number CA50 was defined as the crank angle between TDC and 50% combustion point of the Wiebe

curve. The CA50 in this model was controlled by a PID controller to keep the KI under specific index. The intake exhaust valve timing was optimized with genetic algorithm for both the DEP concept model and the original R2S model for a sensible comparison. Details will be given in the Genetic Algorithm section. The exhaust valve diameter was increased to the same size as the intake valve to ease the exhaust flow choking when only one valve is involved for the DEP engine.

9.2.2 Genetic algorithm

Genetic algorithm (GA) is literally an adaptive heuristic search method based on the evolutionary concepts of natural selection and genetics. It represents an intelligent approach to solve optimization problems. The basic idea of GA is to mimic the processes of evolution in natural systems and follow the principles of "survival of the fittest" first proposed by Charles Darwin. It aims at the results that the fittest individuals dominate over the weaker ones through optimization, which is the similar case for the nature. Although the algorithm is randomised by definition, it actually iterates historical information to continually direct the search towards the region of better solution within the search space. When comparing with conventional artificial intelligence, GA shows more robust performance, which means it does not break easily even if the inputs change, or considerable noise is presenting.

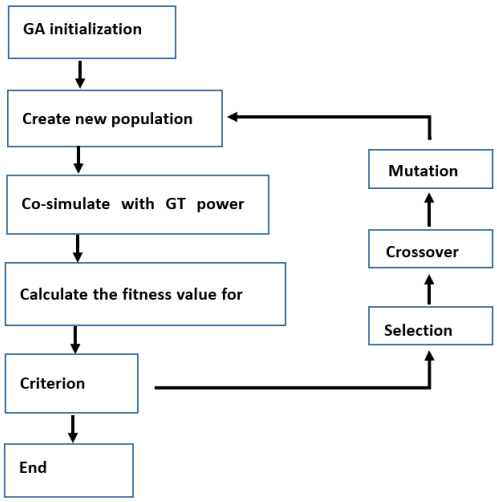

Figure 9.2. Working procedure of genetic algorithm.

The operating structure of the genetic algorithm is shown in Figure 9.1.

GA mimics the principle of the nature, which is survival of the fittest, to explore the best solution to a specific problem with consecutive generations of candidates. Each generation consists of a population of character strings. It is analogous to the chromosome in biological

DNA. The individuals can be regarded as a point in the search space and also a possible solution. After the individuals are initialised, the population go through a process of evolution for optimal.

Similar the law of evolution, the theory of GA is based on several principles. Firstly, the individuals in a population compete for resources and mates. More successful ones in each generation will have higher opportunity to produce offspring than those poorly-performing ones. Genes from better individuals are more likely to propagate and combine throughout the population to produce offspring better than either parent. So that, the generation will move closer and closer to the best solution of the given problem.

Searching Space

A population of individuals is maintained within search space for a GA, each representing a possible solution to a given problem. A candidate solution contains several variables. A weight is worked out through a fitness function and assigned to each solution representing the abilities of an individual to "compete". The GA maintains the population of solutions with associated fitness values. Good parents are selected to mate based on their fitness and produce offspring via a reproductive plan. As offspring are born, space must be made for the new arrivals to keep the population at a static size. Old individuals in the population die out and are replaced by the new ones. Consequently, when the evolution opportunities are fully utilised and a new generation is created. In this way, it is expected that generation of the better solutions will continually replace the previous one. Eventually, the optimal (or generally near optimal) solution will be found.

Once the evolution reaches the plateau and is not producing offspring noticeably different from those in previous generations, the algorithm itself is considered to have converged to a set of solutions to the problem. The operation cycle will be ended then.

Details of the operation structure

After initialization, a population is randomly generated within the searching space. The evolution of GA will proceed with three operators, namely selection, crossover and mutation. Just as its name implies, selection determine the survival of the fittest solutions; crossover represents the mating between individuals; mutation introduces random modifications to the candidates.

Specifically, depending on the fitness value calculated from a fitness function, the selection operator assigns higher priority to better solutions, which allows them to deliver their genes to the next generation.

The crossover operator is regarded as the unique factor of GA distinguishing it from other

optimization techniques. It allows two selected individuals to exchange part of the variables. Two new offspring are created in this way containing part of the features from their "parents". For example, through crossover operation, the candidate S1=000000 and S2=111111 exchange part of their bit strings and create S1'=110000 and S2'=001111. The new individuals created from this mating goes into the next generation. Since it recombines part of the features of the good individuals, it is possible to give even better candidates.

Mutation operator is of relatively low probability when comparing with the former two operators. It changes the characters of some of the new individuals randomly within the searching space to maintain the diversity of the population and avoid premature convergence.

Therefore, using selection alone will fill the population with copies of the best individual from the previous generation. Using mutation alone, however, will induce a random sweep through the search space. Instead, using selection and crossover operators tends to converge the process rapidly to a good solution but may not be the optimal one. Using mutation and selection (without crossover), on the other hand, will create a parallel, noise-tolerant, hill-climbing optimization process.

Nowadays, genetic algorithm has been widely applied to real-world problems solving because of the powerful and robust optimisation ability. However, it should be noted that genetic algorithm is not merely a computing method which simply proceeds pre-designed work flow. Considerable effort is required to design a proper fitness function. If a proper fitness function is absent, the operation will either runs into inappropriate converge with a sub-optimum solution or even is struggle to converge at all. Since the primary target of the optimization process was to gain fuel saving subject to specific constraints, the fitness function was defined as formula 9.3.

$$\text{Fitness (x)} = \text{BSFC} + \text{P} \times \left| 1 - \frac{BMEP_x}{BMEP_{target}} \right| \qquad \textbf{9.3}$$

where x refers to a candidate solution containing the variables of valve timing, lift and turbo size . P is introduced as a penalty factor. It determines the penalty for those individuals that do not satisfy the requirement in engine load. Apparently, a larger value of P imposes higher penalty factor on the fitness score and leads to a stricter confinement but worse selection efficiency. Considering the compactness of fitness definition, a static penalty is adopted in this study for the robust and rapid operation. After investigating the converging results for a considerable number of times, P was decided to be 1000 for the original model and 5000 for the DEP concept model.

9.3 Modelling and simulation

From previous studies [142, 220], it was found that decreasing the intake valve diameters by 10% while changing the blowdown-scavenge area ratio from 1 to 2.5 might bring about a fuel saving up to 1%. If the intake valve size was decreased further, however, the fuel consumption would be higher because of the increased intake losses. On the other hand, if the intake area was kept the same as that in baseline model, while the exhaust valve diameters were increased, there would be reduction in BSFC as well, since the DEP engine was more prone to choke when only exhaust valve was opened. But, from the results, only 0.2% fuel saving could be achieved by increasing the exhaust area by 10%. Although increasing the size of the intake and exhaust valves might help to decrease the risk of choke at the exhaust port at high engine speed and load, such layout of the exhaust valves might not be feasible in OEM engines considering the dimensional limits between two exhaust valves and the cylinder block edges. Therefore, the investigation of the effects of different valve size on the engine performance would not be included in this study. The intake and exhaust area would be kept the same as that in original model.

At low engine speed, the scavenging valve duration should be retrenched to allow more exhaust energy to be given to the turbocharger, so that the power output at low speed end can be improved. Besides, the overlap between the scavenging and intake valve could be increased to reduce the residual gas in the cylinders.

As engine speed was increased, exhaust energy became superfluous for satisfying the air boosting requirement. The scavenging valve duration should be then increased accordingly to direct more exhaust mass flow to the power turbine to avoid choking at the turbocharger turbine. By regulating the exhaust mass flow to the turbocharger, the brake torque could be limited for further increasing with the back pressure being effectively reduced. It was of the similar function as the wastegate. But the exhaust energy was still utilised. The power turbine connected with the scavenging valves would convert it into useful mechanical work.

9.4 Optimization procedure

In this study, the optimization of the DEP engine would be carried out in two phases by order. In the first phase, an iterative procedure would be adopted in order to investigate the effects that the sweeping in valve timing, lift and turbine size have on the engine performance respectively. Since there were strong interaction effects between turbine size, valve timing

and valve lifts, it was impossible to clearly embody the impacts of each parameter if all of them were optimized against each other at a time. Instead, by letting the sweeping go through an iterative process, the test matrix could be significantly compacted while the effects of each parameter could be easily analysed. An example would be given here to explain the iterative optimization procedure. It was started with initialised turbocharger turbine size and power turbine size, the intake and exhaust valve timing was swept firstly together with the valve lift. The sweep in exhaust valve timing consists of the changes in both blow-down and scavenge valve. When an optimal match was found for the intake and exhaust valve timing and lift, it was directly utilised in the sweep of the intake valve timing at the next stage. With the optimal match found in this stage, the exhaust valve duration (which was determined by the "angle multiplier" in GT-Power) would be swept to search for the best settings within the limitations to the overlap between the blow-down exhaust valve closing and scavenge exhaust valve opening. Similarly, the turbocharger turbine and power turbine size would be optimised in the following stage. And finally, the same process was carried out for the intake valve lift. Theoretically, this process needed to continue until the same settings were achieved in the new iteration cycle, which unavoidably made it a time consuming process. However, since the primary demand for this phase is to investigate the effects of different parameters, it was the changing trends in engine performance that really matter, instead of the global optimal setting.

In the next phase, however, genetic algorithm would be involved to explore the best engine performance considering the interactive effects of the parameters. A mathematics model of GA would be built in Simulink to simulate cooperatively with the GT-Power model to search for the global optimal setting for all the parameters. The optimization procedure for the first and second phase were only performed for two load point which represent the full load high speed operation and the low speed low load operation respectively. It should be note that, the original engine model was optimized correspondingly to realise a fair comparison between baseline and DEP engine. Obviously, there are many more parameters that might need optimization before being applied to the DEP concept, for example, the injection strategies, manifold geometry, but further optimization of the complete engine system was deemed to be outside the scope of this thesis.

9.5 Results and analysis

In this section, the results from two studied cases of the DEP model will be discussed

individually before moving to the comparison with the baseline two-stage boosted engine model.

9.5.1 Full load simulation at high engine speed of 3000 rpm

As mentioned in the optimization procedure section, the first sweep was carried out for the exhaust valve timing, in which the blow-down valve timing was varied from 210 to 300 degree, while the scavenge valve timing was varied from 310 to 400 degree. Both the blow-down and scavenge valve timing were referenced to the angle between the point of maximum lift and the top-dead-centre associate with firing.

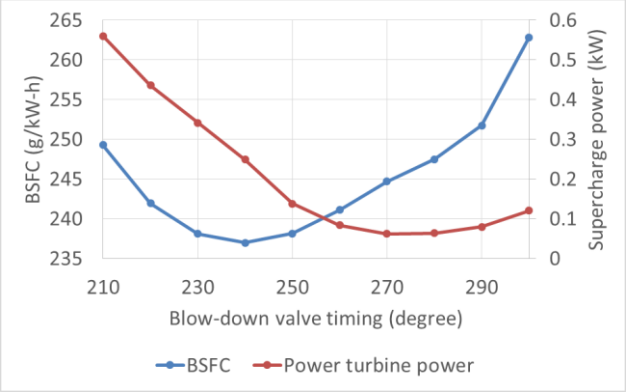

Figure 9.3. Sweep of blow-down valve timing vs fuel consumption and supercharger power.

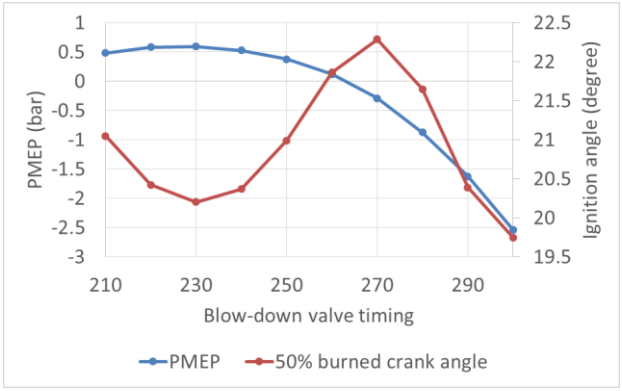

Figure 9.4. Sweep of blow-down valve timing vs pumping work and power turbine power.

From Figure 9.3, it can be seen that the blow-down valve timing itself imposed significant impact on fuel consumption. Specifically, as shown in figure 9.4, when the blow-down valve timing was retarded from 210 to 240 degree, the pumping work was slightly reduced due to the increased overlap between the blow-down and scavenge valve opening. At the same time, the residual gas fraction was reduced significantly because of the better scavenging, which

led to an advanced ignition timing (it was referenced to the 50% burned crank angle) for the same knock index. When the blow-down valve timing was continually moved backward from 250 to 270 degree, the fuel consumption increased rapidly duel to the sharp reduction in PMEP, because the availability of exhaust energy for the turbocharger was reduced. It was also reflected by the increasing power consumption of supercharger. At the same time, ignition had to be retarded because of the increased residual gas fraction. From 270 degree and on, the residual gas was decreased by the larger overlap between the exhaust and intake valve which led to a sweep effect of the burned gas in cylinders. However, since the PMEP continued to decrease, the fuel economy was still deteriorated. It should be noted that the mechanical power spent on driving supercharger was very little, which means turbocharger provided most of the boosting at a high engine speed of 3000 rpm.

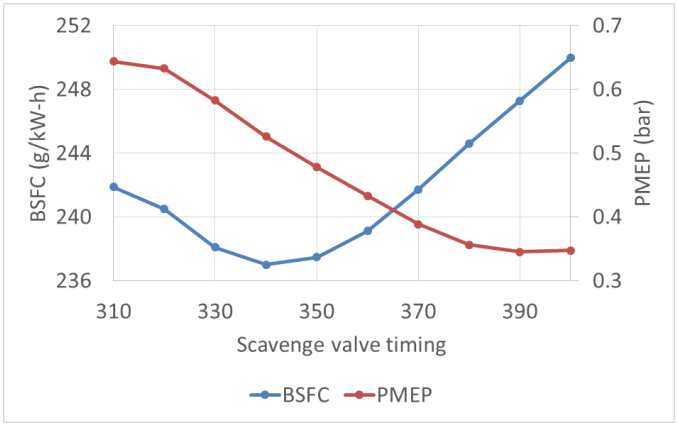

Figure 9.5. **Sweep of scavenge valve timing vs BSFC and PMEP.**

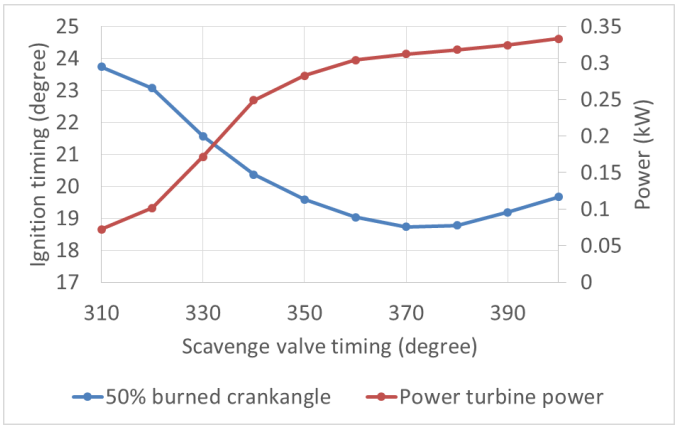

Figure 9.6. **Sweep of scavenge valve timing vs ignition timing and power turbine power.**

The scavenge valve timing, however, had much smaller effects on fuel economy of the engine system, since only a smaller portion of the exhaust gas was flow out via the scavenge valve, as shown in figure 9.5. Nevertheless, the sweep of it from 310 to 400 degree decreased PMEP

by about 0.3 bar, while increased the power turbine work by about 0.3 kW as shown in figure 9.6. More significantly, as illustrated in figure 9.6, the retarding of scavenge valve timing and thus a larger overlap with the intake valve timing reduced the residual gas fraction greatly and led to a significantly advanced ignition timing, which was also beneficial for improving the fuel efficiency. It should be note that although the sweep in scavenging valve timing would change the overlap with the blow-down valve and switch the working status of supercharger, the correlated effects was very limited since turbocharger had done most work for air boosting, as mentioned before.

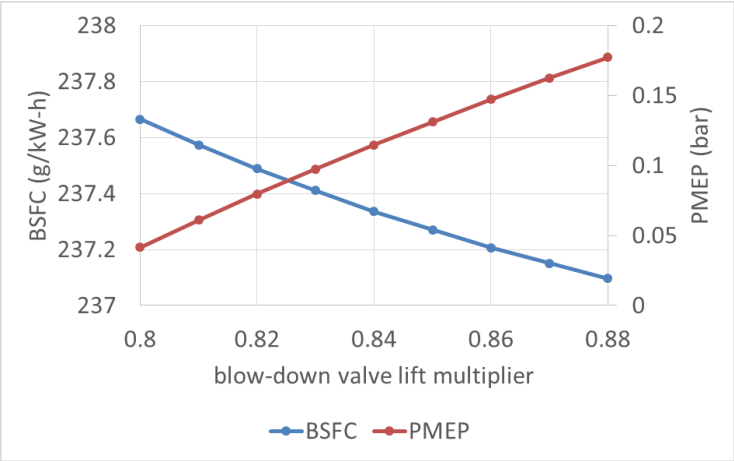

Figure 9.7. Sweep of blow-down valve lift vs BSFC and PMEP.

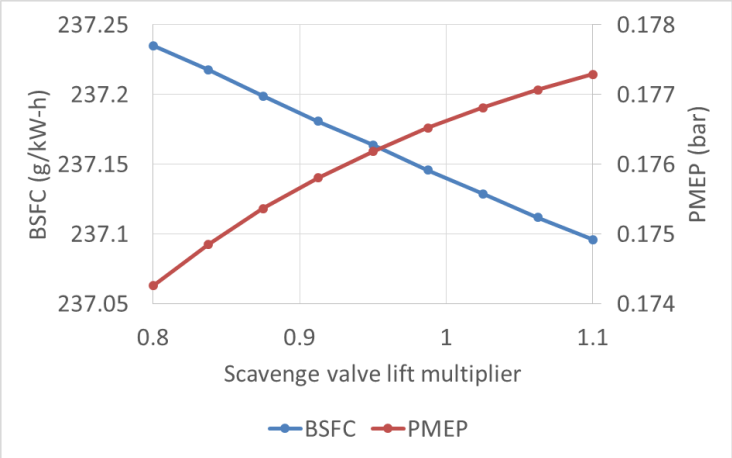

Figure 9.8. Sweep of scavenge valve lift vs BSFC and PMEP.

In the next stage, simulation was carried out to sweep the exhaust valve lift. From the results, it showed very little effects on the engine performance, as shown in figure 9.7 and 9.8. The general trend was that the pumping work could be reduced with enlarged lift multiplier for

both blow-down and scavenge valve. From a previous study conducted by Bo [7], a high exhaust valve lift multiplier may lead to a loss of fresh charge because of the blow through effect which sweep fresh air out of cylinders before the occurrence of combustion. Besides, a higher lift might introduce a larger back flow from the exhaust manifold to the cylinder, which resulted in a reduction of volumetric efficiency. However, those phenomenon was not seen in this work, because the exhaust valve duration was not changed accordingly. The isolated changes in valve lifts did not affect engine breathing much. In brief, it was only the slight change in pumping work that affected the engine fuel economy in this sweep. The gas flow in and out of cylinders was not greatly affected.

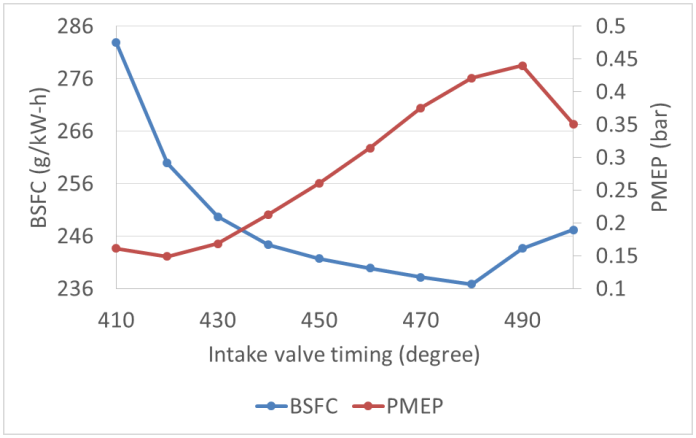

Figure 9.9. Sweep of intake valve timing vs BSFC and PMEP.

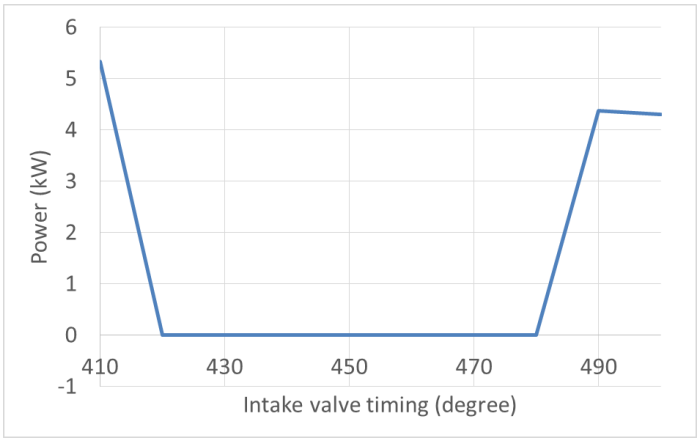

Figure 9.10. Sweep of intake valve timing vs supercharger power.

Figure 9.9 and 9.10 shows the simulation results by sweeping the intake valve timing. From the results, an optimal point existed around 480 degree for the intake valve timing, as shown in figure 9.9. An advanced valve timing resulted in a sweep out of exhaust gas from the overlap between exhaust and intake valve, which would reduce the energy availability for

the turbocharger and thus PMEP, while a retarded valve timing might lead to a deficit in fresh air charging which had to be compensated by supercharger, as shown in figure 9.10. They were both violence against the fuel economy. Besides, from figure 9.10, when the intake valve was advanced to 410 degree, the blow through effect would emerge. Some of the fresh charge would be carried out of cylinders without burning. Supercharger had to be engaged in this case to make up the loss, which would damage the fuel efficiency badly.

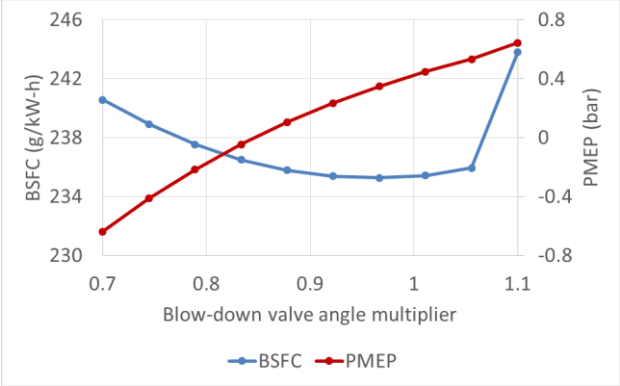

Figure 9.11. Sweep of blow-down valve angle multiplier vs BSFC and PMEP.

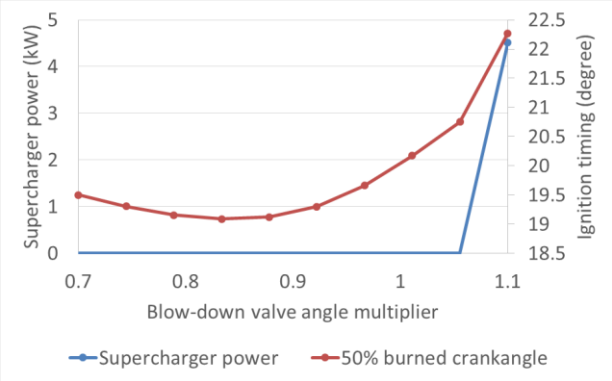

Figure 9.12. Sweep of blow-down valve angle multiplier vs supercharger power.

The effects of blow-down valve duration on engine performance was shown in figure 9.11 and 10.12. In GT-power, the exhaust duration can be varied through adjusting the scaling factor of angle multiplier. When the scaling factor was increased from 0.7 to 1.05, PMEP increased accordingly due to the reduced resistance to exhaust mass flow and thus lower back pressure. Besides, a smooth gas exchange process reduced the residual gas in the cylinder, which allowed an advanced ignition timing, as shown in figure 9.12. So that, the fuel consumption could be reduced by about 2% because of the synthetic effects. When the angle multiplier was increased further, PMEP would keep increasing. However, because a larger portion of exhaust flew back into the cylinder in this case, the ignition timing should be

retarded to avoid violating the knock limits, as shown in figure 9.12. Consequently, the fuel economy deteriorated, as shown in figure 9.11. Furthermore, with an extended exhaust valve duration multiplier above 1.05, the loss of fresh charge would become more serious because of the blow through effect. So that the supercharger had to be engaged to provide additional boosting to compensate loss of intake air, which also damage the fuel economy severely. At the same time, residual gas fraction would increase significantly. Therefore, the fuel consumption went back to a high level rapidly then, even though the pumping loss was lower.

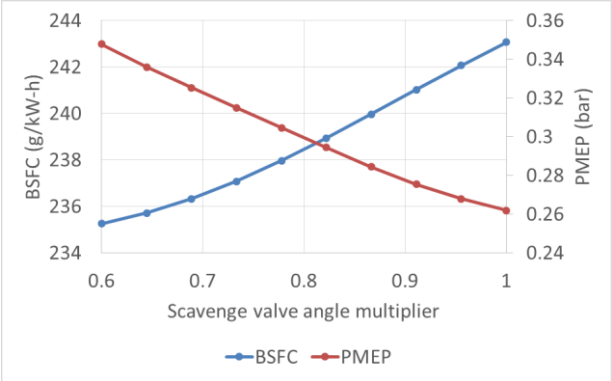

Figure 9.13. Sweep of scavenge valve angle multiplier vs BSFC and PMEP.

For scavenge valve, as shown in figure 9.13, a smaller angle multiplier was preferable to allow more exhaust go through the turbocharger turbine and provide energy for air boosting. From the result, PMEP would decrease by 0.1 bar with longer duration for scavenge valve leading to increased fuel consumption by about 3.3%. However, the scavenge valve duration had little impact on the residual gas fraction and supercharger operation status, since only a small portion of exhaust was expelled through the scavenge valves. Therefore, the ignition timing was mainly determined by the boosting pressure and fresh charge temperature. The overall change of it was very little.

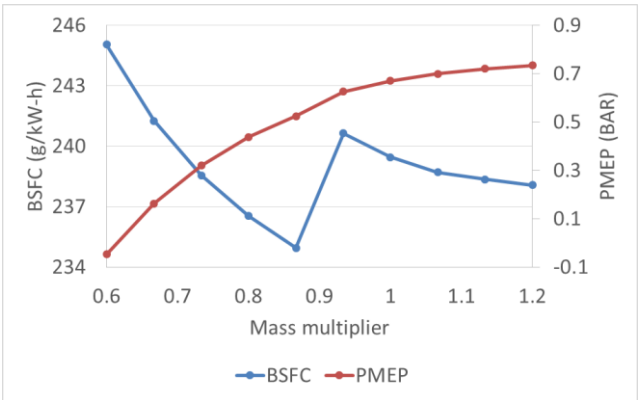

Figure 9.14. Sweep of turbocharger turbine size vs BSFC and PMEP.

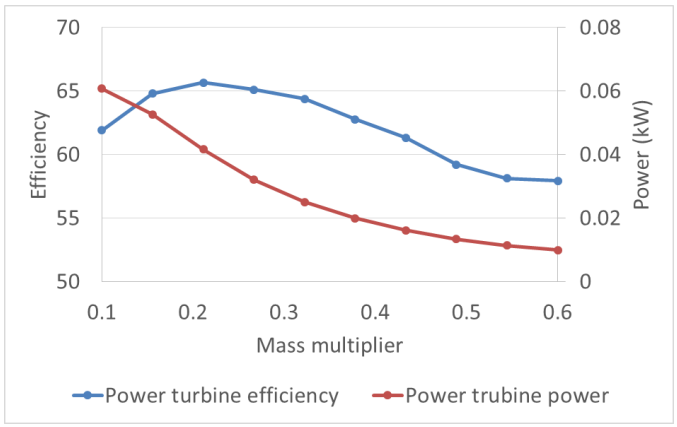

Figure 9.15. Sweep of power turbine size vs power turbine size and power turbine power.

From figure 9.14, it can be seen that a larger turbocharger turbine would brought out lower back pressure and higher PMEP and eventually better fuel economy. However, when the mass multiplier for the main turbine was increased bigger than 0.9, the turbocharger turbine became less effective to capture the energy in exhaust pulse and unable to provide enough boosting for the engine. Therefore, an optimal point existed at around 0.9 for the main turbine mass multiplier. The power turbine, on the other hand, had very little effect on the engine performance, since it contributed very little to the power output and engine breathing, as shown in figure 9.15.

9.5.2 Full load simulation at low engine speed of 1000 rpm

In this section, the similar sweep procedure would be carried out for the simulation at low engine speed of 1000 rpm.

Figure 9.16 and 9.17 show the effects of blow-down valve timing having on engine performance.

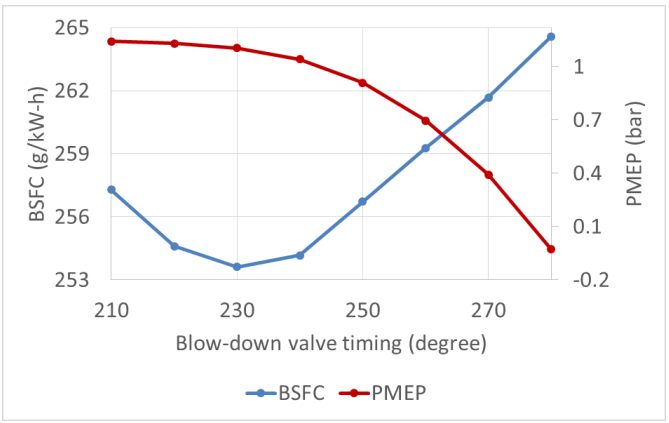

Figure 9.16. Sweep of blow-down valve timing vs BSFC and FMEP at 1000 rpm.

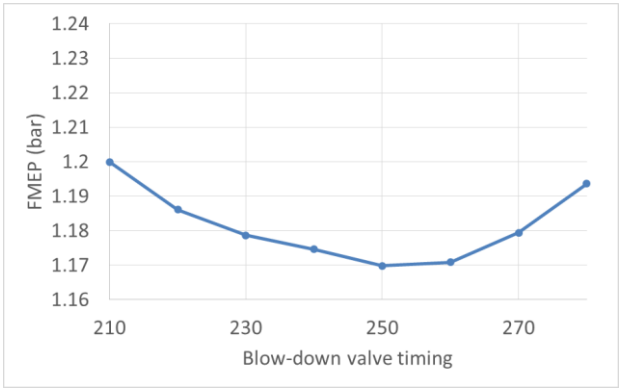

Figure 9.17. **Sweep of blow-down valve timing vs FMEP at 1000 rpm.**

From the plots, it can be seen that the blow-down valve timing had less influences on engine performance at 1000 rpm when compare to the results at higher engine speed of 3000 rpm. It was mainly due to the fact that the back pressure was much lower at low engine speed. It means that the DEP arrangement in this case was less effective to improve PMEP of the engine system. As shown in figure 9.16, a variation in blow-down valve timing led to a drop in PMEP by about 1.2 bar and an increasing in specific fuel consumption by about 3.9%. The change of FMEP, as shown in figure 9.17, also affected the overall fuel economy. But the effect was very limited, since only a slight variation was seen.

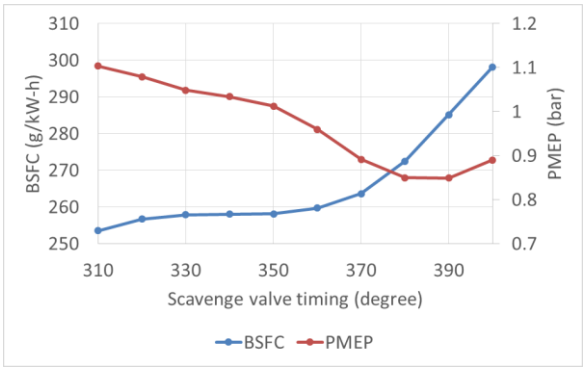

Figure 9.18. **Sweep of scavenge valve timing vs BSFC and PMEP at 1000 rpm.**

As for the scavenge valve timing, it imposed even less impact on the gas exchange and fuel efficiency of the engine, as shown in figure 9.18. However, when the scavenge valve timing was retarded to 370 degree and backwards, a large overlap between exhaust and intake valve timing arose. And then a great portion of fresh charge would be swept out of the cylinders without burning due to the blown through effect. So that, the supercharger had to be engaged to assist boosting to satisfy the load target, as shown in figure 9.18. At the same time, the increasing in FMEP also contributed to the fuel consumption.

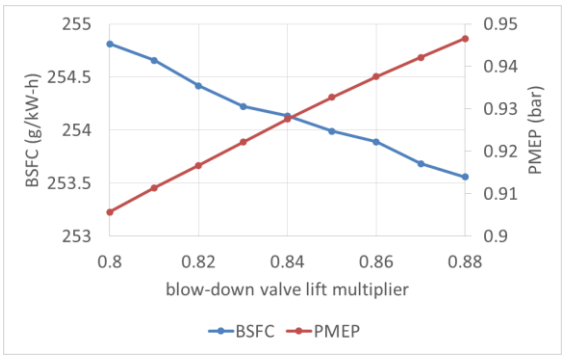

Figure 9.19. **Sweep of blow-down valve lift vs BSFC and PMEP at 1000 rpm.**

From figure 9.19, exhaust valve lift had very limited effects on engine performance, which coincided with the results at high engine speed. Figure 9.19 shows that the pumping work could be reduced by 4%, while the fuel economy could be improved by 0.7% by increasing the blow-down valve lift multiplier from 0.8 to 0.88. The impact of sweeping the scavenge valve lift was negligible, and did not be displayed in here.

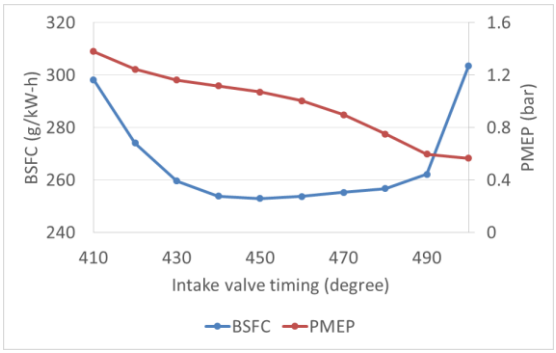

Figure 9.20. **Sweep of intake valve timing vs BSFC and PMEP at 1000 rpm.**

The results shown in figure 9.20 suggests that an optimal setting for intake valve timing existed at the point around 450 degree. If the intake valve timing was retarded too much, PMEP would suffer from a notable decline.

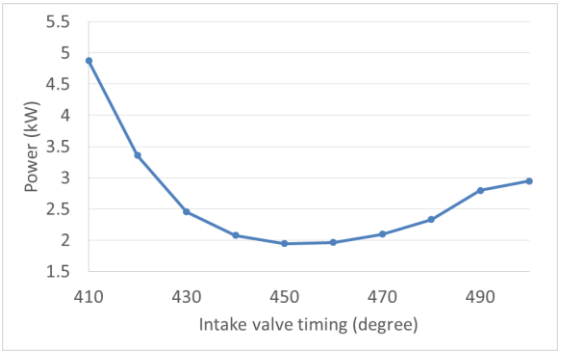

Figure 9.21. **Sweep of intake valve timing vs supercharger power at 1000 rpm.**

Meanwhile, supercharger would consume more power to cover the pumping work, as shown in figure 9.21. On the other hand, if the intake valve timing was advanced too much, fuel efficiency would also deteriorate due to the loss of fresh charge, which was the similar case with retarded scavenge valve timing.

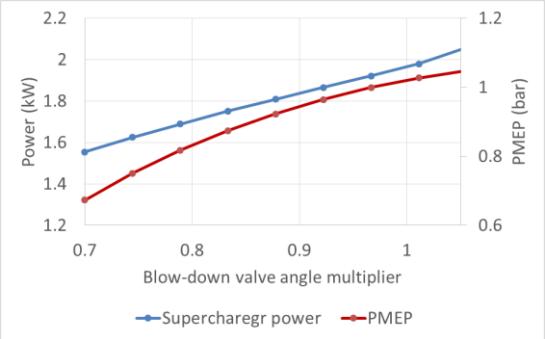

Figure 9.22. Sweep of blow-down valve duration vs supercharger power and PMEP at 1000 rpm.

From figure 9.22, PMEP could be effectively improved by increasing the blow down valve duration. However, the power consumption of supercharger was also increased. Consequently, the synthetic effect on overall fuel economy was negligible.

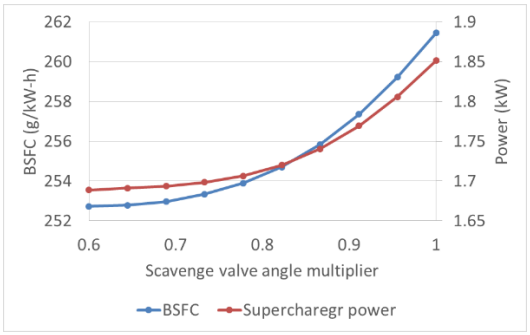

Figure 9.23. Sweep of scavenge valve duration vs BSFC and supercharger power at 1000 rpm.

The scavenge valve, however, imposed notable impact on fuel efficiency of the whole system. As shown in figure 9.23, an extended duration led to a large overlap with the intake valve. Supercharger was then expected to work harder to compensate the fresh charge, which consequently increased the fuel consumption.

From figure 9.24, it can be found that the effect of turbine size on fuel consumption was very limited. The back pressure could be reduced slightly, while the supercharger had to share more work to remedy the loss in turbocharger boosting, as shown in figure 9.25. Ignition timing could be advanced with larger turbine size, because of the better scavenge process. But the change turned out to be very limited. Efficiency of the power turbine was much lower at low engine speed (around 30%) because the mass flow rate was much lower. Therefore,

the sweep of power turbine size had very little effect on engine performance.

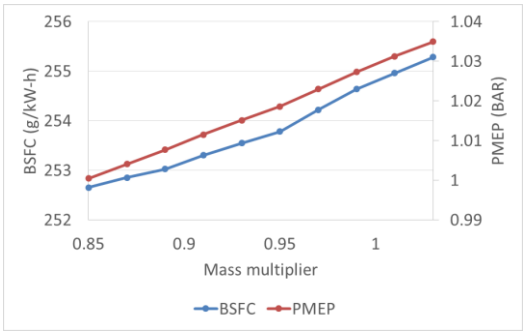

Figure 9.24. Sweep of main turbine size vs BSFC and PMEP.

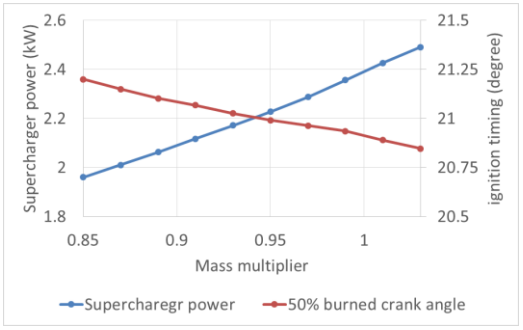

Figure 9.25. Sweep of main turbine size vs supercharger power and ignition timing.

9.5.3 Low load simulation at 3000 rpm

Under low load condition, because the mass flow rate of engine system was reduced significantly, meanwhile the turbomachinery imposed less back pressure to the exhaust flow, it was assumed that DEP was less effective in improving the gas exchange process. Therefore, it was no longer necessary to investigate all the parameters, as what have been done in the full load operation, instead, only the blow-down and scavenge valve timing was optimised at this stage. Besides, it should be note that the power turbine was bypassed in the low load simulation aiming to reduce the back pressure further, since the power generation was very limited in this case.

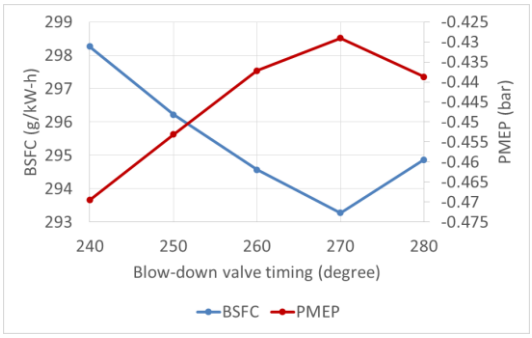

Figure 9.26. Low load sweep of blow down valve timing vs BSFC and PMEP at 3000 rpm.

From figure 9.26, it can be seen that the impact that blow-down valve timing had on fuel efficiency was relatively smaller than that in full load simulation. Only a variation of about 1.7% was found in BSFC, which was mainly due to the reduction of pimping work when increased the overlap between the intake and exhaust valve timing, as shown in figure 9.26. The scavenge valve timing, however, had very little effect on the fuel economy because of the low mass flow rate.

The scenario was similar at 1000 rpm, as shown in figure 9.27 and 9.28. It was the blow-down valve timing that had relatively more significant influence on BSFC due to the capability to shift the gas exchange characters.

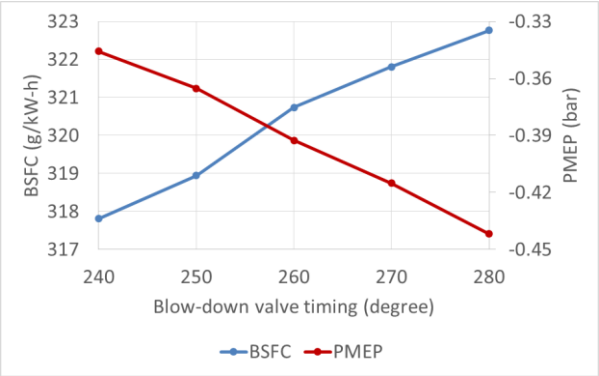

Figure 9.27. Low load sweep of blow down valve timing vs BSFC and PMEP at 1000 rpm.

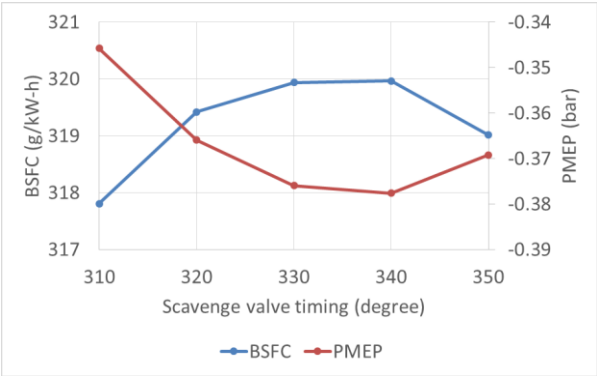

Figure 9.28. Low load sweep of scavenge valve timing vs BSFC and PMEP at 1000 rpm.

9.5.4 Comparison of baseline and DEP engine performance under full load condition

In this section, a comparison between the optimised DEP and original engine models will be carried out. As mentioned before, genetic algorithm was utilised to search for the global optimal setting for both the novel and baseline engines. Four operation points were investigated successively, which were the full load simulation at 3000, 2000, and 1000 rpm and the low load simulation of 4.99 BMEP at the engine speed of 3000 and 1000 rpm.

From the results shown in table 9.2 to table 9.4, DEP arrangement does have advantages in improving the fuel efficiency in a highly boosted gasoline engine. It was mainly due to the ability to regulate the mass flow in and out the cylinders. It was a general trend that the PMEP of the DEP model was reduced under full load condition because of the increased back pressure when only one exhaust valve was engaged. However, the loss in pumping work could be effectively compensated with a higher efficiency for air boosting. The turbocharger with optimized size would be more effective and share more work for fresh charging. The mechanical work spent on driving supercharger was saved. Besides, the larger overlap between the intake and exhaust valve timing and smooth exhaust flow from each cylinder without interruption helped to reduce the residual gas fraction in the cylinder, which is beneficial for advancing the ignition timing (almost the same at 1000 rpm though), providing further improvement to fuel economy. It should be not that the power turbine employed in the DEP system was extremely small (a mass multiplier of 1.5 was applied) to effectively capture the exhaust pulse energy. Since the mass flow rate through the power turbine was much lower, it was not necessarily cause apparent increasing in back pressure. The power generation from power turbine was nearly 2 kW and smaller at lower engine speed.

Table 9-2. **Full load performance of baseline and DEP engine at 3000 rpm.**

	Baseline engine	**DEP engine**	**Promotion**
BSFC (g/kW-h)	244.79	235.13	4.1%
PMEP (bar)	0.656	0.486	-0.17
Supercharger power (kW)	4.31	0	4.31
Turbocharger efficiency (%)	65.48	67.40	3.1%
Ignition timing (degree)	23.34	19.69	3.56
Power turbine power (kW)	--	1.89	--

Table 9-3. **Full load performance of baseline and DEP engine at 2000 rpm.**

	Baseline engine	**DEP engine**	**Promotion**
BSFC (g/Kw-h)	247.36	239.17	3.4%
PMEP (bar)	0.744	0.659	-0.085
Supercharger power (Kw)	3.00	1.51	1.49
Turbocharger efficiency (%)	62.96	64.85	2.9%
Ignition timing (degree)	22.86	20.24	2.62
Power turbine power (kW)	--	0.942	--

Table 9-4. Full load performance of baseline and DEP engine at 1000 rpm.

	Baseline engine	DEP engine	Promotion
BSFC (g/Kw-h)	261.78	253.65	3.2%
PMEP (bar)	1.065	1.000	-0.065 bar
Supercharger power (Kw)	2.926	1.960	0.966
Turbocharger efficiency (%)	60.25	61.97	2.9%
Ignition timing (degree)	20.972	21.200	-0.228
Power turbine power (kW)	--	0.317	--

9.5.5 Comparison of baseline and DEP engine performance under low load condition

Under low load condition, however, exhaust mass flow rate was much lower and imposed much lower back pressure to the engine, so that the advance of DEP arrangement was weakened. From table 9.5 and 9.6, the improving in fuel consumption was less than 0.5%. The promotion mainly came from the increasing in turbocharger efficiency, since a smaller turbocharger turbine was utilised for the DEP engine, which was more suitable for the operation with lower mass flow. And also, by eliminating the interruption between exhaust flows from adjacent cylinders, the operating points were shifted to the region with higher efficiency.

Table 9-5. Part load performance of baseline and DEP engine at 3000 rpm.

	Baseline engine	DEP engine	Promotion
BSFC (g/kW-h)	293.63	292.87	0.43%
PMEP (bar)	-0.4321	-0.4387	-0.0066
Turbocharger efficiency (%)	55.56	58.24	4.8%

Table 9-6. Part load performance of baseline and DEP engine at 1000 rpm.

	Baseline engine	DEP engine	Promotion
BSFC (g/kW-h)	318.07	317.807	0.063%
PMEP (bar)	-0.3677	-0.3557	0.012
Turbocharger efficiency (%)	43.76	44.23	1.1%

9.5.6 Comparison of the transient performance of baseline and DEP engine

From figure 9.29, it can be seen that the response speed of DEP engine was about 0.5 second faster than that of the baseline engine. It was mainly due to the reduced turbo lag, since the turbocharger turbine utilised in DEP engine had smaller inertial. As shown in figure 9.30, the turbocharger in DEP system was able to provide the required boost pressure more rapidly

than the baseline turbocharger. The response time was shorten by 0.5, 0.8 and 1 second at 3000, 2000 and 1000 rpm respectively. Besides, the results also suggested that the turbocharger in DEP system worked harder than in the baseline, so that the load on supercharger for air boosting was eased, which is also reflected by the fuel consumption under full load condition. It should be note that the power turbine in DEP system did not have any influence on transient performance, since it had be totally bypassed before the operation in this case.

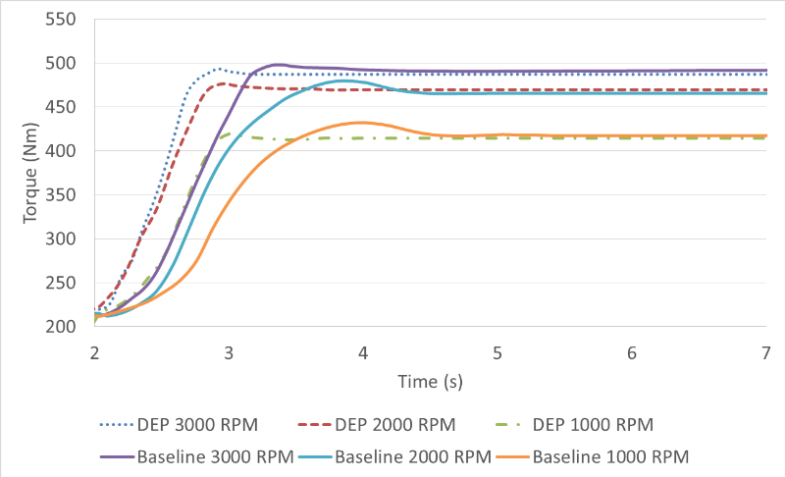

Figure 9.29. Transient performance of DEP and baseline engine.

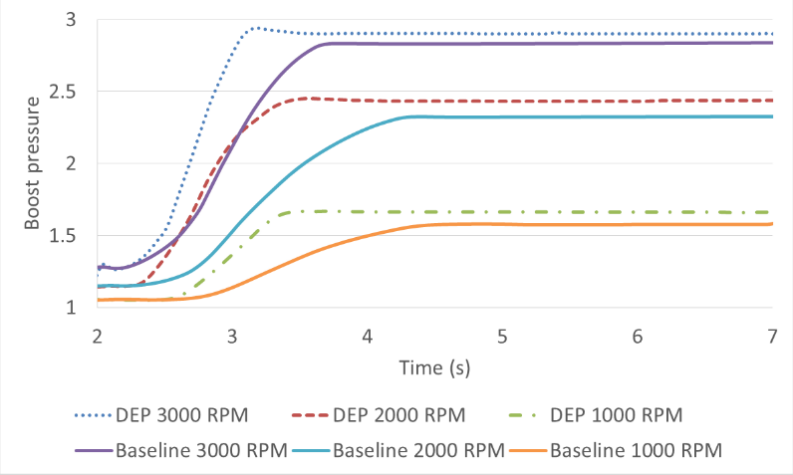

Figure 9.30. Transient performance of DEP and baseline turbocharger.

9.6 Conclusion

The simulation work demonstrated in this chapter shows the potential of DEP turbo-compounding system in reducing the fuel consumption and improving the response speed of

a highly downsized gasoline engine. However, the gains in fuel economy was largely dependent on the refined optimization of intake and exhaust profile and turbine size, since the gas exchange process, combustion phasing and turbocharger performance were all proved to affect the fuel economy of the engine system. On the one hand, since the exhaust mass flow was divided into blow-down and scavenge directed into separate manifold, the interference between the exhaust flows from adjacent cylinders could be avoided. Besides, by adjusting the exhaust valve timing and duration, the mass flow through the turbocharger turbine could be regulated with reduced back pressure, and meanwhile the turbocharger working could be improved by concentrating the operating points in the region of the highest efficiency. On the other hand, because only one exhaust valve was involved at the beginning and end of the discharge stroke for the DEP arrangement, it was more prone to choke, especially for the operation at high engine speed. This could also partly explain the decline in PMEP at higher speed and when the overlap between the blow-down and scavenge valve decreased. Therefore, a proper optimization was needed for a variety of parameters.

In fact, effects of the system specifications such as intake and exhaust valve profile and turbine size are strongly interrelated. It was considered as the main challenge for the optimization procedure. In this chapter, an iterative sweep simulation was carried out to investigate the general trend of each parameters affecting the engine performance before a co-simulation was conducted utilising the genetic algorithm to search for the global optimum value in fuel economy.

From the simulation at under full load condition at 3000 rpm, it was found that the exhaust valve timing had the most significant influence on the engine performance. Specifically, the trade-off between turbine power and pumping work can be adjustable by shifting the valve timing and thus the overlap between exhaust and intake valves. The results showed an optimal setting of 240 degree for the blow-down valve timing and 340 degree for the scavenging. It should be note that the exhaust valve timing could determine the attribution of exhaust mass flow into the main and power turbine.

Similarly, as for the intake valve timing, an optimal point existed at around 480 degree. An earlier intake stroke would be struggle to maintain the energy availability for the turbocharger, and thus PMEP. On the contrary, a retarded timing would cause a severe deficit in fresh air charging which had to be compensated by supercharger.

For the blow-down valve duration, it was slightly extended based on the setting in the original model by a multiplier of about 1.05 to reduce resistance to exhaust mass flow and thus the back pressure. Besides, a smooth gas exchange process could reduce the residual gas fraction

in cylinders, which allowed an advanced ignition timing. However, a further extension in blow-down valve opening would deteriorate fuel economy because of the back flow of exhaust gas into cylinders. In terms of the scavenge valve, a shortened duration was preferable to allow more exhaust gas being directed to the turbocharger turbine.

As expected, the sweep of turbine size was actually a matter of the trade-off between harvesting exhaust energy and imposing back pressure to the engine breathing. Specifically, a larger turbocharger turbine would brought about lower back pressure and thus better fuel economy. However, when the mass multiplier for the main turbine was bigger than 0.9, the turbocharger turbine became less effective to capture the energy in exhaust pulse and unable to provide enough boosting for the engine. The power turbine size, however, had little influence on the fuel efficiency of the whole system.

At 1000 rpm, the trend was similar. But, the engine performance became less sensitive to the turbine size because of the reduced mass flow rate. Since the turbocharger was less effective at low engine speed, the back pressure level became the crucial factor affecting fuel economy. Therefore, it was beneficial to increase the overlap (without causing serious loss of fresh charge) between exhaust and intake valve at 1000 rpm.

At part load operation (frequently used operating points over NEDC), the general trend was similar with diminished degree.

From the results of a global optimization, DEP system could bring about a fuel saving of 4.1% to the engine system under full load operation, because of the promotion in gas exchanging and combustion phase. The improvement became less noticeable at lower engine speed and lower load.

Lastly, since the DEP system utilised a smaller turbine than the baseline engine did, which was significantly beneficial for improving the boosting capability of turbocharger at low engine speed and thus the low-end brake torque. Besides, it also greatly improved the response speed of the whole system, especially at low engine speed when the promotion was more noticeable.

Chapter 10 - Conclusions

This final chapter will summarise the conclusions, contributions and impacts of the work presented in this thesis, followed by some suggestions and recommendations for future study in this area.

10.1 Summary, contributions and impacts

In this thesis, the application and development of turbo-compounding as a waste energy recovery technology for downsized gasoline engine has been presented. With reference to the project aim and objectives laid out in Chapter 1, the results and achievement in this study is summarised specifically.

The work in this thesis started from conventional turbocharged gasoline engine. During the developing, six configurations were built step by step aiming to solve the inherent problem of the former version, as shown in table 10.1. The developing process of the engine system in this work is illustrated in figure 10.1.

Table 10-1. **Studied configurations.**

Phases	Configurations	Issues	Solutions
Step 1	Turbocharged engine	Turbo lag and limited capability in waste energy recovery.	Introducing CVT supercharger to the charging system to eliminate the response delay caused by turbo lag.
Step 2	CVT Supercharger engine	Capability in waste energy recovery is still limited	Introducing turbo-compounding to promote the potential of waste energy recovery and the flexibility in turbomachinery control strategy.
Step 3	Two-stage TC (turbo-compounding) engine	High back pressure results in limited gain in fuel efficiency	Delete the original turbocharger to reduce the back pressure and system complexity.
Step 4	CVT Supercharger single-stage TC engine	A comprehensive evaluation is needed.	Comparing with the novel inverted Brayton cycle engine
Step 5	Inverted Brayton cycle engine	Comparing with turbo-compounding technology.	
Step 6	DEP CVT Supercharger single stage TC engine	A methodology to further reduce the back pressure	

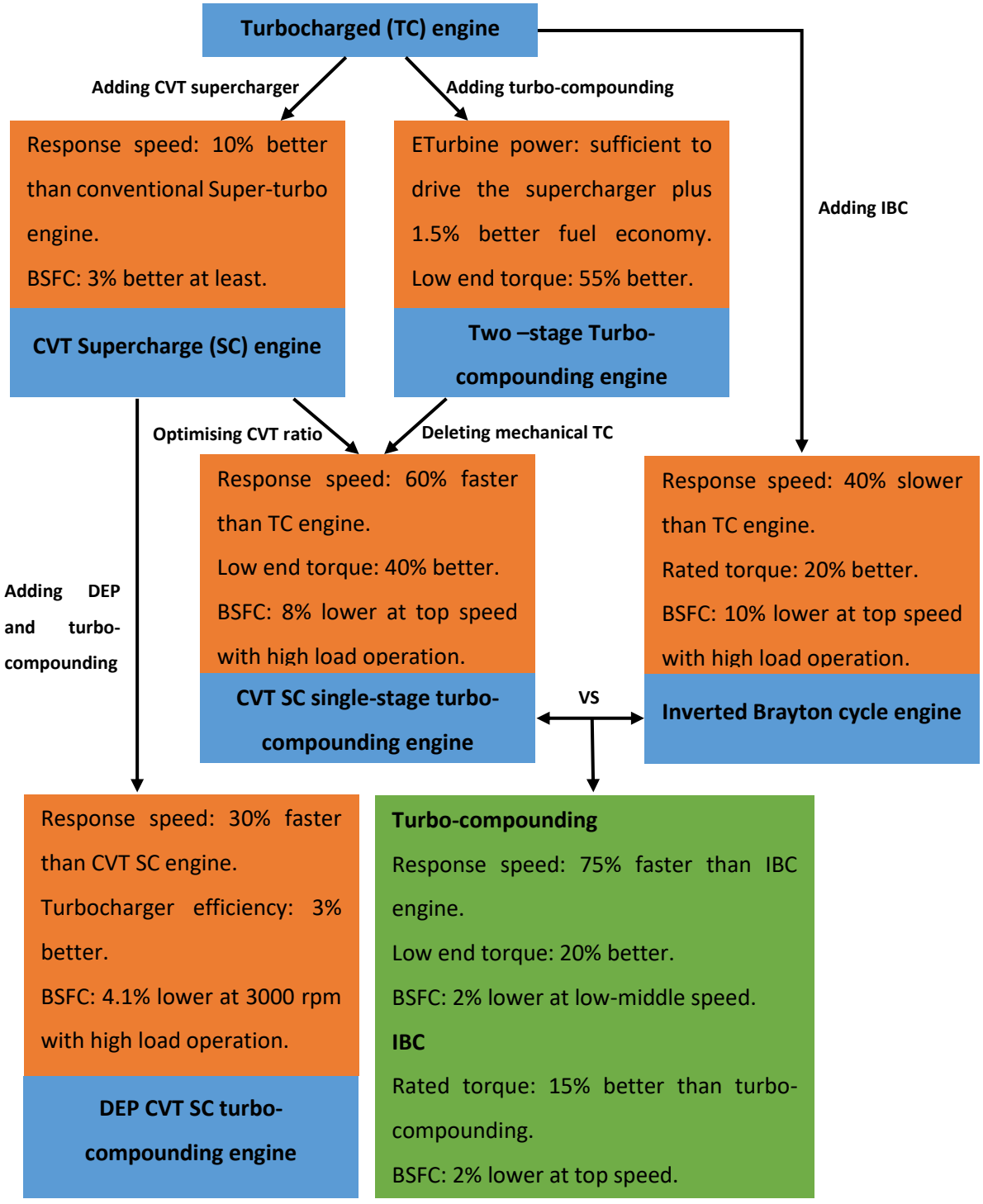

Figure 10.1. Developing process of engine system.

- *Review the dominating technologies to recover exhaust energy of internal combustion engine.*

Except for turbocharger that has been popularised, there are four major approaches to harvest waste heat of internal combustion engine, namely thermoelectric, Rankine cycle, Brayton cycle and turbo-compounding. Among them, Rankine cycle is considered to be infeasible for the application in small vehicle engine because of the bulky volume and weight, despite of the high thermal efficiency to converting waste heat into useful work. On the opposite, thermoelectric is much more compact in size, but inefficient in converting thermal energy into electric power because of the inherent properties of existing material. Therefore, turbo-compounding is regarded as one of the most possible way to save exhaust energy for passenger car engine because of the good thermal efficiency, smaller size, lower weight and simple structure (when comparing with Brayton cycle which requires for multi-stage compressor). However, turbo-compounding has the drawback of imposing higher back pressure to the engine which badly interferes with the gas exchange of the premier cycle. It is the main topic of this work to figure out a solution to this issue.

- *Review the history and typical configuration of turbo-compounding and the sensitivity to different parameters*

Turbo-compounding was initially utilised in aircraft engine and entered automotive industry during 80s in last century. It can be generally classified into mechanical and electrical versions. For both versions, it can be of HP of LP configuration depending on the relative location of the turbocharger turbine and power turbine. It was proven that a variety of parameters, including boosting pressure, compression ratio, ignition timing, air-fuel ratio and so on, have important influence on the performance of turbo-compounding engine system by either leading to a trade-off between combustion power and the magnitude in exhaust energy recovery or affecting the operating condition and efficiency of power turbine. It was also believed that turbo-compounding enables the engine to be operated with retarded ignition timing that helps to reduce the risk of knock without suffering from deterioration in power output. Generally, it can be concluded that a global optimization is needed to determine the best setup for the specification of a specific turbo-compounding engine.

- *Develop the simulation techniques; build and calibration of a 1-D engine model for steady state and transient simulation; determine engine control construction*.

Chapter 4 presents a modelling and calibration theory as a foundation for the study in the following chapters. It includes three sub-sections, namely engine model introduction and calibration for steady state simulation; engine control theory and tuning; and engine modelling and calibration for transient simulation.

- *Modelling the variable drive supercharged engine system*

In this chapter, a CVT Supercharger variable drive supercharged engine model was built. The performance of turbo-super and super-turbo configurations of this system was compared to determine the location of CVT Supercharger compressor followed by the optimization of pulley ratio and CVT ratio change rate regarding the tip-in operation from different starting load. The steady state performance of the whole system was evaluated by examining the fuel consumption at full load, part load and driving cycles. Transient performance was investigated by comparing to the baseline engine model.

It was found that Super-Turbo was proven to be a better configuration than the Turbo-Super counterpart for CVT Supercharger system in consideration of fuel economy. A trade-off exists between the low load fuel consumption and transient response at the lowest engine speed. Similarly, the clutching speed and active bypass valve close rate of the conventional supercharger system were also limited to avoid the sharp decline and over-shooting in engine brake torque. Besides, a general trend was found that the CVT change rate and clutching speed needed to be reduced further for higher starting load.

CVT Supercharger brought about 3% better fuel economy to the whole system when comparing with the positive displacement counterpart. Furthermore, CVT Supercharger embodied further superiority at mid-high load operation when supercharger was less needed for assisting air boosting. At 16 bar BMEP, for example, CVT Supercharger was able to provide about 40% better fuel economy than the conventional fix-ratio supercharger did. However, under low load condition, approximately CVT Supercharger engine consumed 4.5% more fuel than the Eaton system did.

A mini map was produced to imitate the WLTP driving cycle. From the results, the fuel consumption of CVT Supercharger engine is higher than the declutched Eaton system by up to 4.94% at extremely low load operation. When comparing with clutched fix-ratio supercharger, however, the fuel economy could be improved by up to 30.7%. By including weights to each of the operating points, the overall BSFC deficits for the major parts of all the operating points could be worked out that the fuel economy of CVT Supercharger engine was

2.74% worse than the disengaged Eaton and 19.6% better than the engaged Eaton system. From the transient simulation, CVT Supercharger system shorten the response time of the baseline twin charged model by about 0.2 second at 1100 rpm. It also demonstrates that the most significant improvement was seen at 2000 rpm because of the synthetic promotion from both CVT Supercharger and turbocharger.

- *Verification of the Variable Drive Supercharged engine System*

A rig test was carried out for the CVT Supercharger system to prove its capability of enhancing low-end torque, improving the transient driveability and reducing the low-load parasitic losses. It came to the conclusions that CVT Supercharger system was able to significantly enhance an engine's low-end performance without crucially affecting its low load fuel efficiency at steady-state test. It enabled the potential of applying further downsizing or Miller Cycle to mitigate the fuel penalty that is caused by the parasitic losses. A ready-to-use control strategy at the engine's level had been built and calibrated using the steady-state engine test data. The influence of different control calibrations on the engine performance had been found and would guide the later control calibration tuning at the vehicle's level. In transient test, CVT Supercharger system achieved significantly better transient performance in terms of time-to-torque compared with the turbo only configuration with better NVH behavior in comparison to the fixed-ratio positive displacement counterpart with a clutch. Re-optimizing the transmission gear ratio or the shifting strategy, realizing further down-speeding, could further improve the engine's fuel efficiency in a real driving cycle, while maintaining a good driveability.

- *Implementing full electric turbocharging systems on highly boosted gasoline engines*

The performance of a conventional turbocharged engine model was compared with a two-stage boost engine model equipped with a decoupled electric turbocharger, in which a carefully designed control strategy was designed for the electric turbocharger for a variety of engine speed/load conditions. LP mode was selected for the lower eTurbine temperature for thermal protection, although HP mode would be a more economical solution. At full load condition, eCompressor was expected to provide extra boost at 1750 rpm and below to enhance the low end torque by up to 115 Nm. Above 1750 rpm, when the mechanical turbocharger was able to provide sufficient boost on its own, eCompressor was totally bypassed. At the same time, electric turbine was harvesting exhaust energy independently.

The power output from the eTurbine was sufficient to satisfy the power consumption of the eCompressor. At partial load condition, mass flow could be regulated by adjusting the eTurbine bypass valve as an alternative to throttle, so that throttle was less shut. It helped to reduce the throttle loss. At 40% load and higher, the pressure drop across the throttle body was nearly eliminated. Besides, eTurbine was able to harvest up to 8 kW power from the exhaust energy, which could be converted into useful mechanical work. However, similar with the case in full load condition, back pressure and requirement of boost was increased because of the employment of eTurbine. The tendency to knock due to higher back pressure should be further investigated in the experimental phase of the study. Across the part load map the BSFC was reduced by up to 3.6%. At the high engine load, fuel consumption will increase because of the high back pressure as a result of eTurbine trying to harness energy to support eCompressor. The improvement to the fuel economy in driving cycle simulation was less remarkable. The largest reduction in BSFC was seen in HiWay driving cycle, which is 0.8%. In NEDC, the number decreased to 0.4%. The upcoming RDE cycle will be investigated in future works and the eTurbo technology is expected to achieving larger fuel economy benefit due to the higher load/speed of the real world drive cycle.

- *Modelling the Turbo-Compounding Concept*

The effect that a turbo-compounding has on a 2.0 litre gasoline engine model and the benefit of coupling a CVT to the supercharger were examined by comparing its performance data with a conventional turbocharged engine model of the same displacement and compressor characteristics. In this part, both the power recovery by the power turbine and the pumping losses resulted from the higher back pressure were considered. Design of experiments and optimization techniques were used to find the optimal settings for the turbine speed under full load condition. The CVT supercharger in combination with the turbo-compounding contributed to improve the engine performance at lower engine speed range. The simulation results proved the practicability of this concept. The CVT Supercharger helped to increase the brake torque by up to 24% at 1500 revs/min. At higher engine speed, turbo-compounding was able to increase the brake torque evenly by 7% from 3000 revs/min and above. The BSFC was reduced by up to 8% at top engine speed. But the improvement descends as the engine speed slowing down and become vanished at 2000 revs/min because of the weakened power turbine function and the parasitic load imposed by the CVT supercharger.

The performance of a CVT supercharged turbo-compounding engine was further examined for the partial load and transient operation. Under partial load condition, very little improvement was gained from adjusting the turbine speed due to the significant decrease in turbine power output. The improvement in specific fuel consumption of the CVT supercharged turbo-compounding engine was believed due to the windmilling effect of the compressor and the reduced pumping losses.

For the transient performance evaluation, the CVT supercharged turbo-compounding engine was able to provide the rapidest response of boost pressure and torque output (60% faster than turbocharged engine) due to the mechanical connection between the supercharger and the engine crankshaft. A diving in brake torque was seen as the compressor starting to accelerate. These torque losses was proportional to the inertial of the supercharger and the transmission ratio. A proper calibration was needed to rectify this in order improve the drivability.

- *Compare the performance of CVT Supercharged turbo-compounding with Inverted Brayton cycle*

The potential of Inverted Brayton cycle and high pressure turbo-compounding for the augmentation of the power output and fuel economy of conventional turbocharged engine was demonstrated. Design of experiments techniques was used to optimise the compressor and power turbine speed of the turbo-compounding engine and also the size of the turbo-machinery in IBC aiming to achieve the optimal performance of the whole system. It was found that both the brake torque and BSFC of the CVT supercharged turbo-compounding engine were continuously improved along with the acceleration of the supercharger under full load condition. At partial load, a lower supercharger speed was more preferable. Besides, when the engine was operated at middle and low speed, the power output and fuelling efficiency increased significantly with higher turbine speed, while at high engine speed the growth rate was smaller and the plateau appeared sooner. When the throttle was partially closing, the influence of the power turbine speed on the overall engine performance was weakened. By adjusting the size of the power turbine in the inverted Brayton cycle, the inlet exhaust pressure to the bottoming cycle was scaled. Within the engine speed range from 2000 to 5000 rpm, it was found that the IBC engine performance deteriorated rapidly with higher inlet pressure. It was believed resulting from the plummet in PMEP and thus the deterioration of the scavenging process.

When the engines were operated at lower load, the difference in fuel consumption between those two novel models was narrowed. The general trend was that the IBC engine offered

better fuel economy by 1% at lower engine speed (below 2000 rpm, typically), while the CVT supercharged turbo-compounding engine took over the advantages at higher speed (1% better). It was the similar trend that applied to the performance under full load condition. It was also worth noting that the power generation and the fuel consumption from the novel system were both significantly better than the baseline turbocharged model. Furthermore, the low speed torque from the turbo-compounding engine was enhanced impressively with the assistance of CVT.

In terms of the evaluation of the transient performance, CVT supercharged turbo-compounding engine showed the fastest response speed, while the IBC which was delayed by building up the turbine speed took the longest time to achieve the required BMEP, which makes it 75% slower.

- *Model Divided Exhaust Period concept for a turbo-compounding gasoline engine*

The simulation work demonstrated in this chapter shows the potential of DEP turbo-compounding system in reducing the fuel consumption and improving the response speed of a highly downsized gasoline engine. However, the gains in fuel economy was largely dependent on the refined optimization of intake and exhaust profile and turbine size, since the gas exchange process, combustion phasing and turbocharger performance were all proved to affect the fuel economy of the engine system. On the one hand, since the exhaust mass flow was divided into blow-down and scavenge directed into separate manifold, the interference between the exhaust flows from adjacent cylinders could be avoided. Besides, by adjusting the exhaust valve timing and duration, the mass flow through the turbocharger turbine could be regulated with reduced back pressure, and meanwhile the turbocharger working could be improved by concentrating the operating points in the region of the highest efficiency. On the other hand, because only one exhaust valve was involved at the beginning and end of the discharge stroke for the DEP arrangement, it was more prone to choke, especially for the operation at high engine speed. This could also partly explain the decline in PMEP at higher speed and when the overlap between the blow-down and scavenge valve decreased. Therefore, a proper optimization was needed for a variety of parameters.

In this chapter, an iterative sweep simulation was carried out to investigate the general trend of each parameters affecting the engine performance before a co-simulation was conducted utilising the genetic algorithm to search for the global optimum value in fuel economy.

From the simulation at under full load condition at 3000 rpm, it was found that the exhaust valve timing had the most significant influence on the engine performance. Specifically, the trade-off between turbine power and pumping work can be adjustable by shifting the valve timing and thus the overlap between exhaust and intake valves. The results showed an optimal setting of 240 degree for the blow-down valve timing and 340 degree for the scavenging. It should be note that the exhaust valve timing could determine the attribution of exhaust mass flow into the main and power turbine.

Similarly, as for the intake valve timing, an optimal point existed at around 480 degree. An earlier intake stroke would be struggle to maintain the energy availability for the turbocharger, and thus PMEP. On the contrary, a retarded timing would cause a severe deficit in fresh air charging which had to be compensated by supercharger.

For the blow-down valve duration, it was slightly extended based on the setting in the original model by a multiplier of about 1.05 to reduce resistance to exhaust mass flow and thus the back pressure. Besides, a smooth gas exchange process could reduce the residual gas fraction in cylinders, which allowed an advanced ignition timing. However, a further extension in blow-down valve opening would deteriorate fuel economy because of the back flow of exhaust gas into cylinders. In terms of the scavenge valve, a shortened duration was preferable to allow more exhaust gas being directed to the turbocharger turbine.

As expected, the sweep of turbine size was actually a matter of the trade-off between harvesting exhaust energy and imposing back pressure to the engine breathing. Specifically, a larger turbocharger turbine would brought about lower back pressure and thus better fuel economy. However, when the mass multiplier for the main turbine was bigger than 0.9, the turbocharger turbine became less effective to capture the energy in exhaust pulse and unable to provide enough boosting for the engine. The power turbine size, however, had little influence on the fuel efficiency of the whole system.

At 1000 rpm, the trend was similar. But, the engine performance became less sensitive to the turbine size because of the reduced mass flow rate. Since the turbocharger was less effective at low engine speed, the back pressure level became the crucial factor affecting fuel economy. Therefore, it was beneficial to increase the overlap (without causing serious loss of fresh charge) between exhaust and intake valve at 1000 rpm.

At part load operation (frequently used operating points over NEDC), the general trend was similar with diminished degree.

From the results of a global optimization, DEP system could bring about a fuel saving of 4.1% to the engine system under full load operation, because of the promotion in gas exchanging

and combustion phase. The improvement became less noticeable at lower engine speed and lower load.

Lastly, since the DEP system utilised a smaller turbine than the baseline engine did, which was significantly beneficial for improving the boosting capability of turbocharger at low engine speed and thus the low-end brake torque (by 10% at 2000 rpm). Besides, it also greatly improved the response speed of the whole system by 30%, especially at low engine speed when the promotion was more noticeable.

10.2 Outlook

The work presented in this thesis can be considered an analytical foundation for the future research in this area.

1. The verification of CVT Supercharger benefits for gasoline engine has provided a novel option for engine downsizing with air boosting. It is also expected that a similar gains in fuel economy and response speed can be achieved on a downsized diesel engine.
2. The works on electric turbocharger and turbo-compounding has proven the feasibility of applying turbo-compounding in downsized gasoline engine as a waste energy recovery technology. The concept of combining CVT Supercharger with HP turbo-compounding effectively solves the inherent problem of turbo machinery.
3. The analysis on the trade-off between the part-load BSFC and the transient response and recommendation for selecting the drive ratio for a compound charging system could be of reference value for other supercharging projects.
4. The introduction and optimization of DEP turbo-compounding concept can be applied to other complex compound charging systems or WER system

10.3 Further work

1. The DEP and the turbo-compounding concept may need further validation with engine level experimental test. Similarly, the knock model, which is used to determine ignition timing and control the combustion phasing in those simulations, needs to be validated against the test data in a later research.

2. Although the experiment data of the variable-drive supercharging concept and the baseline turbocharged engine are obtained for three pressure analysis, further test is needed to optimize the whole engine system.

3. The control strategy, especially for transient operation, is only briefly described in this work. Rig test is needed to give an optimal performance.

4. Besides, because the superior low-end torque and significantly improved transient behaviour with CVT Supercharger, it is worth exploring the potential of integrating Miller cycle in CVT Supercharger engine to improve the part load fuel economy.

5. Although the system will become more complicated, including the turbo-compounding and IBC in a common arrangement may be worth trying with the expectation of fulfilling the advantages of each unit over the entire engine speed range.

References

1. M Ricardo, P Apostolos and M Yang. “Overview of boosting options for future downsized engines”. Science China Technological Sciences. February 2011, Volume 54, Issue 2.

2. Teo Sheng Jye, A., Pesiridis, A. and Rajoo, S., "Effects of Mechanical Turbo Compounding on a Turbocharged Diesel Engine," SAE Technical Paper 2013-01-0103, 2013, doi:10.4271/2013-01-0103.

3. Wanga TY., Zhanga YJ., Pengb ZJ.and Shua GQ., “A review of research on thermal exhaust heat recovery with Rankine cycle,” Renewable and Sustainable Energy Reviews, 15 (2011) 2862– 2871, 2011.

4. Hendricks TJ, Lustbader JA,. “Advanced thermoelectric power system investigations for light-duty and heavy duty applications: Part I,” In: Proceedings of the 21st international conference on thermoelectrics. 2002.

5. Richard S., Rohitha W., “Heat Recovery and Bottoming Cycles for SI and CI Engines – A Perspective,” Department of Engineering and Design, University of Sussex, 2006.

6. Teng H, Regner G and Cowland C., “Waste energy recovery of heavy-duty diesel engines by organic Rankine cycle Part II: working fluids for WER-ORC,” In: SAE paper 2007-01-0543; 2007.

7. Vazaquez J, Zanz-Bobi MA, Palacios R and Arenas A. “State of the art of thermoelectric generators based on heat recovered from the exhaust gases of automobiles,” In: Proceedings of 7th European workshop on thermoelectrics. 2002.

8. Endo T, Kawajiri S, Kojima Y, Takahashi K, Baba T and Ibaraki S, “Study on maximizing exergy in automotive engines,” In: SAE paper 2007-01-0257; 2007.

9. D.T. Hountalas, C.O. Katsanos and V.T. Lamaris., "Recovering Energy from the Diesel Engine Exhaust Using Mechanical and Electrical Turbo-compounding," SAE Technical Paper 2007-01-1563, 2007.

10. Kamo, R. and Brysik, W., “Adiabatic turbo-compound engine performance prediction”, SAE Paper No. 780068, 1978.

11. Hountalas D.T., Katsanos C.O., Rogdakis E.D.and Kouremenos D., “Study of available exhaust gas heat recovery technologies for HD diesel engine applications”, International Journal of Alternative Propulsion, 2006.

12. Sendyka B, Soczowka J., “Recovery of exhaust gases energy by means of turbocompound”. In: Proceedings of the 6th international symposium on diagnostics and modelling of combustion in internal combustion engines. Yokohama, Japan; 2004.p.99–103.

13. Hopmann, U., “Diesel engine waste energy recovery utilizing electric turbocompound technology”, Catterpillar, DEER Conference, San Diego, California, USA, 2004.

14. Di Nanno, L.R., Di Bella, F.A. and Koplow, M.D, “An RC-1 organic Rankine bottoming cycle for an adiabatic diesel engine”, Thermoelectron Corp., Master Thesis, Waltham, MA, USA 1983, https://archive.org/details/nasa_techdoc_19840024236.

15. P. Brito, F., Martins, J., Goncalves, L. and Sousa, R., "Temperature Controlled Exhaust Heat Thermoelectric Generation," SAE Int. J. Passeng. Cars - Electron. Electr. Syst. 5(2):561-571, 2012, doi: 10. 4271/2012-01-1214.

16. Riffat SB., Ma X.,"Thermoelectrics:a review of present and potential applications," Applied Thermal Engineering 2003;23(8): 913–35.

17. Xu, Z., Liu, J., FU, J. and Ren, C., "Analysis and Comparison of Typical Exhaust Gas Energy Recovery Bottoming Cycles," SAE Technical Paper 2013-01-1648, 2013, doi:10.4271/2013-01-1648.Analysis and Comparison of Typical Exhaust Gas Energy Recovery Bottoming Cycles.

18. Mori M., Yamagami T., Oda N., Hattori M., Sorazawa M.and Haraguchi T., "Current possibilities of thermoelectric technology relative to fuel economy," SAE Paper, No. 2009-01-0170, Presented at SAE World Congress & Exhibition, April 2009, Detroit, MI, USA, Session: Thermal Management Systems (Part1of2).

19. Hsu CT., Huang GY., Chu HS., Yu B.and Yao DJ., "Experiments and simulations on low-temperature waste heat harvesting system by thermoelectric power generators," Applied Energy 2011;88(4):1291–7.

20. Hussain QE., Brigham DR.and Maranville CW., "Thermoelectric exhaust heat recovery for hybrid vehicles," SAE Paper no.2009-01-1327, Presented at SAE World Congress & Exhibition April 2009, Detroit, MI, USA, Session: Advanced Hybrid Vehicle Powertrains-Hybrid Engine & Emissions, Thermo-Electric Conversion (Part1of6).

21. Stobart R, Weerasinghe R. "Heat recovery and bottoming cycles for SI and CI engines—a perspective," SAE Paper no.2006-01-0662, Presented at SAE 2006 World Congress & Exhibition, April 2006, Detroit, MI, USA, Session: Advanced Hybrid Vehicle Powertrains (Part2of5).

22. Stobart, RK., Wijewardane A.and Allen C., "The potential for thermo-electric devices in passenger vehicle applications," SAE Paper no.2010-01-0833, Presented at SAE 2010 World Congress & Exhibition, April 2010, Detroit, MI, USA, Session: Advanced Hybrid Vehicle Powertrains (Part2of3).

23. Bass JC, Campana RJ and Elsner NB., "Thermoelectric generator for diesel engines," In: Proceedings of the 1990 Coatings for Advanced Heat Engines Workshop U.S. 1990.

24. Bass JC, Campana RJ and Elsner NB., "Thermoelectric generator for diesel trucks," In: Proceedings of the 10th International conference on thermoelectrics. 1991.

25. Bass JC, Elsner NB and Leavitt FA., "Performance of the 1 kW thermoelectric generator for diesel engines," In: Proceedings of the 13th international conference on thermoelectrics New York. 1995.

26. Bass J.C., "Thermoelectric generator for motor vehicle," U.S. Patent US5625245, April 29; 1997.

27. Bass J.C., Elsner N.B. and Leavitt F.A., "Method for fabricating a thermoelectric module with gapless eggcrat," U.S. Patent US 5856210, January 5; 1999.

28. Kobayashi M, Ikoma K., Furuya K., Shinohara K., Takao H.and Miyoshi M., “Thermoelectric generation and related properties of conventional type module based on Si–Ge alloys,” In: Proceedings of the 15th international conference of thermoelectric. 1998.

29. Weerasinghe W.M.S.R., Stobart R.K.and Hounsham S.M., “Thermal efficiency improvement in high output diesel engines a comparison of a Rankine cycle with turbo-compounding,” Applied Thermal Engineering, 30 (2010) 2253-2256, 2010.

30. Sherman D., “Turbo Compounding Is the Next Big Thing in Energy Recovery,” http://blog.caranddriver.com/turbo-compounding-is-the-next-big-thing-in-energy-recovery/, 2014.

31. Butcher CJ, Reddy BV. “Second law analysis of a waste energy recovery based power generation system”. Int J Heat Mass Transf 0017-93102007; 50(11-12): 2355–63.

32. Kadota M., Yamamoto K., “Advanced transient simulation on hybrid vehicle using Rankine cycle system,” SAE Paper no.2008-01-0310, Presented at SAE World Congress & Exhibition, April 2008, Detroit, MI, USA, Session: Advanced Hybrid Powertrains (Part2of3) Hydraulic Hybrids, Hybrid Vehicle Designs, and Thermal Energy Recovery and Storage.

33. Gu W., Weng Y., Wang Y.and Zheng B., “Theoretical and experimental investigation of an organic rankine cycle for a waste energy recovery system,” Proceedings of the Institution of Mechanical Engineers, Part A: Journal of Power and Energy 2009;223: 523–33.

34. John BH., “Automotive engines and fuels: a review of future options,” Prog. Energy Combust Sci. 7 (1981) 155e184.

35. Kadota M., Yamamoto K., “Advanced transient simulation on hybrid vehicle using Rankine cycle system,” SAE Paper no.2008-01-0310, Presented at SAE World Congress & Exhibition, April 2008, Detroit, MI, USA, Session: Advanced Hybrid Powertrains (Part2of3) Hydraulic Hybrids, Hybrid Vehicle Designs, and Thermal Energy Recovery and Storage.

36. Hung TC., “Waste energy recovery of organic Rankine cycle using dry fluids,” Energy Conversion and Management 2001; 42 (5): 539–53.

37. Liu B., Chien K.and Wang C., “Effect of working fluids on organic Rankine cycle for waste energy recovery,” Energy 2004; 29: 1207–17.

38. Poling B., Prausnitz J.and Connell JO., “The properties of gases and liquids,” McGraw-Hill Professional; 2000.

39. Chen H., Goswami DY.and Stefanakos EK., “A review of thermodynamic cycles and working fluids for the conversion of low-grade heat,” Renewable and Sustainable EnergyReviews2010;14: 059–67.

40. Ibaraki S., Endo T., Kojima Y., Takahashi K., Baba T.and Kawajiri S., “Study of efficiency on-board waste energy recovery system using Rankine cycle,” Review of Automotive Engineering 2007;28:307–13.

41. Serrano JR., Dolz V., Novella R.and Garc A., “A HD Diesel engine equipped with a bottoming Rankine cycle as a waste energy recovery system. Part2: Evaluation of alternative solutions,” Applied Thermal Engineering 2012; 36(0):279–87.

42. Freymann R., Strobl W. and Obieglo A., “The turbo steamer: a system introducing the principle of cogeneration in automotive applications,” MTZ2008; 69:20–7.

43. Hountalas DT., Mavropoulos GC., Katsanos C. and Knecht W., “Improvement of bottoming cycle efficiency and heat rejection for HD truck applications by utilization of EGR and CAC heat,” Energy Conversion and Management 2012; 53(1): 19–32.

44. Miller EW., Hendricks TJ. and Peterson RB., “Modelling energy recovery using thermoelectric conversion integrated with an organic Rankine bottoming cycle,” Journal of Electronic Materials 2009; 38:7.

45. Hiereth H., Prenninger P., “Charging the Internal Combustion Engine,” 2003 Springer-Verlag, Wien.

46. Woschni G., Bergbauer F., “Verbesserung von Kraftstoffverbrauch und Betriebsverhalten von Verbrennungsmotoren durch Turbo-compounding,” Mtz 51: 108–116, 1990.

47. Wallace FJ., “The differential compound engine-a new integrated engine transmission system concept for heavy vehicles,” School of Engineering, University of Bath, Proc Instn Mech Engrs Vol 197A, IMech E July 1983.

48. He, G. and Xie, H., "Fuel Saving Potential of Different Turbo-Compounding Systems Under Steady and Driving Cycles," SAE Technical Paper 2015-01-0878, 2015, doi:10.4271/2015-01-0878.

49. Göktun S, Yavuz H. “Thermal efficiency of a regenerative Brayton cycle with isothermal heat addition”. Energy Conversion & Management 1999; 40(12):1259-1266.

50. Colin D. Copeland, Zhihang Chen. “The Benefits of an Inverted Brayton Bottoming Cycle as an Alternative to Turbo-Compounding. ASME Turbo Expo 2015: Turbine Technical Conference and Exposition”. Paper No. GT2015-42623, doi:10.1115/GT2015-42623.

51. Zhang W., Chen L. and Sun F., “Power and efficiency optimization for combined Brayton and inverse Brayton cycles”. Applied Thermal Engineering 2009; 29(14): 2885-2894.

52. Frost, T., Anderson, A., and Agnew, B.A. “Hybrid gas turbine cycle (Brayton/Ericsson): an alternative to conventional combined gas and steam turbine power plant”. Proceedings of the IMECHE, Part A: J. of Power and Energy, 1997. 211(2), pp. 121-131.

53. M. Tancreza, J. Galindob, C. Guardiolab, P. Fajardob and O. Varnierb, “Turbine adapted maps for turbocharger engine matching, Experimental Thermal and Fluid Science”, Volume 35, Issue 1, January 2011, Pages 146–153, 17 September 2010.

54. Wood Ridge, “Facts about the Wright Turbo Compound”. New Jersey: Curtiss-Wright Corporation:Wright Aeronautical Division. October 1956. Retrieved 19 February 2016.

55. Gunston, Bill, "Napier Nomad: An engine of outstanding efficiency" (PDF). Flight: 543–551. Retrieved 19 February 2010.

56. Bailey, M. “Comparative evaluation of three alternative power cycles for waste energy recovery from the exhaust of adiabatic diesel engines”. National Aeronautics and Space Administration, 1985. Cleveland, OH (USA). Lewis Research Centre.

57. M. Tancreza, J. Galindob, C. Guardiolab, P. Fajardob, and O. VarnierTurbine. “Adapted maps for turbocharger engine matching. Experimental Thermal and Fluid Science”. Volume 35, Issue 1, January 2011. doi:10.1016.

58. Matsura, Y., Nakazawa, N., Kobayashi, Y., Ogita, H. and Kawatani, T. “Effects of Various Methods for Improving Vehicle Start ability and Transient Response of Turbocharged Diesel Trucks”. SAE paper 920044, 1992.

59. Rose, A. T. J. M., Akehurst, S. and Brace, C. J. “Modelling the performance of a continuously variable supercharger drive system. Proceedings of the Institution of Mechanical Engineers, Part D: Journal of Automobile Engineering”, 225 (10). pp. 1399-1414. ISSN 0954-4070.

60. Dolz V, Novella R, García A and Sánchez J. “HD Diesel engine equipped with a Bottoming Rankine cycle as a waste energy recovery system. Part1:study and analysis of the waste heat energy”. Appl Therm Eng 2012; 36:269–78.

61. Serrano JR, Dolz V, Novella R and García A. “HD Diesel engine equipped with a Bottoming Rankine cycle as a waste energy recovery system. Part2: Evaluation of alternative solutions”. Appl Therm Eng 2012; 36:279–87.

62. Chiara F, Canova M. “A review of energy consumption, management, and Recovery in automotive systems, with considerations of future trends”. Proc Inst Mech Eng: J Automob Eng 2013; 2276914-936.

63. Brands, M., Werner, J., Hoehne, J. and Kramer, S., "Vechicle Testing of Cummins Turbocompound Diesel Engine," SAE Technical Paper 810073, 1981, doi:10.4271/810073.

64. Stobart R, Wijewardane A. and Allen C. “The potential for thermo-electric devices in passenger vehicle applications”. SAE Technical Paper, 2010-01-0833. 2010.

65. Hsiao YY, Chang WC. and Chen SL. “A mathematic model of thermoelectric module with applications on waste energy recovery from automobile engine”. Energy 0360-54422010; 35(3):1447–54.

66. Baines NC. Fundamentals of turbocharging. USA: Concepts NREC; 2005.

67. Kamo R. “Adiabatic diesel-engine technology in future transportation”. Energy 0360-54421987; 12(10-11): 1073–80.

68. Kouremenos DA, Rakopoulos CD. and Hountalas DT. “Prechamber and main chamber insulation effects on the performance of an IDI diesel engine coupled to power turbine”. Heat Recovery Syst CHP0890-43321992; 12 (3):247–56.

69. Assanis DN. “Effect of combustion chamber insulation on the performance of a low heat rejection diesel engine with exhaust heat recovery”. Heat Recovery Syst CHP 1989; 9 (5):475–84.

70. TaymazI. “An experimental study of energy balance in low heat rejection diesel engine”. Energy 2006; 31(2-3): 364–71.

71. Watson N, Janota MS. “Turbocharging the internal combustion engine”. London: MacMillan; 1982.

72. T H Frost, A Anderson and B Agnew. “A hybrid gas turbine cycle (Brayton/Ericsson): An alternative to conventional combined gas and steam turbine power plant”. Journal of Power and Energy March 1, 1997. doi: 10.1243/0957650971537042.

73. Bouton, F. and Winter, R. “Mechanical-draught cooling towers with visible plume abatement”. In IMechE CCGT–II, Second Seminar on Combined Cycle Gas Turbines, April 1992 Mechanical Engineering Publications, London.

74. Silverstein, C. G. “The ICE cycle: high gas turbine efficiency at moderate temperatures”. In Proceedings of Twenty-third Intersociety Energy Conversion Engineering Conference, Vol.1, 1988, pp. 285–289 (IEEE).

75. Chen, Z. and Copeland, C., "Inverted Brayton Cycle Employment for a Highly Downsized Turbocharged Gasoline Engine," SAE Technical Paper 2015-01-1973, 2015, doi:10.4271/2015-01-1973.

76. Wojciechowski, K. T., Schhmidt, M., Zybala, R., Merkisz, J., Fuc, P., and Lijewski, P., 2009, “Comparison of Waste energy recovery From the Exhaust of a Spark Ignition and a Diesel Engine,” J. Elec. Materials, 39, p. 2034–2038.

77. Crane, D. T., and Bell, L. E., 2009, “Design to Maximize Performance of a Thermoelectric Power Generator With a Dynamic Thermal Power Source,” ASME J. Energy Resour. Technol., 131, p. 012401.

78. Wang T., Zhang Y., Zhang J., Shu G. and Peng Z. “Analysis of recoverable exhaust energy from a light-duty gasoline engine”. Appl Therm Eng ISSN: 1359-4311 2013; 53(2): 414–9.

79. Hountalas D, Mavropoulos G. “Potential for improving HD diesel truck engine fuel consumption using exhaust heat recovery techniques”. In: Meng Joo Er (Ed.), New Trends in Technologies: Devices, Computer, Communication and Industrial Systems Chapter 172010 pp. 313-340.

80. Weerasinghe W, Stobart RK. and Hounsham SM. “Thermal efficiency improvement in high output diesel engines a comparison of a Rankine cycle with turbo-compounding”. Appl Therm Eng 2010;30(14–15):2253–6.

81. Aghaali, H. and Angstrom, H., "Demonstration of Air-Fuel Ratio Role in One-Stage Turbocompound Diesel Engines," SAE Technical Paper 2013-01-2703, 2013, doi:10.4271/2013-01-2703.

82. Thompson IGM., Spence SW. and McCartan C. “A review of turbocompounding and the current state of the art”. In: Proceedings of the 3rd international conference on sustainable energy and environmental protection. Dublin; 2009.

83. Varnier ON. “Trends and limits of two-stage boosting systems for automotive diesel engines”. Doctoral thesis. Universidad Politecnica DeValencia, Spain, 2012.

84. Ismail, Y., Durrieu, D., Menegazzi, P.and Chesse, P., "Potential of Exhaust Heat Recovery by Turbocompounding," SAE Technical Paper 2012-01-1603, 2012, doi:10.4271/2012-01-1603.

85. F. J. Wallace. “Second Paper: Differential compound engine”. Proceedings of the Institution of Mechanical Engineers June 1973. doi: 10.1243.

86. Conklin JC, Szybist JP. “A highly efficient six-stroke internal combustion engine cycle with water injection for in-cylinder exhaust heat recovery”. Energy 0360-54422010; 35(4): 1658–64.

87. Shu G, Liang Y, Wei H, Tian H, Zhao J and Liu L. “A review of waste energy recovery on two-stroke IC engine aboard ships”. Renew Sustain Energy Rev 1364-0321 2013; 19: 385–401.

88. T. Briggs, “High efficiency engine systems development and evaluation”. In: Proceedings of the 2011 DOE hydrogen program and vehicle technologies annual meritreview.2011.

89. Briggs I, McCullough G, Spence S and Douglas R, O’Shaughnessy R, Hanna A, “Waste energy recovery on a diesel-electric hybrid bus using a turbogenerator”. In: Proceedings of the SAE 2012 commercial vehicle engineering congress, 2012-01-1945.2012.

90. Thompson IG, Spence SW, Thornhill D, McCartan CD and Talbot-Weiss JMH. “The technical merits of Turbogenerating shown through the design, validation and implementation of a one-dimensional engine model”. Int J Engine Res 2014;15(1):66–77.

91. Michon M, Calverley SD, Clark RE, Howe D and Chambers JDA. “Modelling and testing of a turbo-generator system for exhaust gas energy recovery”. In: Proceedings of the vehicle power and propulsion conference. Arlington, USA; 2007. p. 544–550.

92. Michon M, Calverley SD, Clark RE, Howe D, McClelland M and Sykes P., “Switched reluctance turbo-generator for exhaust gas energy recovery”. In: Proceedings of the IEEE power electron motion control conference. Portoroz, Slovenia; 2006. p. 1801–1807.

93. CH. Weinstein, “Turbogenerator power systems for electric power generation”. In: Proceedings of the SAE aerospace power systems conference. 1998.

94. Briggs I. “Modelling a turbogenerator for waste energy recovery on a diesel-electric hybrid bus”. In: Proceedings of 15th annual Sir Bernard crossland symposium. Dublin; 2012.

95. Kishishita K, Miyajima K and Hirai K. “A study of an electrical turbo-compound system”. JSAE Rev 1995; 16 (1):66–8.

96. Kishishita K, Miyajima K, Hirai K and Fujita S. “Study of the optimization of electrical turbo-compound system through computer simulation”. JSAE Rev 1995; 16 (3):239–43.

97. Thompson I, Spence S, McCartan C and Talbot-Weiss J, Thornhill D. “One dimensional modelling of a turbogenerating spark ignition engine operating on biogas”. SAE Int J Engines 2011; 4 (1): 1354–64.

98. Thompson IGM, Spence SW and McCartan CD. “Design, validation and performance results of a turbocharged turbogenerating biogas engine model”. In: Proceedings of the 9th international conference on turbochargers and turbocharging. London; 2010.

99. Eriksson L, Lindell T, Leufven O and Thomasson A. “Scalable component-based modelling for optimizing engines with supercharging, e-boost and turbo-compound concepts”. SAE Int J Engines 2012; 5(2): 579–95.

100. ATR. Patterson and J. McGuire, “Exhaust heat recovery using electro-turbo generators”. SAE Technical Paper, 2009-01-1604. 2009.

101. Algrain M. “Controlling an electric turbocompound system for exhaust gas energy recovery in a diesel engine”. In: Proceedings of the IEEE international conference on electro information technology. 2005.

102. Fairbanks J, Maronde C and Kruiswyk R. “An engine system approach to exhaust waste energy recovery (High efficiency engine technologies program)”. DOE final report DE-FC26-05NT42423. USA: Caterpillar Inc; 2010.

103. U. Hopmann, M. Algrain, “Diesel engine electric turbocompound technology”. SAE Technical Paper, 2003-01-2294.2003.

104. F.G. Gerke, “Diesel engine waste energy recovery utilizing electric turbocompound technology”, Proc. 7th Diesel Engine Emissions Reduction (DEER) Workshop, Portsmouth, USA, 2001.

105. Hopmann U. “Diesel engine waste energy recovery utilizing electric turbocompound technology”. In: Proceedings of the directions in engine-efficiency and emissions research conference. 2002.

106. Algrain M, Hopmann U. “Diesel engine waste energy recovery utilizing electric turbocompound technology”. In: Proceedings of the directions in engine efficiency and emissions research. 2003.

107. Hopmann U. “Diesel engine waste energy recovery utilizing electric turbocompound technology”. In: Proceedings of the directions in engine-efficiency and emissions research. 2004.

108. Bumby J, Crossland S and Carter J. “Electrically assisted turbochargers: their Potential for energy recovery”. In: Proceedings of the hybrid vehicle conference. The Institution of Engineering and Technology; 2006.

109. F. Millo, F. Mallamo, E. Pautasso and Ganio Mego, “The potential of electric exhaust gas turbocharging for HD diesel engines”. SAE Technical Paper, 2006-01-0437. 2006.

110. Chadwell CJ, Walls M. “Analysis of a Super Turbocharged Downsized Engine Using 1-D CFD Simulation”. SAE Technical Paper, 2010-01-1231. 2010.

111. VanDyn EA, Gendron TA., Superturbocharger. US 7,490,594 B2. 2009.

112. C. Brockbank, “Application of avariable drive to supercharger and turbo compounder applications”. SAE Technical Paper, 2009-01-1465. 2009.

113. E.A. VanDyn, R. Wagner, “Superturbocharger presentation”. In: Proceedings of the directions in engine-efficiency andemissionsresearch.August2008.

114. Zhuge, W., Huang, L., Wei, W.and Zhang, Y. "Optimization of an Electric Turbo Compounding System for Gasoline Engine Exhaust Energy Recovery," SAE Technical Paper 2011-01-0377, 2011, doi:10.4271/2011-01-0377.

115. Ishii, M., "System Optimization of Turbo-Compound Engine (First Report: Compressor and Turbine Pressure Ratio)," SAE Technical Paper 2009-01-1940, 2009, doi:10.4271/2009-01-1940.

116. Ishii, M., "System Optimization of Turbo-Compound Engine (Second Report: Effects of Compression Ratio)," SAE Technical Paper 2012-01-1734, 2012, doi:10.4271/2012-01-1734.

117. Tuttle, J. H. “Controlling engine load by means of late intake-valve closing”, SAE Paper, No. 800794, 1980.

118. Asmus, T. W. “Valve events and engine operation”, SAE Paper, No. 820749, 1982.

119. Rabia, S. M. and Kora, N. S. “Knocking phenomena in gasoline with late-intake valve closing”, SAE Paper, No. 920381, 1992.

120. Saunders, R. J. and Abdual-Wahab, E. A. “Variable valve closure timing for load control and the Otto Atkinson cycle engine”, SAE Paper, No. 890677, 1989.

121. Blakey, S. C., Foss, P. W., Basset, M. D. and Yates, P. W. “Improved automotive part load fuel economy through valve timing”. In XIV Proceedings of Internal Combustion Engine and Combustion, India, 1995.

122. Ham, Y. Y. and Park, P. “The effects of intake valve events on engine breathinging capability”. International Pacific Conference on Automotive Engineering, Seoul, Korea, 1991, Paper No. 912470.

123. Hong H, Parvate-Patil GB and Gordon B. “Review and analysis of variable valve timing strategies – eight ways to approach”. J Auto mob Eng 2004; 218 (10):1179–200.

124. S Siripornakarachai, T Sucharitakul. “Modification and Tuning of Multi-valve Diesel Bus Engine to Run On Biogas for Electricity Production”. International Journal of Renewable Energy. Vol 3, No 2. 2008.

125. T Shudo, K Toshinaga. “Combustion control for waste-heat recovery system in internal combustion engine vehicles: increase in exhaust-gas heat by combustion phasing and its effect on thermal efficiency factors”. International Journal of Engine. April 1, 2010 vol. 11 no. 2 99-108. doi: 10.1243/14680874JER06009.

126. Gumbleton, J., Niepoth, G., and Currie, J., "Effect of Energy and Emission Constraints on Compression Ratio," SAE Technical Paper 760826, 1976, doi:10.4271/760826.

127. Smith, P., Heywood, J., and Cheng, W., "Effects of Compression Ratio on Spark-Ignited Engine Efficiency," SAE Technical Paper 2014-01-2599, 2014, doi:10.4271/2014-01-2599.

128. Ayala, F., Gerty, M., and Heywood, J., "Effects of Combustion Phasing, Relative Air-fuel Ratio, Compression Ratio, and Load on SI Engine Efficiency," SAE Technical Paper 2006-01-0229, 2006, doi:10.4271/2006-01-0229.

129. F Ma, S Li, J Zhao, Z Qi, J Deng, N Naeve, Y He and S Zhao. “Effect of compression ratio and spark timing on the power performance and combustion characteristics of an HCNG engine”. International Journal of Hydrogen Energy. Volume 37, Issue 23, December 2012. doi:10.1016/j.ijhydene.

130. H Aghaali, H Ångström. “A review of turbocompounding as a waste energy recovery system for internal combustion engines”. Renewable and Sustainable Energy Reviews. Volume 49, September 2015. doi:10.1016/j.rser.

131. Hindi, G., Zabeu, C., and Langeani, M., "Turbocharged vs. Turbo-Compounded Ethanol Engine: Fuel-Air Equivalence Ratio Impact," SAE Technical Paper 2009-36-0050, 2009, doi:10.4271/2009-36-0050.

132. Vuk CT. “Turbocompounding, a technology who's time has come”. Diesel Engine Emissions Reduction (DEER) Conference, USA. 2005.

133. R.W. Kruiswyk. “The role of turbocompound in the era of emissions reduction”. 10th International Conference on Turbochargers and Turbocharging. 2012. doi:10.1533/9780857096135.5.269.

134. Japikse D, Baines NC. “Introduction to turbomachinery”. Concepts ETI, Inc. and Oxford University Press; 1995.

135. Moustapha H, Zelesky MF, Baines NC, Japiske D. “Axial and Radial Turbines”. USA: Concepts NREC; 2003.

136. R Zhao, W Zhuge, Y Zhang, Y Yin, Z Chen, Z Li. “Parametric study of power turbine for diesel engine waste energy recovery”. Applied Thermal Engineering. Volume 67, Issues 1–2, June 2014. doi:10.1016/j.applthermaleng.

137. A Boretti. “Numerical Evaluation of the Performance of A Compression Ignition Cng Engine For Heavy Duty Trucks With An Optimum Speed Power Turbine”. International Journal of Engineering and Technology Innovation, vol. 1, no. 1, 2011.

138. Dijkstra, R., Boot, M., Eichhorn, R., Smeulders, D., "Experimental Analysis of Engine Exhaust Waste Energy Recovery Using Power Turbine Technology for Light Duty Application," SAE Int. J. Engines 5(4):1729-1739, 2012, doi:10.4271/2012-01-1749.

139. Hield, P. “The Effect of Back Pressure on the Operation of a Diesel Engine”. DSTO Publications Online. 2011.

140. Ismail, Y., Durrieu, D., Menegazzi, P. and Chesse, P., "Study of Parallel Turbocompounding for Small Displacement Engines," SAE Technical Paper 2013-01-1637, 2013, doi:10.4271/2013-01-1637.

141. Aghaali, H. and Angstrom, H., "Performance Sensitivity to Exhaust Valves and Turbine Parameters on a Turbocompound Engine with Divided Exhaust Period," SAE Int. J. Engines 7(4):1722-1733, 2014, doi:10.4271/2014-01-2597.

142. S Cong, C P Garner and G P McTaggart-Cowan. “The Effects of Exhaust Back Pressure on Conventional and Low-Temperature Diesel Combustion”. Journal of Automobile Engineering February 1, 2011 vol. 225 no. 2 222-235. doi: 10.1177/09544070JAUTO1577.

143. De Ojeda, W. and Rajkumar, M., "Engine Technologies for Clean and High Efficiency Heavy Duty Engines," SAE Int. J. Engines 5(4):1759-1767, 2012, doi:10.4271/2012-01-1976.

144. Edwards, K., Wagner, R., and Briggs, T., "Investigating Potential Light-duty Efficiency Improvements through Simulation of Turbo-compounding and Waste-heat Recovery Systems," SAE Technical Paper 2010-01-2209, 2010, doi:10.4271/2010-01-2209.

145. A Mamat, A Romagnoli, F Ricardo and B Martinez. “Design and development of a low pressure turbine for turbo-compounding application”. International Journal of Gas Turbine, Propulsion and Power Systems. October 2012, Volume 4, Number 3.

146. C Fredriksson, N Baines. “The Mixed Flow Forward Swept Turbine for Next Generation Turbocharged Downsized Automotive Engines”. ASME Turbo Expo 2010: Power for Land, Sea, and Air. 2010. doi:10.1115/GT2010-23366.

147. Tang H, Pennycott A and Akehurst S. “A review of the application of variable geometry turbines to the downsized gasoline engine”. *Int J Engine Res* 2014; 16(6): 810-825.

148. Gamma Technologies. GT-Suite Flow Theory Manual, 2013.

149. Gundmalm S. “Divided Exhaust Period on Heavy-Duty Diesel Engines”. PhD Thesis, Royal Institute of Technology, Sweden, 2013.

150. Gamma Technologies. GT-Suite Engine Performance Application Manual, 2013.

151. Pesiridis A, Salim WSIW and Martinez-Botas RF. “Turbocharger matching methodology for improved exhaust energy recovery”. In: *Institution of Mechanical Engineers 10th International Conference on Turbochargers and Turbocharging*, London, UK, 15 May-16 May 2012, London: Institution of Mechanical Engineers.

152. Holt, Nick. Engine downsizing. “Automotive Manufacturing Solutions”, 2012, p.56-62.

153. Mitchell James Piddock. “Engine optimization for downsizing by experiment and by simulation”. Thesis (Ph.D.) - University of Bath, 2010.

154. Copeland, C., Martinez-Botas, R., Turner, J. and Pearson, R., "Boost system selection for a heavily downsized spark ignition prototype engine," presented at ImechE 10th international Conference on Turbochargers and Turbocharging, UK, May 15-16, 2012.

155. Turner, J., Popplewell, A., Patel, R. and Johnson, T., "Ultra Boost for Economy: Extending the Limits of Extreme Engine Downsizing," SAE Int. J. Engines 7(1):2014, doi:10.4271/2014-01- 1185.

156. Friedfeldt, R., Zenner, T., Ernst, R.and Fraser, A., “Three-cylinder Gasoline Engine with Direct Injection”, MTZ worldwide Edition: 2012-05.

157. Wetzel P. “Downspeeding a Light Duty Diesel Passenger Car with a Combined Supercharger and Turbocharger Boosting System to Improve Vehicle Drive Cycle Fuel Economy”. SAE paper 2013-01-0932, 2013.

158. De Freitas A, Knichel T and Shawe J. “Simulation and verification the performance of the CVT Supercharger variable drive supercharger system on a 1.0L GTDI engine”. In: 21st Supercharging Conference, Dresden, Germany, 15-16 September, 2016.

159. Stone R. “Introduction to Internal Combustion Engines”. 3rd ed. London: MacMillan, 1999.

160. Turner JWG and Pearson RJ. “The turbocharged direct-injection spark-ignition engine”. In: Advanced direct injection combustion engine technologies and development: Vol 1, Gasoline and gas engines: science and technology. 1st edition. Cambridge: Woodhead Publishing, 2009.

161. Lysholm AJR. “A New Rotary Compressor”. Proc IMechE 1943; 150: 11-16.

162. Rose ATJM, Akehurst S and Brace CJ. “Modelling the performance of a continuously variable supercharger drive system”. Proc IMechE Part D: J Automobile Engineering 2011; 225(10): 1399-1414.

163. Froehlich M and Stewart N. “TVS® V-Series Supercharger Development for Single and Compound Boosted Engines”. SAE paper 2013-01-0919, 2013. DOI: 10.4271/2013-01-0919.

164. Birckett A, Engineer N and Arlauskas P. “Mechanically Supercharged 2.4L GDI Engine for Improved Fuel Economy and Low Speed Torque Improvement”. SAE paper 2014-01-1186, 2014. DOI: 10.4271/2014-01-1186.

165. Turner J, Popplewell A and Marshall D. “SuperGen on Ultraboost: Variable-Speed Centrifugal Supercharging as an Enabling Technology for Extreme Engine Downsizing”. SAE Int. J. Engines 2015; 8(4): 1602-1615. DOI:10.4271/2015-01-1282.

166. Rose ATJM, Akehurst S and Brace CJ. “Investigation into the trade-off between the part-load fuel efficiency and the transient response for a highly boosted downsized gasoline engine with a supercharger driven through a continuously variable transmission”. Proc IMechE Part D: J Automobile Engineering 2013; 227(12): 1674-1686. DOI: 10.1177/0954407013492932.

167. Hu B, Copeland C and Lu P. “A New De-throttling Concept in a Twin-Charged Gasoline Engine System”. SAE Int. J. Engines 2015; 8(4): 1553-1561. 2015. DOI: 10.4271/2015-01-1258.

168. Friedfeldt R, Zenner T and Ernst R. “Three-cylinder gasoline engine with direct injection”. Auto Tech Review 2013; 2(2): 32-37.

169. Ross T and Zellbeck H, “New approach to turbochargers for four-cylinder gasoline engines”. MTZ worldwide 2010; 71(12): 46-53.

170. Meghani A, Allen J and Turner JWG, “Effects of Charging System Variability on the Performance and Fuel Economy of a Supercharged Spark-Ignition Engine”. SAE paper 2015-01-1286, 2015. DOI: 10.4271/2015-01-1286.

171. Ostrowski G, Neely GD and Chadwell CJ, “Downspeeding and Supercharging a Diesel Passenger Car for Increased Fuel Economy”. SAE paper 2012-01-0704, 2012. DOI: 10.4271/2012-01-0704.

172. Copland C. “Internal Combustion Engine Technology”. Lecture notes, University of Bath, Bath, UK, October 2015.

173. King J, Heaney M and Bower E. “HyBoost – An intelligently electrified optimised downsized gasoline engine concept”. In: IMechE 10th international conference on turbochargers and turbocharging, London, UK, 15-16 May 2012, pp. 3-14. Cambridge: Woodhead Publishing.

174. Bassett M, Hall J and Hibberd B, “Heavily Downsized Gasoline Demonstrator”. SAE Int. J. Engines 2016; 9(2): 729-738. DOI: 10.4271/2016-01-0663.

175. Brandt M, Rauscher M and Lejsek D. “Scavenging to improve Low-End Torque of a Direct Injected Turbocharged SI Engine”, https://www.gtisoft.com/wp-content/uploads/publication/Bosch_Scavenging.pdf. (2005, accessed 10 August 2015).

176. Karnik AY, Jankovic MJ and Shelby MH. “Scavenging in a turbocharged gasoline engine”. Int. J. Powertrains 2012; 1(4): 420-437.

177. Hu B. “Application of Divided Exhaust Period and Variable Drive Supercharging Concept for a Downsized Gasoline Engine”. PhD Thesis, University of Bath, UK, 2016.

178. Birckett A, Tomazic D and Bowyer S, “Transient Drive Cycle Modeling of Supercharged Powertrains for Medium and Heavy Duty On-Highway Diesel Applications”. SAE paper 2012-01-1962, 2012. DOI: 10.4271/2012-01-1962.

179. Biller BD, Wetzel P and Chandras P. “Vehicle Level Parameter Sensitivity Studies for a 1.5L Diesel Engine Powered Passenger Car with Various Boosting Systems”. SAE Int. J. Fuels Lubr. 2015; 8(2): 441-453. DOI: 10.4271/2015-01-0982.

180. Miller RH. “Supercharging and internal cooling cycle for high output”. Trans. ASME 1947; 69: 453-457.

181. Li T, Gao Y and Wang J. “The Miller cycle effects on improvement of fuel economy in a highly boosted, high compression ratio, direct-injection gasoline engine: EIVC vs. LIVC”. Energ Convers Manage 2014; 79: 59-65. OI:10.1016/j.enconman.2013.12.022.

182. Bassett, M., “E-supercharging for Heavily Downsized Gasoline Engines,” in SIA Powertrain: The low CO2 spark ignition engine of the future and its hybridisation, Versailles, 2015

183. Nick Gibbs, “Audi’s move to e-charger could boost Valeo, Honeywell, BorgWarner,” in Automotive News. http://www.autonews.com/article/20150515/COPY01/305159986/audis-move-to-e-charger-could-boost-valeo-honeywell-borgwarner, 2015. Last accessed: Nov. 2016

184. Stapelbroek, M. , “Fuel Consumption Reduction and Performance Improvement by Electric Driven Supercharger,” in Aachen Colloquium Automobile and Engine Technology, pp1-20, Aachen, 2016

185. Katrašnik, T., “An Analysis of Turbocharged Diesel Engine Dynamic Response Improvement by Electric Assisting Systems,” in Transactions of the ASME, Vol. 127, pp918-926. 2005

186. Ehrhard, J., “Future Emission Legislation Requirements – Contribution of Electrically-Assisted Charging Systems,” in Aachen Colloquium Automobile and Engine Technology, pp1137-1155, Aachen, 2016

187. Panting, J., “Turbocharger motor–generator for improvement of transient performance in an internal combustion engine,” in Proceedings of Institution of Mechanical Engineers Vol 215 Part D, pp368-383, 2001

188. Katrašnik, T., “Improvement of the Dynamic Characteristic of an Automotive Engine by a Turbocharger Assisted by an Electric Motor,” in Transactions of the ASME, Vol 125, pp590-595, 2003

189. Arsie, I., “A Comprehensive Powertrain Model to Evaluate the Benefits of Electric Turbo Compound (ETC) in Reducing CO2 Emissions from Small Diesel Passenger Cars,” SAE Technical Paper 2014-01-1650, 2014

190. Divekar, P., “Coordinated Electric Supercharging and Turbo-Generation for a Diesel Engine,” SAE Technical Paper 2010-01-1228, 201.

191. Kamo, R. and Bryzik, W., “Adiabatic Turbocompound Engine Performance Prediction,” SAE Technical Paper 780068, 1978, doi:10.4271/780068.

192. Hountalas D.T., Katsanos C.O., Rogdakis E.D.and Kouremenos D., “Study of available exhaust gas heat recovery technologies for HD diesel engine applications”, International Journal of Alternative Propulsion, 2006.

193. Kushch, A.S., Bass, J.C., Ghamaty, S. and Elsner, N.B., “Thermoelectric Development at Hi-Z Technology,” Hi-Z Technology Inc, June 2001, pp.422-430.

194. Timothy J., David P., Ana C., and Micheal G., “Effectiveness of Mechanical Turbo Compounding in a Modern Heavy-Duty Disel Engine,” SAE Technical Paper, 2012.

195. “Napier Nomad-An Engine of Outstanding Efficiency,” Flight, April, 1954.

196. Winkler, N. and Ångström, H., “Simulations and Measurements of a Two-Stage Turbocharged Heavy-Duty Diesel Engine Including EGR in Transient Operation,” SAE Technical Paper 2008-01-0539, 2008, doi:10.4271/2008-01-0539.

197. Matsura, Y., Nakazawa, N., Kobayashi, Y. and Ogita, H. “Effects of Various Methods for Improving Vehicle Startability and Transient Response of Turbocharged Diesel Trucks,” SAE Technical Paper 920044, 1992, doi:10.4271/920044.

198. Mitsunori I. “System Optimization of Turbo-Compound Engine (First Report: Compressor and Turbine Pressure Ratio”. SAE International. 2009-01-1940. 2009. doi:10.4271/2009-01-1940.

199. Hiroaki Minegishi, Hiromi Matsushita and Masaru Sakakida, “Development of A Small Mixed-flow Turbine for Automotive Turbochargers”. THE AMERICAN SOCIETY OF MECHANICAL ENGINEERS. 95-GT-53, 1995.

200. Bo Hu, Huayin Tang, Sam Akehurst, Andrew De Freitas, Dave Burtt and James Shawe, “Modelling the Performance of the Torotrak CVT Supercharger Variable Drive Supercharger System on a 1.0L GTDI - Preliminary Simulation Results”. SAE Technical Paper, 2015-01-1971, doi:10.4271/2015-01-1971.

201. Liu Jingping, Yang Yanping and Yang Hanqian. “A Study on the Prospect of Engine Exhaust Gas Energy Recovery” (C). Electric Information and Control Engineering (ICEICE) 15-17 April 2011. Print ISBN:978-1-4244-8036-4.

202. Rich Kruiswyk. “An Engine System Approach to Exhaust Waste energy recovery”. Caterpillar Inc report. DOE Award No.: DE-FC26-05NT42423.

203. John R. Armstead and Scott A. Miers. “Review of Waste energy recovery Mechanisms for Internal Combustion Engines” (C). ASME 2010 Internal Combustion Engine Division Fall Technical Conference. ISBN: 978-0-7918-4944-6.

204. Saidur R, Rezaei M, Muzammil WK and Hassan MH. “Technologies to recover Exhaust heat from internal combustion engines” (J). Renewable and Sustainable Energy ReviewsVolume 16, Issue 8, October 2012, Pages 5649–5659. doi: 10.1016/ j.rser.2012.05.018.

205. Toom R. “Waste heat regeneration: a technology overview and its potential in racing applications”. Professional Motorsport World. November 2007.

206. Wanli Zhang, Lingen Chen and Fengrui Sun. “Power and efficiency optimization for combined Brayton and inverse Brayton cycles” (J). Applied Thermal Engineering, Volume 29, Issues 14–15, October 2009, Pages 2885–2894. doi:10.1016/ j.applthermaleng.2009.02.011.

207. Société Rateau, "Improvements in or relating to Internal Combustion Engines," British Patent 179,926, February 1924.

208. Deutz AG, "Turbocharged four stroke cycle fuel injection engine," United States Patent 2,979,887, April 1961.

209. Fleming Thermodynamics Ltd., "I.C. engine with an exhaust driven turbine or positive displacement expander," British Patent 2,185,286, July 1987.

210. SAAB Automobile AB, Family of Swedish Patents SE507030C2, SE521615C2, SE521174C2, SE514806C2, SE514969C2, SE512943C2, SE518687C2, 1998-2003.

211. D. Roth and P. Keller, "Valve-Event Modulated Boost System", SAE Technical Paper 2010-01-1222.

212. D. Roth and M. Becker, "Valve-Event Modulated Boost System: Fuel Consumption and Performance with Scavenge-Sourced EGR", SAE Int. J. Engines, vol. 5(2):538-546, 2012.

213. Hu, B., Akehurst, S., Brace, C. and Copeland, C., "1-D Simulation Study of Divided Exhaust Period for a Highly Downsized Turbocharged SI Engine - Scavenge Valve Optimization," SAE Int. J. Engines 7(3):1443-1452, 2014, doi:10.4271/2014-01-1656.

214. Stefan Gundmalm, “Divided Exhaust Period on Heavy-Duty Diesel Engines”, Academic thesis, Department of Machine Design, Royal Institute of Technology 25th of January 2013.

215. Hu, B., Akehurst, S., Brace, C., Lu, P., Copeland, C. and Turner, J. W. G., 2016. “Fuel efficiency optimization for a divided exhaust period regulated two-stage downsized spark ignition engine”. Journal of Engineering for Gas Turbines and Power: Transactions of the ASME, 138 (5), 051507.

216. Turner, J.W.G., “Ultra Boost for Economy: Extending the Limits of Extreme Engine Downsizing”, SAE Int. J. Engines 7(1):387-417, 2014, doi:10.4271/2014-01-1185.

217. Douaud, A. and Eyzat, P., "Four-Octane-Number Method for Predicting the Anti-Knock Behavior of Fuels and Engines," SAE Technical Paper 780080, 1978, doi:10.4271/780080.

218. GTI, 2014, GT-SUITE Manual, Version 7.4.0 Build 1, Gamma Technologies Inc., Westmont, IL.

219. Gundmalm, S., Cronhjort, A., and Angstrom, H., "Divided Exhaust Period: Effects of Changing the Relation between Intake, Blow-Down and Scavenging Valve Area," SAE Int. J. Engines 6(2):739-750, doi:10.4271/2013-01-0578, 2013.

220. Energy & Fuels Road Map, Automotive Council UK, http://www.apcuk.co.uk/wp-content/uploads/2014/07/AC-Fuels-and-Energy-Roadmap-Final.pdf, 2016.